J. L. van Egmond 4666852

Groundwater Quality in Curaçao

A hydrochemical multi-annual (1977-2021) assessment of a Caribbean island

TUDelft

Groundwater Quality in Curaçao

A hydrochemical multi-annual (1977-2021) assessment of a Caribbean island

By

J. L. van Egmond

in partial fulfilment of the requirements for the degree of

Master of Science
in Environmental Engineering
Faculty of Civil Engineering and Geosciences (CEG)

at the Delft University of Technology,
to be defended publicly on Friday March 31, 2023 at 13:00 AM.

Supervisor:	Dr. B. M. van Breukelen,	TU Delft
Thesis committee:	Prof. Dr. Ir. M. K. de Kreuk,	TU Delft
	M. Wit, MSc	TU Delft

TU Delft

Preface

For this master's thesis a hydrochemical groundwater survey was carried out on the Caribbean island Curaçao as part of the SEALINK project and for the Environmental Engineering (Technology) master track of the Faculty of Civil Engineering and Geosciences, TU Delft.

This thesis is the culmination of a journey of academic and personal growth. It represents the fruit of many years of hard work, research, and writing and it would not have been possible without the help, guidance, and support of a number of people.

First and foremost, I would like to express my gratitude to my supervisor, Dr. B. M. van Breukelen, for his invaluable guidance and support throughout the entire process by providing valuable feedback at every step. His expertise has been instrumental in helping me to shape and refine my research.

I would also like to thank Prof. Dr. Ir. M. K. de Kreuk, not just as a member of the thesis committee, but also for the encouragement and support I was provided with throughout my entire academic program and career. I am deeply grateful for her guidance, advice and insights, and for the time that was taken to share her knowledge and experiences with me.

Furthermore, I would like to extend my thanks to PhD Candidate M. Wit for his insights and feedback. His support has been very helpful in developing a robust argument, and I am appreciative for the time and effort invested in commenting on my work.

I would also like to thank TU Delft's Faculty of Civil Engineering, the Water Lab and Armand Middeldorp for providing me with the resources and support necessary to complete my research. In addition, I would like to thank the kind and warm-hearted people of Curaçao that took it upon themselves to assist in the challenging practice of chasing down wells.

Finally, I would like to thank my family and friends, with a special shoutout to my wonderful and absolutely fabulous cousin Aaron Cassou for his unwavering support and encouragement throughout the fieldwork campaign. Without his love, support and commitment this master's thesis would not have been possible.

Link to video on this thesis from Student Stories TU Delft: " A Deep Dive into the Blue Waters of Curaçao":
https://www.tudelft.nl/en/ceg/education/student-stories/a-deep-dive-into-the-blue-waters-of-curacao

J. L. van Egmond
Delft, 7 January 2023

Contents

List of Figures

List of Tables

Abstract

For this thesis a hydrochemical groundwater survey was carried out on the Caribbean island of Curaçao in 2020 as part of the NWO SEALINK project. In order to be well-adapted against anthropogenic and natural pressures, Curaçao needs representative data, yet thorough hydrochemical datasets were only sparsely collected in the wet seasons of 1977 and 1992. The aim of this thesis was to determine the current chemical state of the groundwater and analyze for long-term pollution trends with an extended database spanning four decades, also including data that was collected in another fieldwork campaign in 2021.

Curaçao was divided into a western and eastern section to facilitate data interpretation. Willemstad is located in the east, with a higher population density and most drinking/wastewater treatment plants and pipelines. The west is less populated, more rural and mostly agricultural. Four geological formations occur: Diabaas, Knip Group, Limestones, and Mid Curaçao Formation, of which the Diabaas is distinctly present as both Diabaas East (DE) and Diabaas West (DW). During the 2020 fieldwork campaign, wells that were sampled in 1992 were revisited (n=96), of which 20 could be remeasured, but 76 were inaccessible. To acquire more data, an additional 71 wells were sampled, bringing the total to 91 (n_{east}=52; n_{west}=39). To obtain representativity, wells were as homogeneously distributed across the island as fieldwork conditions allowed for. 27 water quality parameters were analyzed in the field and lab (EC, DO, pH, turbidity, T, alkalinity, NO_3, NO_2, NH_4, Al, B, Br, Ca, Cl, Fe, F, K, Mg, Na, Ni, P, PO_4, S, Si, SO_4, V and Zn). Datasets were assessed with a variety of boxplots, diagrams, descriptive and multivariate statistics (e.g. cluster analysis).

Of the groundwater wells measured in 2020, 29% were fresh, 53% slightly brackish (EC = 1.5 – 5 mS/cm), 17% brackish (5 – 15 mS/cm) and 1% saline. The majority was used for private irrigation (51%) or commercial agriculture (11%). The expectation was that the 2020 and a later obtained 2021 (n=72) dataset could be combined, but the results showed that this was not possible; reasons are further discussed within this thesis. To determine the influence of field methodology, wells measured in 2020 and 2021 (n=8) were compared for EC and sampling strategy, and wells situated closely together (n_{2020}=7; 21-74 m) were assessed for heterogeneity (EC, pH, NO_3, Ca, Cl), showing the effects of different sampling techniques (<152%; Δ2.7mS/cm) and well choice (<450%; Δ175 mg-NO_3/L; 21m). For this reason, extra attention was paid to representativity and sets of identical wells shared between all datasets. With the cluster analyses of ‘21 five clusters were identified: fresh, fossil seawater, anthropogenic, and two brackish clusters.

Over the decades, groundwater freshening was observed for the east between the years 1977 and 1992 (EC_{1977}=2.6±2.4 mS/cm, n=126; EC_{1992}=2.1±1.6 mS/cm, n=52; DE) and between the years 1977 and 2020/2021 ($EC_{2020/21}$ = 1.8±1.2/1.9±1.2 mS/cm; n=41/43), as determined with student t-tests. Eastern freshening is probably caused by leaking wastewater and drinking water, to which the urban east would be more susceptible than the west. Between 1992 and 2020/2021 the extent of freshening declined, presumably due to simultaneous salinization processes (over-extraction and/or seawater intrusion). For nitrate no trend was observed, yet nitrate pollution is present for all years (NO_3>3 mg/L$_{'92,'20,'21}$=81%, 87%, 65%; NO_3>50 mg/L$_{'92,'20,'21}$=38%, 39%, 47%), likely linked to wastewater and fertilizer inputs.

Throughout the years, groundwater acidified, but the rural west did so with a higher onset pH (pH_{1977}=7.83, DW) and steeper decline (ΔpH=0.7) than the urbanized east (pH_{1977}=7.49; ΔpH=0.25, DE). An upward alkalinity trend is observed for the east, but not the west. Eastern acidification is likely caused by leaking wastewater. This is substantiated by higher eastern NO_3 concentrations (east: 74±63 mg/L, west: 27±44 mg/L; p<0.001), more exposure to wastewater due to the presence of Willemstad, and a negative correlation between alkalinity and pH only found in the east, probably caused by the conversion of wastewater-related organics to HCO_3/H^+. For the rural west, acidification is also attributed to wastewater pollution, but to a much lesser extent than the east. Instead, exploratory assessments point towards a plausible influence of atmospheric pollution spreading westward from the petrochemical facility “Isla Refinería” during its operating years. More vegetation, increasing the degradation of subsurface organic matter, is speculated to have an acidifying effect in the west, but no detailed analyses was done. Overall, further research into the causations and influences on long-term groundwater trends is recommended.

As was shown in this thesis, multi-annual datasets are valuable tools to disclose long-term groundwater quality trends regarding contamination, freshening, salinization and acidification. Such knowledge can greatly support the management and protection of groundwater resources and interlinked systems, such as marine aquatic life. This underlines the value of extended research, and also stresses the importance of an accessible network of groundwater wells, allowing for more representative data, further improving the advisory potential of such fieldwork campaigns.

1 Introduction

This thesis on groundwater hydrochemistry in Curaçao was performed at the Civil Engineering and Geosciences faculty of TU Delft, in relation to the NWO SEALINK project: an interdisciplinary research project that focuses on the aquatic and terrestrial processes that influence coral health in the Dutch Caribbean. The thesis research was pre-exploratory and took place before the onset of the SEALINK project. This thesis' results and aim are related to the groundwater section and land-derived processes of the project.

1.1 Problem statement

Fresh and unpolluted water is one of the world's most valuable resources, yet it is becoming increasingly scarce - especially in decentralised regions such as islands. An increasing amount of island states have been experiencing contamination and depletion of their (ground)water resources and are expressing concerns, not just for decreased availability of clean and fresh water (Santo Tomás Seccional Tunja et al., 2018), but also for the adverse effects that terrestrial water resources can have on interlinked systems upon contamination, such as coral reefs (Estep et al., 2017). The Caribbean island Curaçao (Figure 1) is no exception to these concerns, as there are several anthropogenic and natural hazards that pose as a possible threat to (further) affect its groundwater, ranging from over-extraction to climate change.

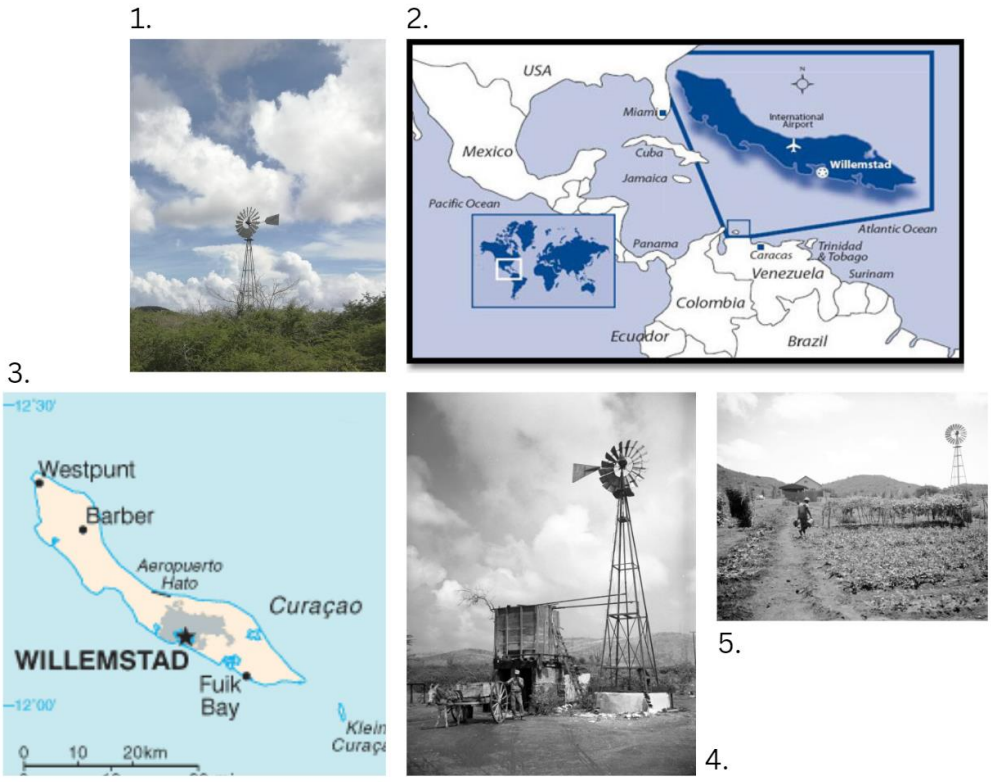

Figure 1. Location Curaçao and well pictures 1. Groundwater well, picture taken during field campaign '20, 2.-3. Location of Curaçao: Curaçao is a semi-arid Lesser Antilles island country located in the Southern Caribbean sea, 70 km of the coast of Venezuela (Marine Caribbean, n.d.)*, 4.-5. Groundwater wells on farmland in Curaçao* (Nationaal Archief Curaçao, n.d.).

In Curaçao, groundwater is of particular importance as there are not many surface water resources, besides small dams (Van Buurt, 2018). In addition, tap water is costly (Aqualectra, 2022) and groundwater is being relied on for a variety purposes, such as agriculture or industries (UNDP, 2018). A permit is not needed to drill for wells (ter Meer et al., 2007)

and the estimation is that there is a vast network of unregistered household, agricultural and industrial wells (Erdogan, 2021). For these wells there is no official supervision of groundwater use, nor are there groundwater quality directives (ter Meer et al., 2007). The unmonitored use of these wells could lead to over-extraction and a subsequent decline in the water table, which could cause a number of problems, such as land subsidence (Jones, 2011), and seawater intrusion (Cashman, 2014). Seawater intrusion could in turn lead to a degradation of groundwater quality by salinization (Shahid et al., 2017), which could ultimately give rise to groundwater that is unsuitable for purposes it now is extracted for. Agricultural practices can also impair groundwater quality, along with its effect on possible over-extraction by pumping up groundwater for irrigation. Adverse quality effects are mostly related to pesticide use, synthetic fertilizers or manure, livestock waste and soil erosion (Bijay-Singh & Craswell, 2021; Khan et al., 2017).

Islands in the Wider Caribbean Regions are also under threat from wastewater pollution (Erdogan, 2021). Such pollution can come from the leaching of untreated sewage, failing treatment and collection systems and industries that lack the capacity to properly treat their wastewater. In Curaçao, around one-third of households is connected to a sewage system (Jager, 2017) and roughly 16% of wastewater is treated, but even then, wastewater treatment is generally lacking, and both treated and untreated disposal is affecting the terrestrial and marine environment (Erdogan, 2021). Wastewater can have several consequences on water resources related to the contaminants its carries, i.e. nutrients, suspended solids, pathogens and organic matter (Robertson, 2021).
Curaçao used to be home to one of the world's largest oil-refineries in the world, "Isla Refinieriá", centrally located in the island's main port (Pulster, 2015), processing oil from nearby reserve Lale Maracaibo, Venezuela (Bonnélye et al., 2007). During its operating years (1918-2019 (Reuters, 2022)), oil refining was Curaçao's principle industry (Bonnélye et al., 2007). In an assessment done by TNO (ter Meer et al., 2007) surrounding the "Isla Refinieriá" location, several refinery-related contaminants were found in groundwater wells.

Climate change predictions show that the Caribbean is anticipated to experience more extensive drought (Cashman et al., 2010) and a rise in more variable weather (Farrell et al., 2010). Managing the variety of water can be an even greater challenge than water scarcity alone, as both excess rainfall and drought now need to managed, and under greater uncertainty (Sadoff & Muller, 2009). Both drought and rainfall play a role in aquifer depletion. Drought directly inhibits the island's natural groundwater recharge mechanism, whereas more intense rainfall increases localized run-off, leading to both reduced recharge of the aquifers and flooding (Farrell et al., 2010). In addition, sea level rise is another threat for seawater intrusion and salinization in the Caribbean region (Cashman, 2014). Furthermore, Curaçao will continue to experience population growth (United Nations, 2022) increasing the competition for water use, further stressing the quantity and quality of available water resources (Cashman et al., 2010).

The effects of anthropogenic pollution can extend beyond groundwater challenges or water supply. With intense rainfall, surface runoff can form and move sediments, nutrients and other forms of pollution overland towards the sea (Van Houselt, 2021), negatively affecting marine life and coral (Estep et al., 2017). Another way that (contaminated) groundwater can enter the marine environment is through submarine groundwater discharge (SGD), which has been noted as a key source of nutrients to coral reefs, although difficult to track and research. SGD is nonetheless known to occur anywhere where the aquifer head is above the ocean, and there is a connection through permeable rocks (Paytan et al., 2006). Coral in Curaçao is important for tourism, fishing, biodiversity, serves as a home for marine life, and aids in the protection of coastlines against wave impact and erosion (Waitt, 2016). The main components found in terrestrial sources (surface runoff and/or SGD) that could adversely affect coral health are nutrients, sedimentation and turbidity-related light limitations (Fabricius, 2005). In other words, contamination does not limit itself to land-sea boundaries. Land-derived pollution can have a negative effect on coral development, but go unnoticed through sectoral research that stays within the bounds of its own terrestrial discipline. This is also why interdisciplinary projects combining land and sea-based research, such as the NWO SEALINK project are essential.

1.2 Previous Research

In order to be well-adapted against the range of challenges linked to decreased fresh groundwater availability and aquifer contamination, high-quality data is necessary, yet Curaçao lacks an abundance of scientifically collected datasets. At the time of this thesis' fieldwork the last thorough hydrochemical assessments of Curaçao's groundwater system were

conducted in 1992 (De Bruijne & Louws, 1994) and 1977 (Abtmaier, 1978). A year after this thesis' fieldwork campaign a similar assessment was done in '21 by a master student from Wageningen University Research in the framework of SEALINK (**Table 1**). All the hydrogeological research campaigns ('92, '77, '20 and '21) have focused on different aspects of Curaçao's groundwater resources.

Table 1. Hydrogeochemical fieldwork campaigns in Curaçao over the years

Year	# of wells	Researcher & Institute
1977/78	233 (750)	Abtmaier, the Department of Agriculture of Curaçao
1992	96	Louws et al., Faculty Earth Sciences, Utrecht University
2020/21	91	This Master Thesis, Civil Engineering & Geosciences, Technische Universiteit Delft
2021/22	76	Master Thesis, Verstappen, Wageningen University Research & TU Delft

1977/'78 research

In 1977/1978 (Abtmaier, Department of Agriculture of Curaçao) different borewells were drilled and pumping tests were done. In addition, water balances were made of catchments throughout Curaçao and the transmissivity of different geologies were measured. 750 groundwater conductivity measurements were done and a sub-selection (233) was measured for the major ions K^+, Na^+, Ca^{2+}, Mg^{2+}, HCO_3^-, SO_4^{2-}, Cl^-, alkalinity and Total Dissolved Solids (TDS). The conclusions were that in several areas groundwater was over-extracted and seawater intrusion was found (among which St. Joris Baai). The highest salinities were observed in the Mid Curaçao Formation (MCF) and Knip Group. Rainwater was generally not found to have a big influence on the aquifers. The only formation that was deemed suitable for groundwater extraction was the Curaçao Lava Formation (CLF), due to the higher permeability and lower salinities than the other formations. (Abtmaier, 1978)

1992 research

In 1992, 96 wells were sampled, of which 62 overlapped with the research that was done in 1977. Both one-on-one and general comparisons (e.g. cluster analyses) were done to assess the differences between '77 and '92. With the cluster analyses the following clusters were identified: seawater cluster (± half EC of seawater), arid-zone cluster, sub-oxidized cluster and precipitation cluster. The high sodium adsorption ratio of the seawater cluster was linked to salinization and seawater intrusion in coastal regions and bays, whereas the higher salinity samples in the MCF were linked to fossil seawater. From the pairwise comparison it came forward that 30% of the wells increased in chloride concentration, and 45% decreased in chloride concentration. Freshening was attributed to leaking drinking water and/or wastewater pollution, as infiltrating wastewater can have a desalinizing effect. In addition, nitrate was measured and found to be well beyond the WHO drinking water standard of 50 mg/L (2022). Nitrate pollution was mainly found in regions with higher population density and linked to septic tanks, cess pits and leaking wastewater. In addition, several geochemical processes influencing the anion and cation concentrations were found, such as calcite dissolution, cation exchange and silicate weathering. Wells situated along the coast and in the MCF were found to have the highest EC, the higher salinity MCF samples were linked to fossil seawater. (De Bruijne & Louws, 1994)

2021 research

In 2021, one year after this thesis' fieldwork campaign, Verstappen (2022) did a hydrochemical survey where trends were analysed between '77, '92 and '21 with a distinction between the different geologies. Verstappen found that seawater intrusion increased in the Knip and Mid Curaçao Formation. Both nitrate pollution and the decreasing pH were attributed to ongoing leaching of cesspits and septic tanks. Overall, the hydrochemical status of Curaçao was explained with geological interactions, recharge, salinization, pollution and other chemical processes. (Verstappen, 2022)

'20 research - this thesis

As the fieldwork campaign of this thesis and Verstappen were measured only one year apart and in similar months and rainy seasons, the expectation was that the results would be similar and allow for insight into the representativity of the applied fieldwork methodology in both years. For this reason, a comparative assessment was not just done between all years, but also done between the '20 and '21 with focus on the methodologies and representativity of these datasets. Furthermore, in the previous campaigns, most focus was put on the analyses of different geologies, yet no attention had

been paid to a more general division between the west and east, which is what this thesis' has made a geographical distinction between (Figure 2; Figure 3). More information on the west and east can be found in Chapter 2 Background.

Overall, understanding the dynamics of water quality variability and pollution trends in Curaçao is a much-needed step towards the avoidance of the manifold consequences that can arise from poor or inadequate water management. Enabling better water resources management will strengthen the island's resilience to natural and anthropogenic hazards and climate challenges, whilst building up the capacity to better adapt.

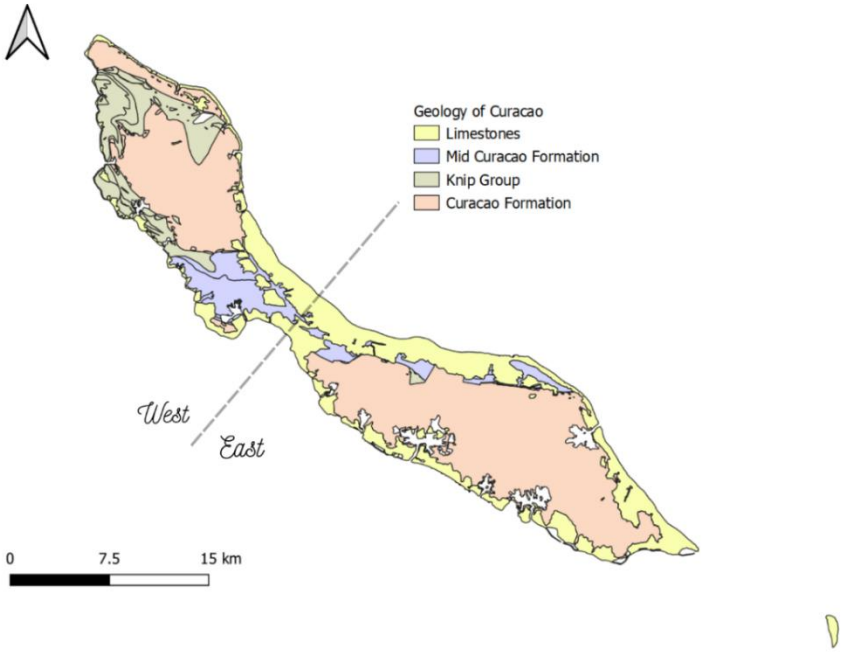

Figure 2. Simplified geological map of Curaçao (Beets, 1972). Within this thesis the focus mainly lies on the eastern side of Curaçao.

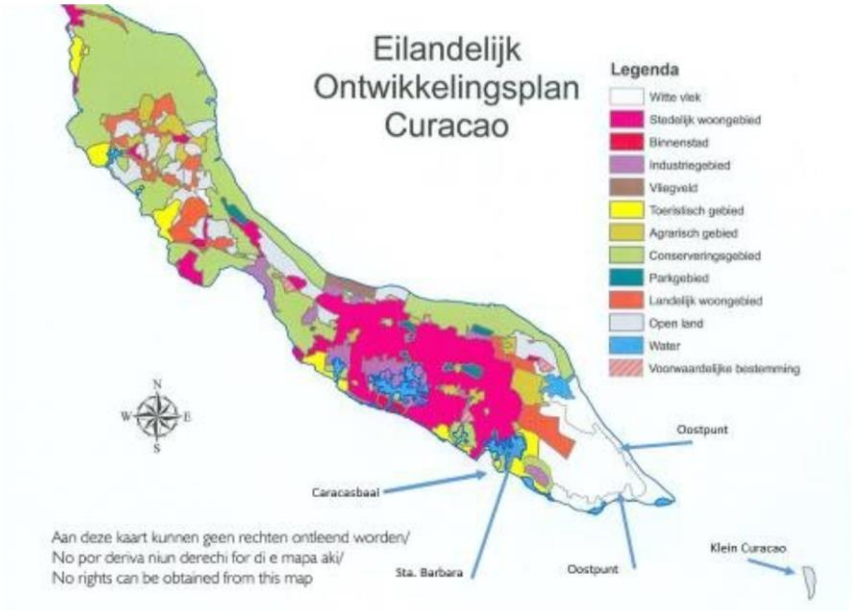

Figure 3. Land use map of Curaçao The east holds more urbanized areas (dark pink), whereas the west contains more nature, conservation area (green) and agriculture. More information on the distinction between east and west is presented in 2.1.2 Eastern side versus western side of Curaçao.

1.3 Research Objective and Research Questions

The main objective of this research thesis is to determine the hydrochemical groundwater characteristics of Curaçao in 2020's wet season through field research of deep-wells and analyze for long-term pollution trends with an extended database including data from '77, '92, '20 and '21. This is motivated by below-listed main research question, supported by five sub-questions.

1) **Geochemical groundwater trend**
   What general hydrochemical trends can be found throughout the decades for eastern and western Curaçao when comparing datasets from '77, '92, '20 and '21, and how can these trends be explained?
   a) What is the (hydrogeochemical) groundwater status in Curaçao during the '20 fieldwork campaign?
   b) How has the state of wells developed over the last 30 years (1992 - 2020) and how could this influence the results?
   c) How do the groundwater samples collected in '20 compare themselves to the groundwater data collected in '21? What differences and similarities can be found and can the two datasets be combined for further analyses?
   d) How representative are the datasets and how does field methodology affect the comparative assessment and analyses of long-term pollution trends?
   e) What is the influence of different processes on the observed geochemical trends, and how do they relate to eastern and western Curaçao?

In addition to the geochemical trend, exploratory assessments of runoff and rainwater were made to gain more insight into the surface processes that might link to the disruption of marine aquatic life, such as runoff streams. This resulted in the following additional question:

2) **Runoff, rain and groundwater relations**
   What water quality characteristics can be attributed to runoff water in relation to rain?

1.4 Thesis Structure

In Chapter 2 Background the background of the thesis topics will be discussed: geographic location, geology and water management practices within Curaçao. Chapter 3 Methods, consists of the field and lab methods and data analysis. In Chapter 4 Results, the results are presented and sectioned into groundwater, multivariate statistics, water use and rain and runoff, after which they are discussed in Chapter 5: Discussion. Chapter 6 provides the conclusion of the work performed within this thesis research, with the Recommendations in Chapter 7.

2 Background

2.1 Description of the location

2.1.1 Geographic description

Curaçao is a Lesser Antillean island located 64 kilometres north of the coast of Venezuela, in the southern Caribbean Sea. Its highest point is at 372 meters, the Christoffelberg in Christoffel Park (Van Sambeek et al., 2000). Curaçao has 152 000 inhabitants (United Nations, 2021) and a land mass area of roughly 444 km^2 (64 km long and 10-16 km wide) (Van Sambeek et al., 2000) making it the most densely populated island of the three islands previously known as the Dutch "Leeward" Islands (Aruba, Bonaire, Curaçao) (Bonnélye et al., 2007). Its diverse population counts 50 different nationalities and the official language is Papiemento and Dutch (Pulster, 2015). The island has rocks and distinct cliffs. The vegetation in Curaçao consist of thorn-like bushes (Van Sambeek et al., 2000), xeric shrubs like Euphorbiaceae, Fabaceae and Ribaceae (Van Leeuwen, 2017), and columnar cacti. Dense mangroves are present around semi-closed and inland bays. Around 30% of the island is covered with industries or accommodation, and another 30% is reserved for conservation (Debrot & Wells, 2009).

2.1.2 Eastern side versus western side of Curaçao

The island of Curaçao can roughly be divided into a north-western and south-eastern section (Table 2; Figure 4), regionally also known as Band'abou ("downside") and Band'ariba ("upside"), respectively (Van Leeuwen, 2017). Band'ariba (eastern side) is more urbanized, as the majority of the population lives in eastern-located Willemstad (Verstappen, 2022). The eastern side also has more exposure to (leaked/discharged) wastewater and the infrastructure for distributing desalinated seawater (UNOPS, 2018). Oil refinery "Isla Refineria" is located around Schottegat on the eastern side of the island (Pulster, 2015). During its operating years 1918-2019 (Reuters, 2022), oil refining was Curaçao's main industry, followed with tourism and the ship industry (Bonnélye et al., 2007). In the far east is an inaccessible, privately owned, part of Curaçao (Verstappen, 2022). Band'abou (western side) is more rural than the east, with less people, more agricultural practices and Christoffelpark, a nature conserve. In the past, repeated cultivation of crops, livestock and charcoal production affected the soil and vegetation of the island. Due to several factors (heavy theft of livestock and produce, economic reasons and/or increased land ownership), agriculture has reduced and because of that vegetation, such as dense woodlands, is recovering and returning, especially on the western side of the island (Debrot & Wells, 2009). Another reason that is mentioned for increased vegetation coverage is that nature management has reduced the amount of "wild goats" over the years (Van Leeuwen, 2017).

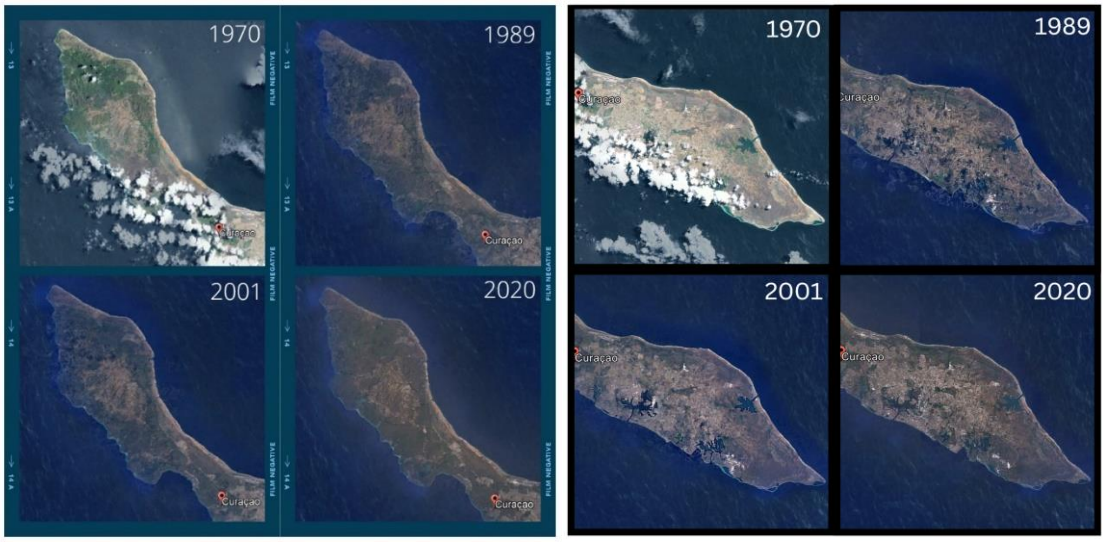

Figure 4. Satellite images of the western (left) and eastern (right) side of Curaçao, taken in different years, all in the month December (Google Earth Pro).

Table 2. Characteristics western and eastern Curaçao

West (Bandabou)	East (Bandariba / Eastpunt)
More rural, less populated	More urban, densely populated
More (returning) vegetation in the west	Willemstad
More agriculture	Most wastewater treatment plants
Christoffelpark, highest point	Desalination facilities
	Oil refinery Isla Refineria

2.1.3 Climate

As Curaçao is situated in the "Southern Caribbean Dry Zone" it has a (semi)arid climate with desert-like characteristics, and a clear dry and rainy season (Bonnélye et al., 2007). The dry season goes from February to June, and the rainy season from September – January, the in-between months (July, August) are transitional between the wet and dry season. All fieldwork campaigns measured in rainy season. The precipitation variations between the years is large, and the standard deviation is larger than the average. A strong, but delayed, relationship is found between the El Nino-Southern Oscillation and precipitation on Aruba, Bonaire and Curaçao (Martis et al., 2001). The temperature in Curaçao is tropical; the ocean around the Leeward islands has an average of 27C. The average annual rainfall is 581 mm year, based on the averages of all years between 1981 and 2020. The total rainfall in 2020 was 646 *mm*, with 79 rainy days (Central Bureau of Statistics Curaçao, 2022). The evaporation in the earthen dams of Curaçao was estimated to be 4-6 mm per day (Van Buurt, 2018). The potential evapotranspiration is 2400 mm/year and exceeds the average yearly rainfall (van Sambeek et al., 2000).

2.1.4 Geology of Curaçao

In terms of geology, Curaçao has four main lithologies: Curaçao Lava Formation (CLF), Knip formation (K), Mid Curaçao Formation (M) and Limestones (L)(Figure 2). The CLF is also known as Diabaas and can be divided into Diabaas East and West (Beets, 1972).
For the eastern section of Curaçao, the main focus for this thesis, three of these geologies are present: Diabaas East (DE), Limestones (L), and Mid Curaçao Formation (M) (Table 3). The CLF (a.k.a. Diabaas) consist chlorite-like minerals, clinopyroxene, and plagioclase, which is mainly substituted by turbid alite or to lesser extent by labradorite. Other minerals present in the CLF, but in lesser quantities are: ore, titanite, zeolites, phrenite, carbonates, quartz, pumpellyite, magnetite and leucoxene. After weathering of the Diabaas formation present (clay) minerals are: kaolinite, illite and montmorillonite. The L, present in both the east and west, consist of calcareous lithologies, in addition to terrigenous material. The MCF, which is only located in the west, contains mudstones, shales, sandstones and fine-grained

conglomerates. The latter consists of both calcareous and siliceous rocks, and also contain smaller pieces of the basalts that are found in the CLF. When looking at minerals the ones that most frequently occur in the MCF are: quartz, pyroxenes, chlorites and plagioclase (De Bruijne & Louws, 1994).

Table 3. Geological formations eastern Curaçao (De Bruijne & Louws, 1994; Geology, 2022; Mindat, 2022)

Curaçao Lava Formation (CLF) / Diabaas East (DO)	Chlorite group	$A_{5\text{-}6}T_4Z_{18}$, where A can be Al, Fe^{2+}, Fe^{3+}, Li, Mg, Mn, or Ni, while T = Al, Fe^{3+}, Si, or a combination. Z = O and/or OH
	Clinopyroxene	XYZ_2O_6. X: Ca, Na, Fe++, Mg, Zn, Mn, or Li. Y: Mg, Fe^{+++}, Fe^{++}, Cr, Al, Co, Mn, Sc, Ti, or Vn. Z: Si, Al, or a combination
	Plagioclase / turbid alite / labradorite	$NaAlSi_3O_8$ to $CaAl_2Si_2O_8$
	Ore	Sediment with range of valuable minerals, often metals, such as Zn or Sn.
	Titanite	$CaTiSiO_5$
	Zeolites	Example: $Na_2Al_2Si_3O_{10}{\cdot}2\ H_2O$
	Phrenite	$Ca_2Al_2Si_3O_{10}(OH)_2$
	Carbonates	$CaCO_3$ (s)
	Quartz	SiO_2
	Pumpellyite	$Ca_2Al_2(OH)_2$
	Magnetite	A main iron ore: $Fe^{2+}Fe^{3+}{}_2O_4$
	Leucoxene	Mixture of Fe-Ti oxides
	Kaolinite (clay mineral)	$Al_2Si_2O_5(OH)_4$
	Illite (clay mineral)	$(Al, Mg, Fe^{2+})_2(Si, Al)_4O_{10}[(OH)_2$,
	Montmorillonite (clay mineral)	$(Na,Ca)_{0.33}(Al,Mg)_2(Si_4O_{10})(OH)_2{\cdot}nH_2O$
Mid Curaçao Formation (M)	Quartz, quartz diorites	In summary M consist of sand stones, shales, mudstones, and conglomerates with calcareous and siliceous sediments, and fragments of basalt. See CLF for mineral formulas.
	Pyroxines	
	Chlorites	
	Plagioclase	
Limestone Formation (L)	Calcite, aragonite	Main component of limestone is calcite: $CaCO_3$ (s). In water this mostly means higher Ca^{2+}, and bicarbonate ions after dissolution.

2.1.5 General water use and water management in Curaçao

During the 19th century, rain and groundwater were used to supply the island with fresh water. In 1908 there were 34 wells on the island, used by the then 30 000 inhabitants. In 1915 the main refinery was built by Shell who subsequently purchased freshwater plantations, that it used till 1973, after which it made the switch to distilled seawater (Van Sambeek et al., 2000). The first desalination facility in Curaçao was set up in 1928, because of a shortage of drinking water. Initially, evaporation technologies were used; nowadays, Curaçao's Aqualectra has a multi-stage treatment line including Reverse Osmosis systems, producing 69 000 m^3 of drinking water per day (Figure 5) (Bonnélye et al., 2007).

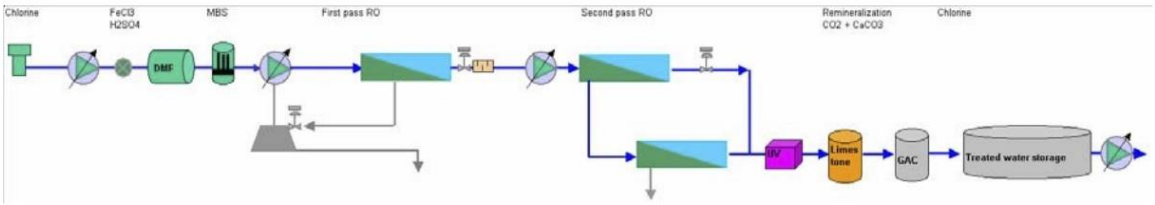

Figure 5. Curaçao's desalination treatment line(Bonneleye, 2006).

Around a third of Curaçao's inhabitants is connected to centralized sewage, with a combined sewage overflow system, collecting both domestic sewage and rainwater. There are four wastewater treatment facilities on the island: Abbatoir, Klein Kwartier, Klein Hofje and Tera Kora, of which only the first three were active as of February 2021. There are several challenges with wastewater management on the island, and the majority of the wastewater treatment facilities are not (properly) functioning, require renovation and exceed their design capacity (Erdogan, 2021). Ultimately, around 16% of Curaçao's wastewater is treated (inadequately) (Figure 6; Figure 7) and disposed of in the terrestrial environment of ocean, and 84% is directly disposed of in an untreated form (UNOPS, 2018). The treated wastewater of Klein Kwartier is being used for irrigational practices for e.g. golf courses and agriculture; the treated water of Klein Kwartier is infiltrated with infiltration ponds (Verstappen, 2022). The regions that are not connected to centralized sewage collection use septic tanks or cesspits; there are no regulations for such septic systems and they do not undergo any inspections. In the moments that sludge is collected, it either goes to sludge treatment facilities, or disposed of in the landfill or ocean (UNOPS, 2018).

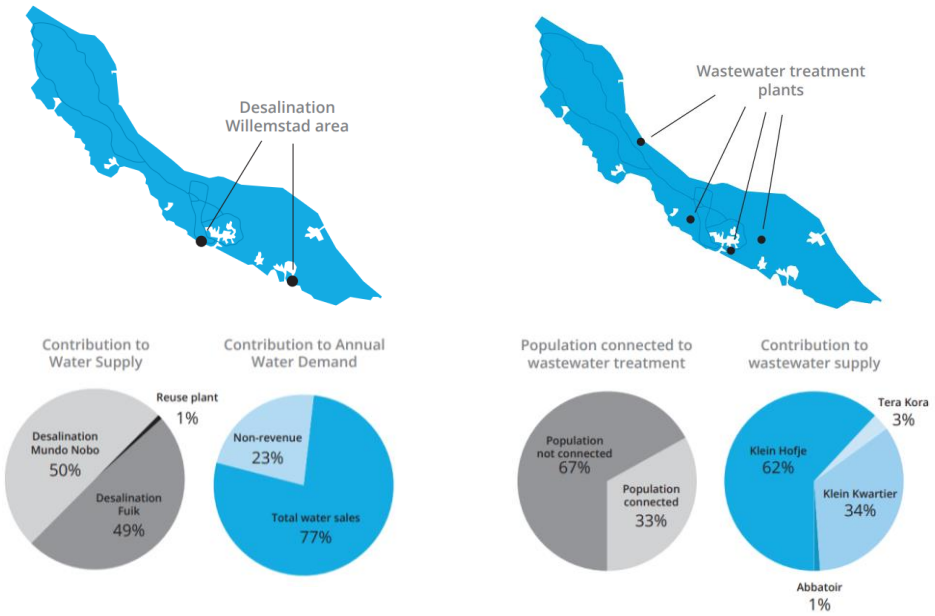

Figure 6. Locations of desalination in Willemstad and their contribution to water supply (left) and Curaçao's wastewater treatment plants (right): Tera Kora (west), Klein Hofje (east), Klein Kwartier (east) and Abbatoir (east) (UNOPS, 2018). The western Tera Kora was not active in February 2021 (Erdogan, 2021).

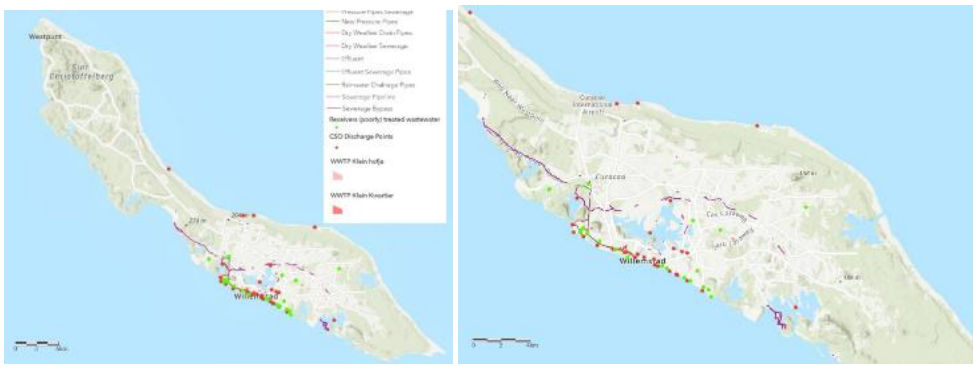

Figure 7. Locations of sewage discharge points and treatment plants in Curaçao (Erdogan, 2021).

The island has 47 discharge areas, with an average size of 5 km^2. There are no rivers or lakes on Curaçao (van Sambeek, 2000). A significant part of the precipitation evaporates or flows out into the ocean as surface runoff (Bonnélye et al., 2007); it is estimated that roughly 4% infiltrates as groundwater. Rainfall mainly occurs between October and January, and groundwater recharge and surface water mainly occur during this period. The research done in 1968 (Grontmij & Sogreah) mentions that there are eight important aquifers. When comparing Curaçao to other Caribbean islands there is less topography and only highly seasonal rainfall, resulting in less runoff. This could also be a potential explanation as to why Curaçao's coral reefs are considered to be more healthy than other regions of the Caribbean (Verstappen, 2022), despite the fact that Curaçao also experiences a considerable decline (50%) in coral cover between 1980 and 2015 (Estep et al., 2017). There are many smalls dams around the island that retain surface runoff, and aid groundwater infiltration. These dams have, however, severely decreased in numbers, from 1500 to 800, and have not been properly maintained (Van Buurt, 2018).

Groundwater is used for different purposes, such as irrigation, laundry, toilet flushing and showering (Verstappen, 2022). In 1979 it was estimated that there were 4000 wells, with an 800 wells being added to this number each year. At that time, most wells were situated in the CLF, with the most important aquifers were located there. Overall, wells in Curaçao are either hand dug (with a diameter of 2 - 4 meter) or drilled (boreholes with a diameter of 0.2 – 0.4 meter) and groundwater is won with windmills or electricity-driven pumps ((Van Sambeek et al., 2000; Verstappen, 2022). The hand dug wells often originate from the times of the plantations (Verstappen, 2022). The current number of wells is unknown, as no permit is needed to drill a well (ter Meer et al., 2007) and most boreholes are drilled by private companies (Verstappen, 2022). There is also no official check on groundwater usage, nor are there regulations for groundwater quality (ter Meer et al., 2007).

3 Methods

In this chapter the field and lab methodology and data analyses of this thesis' research campaign are explained. The methodology is divided in several section: 3.1 Field Methodology, 3.2 Lab Analyses and Data Validation, 3.3 Data Analyses and 3.4 Methodology of previous research.

3.1 Field Methodology

3.1.1 Well selection strategy and well access challenges

During the hydrochemical assessments of '77 and '92, over 233 and 97 wells were measured, respectively. At that time, research was conducted in cooperation with Directie Landbouw, Veeteelt en Visserij en Markthallen (DLVV). For the fieldwork campaign of '20 (11th of November 2020, till the 3rd of January, 2021), the initial idea was to visit the exact same 97 wells of the '92 fieldwork. Maps were set up on the basis of the GPS coordinates of the 90s and attempt were made to track them down. However, within the first weeks of this thesis fieldwork, it became apparent that it was challenging to find and measure these wells.

Over the last 28 years, many wells had not been maintained, others had been damped, covered or were so overgrown that they were completely concealed by thick bush, inaccessible even with hedge cutters. To give an example, for one well it took three hours of hiking and bush cutting to access it, only to find out the water could not be retrieved from the well as the lid was could only be removed with special equipment. After 9 days of fieldwork, wells were only attempted to be accessed for a time period up to 30 minutes. If the attempt to access the "original" well was not successful within this given time limit, a "substitute" well was sought out in the nearby region whenever available, given the substitute had the same geology and surrounding land-use.

This, however, also became challenging, as many wells were located on private terrain and access to these wells is subjected to the availability and cooperation of the owners. When "substitute" wells also became too hard to find in close proximity of "original" wells, the well selection strategy of this fieldwork was fully altered to one where the main goal was to establish a spatial variation of wells over the island, located in Curaçaos different geologies, regardless of the type of well or if it had been measured before. Still, even with this altered strategy, the "original" 1992 were all attempted to be found and accessed throughout the entire fieldwork period, as to gain insight as to what had happened to the wells of Curaçao over the last 28 years, between 1992 and 2020. To establish the fate of the wells measured in 1992 the following coding was used:

- **Access not granted (NG)**
  Well still existed, but owners of terrain did not allow access for groundwater sampling.
  Well was fenced off by company or institution in charge of well.
  Appointments were attempted to be made, but access was not granted in time.
- **No access (NA)**
  Well could not be accessed, because it was overgrown by thorned bush.
  Well was fully closed off by lid and could not be accessed without specialized equipment.
- **No one home (NH)**
  Wells were on private terrain, but upon several visits no one was home to allow access to well.
- **No well (NW)**
  Upon arrival at 1992 GPS point, there were no traces of there ever being a well.
  There used to be a well, but not anymore. This could be because a neighborhood was built in a previously rural region, or because wells were damped after (lethal) accidents.

- **Accessed and unreliable measurement (AU)**
  Well was accessed, but an unreliable sample was taken.
- **Accessed and reliable measurement (AR)**
  Well was accessed and a reliable sample was taken.

As sampling took place during monsoon season, wells were first aimed to be preselected on a daily basis, so that consideration could be taken to only collect from wells where it had not rained for at least 72 hours. This, however, ended up being unfeasible, as the predictions were often off due to highly localized rainfall. In addition, as access to the wells ended up being the main challenge in sampling, whenever there was an opportunity to sample, this was immediately taken, regardless of previous rainfall or not.

3.1.2 Water use questions

If wells were located on private property, and inhabitants were willing to participate, additional open questions were asked after groundwater collection and sampling was completed. Questions were asked in either Dutch, English or Spanish.

- How often is the groundwater well used?
- For what purpose is the well water used?
- If possible, can you give an estimate of the well water use?
- How long have you lived at this location?
- How was the well made and how deep is the well?
- In your experience, has the groundwater changed in quality or quantity throughout the years?
- Do you have any worries about the quality of the well water?
- What kind of sanitation facility is used on site?

3.1.3 Water level

Before groundwater collection, the depth of the well water was measured from the upper side of the well to the water level in m using a Heron dipper. At times, when the sound of well would be too loud, the dipper was substituted with a bag of weights or rocks, to be able to hear over the squeaking noises of the working windmill. The bottom of the wells was not measured, as the measuring device was not long enough for most wells: during the first period the measuring device was 8 meters, later 12, and in the last weeks 30 meters.

3.1.4 Groundwater collection

The groundwater samples were collected in a PVC tube that is closed on one side, which was connected to a 8-30 meter glass fiber rope (
Figure 8). The top was covered with cut panty hose attached with an elastic, preventing any larger objects from entering. Weights were stripped on one side of the tube with a band, allowing the device to flip and sink into the groundwater. It was made sure to not sample from the first 10 cm and the well was sampled at a depth of 3 meters from groundwater level. Whenever possible, the wells were purged for some time before sampling, although this was not possible for all wells. If not, it was registered how active the well was and if inhabitants or users could estimate their daily, weekly or monthly use. This way, it could roughly be determined if the well was used often enough that purging was not necessary and if not, a note was made so the inactivity could be taken into account for the analysis of the results. Before the water from the well was stored, it was made sure that the collection device was properly rinsed.

Figure 8. Field work material. Left: groundwater sampling device. Right: hedge cutters to get through bushes.

3.1.5 Field parameters

After water sample collection, measurements of the electroconductivity (EC), dissolved oxygen (DO), pH, temperature, turbidity were directly performed. For DO, the sensor was submerged at least 3 cm and an ‘’artificial’’ flow was created by moving the sensor around, whilst also making sure that the sensor did not touch any of the sides. Subsequently, the DO concentration was determined with an accuracy of 0.5-1 mg/L with the following categories:

- Category 1: Unsaturated (0-1 mg/L)
- Category 2: Lower saturation (1-2 mg/L)
- Category 3: Higher saturation (3-4 mg/L)
- Category 4: Saturated (>5 mg/L)

Depending on the level of saturation, an indication of the nitrate- was obtained by means of test strips, either immediately or at a later moment in the day. With low saturation (category 1 and 2), strips were immediately applied to avoid ammonium oxidation within the groundwater sample. With higher oxygen saturation levels (category 3 and 4), test strips were applied within 24 hours to save on time in the field. When the nitrate concentration exceeded 10 mg/L, or if there was any other indication of pollution by sanitation, another strip test was performed for ammonium. After two weeks, the DO meter stopped working and a substitute meter could not found, for this reason DO measurements were no longer taken and nitrate strips were used for all groundwater samples.

The idea was to also perform E. Coli measurements, but unfortunately a swap-out took place in the lab and Total Coliform plates were sent instead of E. Coli plates. The total coliform measurements were nonetheless also performed in the field, within 2 hours of sampling. 1 mL of the groundwater was taken with a plastic Pasteur pipette. The coliform plate was gently closed afterwards, after which a provided ‘’spreader’’ was used to equally spread the 1 mL sample. After one minute, the plate was placed in a hardcovered bag between 20-40 Celcius, away from direct sunlight, stacking no more than 20 samples. After 24, 36 and 72 hours (1, 2 and 3 days), the number of blue colonies was counted, using the Promega Colony Counter app and filled into the AKVO form, after which it was uploaded to the online database. To make sure the colonies could be counted after exactly 24, 48 and 72 hours, the container was brought to the field and reminders were set as alarms for each water sample. For total coliform was counted manually three times, and an average was taken. An overview of all measured field parameters and their brief methodology is presented in **Table 4**.

Table 4. Measured field parameters and brief methodology

Field Parameter	Measured	Time limit	Material
GPS coordinates	At well site		GPS coordinates were tracked in both the application ‘’AKVO Flow’’ and ‘’MapMarker’’.
Depth	At well site	NA	Heron Dipper
Dissolved Oxygen	At well site	< 10 minutes	Greisinger

pH	At well site	< 10 minutes	pH/Conductivity Meter Delta Ohm HD 2156.2
EC	At well site	NA	pH/Conductivity Meter Delta Ohm HD 2156.2
Turbidity	Field lab	NA	Turbidity Field
Alkalinity	Field lab	< 24 hours	Lovibond MD610 HACH
Total Coliform	Field lab	< 2 hours	3M Petrifilm Total Coliform
Nitrate	Field lab	NA	HACH NO_3 test strips
Ammonium	Field lab	NA	HACH NH_4 test strips

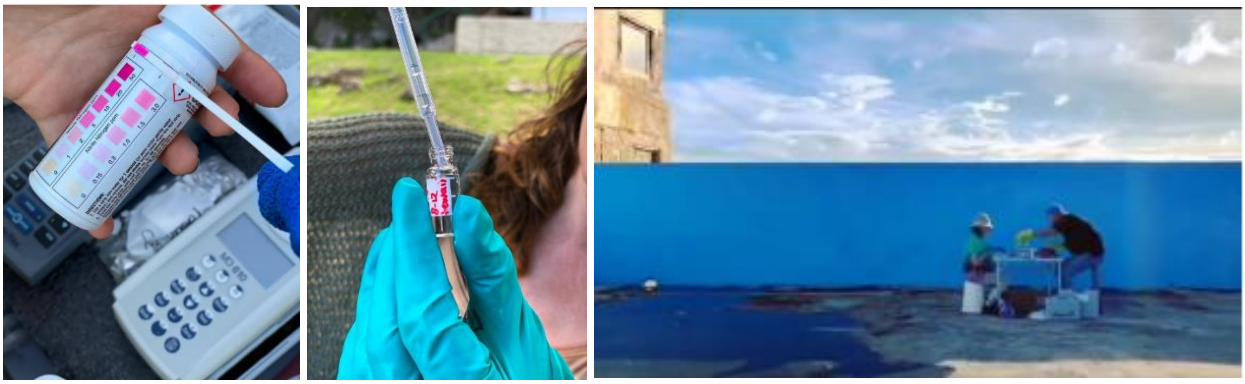

Figure 9. Fieldwork material & portable field lab. Left: Nitrate strips and Lovibond MD610. Middle: Filling the 2 mL vial for stable isotope analysis in the Netherlands. Right: making sue the parameters are measured in time.

3.1.6 Sample storage for further analysis

After initial measurements, the groundwater was subsequently filtered and stored into a collection of vials. Filtration was done with a 15 mL syringe, after it was rinsed several times with the groundwater sample. The first few drops were spilled before the different vials (Table 5) were filtered over the 0.45 µm.

Table 5. Water sample vials and storage methods

Sample bottle	Method	Used for
15 mL vial (14 mL filled)	A plastic 15 mL vial was filled until about 14 mL to keep about 1 mL headspace for later acidification 1:100 in the lab with concentrated HNO3 p.a. (thus 140 µL HNO3 per 14 mL sample) for further analysis with ICP-MS.	ICP-MS (Waterlab, TU Delft, the Netherlands)
15 mL vial (15 mL filled)	A 15 mL vial for IC A plastic 15 mL vial was filled completely for further analysis with IC.	IC (Waterlab, TU Delft, the Netherlands)
A 2 mL vial for isotope analysis	A 2 mL vial for isotope analysis A glass isotope vial was filled to the rim, making sure no air was present in the sample and evaporation was not possible, as it can alter the isotope composition, for further analysis with [fill in].	Stable isotope analysis (Waterlab, TU Delft, the Netherlands)
20 mL back up vial	Backup samples were made in case anything happened to the original sample	Backup
50 mL	A 50 mL vial was filled to use for field parameter analyses in the portable field lab or in-house lab in Curaçao. For example for turbidity, alkalinity and other field parameters that were not measured immediately on-site.	Field parameters (alkalinity, turbidity)

All vials were stored in a cool box in the field and immediately transferred to the fridge at site of accommodation, before they were either analyzed, or flown back to the Netherlands for further analysis in TU Delft's Waterlab. During the fieldwork period there were several moments when all electricity on the island was cut off, for periods of up to 10 hours. During these times, the samples were kept cool on ice.

3.1.7 Runoff and rain collection

For each run-off sample the EC, pH, turbidity and water color were determined. Samples were taken away from the sides of the runoff stream and when possible not in stagnant zones of the water body. For each run-off 1x 50 mL vial was used for collection. For a few run-off samples an isotope vial was filled as well.

During the fieldwork period, rainwater would flow downhill in the form of terrestrial streams at several locations across the island. At times, these streams were witnessed entering the ocean, creating plumes. The size of the runoff would range from several millimeters and centimeters to full streets or a waterfall-type flow, depending on the location and gradient.

Runoff was measured at four locations (A, B, C, D; Tewaii field codes: A1.1, B4.4, B4.5, C11.1, D17.1, D17.2). Runoff was sampled at the following spots. All the points where runoff samples were taken can be found in the following Google Maps Locations.

- Location A at Westpunt, Bandabou, Curaçao
- Location B at an unofficial landfill up North, Curaçao
- Location C at Santa Rosa, Willemstad, Curaçao (*Figure 10*)
- Location D at Willemstad, Curaçao

There were several challenges that obstructed the ability to properly measure the sampled runoff streams, and also prevented the capacity to sample more. The amount of runoff samples are limited, as there were several challenges during this fieldwork period that obstructed the ability to properly measure these runoff streams, namely:

- Rainfall was short-lived and very localized, making it difficult to “catch” these runoff streams in time, especially with traffic. Accommodation close to the runoff streams did not fit within the fieldwork budget. Often upon arrival, the runoff stream had either stopped or the weather prediction application was off in its forecast.
- Additional obstacles were the unpaved and muddy nature of some roads close to the ocean, which made it easy for the rental car to get stuck in areas with bigger runoff streams and puddling. Especially when trying to measure for a longer period to see potential water quality changes over time (e.g. sample every 5 minutes for the duration of rainfall). Several attempts were made, but had to be cut off quickly as the car was not able to drive through the deepening puddles. If measurements continued, car would have gotten (more) stuck. To illustrate: at one location, the car’s license plate got lost in one of the puddles, even after the rainfall had already stopped. Damage on the car went from scratches on the sides to part of the bottom of the car scraping off, resulting in a range of costs.
- For paved and busier regions within Willemstad, it could be challenging to remain parked to do measurements during rainfall.
- Not all equipment was suitable to use in heavy rainfall.
- Weather predictions were not consistently accurate, which made following them to get ahead of rainfall and runoff a time costly practice, with little result.
- Also relevant for groundwater measurements, it was not possible to find out where rain had fallen in the past, as there were no (unpaid) weather applications that allowed to check where rainfall had fallen over the last hours / days, which would have allowed to check for potential plumes, *if* presented past data would have also been accurate.
- Unfortunately during the fieldwork, a burglary had also occurred and a significant amount of money was stolen, including my laptop. Because this research was performed pre-SEALINK, the research was paid for with individually gathered funding, covering flights, accommodation, car rental, gasoline, electricity and fieldwork material (nitrate strips, ammonium strips, alkalinity reagents). This cut the fieldwork period short and caused there to only be a limited amount of runoff samples.

Figure 10. Sampling runoff at location C, Willemstad.

Despite the lack of thorough measurements, the preliminary data on runoff might give an initial glimpse into the runoff situation in Curaçao, and allow follow-up researchers to start their measurements with more insight in what is needed to measure runoff in Curaçao. For comparison, average and standard deviation of rainfall measurements were taken. Rainwater was collected with a bottle-made rain gauge. Care was taken that rainwater was not captured from roofs as some had different metal parts and large amounts of sediments.

3.2 Lab Analyses and Data Validation

3.2.1 Lab analysis

Upon return to the Netherlands, the samples were prepared according to the “Standard Methods for the Examination of Water and Wastewater” (1985). Samples were measured in the IC, ICP-MS and DA (Figure 11).

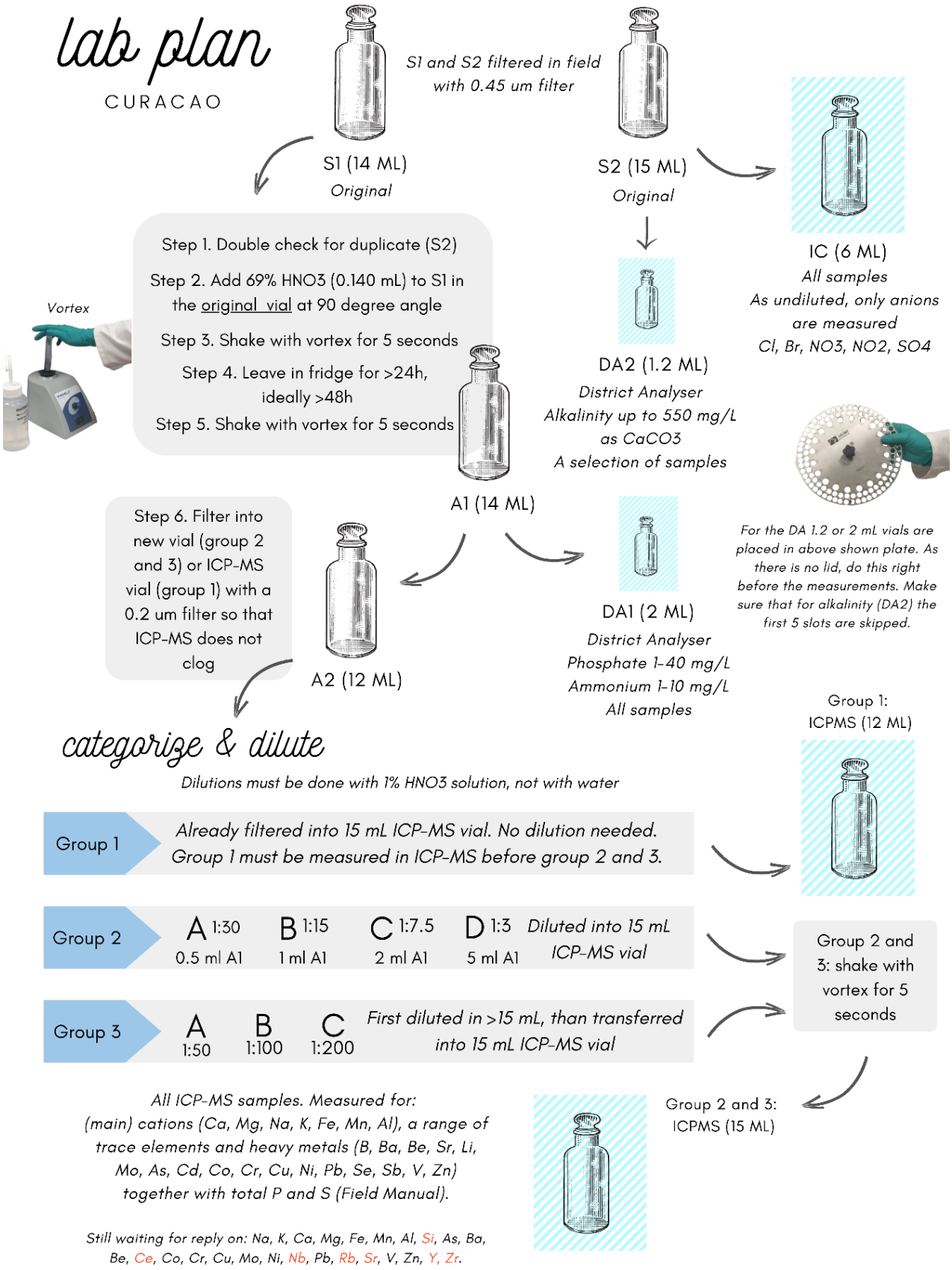

Figure 11. Overview of lab methodology.

3.2.2 Missing components of dataset, eastern focus

During the lab analysis of the groundwater, rain and runoff samples, there were consistent issues with the ICP-MS in the Water Lab of TU Delft. After the first sample run, the leftover samples were accidentally thrown out in a Waterlab clean. This meant that the samples that were over- or underrange could not be remeasured. After this, a lengthy procedure took place to reprepare backup samples, for the wells that actually still had some backup water available (roughly 60%). When these samples were ready to be measured to get closer to completing the dataset, the ICP-MS itself stopped working and had reoccurring issues. This meant that the second batch of samples could not be analyzed, leaving a large hiatus in the dataset. Nevertheless, it was decided to proceed with only a part of the '20 dataset, so that graduation could take place. In Appendix I an overview was made of the effects of this hiatus on the results. Based on these effects it was decided to focus on the *eastern* '20 dataset only, when it comes to the lab parameters, and only include the samples that could be validated with the electrical balance. For field parameters, such as EC and pH, the entire '20 dataset is still be used. When the ICP-MS is properly working again, the prepared samples can be run to complete the dataset, but this is now out of the scope of this thesis.

3.2.3 Validation of dataset

To validate the accuracy of the dataset the concentration of the major ions was used to calculate the electrical balance (E.B.) by taking the sum of the positive and negative charges of following cations: Mg^{2+}, Ca^{2+}, K^{+}, Na^{+}, and anions: Cl^{-}, $SO4^{2-}$, HCO_3^{-} and NO_3^{-}. To retrieve HCO_3^{-} values, the alkalinity field measurements (as mg/L $CaCO_3$) have been multiplied with 1.22, as the pH of all samples are below 8.4. For an additional check the anions and cations (in meq/) are compared with the EC / 100, if EC was below 2 mS/cm (Appelo & Postma, 2005).

The data used to construct all analyses within this thesis have less than 10% charge imbalance. All other samples have not been taken into consideration. The reason why the charge imbalance has been taken more amply than what would be the case regularly (<5%) is because the field measurements for e.g. alkalinity are not as accurate and over- and underestimations are expected.

3.2.4 Detection limits

The samples that were below the detection limit (**Table 6**), and could not be re-analyzed, the limit was multiplied with the dilution ratio. If substantial amounts (>50%) of a specific parameter was below the detection limit, it was excluded from analyses. For the multivariate statistics it was excluded at >30%.

Table 6. Detection limits of lab analyses

Parameter		Unit	Mn	1	µg/L
Ag	1	µg/L	**Mo**	1	µg/L
Al	1	µg/L	**Na**	0.1	mg/L
As	1	µg/L	**NH_4**	0.1	mg/L
B	1	µg/L	**Ni**	1	µg/L
Ba	1	µg/L	**Nitrate**	0.03	mg/L
Be	1	µg/L	**Nitrite**	0.009	mg/L
Bromide	0.001	mg/L	**Os**	1	µg/L
Ca	0.5	mg/L	**P**	0.001	mg/L
Cd	1	µg/L	**Pb**	1	µg/L
Chloride	0.2	mg/L	**Phosphate**	0.06	mg/L
Co	1	µg/L	**S**	0.001	mg/L
Cr	1	µg/L	**S**	0.001	mg/L
Cu	1	µg/L	**Sb**	1	µg/L
Fe	0.001	mg/L	**Se**	1	µg/L
Fe	0.001	mg/L	**Si**	0.5	mg/L

Fluoride	0.005	mg/L	**Sr**	1	µg/L
K	0.1	mg/L	**Sulphate**	0.2	mg/L
Li	1	µg/L	**Ti**	1	µg/L
Mg	0.1	mg/L	**V**	1	µg/L
Mg	0.1	mg/L	**Zn**	1	µg/L

3.3 Data analysis

3.3.1 Descriptive statistics, representativity and comparative assessments

To gain insight into the '20 datasets, data was first graphically displayed into descriptive tables (min, max, range, mean, average, standard deviation, standard error), boxplots and correlation matrices (Pearson's method). All lab parameters were subsequently compared to the eastern datasets of '21 to establish (dis)similarities between the two adjacent years, significant differences were established with non-parametric, pairwise Wilcoxon tests. To exclude the influence of geology, a sub-selection of wells located in the "Diabaas East" formation was added to this comparison.

For the comparative assessments between all years and assessment of trends (Table 7), ANOVA and Wilcoxon t-tests were done (1977-1992, 1977-2020, 1977-2021, 1992-2020, 1992-202, 2020-2021) for alkalinity, pH and EC for the total island, the eastern side and the western side. In addition, for pH and EC, the significant changes over the decades were also obtained per geology, per year, and a distinction was made between "Diabaas East" and "Diabaas West", to exclude the influence of geology affecting the overall trends found in the west and east. In addition to EC, pH and HCO_3^- comparative analyses were done for: B, Ca, Cl, Fe, F, K, Mg, Na, NH_4, NO_3, PO_4, Si, SO_4 and temperature. For EC and pH significant differences between the east and west for each year were also determined, on top of the already mentioned differences between pH and EC between the years for the east and west separately. For the data of 2021, additional pCO_2 comparisons were made between the east and the west, with calcite saturation indices provided by PhD candidate M. Wit.

Table 7. Comparative assessments between datasets

Comparison in years	Total Island	Eastern (+ Diabaas East)	Western (+ Diabaas West)
1977 – 1992	EC, pH, HCO_3^-	EC, pH, HCO_3	EC, pH, HCO_3
1977 – 2020	EC, pH (only field)	EC, pH (only field)	EC, pH (only field)
1977 – 2021	EC, pH, HCO_3^-	EC, pH, HCO_3^-	EC, pH, HCO_3^-
1992 – 2020	EC, pH (only field)	EC, pH (only field)	EC, pH (only field)
1992 – 2021	EC, pH, HCO_3^-	EC, pH, HCO_3^-	EC, pH, HCO_3^-
2020 – 2021	EC, pH (only field)	Lab and field parameters	EC, pH (only field)

There were 7-9 "identical wells" shared between '20 and '21, that were zoomed in on and compared for EC, geology, water level, well depth, purging methodology, well type and sampling date to investigate the representativity. The identical wells measured in 1977, 1992 and 2020 were also used to support in findings of the overall hydrochemical trend, as well type is excluded as influence for these measurements (Table 8).

Table 8. Identical wells

Comparison in years	# of identical wells	Compared between parameters
1977 – 1992	62	EC
1977 – 2020	12	EC, pH
1977 – 2021	3	EC
1992 – 2020	20	EC, pH, SO_4, SAR, NO_3
1977 – 1992 – 2020	12	EC, pH, SO_4, SAR, NO_3
1992 – 2021	5	EC, pH
2020 – 2021	7	EC, pH

As is witnessed in Table 9, not all datasets have a substantial amount of identical wells between them. To determine how to handle this best, the heterogeneity of water quality was determined on a zoomed in scale (21-74 meters) with wells that are located close together, have the same well type and the same geology. This was done to evaluate if the wells between different datasets could be coupled based on distance, and then in turn used to determine differences in quality and geochemical trend over the decades, as was done in 2021. Verstappen (2022) coupled the 2021 data to the previous research results by generating “well code reference” based on distance with ArcGIS Pro. However, when assessing the heterogeneity for this thesis and previous research, it was found to be very high, even at close distances. It was therefore determined not to couple datasets based on well distance. Instead, comparisons were made through larger collections of samples, or with wells that were actually identical, not just situated close together. This meant that for each dataset there were different amount of wells available to compare for EC and pH for the total island, the total east, the total west, Diabaas East and Diabaas West (Table 9 and Table 10).

Table 9. Amount of wells sampled per year (east, west, total, Diabaas East, Diabaas West)

	1977	**1992**	**2020**	**2021**
East	151	56	49	46
West	82	40	42	26
Total	233 (750)	96	91	72
Diabaas East	126	52	41	43
Diabaas West	43	21	20	13

Table 10. Amount of wells for each of the comparisons between datasets

	1977 – 1992	1977 – 2020	1977 – 2021	1992 – 2020	1992 – 2021	2020 -2021
Total	233 (750) - 96	233 - 72	233 - 72	96 - 91	96 - 72	91 - 72
East	151 - 56	151 - 49	151 - 46	56 - 49	56 - 46	49 - 46
West	82 - 40	82 - 42	82 - 26	40 - 42	40 - 26	42 - 26
Identical wells	62	12	3	20	5	7

3.3.2 Water quality standards

To results of the ’20 fieldwork campaign are compared to the WHO drinking water standard (WHO, 2022) and classified according to salinity. In addition, the Sodium Adsorption Ratio (SAR) (Eq. 3-1; Table 11; Table 12) is used to determine the suitability for irrigation and plotted against EC to determine relative sodification and salinization (Ahmad Cahyadi et al., n.d.; FAO, 1985).

$$SAR = \frac{Na^{+}}{\sqrt{\frac{Ca^{2+} + Mg^{2+}}{2}}} \quad (Eq.\ 3-1)$$

Table 11. SAR classification

SAR	**Water class**
<10	Excellent
10-18	Good
18-26	Doubtful
>26	Unsuitable

Table 12. Salinity classification

Salinity	Threshold [µS/cm]
Fresh	< 1500

Slightly brackish	1500 - 5000
Brackish	5000 – 15 000
Saline	15 000 – 50 000

3.3.3 Graphical technique

For this thesis, all datasets (1977-2021) were plotted in the piper diagram for the eastern side of the island. Piper diagrams (
Figure 12) can be used to display the relative percentages of the major cations and anions: Mg, Ca, K + Na, Cl, SO_4 and $HCO_3 + CO_3$. This classification can aid in the determination of the type of groundwater, their evolution and the potential mixing between these water types (Table 13). The different Piper groups that groundwater can be divided in the following water types: (1) calcium chloride type, (2) mixed type, (3) sodium chloride type, (4) magnesium bicarbonate type, (5) sodium bicarbonate type. The anions and cations are represented in the smaller triangles at the bottom, the diamond shape in the middle stands for the combination of cations and anions. Mixed zone water means that the water is neither anion or cation dominant. Possible challenges with piper diagrams are when other ions, besides those visible in the Piper plot, are significant, and the fact that it renormalizes the concentrations. The salinity between samples can be very different, yet they can plot on the exact same spot if the relative concentrations are similar. This is overcome by distinguishing between higher and lower salinity samples, by either grouping them before plotting separately or by indicating the EC in width of each sample point: with increasing EC, an increased point size diameter. (Ging et al., 1996) In addition to piper diagrams, Cl / Br ratios (molar) were plotted against the Cl concentration (mg/L) (Figure 13) (Alcalá & Custodio, 2008).

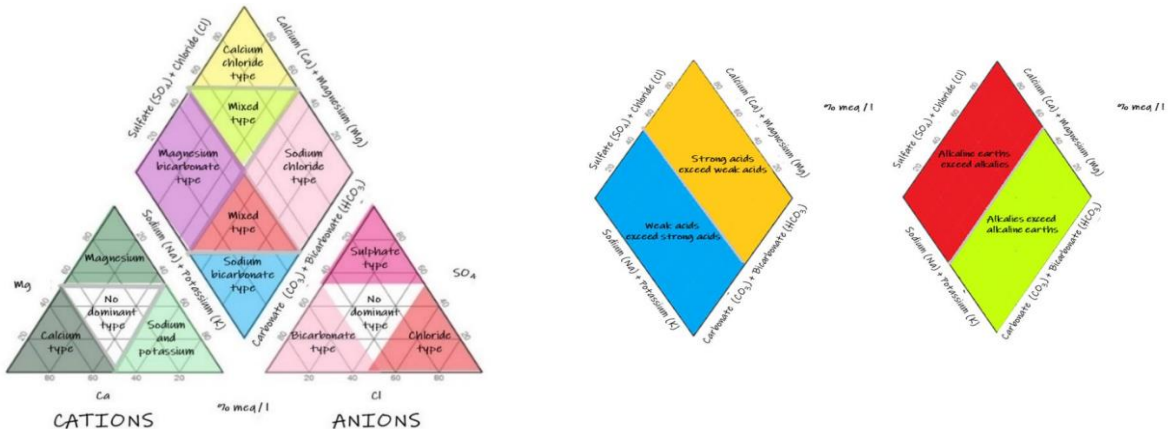

Figure 12. Piper diagram examples, adjusted from Piper (1994).

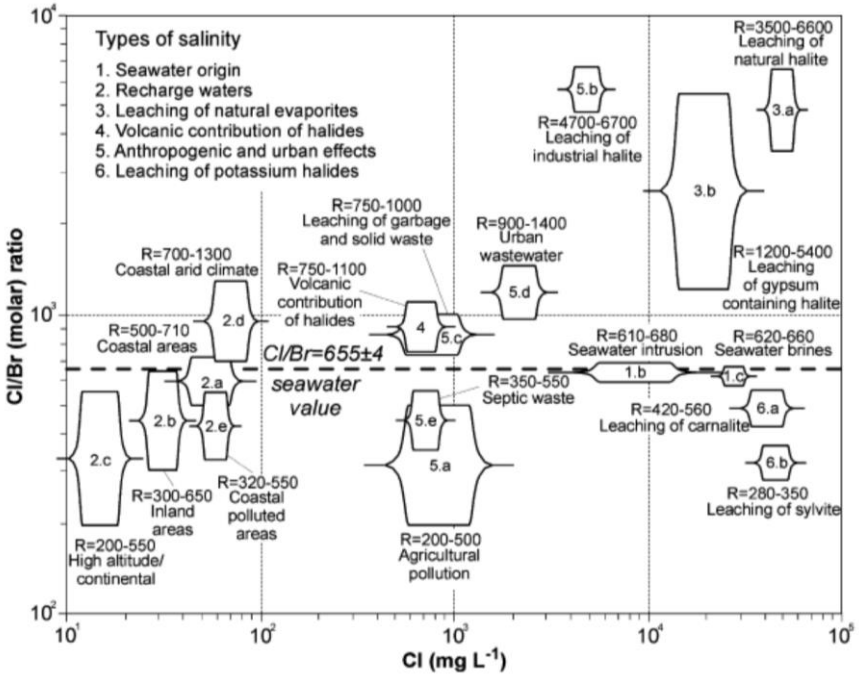

Figure 13. Cl/Br ratio plotted against Cl concentration (mg/L) (Alcalá & Custodio, 2008).

Table 13. Piper plot water types

Water type	
Ca-SO_4 waters	Typical of gypsum ground water and mine drainage
Ca-HCO_3 waters	Typical of shallow, fresh groundwater
Na-Cl waters	Typical of marine and deep ancient groundwaters
Na-HCO_3	Waters – typical of deeper groundwaters influenced by ion exchange

3.3.4 Multivariate statistical techniques

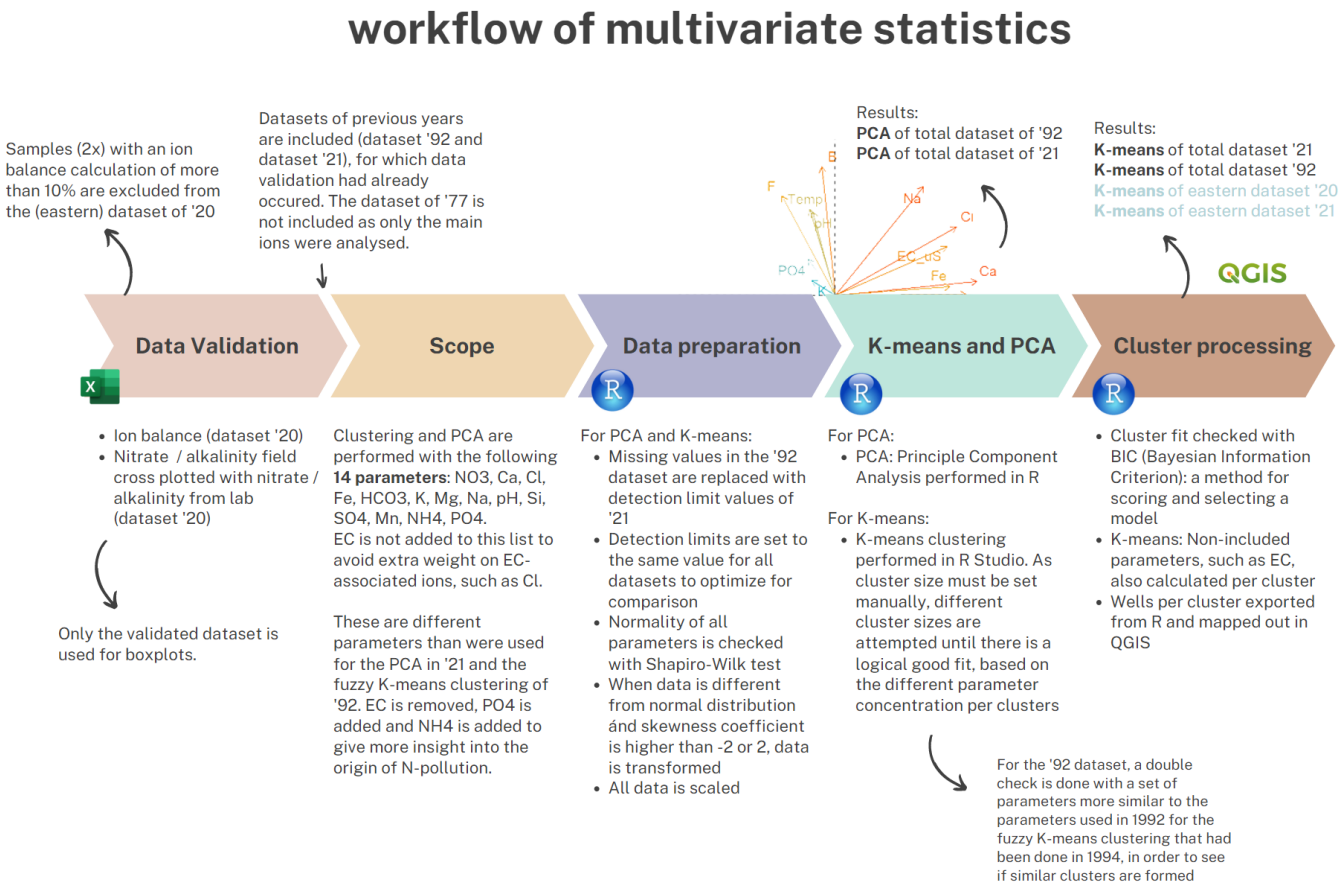

Figure 14. Overview methodology of data analysis, multivariate statistics

Before any multivariate statistics (MVS) were applied, the skewness of the samples was checked with a normality test (Shapiro-Wilk), to check how far parameters deviate from a normal distribution. Parameters that had a skewness coefficient that exceeded 2 or -2, were log transformed so that they can be used for further analyses. Subsequently, all parameters were scaled before doing Principle Component Analyses (PCA) and Cluster Analyses (CA). The dataset of '77 was not used for any MVS, as only the main ions were measured during this fieldwork campaign. Samples that were missing for the '21 dataset, were either removed or substituted in the same way as described by Verstappen (2022). For '92 there were no missing values, so no adjustments needed to made. Subsequently, several (rigid and fuzzy) k-means clustering analyses were tested. An overview of the methodology of data analyses is presented in Figure 14.

A rigid k-means clustering and PCA was done on the '21 and '92 dataset with the following 14 parameters: pH, NH_4, Na, K, Ca, Mg, PO_4, Cl, SO_4, HCO_3, Mn, NO_3, Si and Fe (Table 14). Several tests were also done with eastern datasets of '21, '92 and '20, but due to the lack of a complete dataset for '20, it was decided to stay with '92 and '21 datasets only, and for the total island, not just the east.

In previous data analyses, a (fuzzy) clustering analyses was also done, namely in the doctoral report on Curaçao's groundwaters based on the '92 dataset (de Bruijne & Louws, 1994). There are, however, two main differences between the analysis in this thesis, and that of '94.

1. The set of parameters

   In ’94 the following 19 parameters were (likely) used to cluster the ’92 dataset with: pH, EC, Na, K, Ca, Mg, Cl, SO_4, HCO_3, and minor elements Al, Mn, Zn, Ti, Cd, Co, Cr, Cu, Ni en V. In this thesis Fe, NO_3, PO_4, NH_4, and Si were also included, and of the minor elements only Mn was used. EC was excluded for this thesis. This resulted in the following 14 parameters for this thesis: pH, NH_4, Na, K, Ca, Mg, PO_4, Cl, SO_4, HCO_3, Mn, NO_3, Si and Fe.

2. The amount of wells

   For the analyses of de Bruijne & Louws (1994), 88 groundwater wells were included for the ’92, whereas in this thesis all 97 wells measured in ’92 were included, as it is not known which 9 wells were excluded from the fuzzy k-means of the ’94 report; there are currently no available maps of the k-means analyses that was presented in the ’94 report.

For this reason, a cluster analyses with 19 parameters that were used in the ’94 report was also done (**Table 14**), to see what type of clusters were formed and if they - to an extent - coincide with the results from the methods used within this thesis.

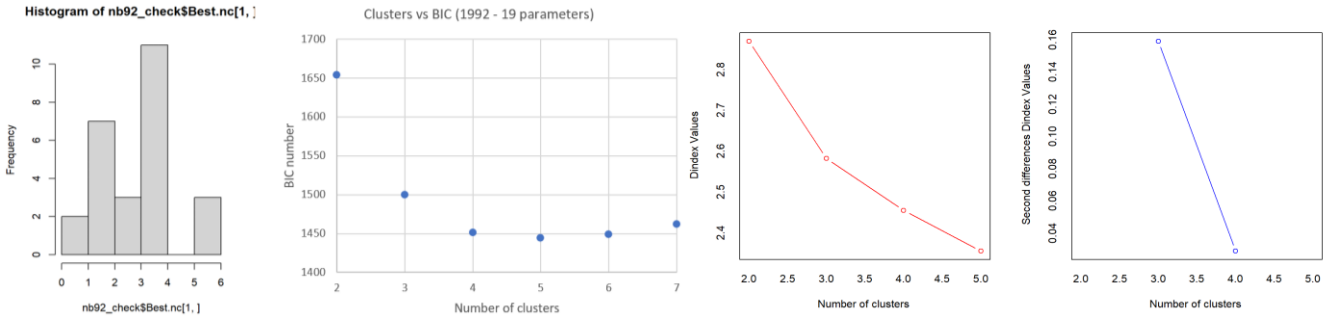

Figure 15. Finding the optimal amount of clusters. Done with BIC number, k-values, and the “elbow method”.

The fit of all clusters was checked with Bayesion Information Criterion (BIC), to determine the amount of clusters. In addition, attention was paid to the k-value and the “elbow method” was used where adding an additional cluster would not give much more explanation of the variance (Figure 15). For each configuration, the quality was checked to see if logical clusters had formed based on different water quality characteristics.

Table 14. Cluster parameters for ’92 and ’21

MVS	Years	Parameters
Rigid k-means clustering / PCA	’92 / ’21	pH, NH_4, Na, K, Ca, Mg, PO_4, Cl, SO_4, HCO_3, Mn, NO_3, Si and Fe (14 parameters)
Rigid k-means - Test	’92 / ‘21	pH, EC, Na, K, Ca, Mg, Cl, SO_4, HCO_3, Al, Mn, Zn, Ti, Cd, Co, Cr, Cu, Ni and V (19 parameters)

3.3.5 Rain, runoff and groundwater relations

Due to the lack of a substantial amount of samples, the rain and runoff samples of ’20 and ’21 were joined together. Only a very general and explorative assessment was done by comparing with averages and standard deviations between the groups.

3.4 Methodology of previous research

In ’77, ’92, ’20 and ’21 different methodologies were used for the collection and analyses of both the field and lab campaigns, shown in **Table 15**. The different approaches for data analyses (graphical, multivariate statistics, comparative assessments, etc.) are touched on in **Table 15** but shown in more schematic detail in **Table 16.**

Table 15. Overview of different field methodologies and circumstances for 1977, 1992, 2021 and 2022, that could potentially influence the results.

Field method for	1977	1992	2021	2020
Well measurement period	August 1976 - March 1978 (1.5 years)	14 September 1992 - 31 October 1992 (<2 months)	25 October 2021 – 23 December 2021 (<2 months)	11 November 2020 – 03 January 2021 (<2 months)
Precipitation*	Wet season dryer than average	Wet season dryer than average Year: 574 mm (-4.3%)	Wet season wetter than average Year: 623 mm (+3.5%) Weak La Nina	Wet season wetter than average Year: 646 mm (+7.7%) Dec Min: 12.4mm. Dec Max: 3.11mm Dec Sum: 96.4mm
Well sampling strategy	Uniform, also drilled 48 bores themselves (between 20 – 60 m depth).	Aiming for a uniform distribution over the island and checked with x^2 test.	Strategy to obtain wells in different geologies and with spatial variability throughout the island.	See paragraph: “Well sampling strategy”. Ultimately a strategy to obtain wells with distribution over the island.
Overlapping / identical wells	233 wells were sampled for geochemical analyses. 750 (periodical) conductivity measurements were taken.	96 wells were sampled. 62 of those overlap with wells from 1992.	72 groundwater locations were sampled. 5 of these wells overlap with wells in 1977.	91 wells were sampled for geochemical analyses. 20 of those wells overlap with 1992. 12 of 20 wells also overlap with 1977. 7-8 wells overlap with 2021.
Groundwater collection device	Unclear what device was used to retrieve groundwater	Glass weighted bottle connected to a rope (Figure 16)	Groundwater was collected with a bailer, when pump (stationary, hand pump or vacuum pump) couldn’t be used.	Weighted PVC. No (personal) pump during fieldwork campaign.
Groundwater collection depth / purging method	Over different depths and well documented.	Unclear at what depth the groundwater was sampled.	Well was pumped with stationary pump when available, otherwise bailer, hand pump or vacuum pump was used.	Pumped when possible (with pump of well owners). Otherwise: between 0.5 – 3 meters below surface, but influenced by surface water as no bailer was available.
Well depth measurement	Measured water level from well rim, depth of measurement and depth of well (as drilled most wells themselves)	Measured distance between well rim and water level	Measured distance between water level and bottom of well, and well rim and water level	Measured distance between well rim and water level
Field parameters	EC, it is unclear if pH was measured in the field or in the lab	EC, pH, temperature, field strips for nitrate-, sulfate, phosphate, chloride and ammonium. Field lab: HCO_3 with HCl titration.	EC, pH, E. Coli, DO, redox (pE), temperature, field strips (NO_3/NO_2). Field lab: alkalinity with titration.	EC, pH, DO, total coliform, temperature, field strips (NO_3/NO_2 and NH_4). Field lab: alkalinity with colorimetric method.
Lab parameters	K^+, Na^+, Ca^{2+}, Mg^{2+}, HCO^{3-}, SO_4^{2-}, Cl^-	Fe, Na, K, Ti, Cd, Zn, Cr, Cl, NO_3, Br, Mg, Al, P, Mn, Co, Cu, NO2, NH_4, Si, Ca, S, Pb, V, Ni, SO_4, HCO_3, PO_4	Ca, Mg, Na, K, Fe, Mn, Al, B, Ba, Be, Sr, Li, Mo, As, Cd, Co, Cr, Cu, Ni, Pb, Se, Sb, V, Zn, P & S, Cl, Br, F, NO_3, NO_2, SO_4 & PO_4, NH_4 & PO_4, Alkalinity	Ca, Mg, Na, K, Fe, Mn, Al, B, Ba, Be, Sr, Li, Mo, As, Cd, Co, Cr, Cu, Ni, Pb, Se, Sb, V, Zn, P & S, Cl, Br, F, NO_3, NO_2, SO_4 & PO_4, NH_4 & PO_4, Alkalinity. Due to problems with equipment in the Waterlab of TU Delft, overrange samples could not be remeasured. They are all prepared, however, and ready for future analyses.
Lab preparation samples			Acidified during fieldwork	Acidified in Waterlab
Below detection limit samples	Not mentioned in report, but only major cations and anions were measured in lab.	Pb removed (all samples BDL). Other samples beneath detection limit multiplied with -0.7.	For samples BLD, threshold multiplied with dilution ratio, no further alterations.	For samples BLD, threshold multiplied with dilution ratio. Components where results are distorted due to majority of samples being below detection limit, yet multiplied with a higher dilution ratio, are left out.
Data validation	Not mentioned	Ion balance <10% (97% below 10%)	Ion balance, threshold not mentioned	Ion balance for eastern dataset <10% (97% below 10%)
Clustering	No clustering	Fuzzy c-means clustering on 1992 dataset	Mentioned HCA and K-means for 2021 dataset, but not in detail	K-means clustering for all datasets: 2020 (east), 2021 (east), 2021 (total) 1992 (total) and 1977 (total)
PCA	No PCA	No PCA	PCA on 2021 dataset	PCA on 2021, 2020 (east) and 1992 dataset
Parameters used for PCA and clustering	No clustering and PCA performed	Clustering with the following parameters: Na, K, Ca, Mg, Cl, SO4, and HCO3, the minor, pH and EC.	Clustering and PCA with following parameters: pH, pE, T, EC, NO3, PO4,HCO3, Ecoli, F, Cl, SO4, NH4, Br, B, Ca, Fe, K, Mg, Na and Si	Clustering and PCA with the following parameters: B, Ca, Cl, EC, F, Fe, HCO3, K, Mg, Na, NH4, NO3, PO4, pH, Si, Temperature

* Based on average of: 600 mm / year and monthly mm rain in rain season maximum of 120 (Central Bureau of Statistics Curaçao, 2022).

Table 16. Table met data analyses over the years.

Analyse	Data:	'20	'21	'92	'77
Descriptive statistics groundwater of current year fieldwork campaign		(E)	(V)	(B)	(A)
				(B)	
				(V)	
		(E)			
Rainwater		(E)	M	X	(A)
Initial assessment rain and runoff		20/21 (E)		X	X
Boxplot (Graphical), including t-tests		(E)	(V)	X	X
				X	
				(V)	
Total, west and east		20-21-92-77 (E)			
		20/21 (E)			
PCA / clustering (Multivariate Statistics)		(E)	(V)	(B)	X
PCA only done in '20/'21. Clustering done in '92'/'20 (fuzzy c clustering). In 2020 clustering done for '92, '21 and '20, both east and total island. PCA done for '21 and '92.				(B)	
				X	
		20/21 – 92-77 (E)			
		20/21 (E)			
Piper diagram		(E)	(V)	(B)	(A)
				X	
				X	
Piper for eastern side:		20/21 – 92-77 (E)			
		20/21 (E)			
Scatter	*Ca, Na, Mg, SO_4, K, HCO_3 - Cl*	X	(V)	(S)	X
	Mg, Na, HCO_3, Cl, pH, EC, SAR. RSC			(B)	
				X	
1-on-1, identical	*EC, pH, SO_4, SAR, NO_3*		(E)		X
Correlation matrices (based on scatter)		X		(B)	
			X		
Irrigation Return Flow		X	X	X	X
		20/21 – 92-77 (E)			
SAR (vs EC)		(E)	(V)	(B)	(A)
Production / consumption of SO_4		X	(V)	X	X
Cl / Br ratio against Cl		A	A	X	X
Saturation Indices		X	(V)	(S)	X
Eh – pH diagram		X	X	(B)	X
Distance well coast / depth / EC		X	(V)	X	(A)
Social survey water use		(E)	X	X	X
Heterogeneity		(E)	X	X	X
Isotopes		M	M	(S)	X
Pumping tests, water availability, infiltration and drainage areas		X	X	X	(A)

RQ = research question, O = optional, M = measured, but nothing done with it, (X) = this analysis was never done, A = analyses done, but not used for discussion, (A) = Abtmaier., 1978 (dataset '77) "Report to the Island Government of Curaçao", (B) = de Bruijne & Louws., 1994 (dataset: '92), (H) = H2O artikel , (S) = van Samebeek et al., 2000 (dataset: '92), (V) = Verstappen et al., 2022 (dataset: '21), (E) = this thesis (dataset '20)

Figure 16. Sampling in 1992. In 1992 a heavy bottle was used to retrieve the groundwater.

4 Results

In this chapter the results of the 2020 field campaign to Curaçao are showcased in four sections: 4.1 Groundwater, 4.2 Multivariate Statistics, 4.3 Water Use and Well Practices, 4.4 Rain and Runoff and 4.5 Key Figures. The first section accounts for all groundwater-related results and is subdivided in: the descriptive statistics and spatial variation of the entire dataset (4.1.1), thresholds and water quality limits (4.1.2), the chemical trend throughout the years when looking at the datasets from ’77, ’92, ’20 and ’21 (4.1.3) and hydrochemical processes (4.1.4). In 4.1.5 the pCO_2 calculations over 2021 are presented. In the last four subsections of 4.1 Groundwater, different sub-selections of groundwater wells are zoomed in on, namely 4.1.6 Heterogeneity (two groups of wells that are located very close together), 4.1.7 Identical Wells for 2020 and 2021, and 4.1.7 and 4.1.8 Identical Wells for 2021, 2020, 1992, and 1977. In section 4.2 Multivariate Statistics the principle component and cluster analyses of the 1992 and 2021 dataset are shown. In section 4.3, Water use, well practices and the fate of the wells measured in 1992 is described, together with the current well practices. The Rain and Runoff section (4.4) presents the water quality results of the exploratory measurements taken of precipitation and surface runoff. In 4.5 the key figures are repeated, for ease of reading the Discussion chapter.

4.1 Groundwater

4.1.1 Descriptive statistics and spatial variation ‘20

Exclusion of samples from the ’20 dataset

As mentioned in Chapter 3 Methodology, a total of 91 groundwater, 12 runoff and 4 rainwater samples were collected during the 2020 field campaign. Because there were several issues with equipment (ICP-MS) in the Waterlab, samples could only be measured once, which meant that the samples that contained over-range and under-range parameters could not be re-diluted and re-analysed to obtain the values that were needed to validate the ion balances for this dataset. Looking at the missing analyses of the major ions from the ICP-MS (Na, K, Mg, Ca), of the 39 samples taken in western Curaçao, 19 could be fully analysed, and 20 are still waiting to be re-analysed in the ICP-MS. Of the 52 groundwater samples taken in eastern Curaçao, 40 could be fully analysed and did not need to be re-analysed, of which 1 was excluded based on the ion balance exceeding 10%; in other words 12 samples of the eastern dataset are still waiting to go through the ICP-MS. A decision was made to only continue with the fully analysed samples from the eastern dataset of ‘20, the argumentation for this is presented in Appendix I. The descriptive statistics are therefore divided into the field parameters (EC, pH, strips, turbidity) of all wells for the total island (Table 17) and the lab parameters of only the eastern island (Table 18; Table 19). An overview of the fully analysed and semi-analysed samples of the western and eastern 2020 dataset and the selection for this thesis are summarized in Appendix I. In addition, Ag, As, Ba, Be, Cd, Li, Mn, Mo, Pb, Sb, Se and Ti were excluded as parameter from the 39 eastern wells of ‘20, because a large section of the results for these parameters on are below the detection limit. As they could not be re-analysed due to above-mentioned issues with ICP-MS, they have also been excluded from the results for the 2020 (eastern) dataset.

Spatial variability ’20 and ‘21

When comparing the spatial variability between 2021 (n=71) and 2020 (n=91), it is observed that in 2020 more samples were taken on the eastern side of island around the Fuik area (Figure 17; Figure 18). In 2021, nine samples were taken from the Knip formation, while zero wells could be accessed in 2020 in this geology. In 2020, six wells were sampled in the Limestone formation, whereas one well in this formation was sampled in 2021. The spatial variation of EC, pH and nitrate of ’20 is shown in Figure 18 (a, b, c). The groundwater EC range is considerable and goes from 0.113 to 18.8 mS/cm. The lowest ECs are measured on the eastern side of Curaçao in the Curaçao Lava formation; the highest ECs are measured on the western side of Curaçao in the Mid Curaçao Formation. When considering the eastern side only, the highest EC measurements are found closer to St. Joris Baai en the Fuik region, towards the eastern end of the island. For the 91 wells measured in 2020, over half (53%) had a salinity between 1.5 and 5 mS/cm, 29% under 1.5

mS/cm, 17% was brackish, and one well had saline groundwater over 15 mS/cm (Table 20). The most saline wells are located in the west, as well as most of the brackish wells (Figure 18 (b)). The eastern side has two brackish wells and zero saline wells (Table 21).

The groundwater pH ranges from 6.2 to 8.15. The lowest pH is measured in the western side of Curaçao in the Curaçao Lava Formation, the highest pH is measured in the Limestones formation (Figure 18 a). The nitrate concentrations measured in the lab for '20 can only be shown for the eastern side of the island (Figure 18 c), due to above mentioned challenges with the analyses, with the highest measurement at 339 mg-NO_3/L (Table 18). For the entire island, based on field strips, the NO_3 concentrations ranges from 0 to 221 mg-NO_3/L (Table 17). For the relationship between strip measurements and IC lab measurements, see Appendix I; Lab results versus field results. The range in ammonium concentrations is between 0.0 and 3.9 mg-NH_4/L when looking at strips, and between 0.0 and 6.4 mg-NH_4/L for the eastern side of the island when measured in the lab. The highest concentrations are found around Willemstad. The turbidity goes from completely clear (<0.01 NTU) to very turbid (436 NTU), with an average of 26 NTU.

Table 17. Descriptive statistics groundwater fieldwork, field parameters, all of Curaçao, 2020. *n*=90

Parameter	Min	Max	Range	Mean	Average	Std. Dev	Std. Error	Count
EC [mS/cm]	0.113	18.8	18.7	1.82	2.96	2.92	0.310	89
pH [-]	6.2	8.15	1.95	7.31	7.3	0.4	0.0	90
NO_3 [mg/L]*	0	221	221	44	67	72	8	85
NO_2 [mg/L]*	0.0	9.9	9.9	0.0	0.5	1.7	0.2	85
NH_4 [mg/L]	0.0	3.9	3.9	0.0	0.4	0.6	0.1	70
Turbidity [NTU]	0	436	436	2	26	71	8	77

*Nitrate and ammonium concentrations are from HACH strips, as this table only contains field parameters. NO_3 from the lab is presented in the table containing information on easter Curaçao.

Table 18. Descriptive statistics groundwater fieldwork, field parameters, eastern Curaçao, 2020. *n*=51

Parameter	Min	Max	Range	Mean	Average	Std. Dev	Std. Error	Count
EC [mS/cm]	0.113	6.92	6.81	16.4	1.90	0.191	1.36	51
pH [-]	6.2	8.15	1.95	7.44	7	0.1	0.4	52
NO_3 [mg/L] - strips	0	221	221	44	76	10	74	50
NO_3 [mg/L] - IC	0	339	339	48	80	12	87	51
NO_2 [mg/L] - strips	0	7	7	0	0	0	1	50
NO_2 [mg/L] - IC	0.005	1.4	1.4	0.01	0	0	0	51
NH_4 [mg/L]	0	6	6	0	0	0	1	39
Turbidity [NTU]	0.01	316	316	1.53	23	9	61	49

Table 19. Descriptive statistics groundwater fieldwork, lab parameters, eastern Curaçao, 2020. *n*=39-52

Parameter*	Min	Max	Range	Mean	Average	Std. Dev	Std. Error	Count
Alkalinity [mg/L as $CaCO_3$]	104	415	311	319	308	10	73	52
Al [µg/L]	7.5	199	191	39	47	6	38	39
B [µg/L]	90.4	863.6	773.1	305.4	336	22	138	39
Br [µg/L]	0.1	2.5	2.5	0.8	1	0	1	39
Ca [mg/L]	31.0	224.6	193.6	90.4	98	7	45	39
Cl [mg/L]	29.9	811.0	781.1	235.0	250	28	172	39
Fe [mg/L]	0.1	0.8	0.7	0.4	0	0	0	39
F [mg/L]	0.0	0.2	0.2	0.1	0	0	0	39
K [mg/L]	1.5	37.5	36.0	3.0	6	1	8	39

Mg [mg/L]	13.0	157.6	144.6	59.7	62	6	36	39
Na [mg/L]	33.6	370.6	337.0	166.7	158	9	56	39
NH_4 [mg/L]	0.0	6.4	6.4	0.0	0	0	1	39
Ni [µg/L]	1.7	514.0	512.3	3.7	17	13	81	39
P [mg/L]	0.0	3.7	3.7	0.1	0	0	1	39
PO_4 [mg/L]	0.0	12.2	12.2	0.1	1	0	2	32
PO_4 [mg/L]	0.0	10.4	10.4	0.0	0	0	2	39
S [mg/L]	0.0	94.1	94.0	25.3	29	3	21	39
Si [mg/L]	7.8	50.0	42.2	27.8	27	1	9	39
SO_4 [mg/L]	12.7	276.0	263.3	68.0	80	9	55	39
Temperature [C]	28.1	34.0	5.9	29.3	29	0	2	39
V [µg/L]	30.0	349.1	319.1	163.6	169	16	99	39
Zn [µg/L]	25.3	2361.3	2336.0	284.7	440	88	546	39
SAR [-]	0.8	4.4	3.6	2.1	2	0	1	39

* More parameters have been analysed, yet not included because between 80% and 100% of the results were below the detection limit. When multiplying these detection limits with the dilution ratios of each sample, the results would give a distorted picture of found concentrations, as they at times far exceed concentrations of concentrations above the detection limit. For this reason, the following parameters are not included in this table: Ag [µg/L], As [µg/L], Ba [µg/L], Be [µg/L], Cd [µg/L], Li [µg/L], Mn [µg/L], Mo [µg/L], Pb [µg/L], Sb [µg/L], Se [µg/L] and Ti [µg/L]. The parameters could not be remeasured due to continuous problems with the ICP-MS in the Waterlab of TU Delft (see Methods: missing components of dataset).

Table 20. Groundwater salinity Curaçao, 2020. *n*=90

Salinity	Threshold [mS/cm]	Wells	%
Fresh	< 1.5	27	29%
Slightly brackish	1.5 – 5	47	53%
Brackish	5 – 15	15	17%
Saline	15 – 50	1	1%

Salinity classification based on Cahyadi, 2018.

Table 21. Groundwater salinity eastern Curaçao, 2020. *n*=50

Salinity	Threshold [mS/cm]	Amount	%
Fresh	< 1.5	20	39%
Slightly brackish	1.5 – 5	28	56%
Brackish	5 – 15	2	5%
Saline	15 – 50	0	0%

Salinity classification based on Cahyadi, 2018.

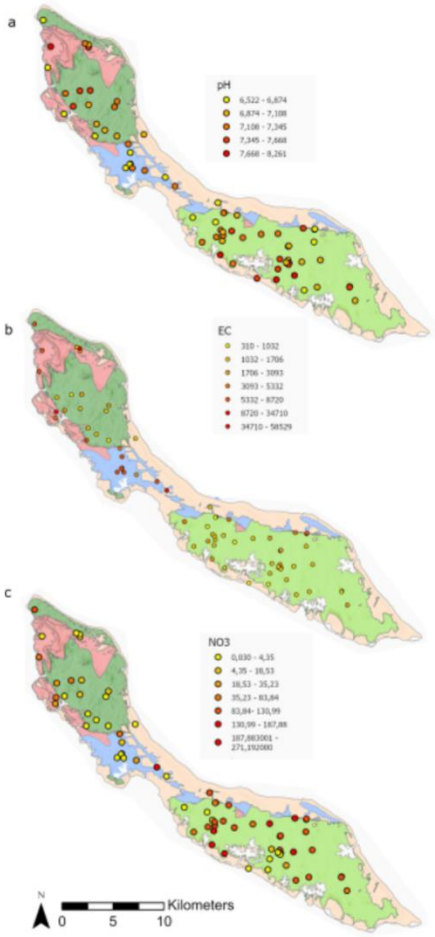

Figure 17. Spatial variation of parameters '21. a) pH, b) EC and c) nitrate for the fieldwork campaign in 2021(Verstappen, 2022).

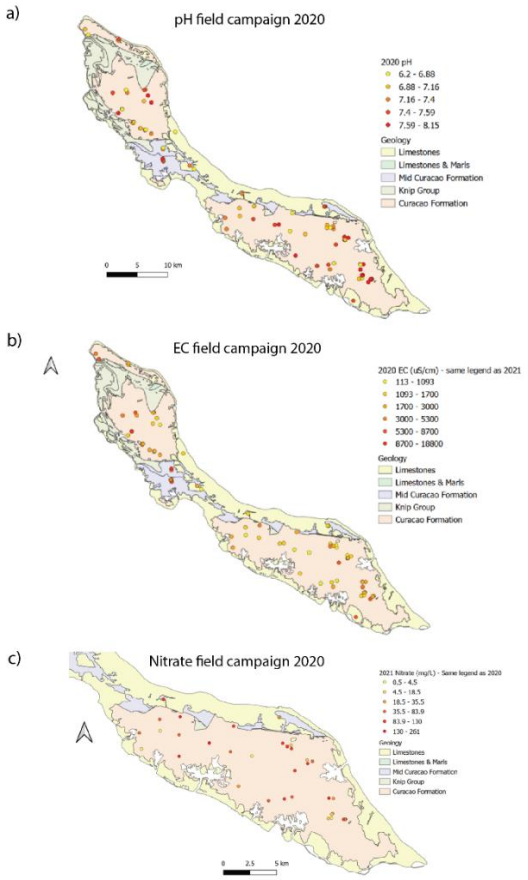

Figure 18. Spatial variation of parameters '20 . a) pH, b) EC and c) nitrate for the fieldwork campaign of this thesis in 2020.

4.1.2 Thresholds and water quality standards

When comparing the groundwater quality of all wells measured in 2020 to drinking water standards (WHO, 2022), as based on NO_2, EC, turbidity, pH, NO_3 and NH_4 (Table 22) 44% of wells are unsuitable as drinking water. Notably 81% of wells has a nitrate concentration higher than 10 mg/L, and 39% over 50 mg/L. E. Coli measurements were not performed in the 2020 field campaign, so the amount of unsuitable wells could be higher based on pathogenic contamination.

Table 22. Groundwater compared to drinking water standard (WHO, 2022) for all of Curaçao (2020), *n*=90.

Parameter	Threshold	# wells over threshold	% of total wells	Threshold for:
EC [mS/cm]	1.56	58	65%	Scaling, taste
pH [-]	6.5 - 8.5	0	0%	Operational, not health

NO_3 [mg/L]**	50	33	39%	Health concern
NO_2 [mg/L]**	3	5	6%	Health concern
NH_4 [mg/L]	1.5	0	0%	Mainly taste
E. Coli	0 / 100 mL	Not measured		Health concern
Turbidity [NTU]	5	24	31%	Social acceptance

*Nitrate thresholds are 50 mg NO_3/L, but concentrations over 1-3 mg/L indicate anthropogenic influence. Concentration over 50 mg/L will often indicate significant amounts of pollution and health risks
**Nitrate in this table over are HACH strips measurements as table for entire island.

When comparing the groundwater quality of the eastern wells to drinking water standards (WHO, 2022), as based on parameters measured in the lab (Table 23) 49% of wells are unsuitable for drinking water due to high nitrate concentrations.

Table 23. Groundwater compared to drinking water standard (WHO, 2022) for eastern Curaçao (2020), *n*=39.

Parameter	Threshold	#wells over threshold	% of total wells	Threshold for:
Al [µg/L]	200	0	0%	Consumer complaints
B [µg/L]	500-2400	0 - 3	0 - 8%	Health concern
Ca [mg/L]	75	23	59%	Scaling, acceptance, not health
Cl [mg/L]	250	17	44%	Taste, not health
Fe [mg/L]	0.3	28	72%	Laundry, staining, not health
F [mg/L]	1.5	0	0%	Health concern
K [mg/L]	No guideline value			No health concern
Mg [mg/L]	50	25	64%	Scaling, acceptance, not health
Na [mg/L]	200	7	18%	Taste, not health
NH4 [mg/L]	1.5-35	2	5%	Odor and taste, not health
Ni [µg/L]	0.1	1	3%	Sensitivity for certain people
NO_3 [mg/L]**	10-50	44-25	86% - 49%	Health concern
NO_2 [mg/L]**	3	1	2%	Health concern
SO4 [mg/L]	250	1	3%	Taste
Zn [µg/L]	5	39	1	Taste
Hardness [mg/L]	200 - 600		0	Scaling, taste

**measured with IC.

4.1.3 Chemical trend

In this subsection the results for the chemical trend over the decades (’77, ’92, ’20, ’21) and between ’20 and ’21 are presented. At first a comparison is made between the results of ’20 and ’21 for the lab and field parameters of the eastern side of Curaçao (Table 24). In Table 25 and Table 28, ANOVA and Wilcoxon t-tests for all datasets are done (1977-1992, 1977-2020, 1977-2021, 1992-2020, 1992-202, 2020-2021) for three important field parameters that were analyzed for the total island in all years, namely: alkalinity, pH and EC. This is done to gain insight into the changes in pH, alkalinity and EC that have occurred over the decades. Not just for the total island, as was done in previous research campaigns, but also for the eastern and western side separately. In addition, for pH and EC the significant changes over the decades are also obtained per geology, and a distinction is made between Diabaas East and West, as shown in Table 28, Figure 20 and Figure 21. As different trends between the east and west are clearly present, further checks were performed to see if there is a significant difference for pH and EC between the east and west, when looking at the samples that were acquired within each specific year (Table 27 and Table 29). To acquire information on the influence of geology between the differences for the west and east, these checks are also done between Diabaas East (DE) and Diabaas West (DW), of which the results are shown within the same tables and Table 26.

Comparison between ’20 and ‘21

For lab parameters of the ’20 and ’21 dataset only the eastern dataset can be compared, where it is witnessed that there is a significant difference for alkalinity, Fe, F, K, Mg, NH_4, PO_4 and temperature (Table 24) between ’20 and ’21. There is no significant difference between ’20 and ’21 for nitrate, B, Cl, Si and SO_4 (Appendix II).

Table 24. Significant difference of parameters between the ’20 and ’21 dataset, eastern Curaçao (t-test) and between east ’77, ’92 and ’20.

Test Years. East	Anova, east 1977, 1992, 2020	Anova, east 1977, 1992, 2021	2020	2021	T-test, east 2020 – 2021
Alkalinity (as mg/L HCO_3)	ns	***	376±90	509±185	****
B	-	-			ns
Ca (mg/L)	ns	ns	104±59	147±114	*
Cl	ns	ns			ns
Fe (mg/L)	-	-	0.42±0.19	0.013±0.25	****
F	-	-			**
K (mg/L)	ns	ns	7±10	4±9	****
Mg (mg/L)	ns	*	73±45	104±76	*
Na	ns	ns			ns
NH_4	-	-			****
NO_3	-	-			ns
PO_4	-	-			****
Si	-	-			ns
SO_4	ns	ns			ns
Temperature	**	**			*

*Symbol meaning: ns p > 0.05, * p ≤ 0.05, ** p ≤ 0.01, *** p ≤ 0.001, **** p ≤ 0.0001. Alkalinity as mg/L $CaCO_3$, EC in µS/cm.*

EC comparison for all datasets

When looking at field parameter EC only (Table 25; Table 26) over the total island (Table 25; row #1), there is no significant different in EC over the decades, except for the comparison between 1977-1992, where a decrease in salinity is observed for the total dataset (*). When only considering the wells located on the eastern side of the island (Table 25: row #2), as opposed to the total island, a drop in salinity can be witnessed between 1977 and 1922 (*), and between 1977 and 2020/2021 (***), which is also visible for the Diabaas East formation when looking at the geologies separately (Table 25: row #4). For the west and all the other geologies, no significant differences in EC are found. In '77, '20 and '21 the wells sampled in western Curaçao were on average more saline than in the east (Table 27). Salinization around St. Joris Baai is presented in Appendix III.

Table 25. Significant difference of EC over the decades, between '77, '92, '20 and '21 dataset: for total island, eastern island, western island and per geology.

Parameter (anova)	1977-1992	1977-2020	1977-2021	1992-2020	1992-2021	2020-2021
[1]EC – total (*)	*↓	ns	ns	ns	ns	ns
[2]EC – east (***)	*↓	*** ↓	***↓	ns	ns	ns
[3]EC – west (ns)	ns	ns	ns	ns	ns	ns
[4]EC – Diabaas East (**)	*↓	**↓	**↓	ns	ns	ns
[5]EC – Diabaas West (ns)	ns	ns	ns	ns	ns	ns
[6]EC – Knip (ns)	ns	-	ns	-	ns	-
[7]EC – Limestones (ns)	ns	ns	-	ns	-	-
[8]EC – Mid Curaçao (ns)	ns	ns	ns	ns	ns	ns

*Symbol meaning: ns p > 0.05, * p ≤ 0.05, ** p ≤ 0.01, *** p ≤ 0.001, **** p ≤ 0.0001. Some geologies for certain years did not have any measurements, for those comparisons a "-" sign is present.*

Table 26. EC (mS/cm) per year (east, west, total, Diabaas East, Diabaas West)

	1977	**1992**	**2020**	**2021**
East	2.82 ± 2.74	2.51 ± 2.22	1.89 ± 1.36	2.10 ± 1.65
West	4.44 ± 6.36	4.48 ± 6.42	4.38 ± 3.74	7.34 ± 11.73
Total	3.52 ± 4.45	3.52 ± 4.55	2.95 ± 2.92	3.52 ± 5.26
Diabaas East	2.58 ± 2.37	2.07 ± 1.55	1.83 ± 1.23	1.90 ± 1.21
Diabaas West	2.65 ± 1.42	2.84 ± 4.55	3.14 ± 2.37	2.59 ± 2.24
MCF (only in west)	9.18 ± 11.16	5.87 ± 6.88	6.28 ± 4.57	7.13 ± 4.83

Table 27. EC of all datasets, comparison between east / west and DO / DW

Parameter	**West '77 – East '77**	**West '92 – East '92**	**West '20 vs East '20**	**West '21 – East '21**
EC average (stat. diff)	*** (west higher)	ns	**** (west higher)	*** (west higher)
Parameter	**DW '77 vs DO '77**	**DW '92 – DO '92**	**DW '20 – DO '20**	**DW '21 – DO '21**
EC average (stat. diff)	ns	ns	** (DW higher)	ns

*Symbol meaning: ns p > 0.05, * p ≤ 0.05, ** p ≤ 0.01, *** p ≤ 0.001, **** p ≤ 0.0001. Alkalinity as mg/L $CaCO_3$, EC in µS/cm.*

pH and alkalinity comparison for all datasets

The pH shows an overall downward trend from ’77 to ’92 to ‘20/’21 (Table 28: row #1; Figure 19 a). When splitting the wells into a western and eastern side, it is observed that the downward trend is more distinct for the western wells, where there is a decrease in pH between 1977-1992, 1977-2020, 1977-2021, 1992-2020 and 1992-2021 (Table 28: row #3; Figure 19 c). In the east of Curaçao there is also a decrease in pH between 1977-2021 (Table 28: row #2; Figure 19 b). In addition, the pH measured for the ’20 dataset was on average higher than for ’21.

When comparing the different geologies per year for pH (Figure 20; Table 28: row #4-8), it is shown that the decrease in pH is most apparent for western formations Diabaas West (CLF) (Figure 20 b) and Mid Curaçao formation (Figure 20 e), and to a lesser extent the eastern formation Diabaas East (CLF) (Figure 20 a). To illustrate, for Diabaas West, the drop is 0.7 pH unit, between a pH of 7.83 (1977) and 7.13 (2021). Although there is a long term decrease in pH in Diabaas East as well, 0.25 pH unit between 7.49 (1977) and 7.24 (2021), the relative and absolute decrease is larger in the west and DW.

Table 28. Significant difference of pH and alkalinity (per year and geology), all of Curaçao.

Parameter (anova)	1977-1992	1977-2020	1977-2021	1992-2020	1992-2021	2020-2021
[1]pH – total (≥***)	****↓	****↓	****↓	ns	***↓	*↓
[2]pH – east (*)	**↓	ns	****↓	ns	ns	**↓
[3]pH – west (≥***)	***↓	****↓	****↓	*↓	**↓	ns
[4]pH – Diabaas East (≥***)	ns	ns	****↓	ns	ns	* ↓
[5]pH – Diabaas West (≥***)	***↓	****↓	****↓	*↓	**↓	ns / *↓
[6]pH – Knip (ns)	ns	-	ns	-	ns	-
[7]pH – Limestones (ns)	ns	ns	-	ns	-	-
[8]pH – Mid Curaçao (**)	*↓	**↓	**↓	ns	*↓	ns
[1]Alkalinity – total (**)	**↑	ns	****↑	**↑	ns	****↑
[2]Alkalinity– east (*)	**↑	ns	***↑	**↑	ns	****↑
[3]Alkalinity – west (ns)	ns	ns / -	ns	*↑ / -	ns	ns / -

*Symbol meaning: ns p > 0.05, * p ≤ 0.05, ** p ≤ 0.01, *** p ≤ 0.001, **** p ≤ 0.0001. HCO_3 measurements for ’20 were taken with different methodology and most likely gave an underestimation of the alkalintiy. For alkalinity, the ’20 results could in addition not be validated with the ion balance and therefore also have an “-“ sign present.*

When considering all geologies, for the total west, the drop is 0.57 pH unit between an average of 7.66 (1977) and 7.09 (2021) (Figure 20 b), whereas in the east the drop is 0.26 pH unit between 7.48 (1977) and 7.22 (2021) (Figure 20 a). For both the total east, and DE, the drop is not incremental, like it is for the total west and for DW, but first decreases, then increases, and then decreases again. The alkalinity concentration shows a significant upward trend for the eastern side, rises when the pH drops, and drops when the pH rises; in the west there is no significant difference between the years (Appendix II).

The Limestones and Knip formation show no significant difference in pH (Table 28: row #6-7), but also have a relatively smaller sample size than the CLF and MCF (Figure 20). When looking at the difference within the Curaçao Lava formation (Diabaas West versus Diabaas East) within the same years (Table 29), it shows that in ’77 and ’92 the pH is higher in DO than DW, while in ’21 it is reversed and DW has a lower pH than DO. This is also witnessed in Figure 21, where the pH per year is shown with each geology separately in boxplots.

Table 29. pH of all datasets, comparison between east / west and DO / DW field campaign, DO/DW

Parameter pH (average, stat. diff)	**'77 west-east** 7.66 - 7.48 (***)	**'92 west-east** 7.33 – 7.19 (ns)	**'20 west-east** 7.12 – 7.40 (***)	**'21 west-east** 7.09 - 7.22 (ns)
Parameter pH (average, stat. diff)	**'77 DW-DE** 7.83 – 7.49 (****)	**'92 DW-DE** 7.42 – 7.22 (*)	**'20 DW-DE** 7.22 – 7.39 (ns)	**'21 DW-DE** 7.13 – 7.24 (*)

*Symbol meaning: ns p > 0.05, * p ≤ 0.05, ** p ≤ 0.01, *** p ≤ 0.001, **** p ≤ 0.0001. Alkalinity as mg/L $CaCO_3$, EC in µS/cm.*

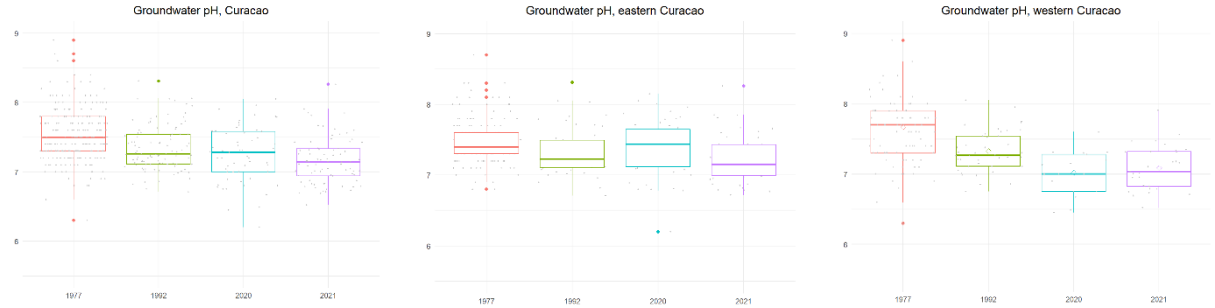

Figure 19. Results Groundwater pH . a) pH groundwater comparison for entire island between 1977, 1992, 2020 and 2021. ***b)*** *Boxplots pH groundwater comparison for eastern island between 1977, 1992, 2020 and 2021* *c) Boxplots pH groundwater comparison for western island between 1977, 1992, 2020 and 2021.*

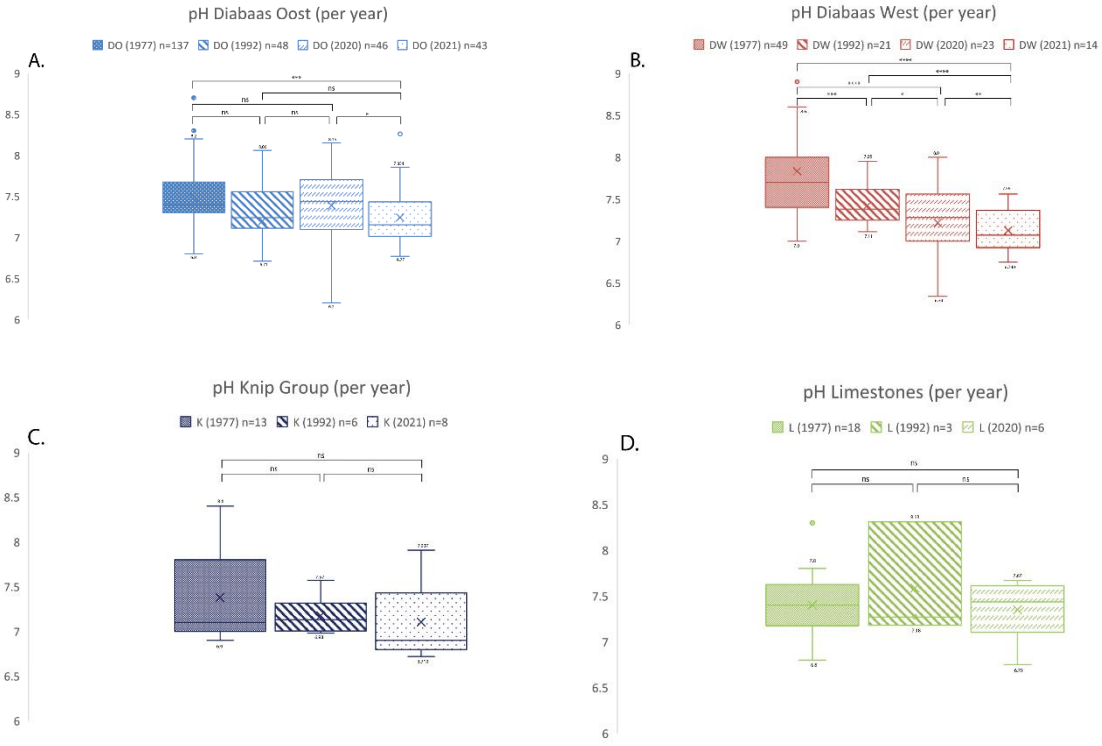

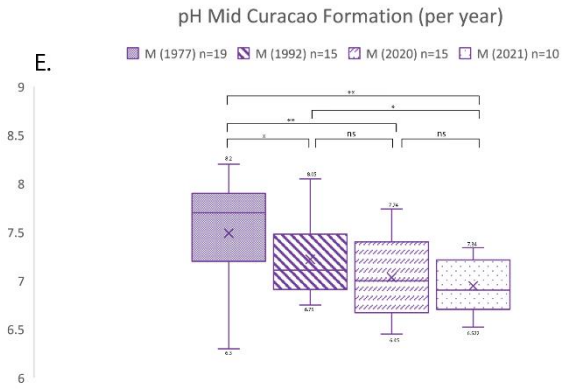

Figure 20. Boxplot comparison of pH per geology over the decades.. A) pH of Diabaas East (Diabase East) for '77, '92, '20 and '21. B) pH of Diabaas West (Diabase West) for '77, '92, '20 and '21. C) pH of Knip Group for '77, '92, and '21. D) pH of Knip Group for '77, '92, and '20. E) pH of Mid Curaçao formation for '77, '92, '20 and '21.

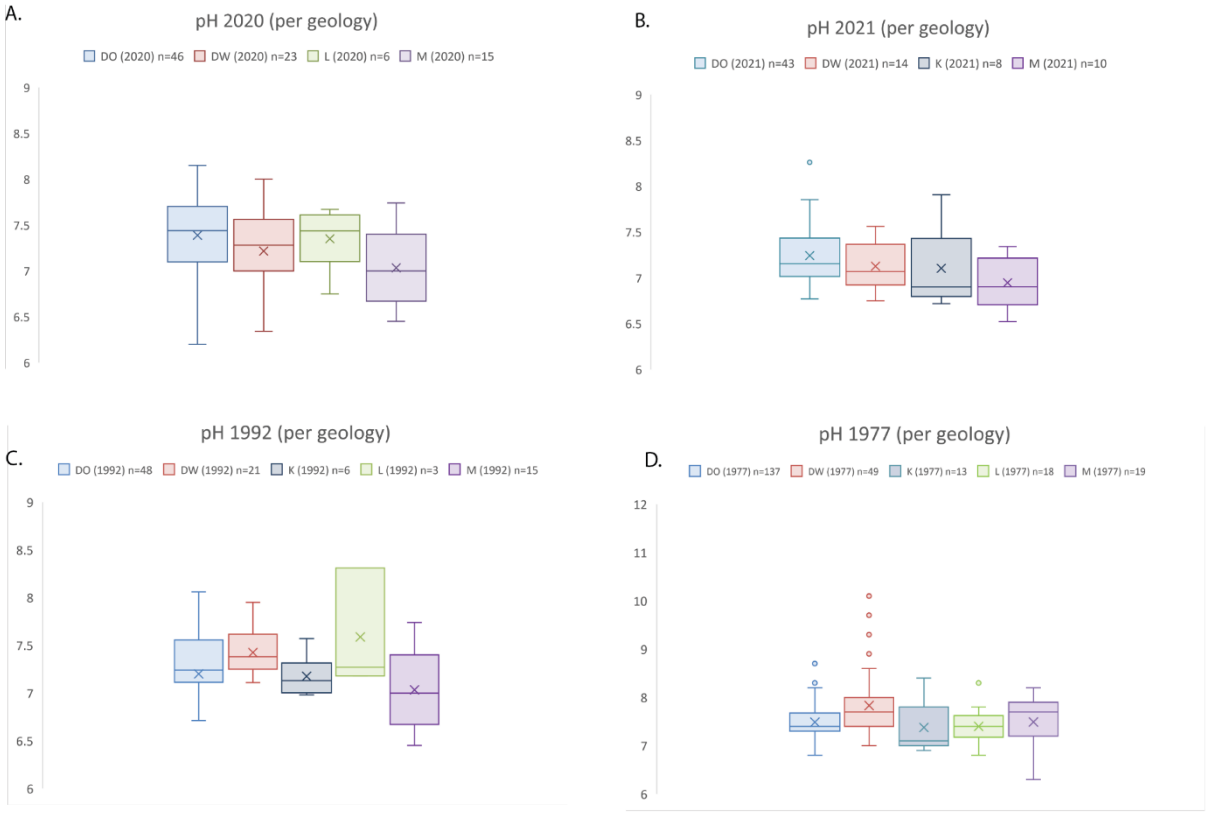

Figure 21. Boxplot comparison of pH per year for each geology. . A) pH of '20. B) pH of '21 C) pH of '92 D) pH of '77.

For the comparison of SO_4, Ca, Mg, K and Na between all datasets please refer to Appendix II. For SO_4, the west has significantly higher concentrations than the east in 1977 and 2021, but there is not increase or decrease between the years itself for east / west (compared for 1977 – 1992, 1992 – 2021, 1977 – 2021).

Sodium Adsorption Ratio

When looking at the Sodium Adsorption Ratio (SAR) and the EC (Figure 22) for all wells located on the eastern side of Curaçao, all samples from '20 (*n*=39) have a low sodium hazard, but a high to severely high salinity hazard. Only four samples have both a low salinity and sodicity hazard. The '21 samples

have a similar distribution, but contain more higher salinity and higher sodicity hazard samples. The ’92 and ’77 samples are also divided similarly, but go up to more extreme values associated with a higher potential hazard for sodification. When comparing SAR specific, for the eastern side of the island, there is no significant different over the decades.

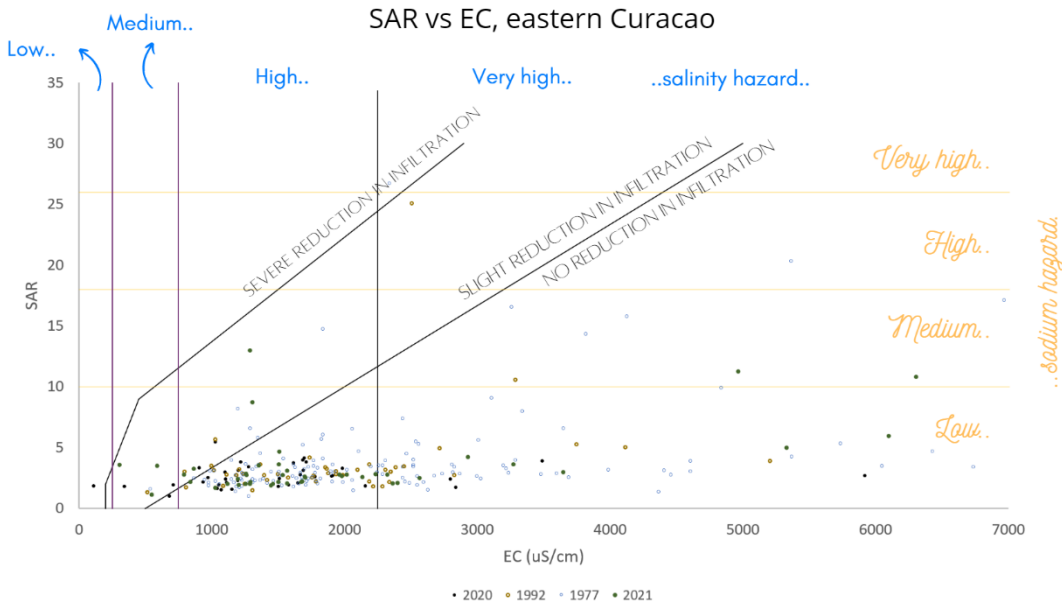

Figure 22. EC versus SAR for eastern Curaçao.

4.1.4 Hydrochemical processes and ionic relations

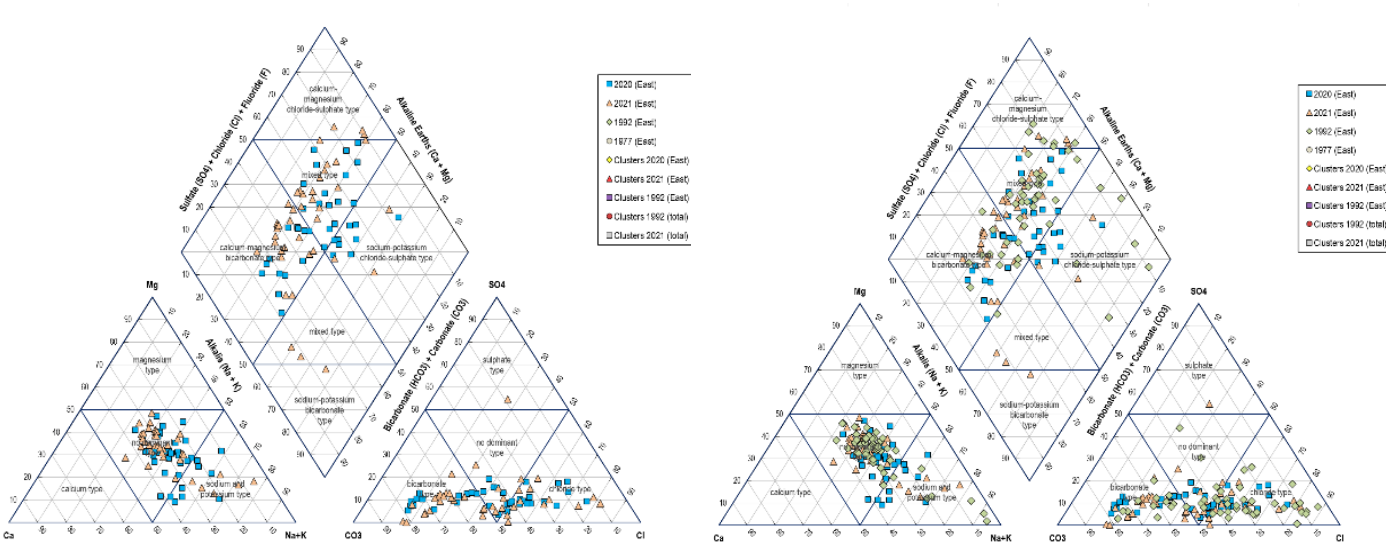

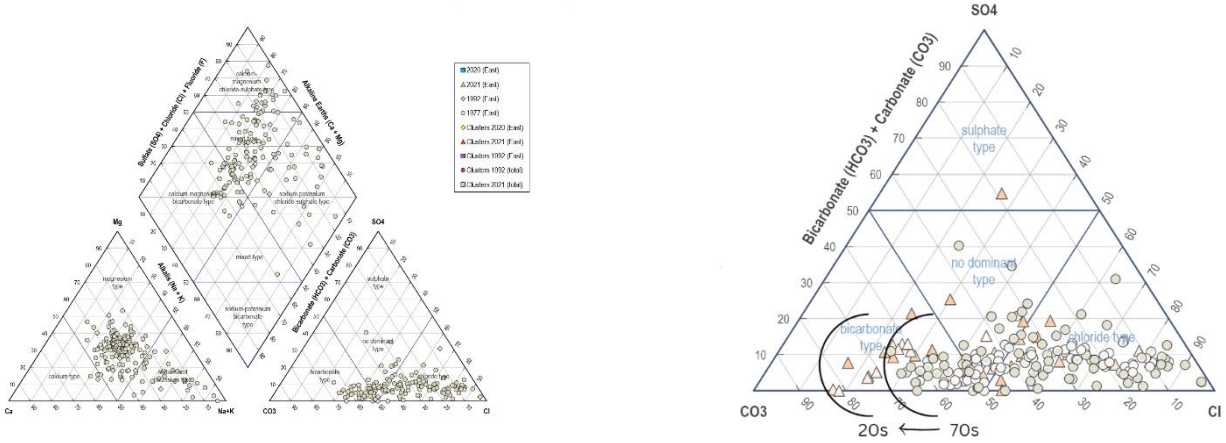

Figure 23. Piper diagrams for different datasets, eastern side.
a). Piper diagram for 2020 and 2021, east
c). Piper diagram for 1977, east.
b). Piper diagram for 2020, 2021 and 1992, east.
d). Anion side for '77 and '20-'21.

The piper diagrams represent the different water types based on the water chemistry of the main ions over different years for eastern Curaçao (Figure 23 a, b, c; Table 30). For all years, Mixed water type (2) and Ca-Mg-HCO3 water type are most present for the wells of the east. The proportion of wells found in the mixed water type (2) section (Table 30), ranges between 38% ('21) and 52% ('92), and the wells found in the Ca-Mg-HCO_3 water type, increase from 23% ('77) to 40% ('21). The wells of '92, '20 and '21 have similar distributions amongst the anion side, dividing most wells into the chloride or bicarbonate anion type. When comparing this to the anion section of '77, it shows that the wells have moved more towards bicarbonate-type when comparing the '92/'20/'21 to the '77 dataset (Figure 23 d). The eastern cation side in '92 has more extreme values in the sodium-potassium type water than '20 and '21, but it must be noted that for the '20 dataset, 13 (higher salinity) samples could not be included as they could not be fully analysed.

Table 30. Classification of groundwater samples eastern Curaçao, as based on Piper trilinear diagram.

Class	Water type	East '77		East '92		East '20		East '21	
1	Ca-Mg-Cl-SO_4	22	15%	6	12%	0	-	3	7%
2	Ca-Mg-HCO_3	35	23%	12	23%	13	33%	17	40%
3	Na-K-Cl-SO_4	28	19%	6	12%	9	23%	3	7%
4	Na-K-HCO_3	0	0%	0	0%	0	-	1	2%
1, 2, 3	Mixed	63	42%	27	52%	17	44%	16	38%
2, 3, 4	Mixed	1	1%	1	2%	0	-	2	5%
	Total (n and %)	149	100%	52	100%	39	100%	42	100%

In Table 31, the Pearson correlation between the parameters is displayed for eastern Curaçao (*n*=39), 2020, excluding the 13 samples, with generally higher salinity, as they could not be fully analysed (Appendix 2). The table shows that EC only moderately correlates with Mg and Na: 0.5 and 0.55, respectively. The expectation is that with the additional eastern samples included this correlation could increase. Br and Cl have a strong correlation (0.96), as do PO_4 and P, expectedly (0.99). The following parameters have a correlation between 0.7 and 0.8: Zn and Al (0.77), Na and Br (0.75), Na and Cl (0.73), S and Ca (0.73), SO_4 and Cl (0.78), SO_4 and S (0.78), and Zn and NH_4 (0.79). Although the latter can be due to the many samples that are below detection limit for NH_4, which could give a distorted view. Calcium is correlated with Cl (0.67), Mg (0.67), Fe (0.65) and SO_4 (0.67); HCO_3 with Si (0.66), NO_3 with SO_4 (0.66), Mg with S (0.66) and Mg with SO_4 (0.62).

4.1.5 pCO_2 over 2021

The pCO_2 (Figure 24 a) for the eastern side of Curaçao has a range between 1.5 x 10^{-10} and 0.08 with an average of 0.032, the pCO_2 for the western side of Curaçao has a range between 1.1 x 10^{-10} and 0.09 with an average of 0.037. There is no significant difference between the east and the west. The log pCO_2 in relation to pH, saturation and atmospheric pCO_2 is shown in Figure 24 b. Note that all wells, both east and west, have pCO_2 values that are higher than that of atmospheric pCO_2 (0.04 vol%; pCO_2 = 4 x 10^{-4} of 1 atm = $10^{-3.4}$ atm; log pCO_2 = -3.4). Log pCO_2 versus the saturation index of calcite is presented in Appendix V.

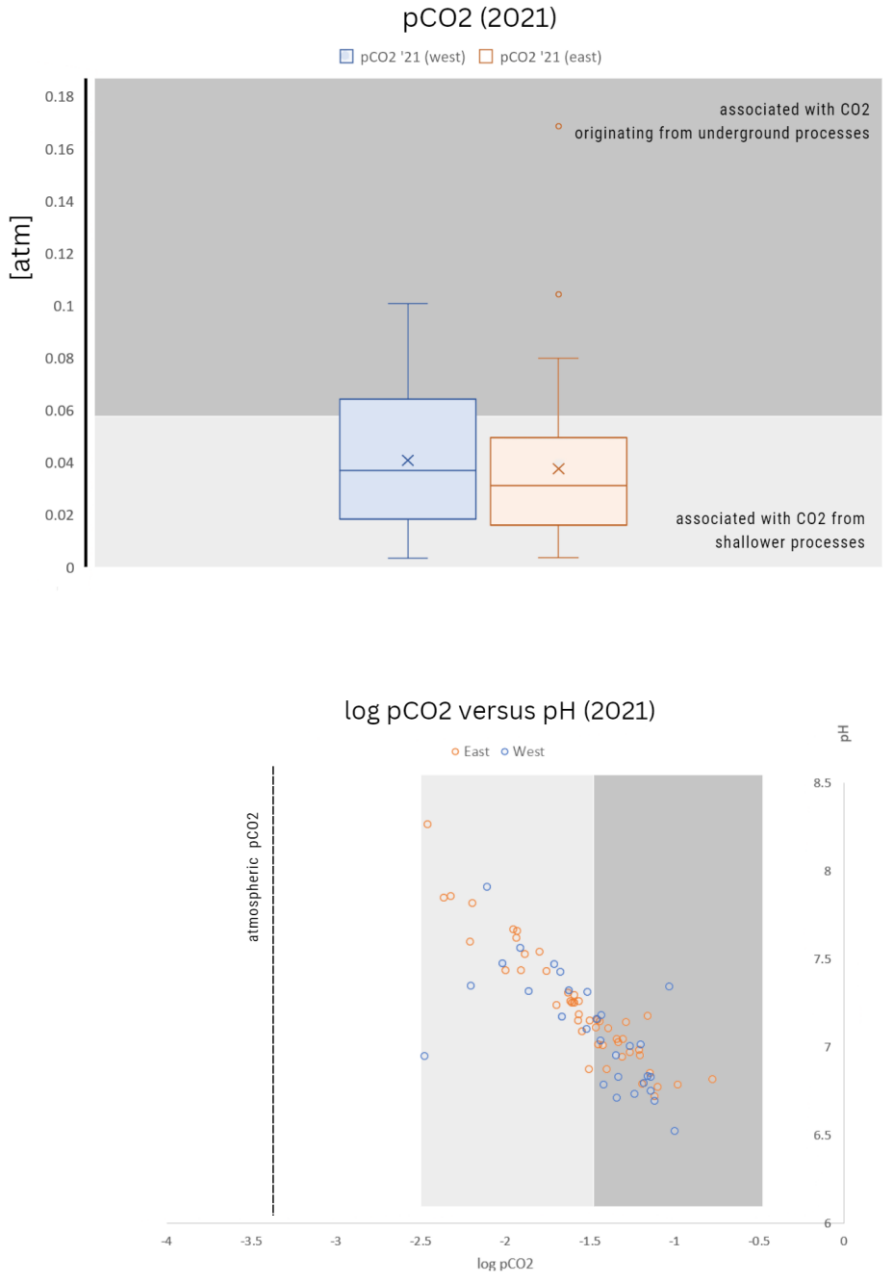

Figure 24. pCO_2 for 2021 . Units is atmosphere a) top: pCO_2 east and pCO_2 west visualized in boxplots for 2021 and b) bottom: log pCO_2 (atm) versus pH over 2021, eastern and western Curaçao. Difference in shallower (e.g. vegetation-related or closer to the surface processes) and deeper underground processes from (Delkhahi et al., 2020).

Table 31. Correlation between the parameters, fieldwork campaign 2020, eastern Curaçao.

	Al	*B*	*Br*	*Ca*	*Cl*	*EC*	*F*	*Fe*	*HCO_3*	*K*	*Mg*	*Na*	*NH_4*	*Ni*	*NO_2*	*NO_3*	*Turb*	*P*	*Pb*	*PO_4*	*pH*	*S*	*Si*	*SO_4*	*Temp*	*V*	*Zn*
Al	1																										
B	-0.11	1																									
Br	0.34	0.16	1																								
Ca	0.25	-0.04	0.58	1																							
Cl	0.36	0.19	0.96	0.67	1																						
EC	0.41	0.13	0.51	0.52	0.56	1																					
F	-0.24	0.61	-0.16	-0.24	-0.11	-0.13	1																				
Fe	0.51	0.04	0.39	0.65	0.47	0.60	-0.28	1																			
HCO_3	0.19	-0.28	-0.08	0.38	-0.03	0.13	-0.16	0.22	1																		
K	-0.13	0.14	-0.09	-0.13	-0.05	0.03	0.00	0.34	-0.19	1																	
Mg	0.15	-0.07	0.49	0.67	0.57	0.50	-0.17	0.38	0.51	-0.20	1																
Na	0.09	0.47	0.75	0.56	0.73	0.55	0.19	0.25	-0.04	-0.08	0.40	1															
NH4	0.93	-0.14	0.24	0.09	0.26	0.08	-0.28	0.39	0.12	-0.07	0.00	-0.07	1														
Ni	-0.03	0.06	0.13	0.11	0.11	0.03	0.20	0.06	0.04	0.05	-0.11	0.23	-0.05	1													
NO_2	0.32	-0.21	-0.20	-0.06	-0.20	-0.06	-0.09	0.05	0.14	-0.10	0.00	-0.20	0.34	-0.04	1												
NO_3	0.59	-0.18	0.47	0.51	0.52	0.37	-0.30	0.45	0.22	-0.26	0.48	0.19	0.49	-0.14	0.08	1											
Turb	-0.05	0.05	0.20	-0.05	0.06	0.01	-0.07	-0.15	-0.26	-0.06	-0.27	0.10	-0.08	0.25	-0.09	-0.37	1										
P	-0.03	0.36	-0.03	-0.12	0.00	0.10	0.02	-0.03	-0.09	0.17	-0.14	0.09	0.07	-0.06	-0.03	-0.20	-0.01	1									
Pb	-0.02	-0.03	0.07	0.05	0.06	-0.04	0.10	0.05	0.11	0.51	0.01	0.12	-0.03	-0.01	-0.06	0.02	-0.08	-0.09	1								
PO4	-0.09	0.34	-0.10	-0.14	-0.05	0.06	0.06	-0.08	-0.07	0.19	-0.16	0.05	0.04	-0.05	-0.01	-0.22	-0.16	0.99	-0.07	1							
pH	0.12	0.16	0.10	-0.22	0.08	0.10	0.26	-0.20	-0.27	-0.21	-0.02	0.12	0.07	0.01	-0.03	0.08	0.23	-0.06	-0.21	-0.08	1						
S	0.12	0.32	0.41	0.73	0.55	0.43	0.07	0.45	0.21	-0.14	0.66	0.55	-0.01	0.02	-0.12	0.42	-0.15	-0.07	0.04	-0.09	0.04	1					
Si	0.21	-0.16	0.04	0.32	0.07	0.35	0.00	0.21	0.66	-0.23	0.53	0.07	0.02	-0.22	0.07	0.36	-0.43	-0.18	0.16	-0.22	-0.26	0.18	1				
SO_4	0.50	0.18	0.63	0.67	0.78	0.52	-0.05	0.55	0.25	-0.16	0.62	0.47	0.39	-0.02	-0.08	0.66	-0.15	-0.02	0.03	-0.07	0.13	0.78	0.26	1			
Temp	-0.04	0.22	-0.04	-0.04	-0.05	-0.03	0.44	-0.01	-0.15	-0.07	-0.06	0.07	-0.04	0.11	0.07	-0.03	0.10	-0.07	0.05	-0.03	0.55	0.19	-0.21	0.10	1		
V	-0.02	-0.19	-0.23	-0.17	-0.18	0.08	0.13	-0.12	0.47	-0.08	0.42	-0.16	-0.09	-0.23	0.04	0.13	-0.48	-0.12	0.05	-0.07	0.20	-0.02	0.55	0.01	0.12	1	
Zn	0.77	-0.09	0.14	-0.10	0.14	-0.16	-0.01	0.12	-0.05	-0.10	-0.14	-0.10	0.79	-0.03	0.25	0.32	0.10	-0.11	0.08	-0.14	0.22	-0.16	0.00	0.22	0.15	-0.01	1

The following components were left out of the analyses due to a considerable amount of values that were below detection limit and would otherwise give distorted correlations: Ag, As, Ba, Be, Cd, Li, Mn, Mo, Sb, Se, Ti. K, Al and NH_4 were left in, even though they too have a distinct amount of values that are below detection limit, this needs to be taken into consideration for the interpretation. The different measurement techniques (DA and IC for PO4, strips and IC for NO3) have also been checked, and have a correlation between 0.99 and 0.86, respectively.

4.1.6 Heterogeneity

During the 2020 field campaign there were several areas where sampled wells with the same well type were located within a 100 meter radius of each other, in the same geology and sampled within 30 minutes of each other. The water quality of two of these regions (Figure 25) are zoomed in on.

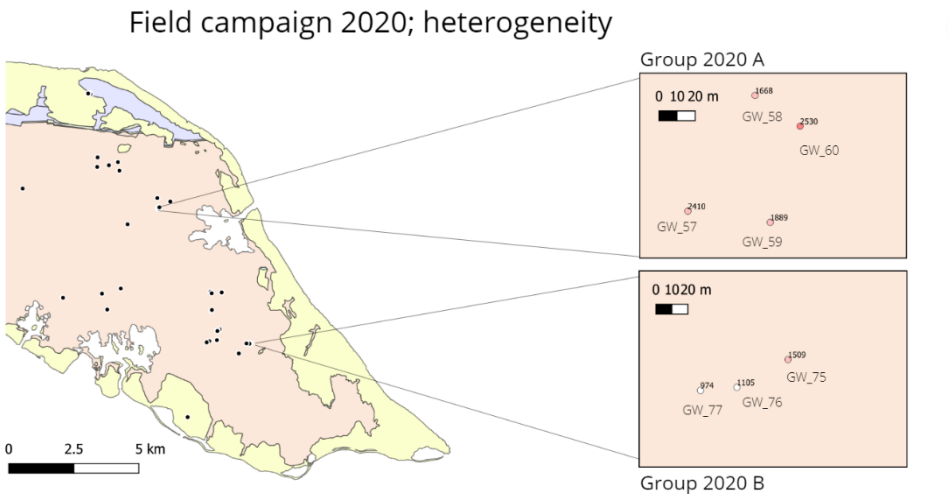

Figure 25. Heterogeneity in groundwater quality for two regions during the 2020 fieldwork campaign.. These are wells that are within 20 – 75 meters of each other, in the same geology and measured within half an hour. Numbers that are shown next to the well points are EC levels in µS/cm*.*

The wells of 2020 Group A (Figure 26) were measured in the four corners of an agricultural field where different vegetables were grown and all wells are of the same owner. The wells are located 29-74 m from each other. Depth (water level) of the wells could not be measured, as the rope of the measurement device got snapped off in another well that morning, dropping the entire PVC device into the well. All wells were actively in use, except for GW_58, which did not have a pump and its sample was therefore collected with a glass jar and a rope. Manure is used to fertilize this field and a small farm house was located adjacent to GW_57. Three out of these four wells did not have a full geochemical analyses, therefore only the field parameters EC, pH and nitrate strips are presented in Figure 26. It is observed that the well close to the farmhouse (GW_57) and GW_59 has a higher nitrate concentration (>220 mg/L) than the other two wells. The EC ranges between 1668 and 2530, lowest being in the well that was not actively used.

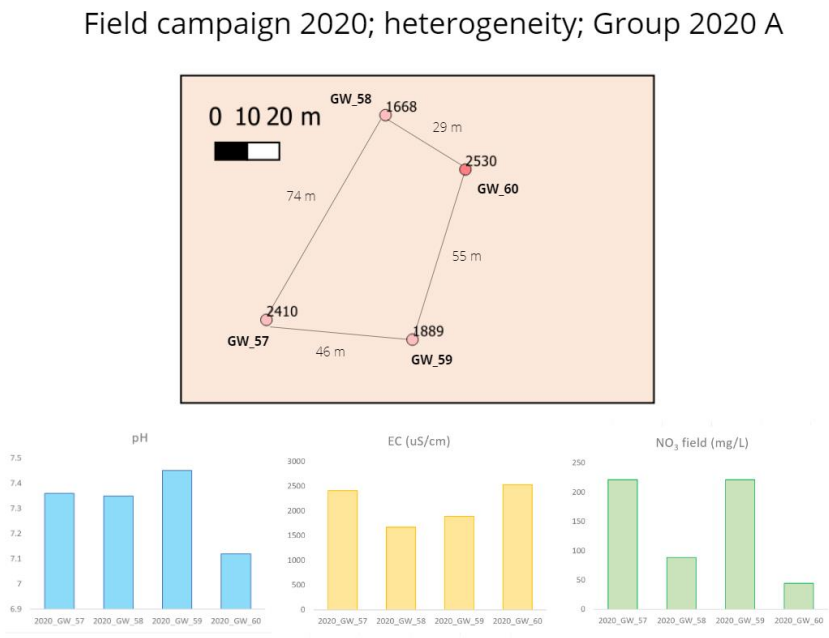

Figure 26. Heterogeneity of four wells in the eastern section (group 2020 A). . The numbers in the map are the EC values for each of the wells in µS/cm*.*

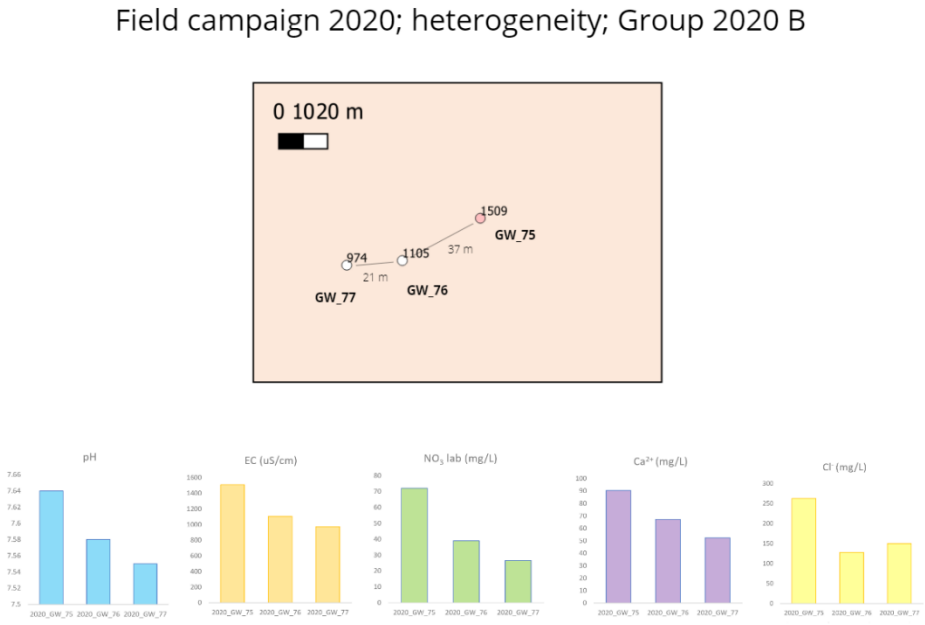

Figure 27. Heterogeneity of three wells in the eastern section (group 2020 B). . The numbers in the map are the EC values for each of the wells in µS/cm*. All three wells had a geochemical analyses, and an E.B. < 10% , therefore NO3, Ca and Cl are showcased, besides EC and pH.*

The wells of 2020 Group B were measured on private semi-overgrown terrain, of which GW_75 was close to the house (<3 m) and used daily. GW_76 (borewell) and GW_77 (hand dug) were further away from the house and no longer in use (Figure 27). Depths of the wells were 3.52 and 3.29 meters from ground level for GW_77 and GW_76 meters, respectively. Water level of GW_75 was not accessible to measure. Notable is the NO_3 concentration close to the house is 72 mg/L, but drops to 39 mg/L at 37 meters, and to 27 mg/L 21 meters further than that. The EC roughly drops 400 µS/cm, Ca^{2+} 40 mg/L and Cl^- 110 mg/L over the same distance.

4.1.7 Identical wells for 2020 and 2021

During the fieldwork period of 2021, between 7-9 wells were measured that were also measured in the fieldwork period of 2020, as shown in Figure 28 and Table 32. For all wells the field values for EC, water levels, sample depths and field methodology are compared.

It is witnessed that the deeper wells (well 1, 2 and 6) are located in MCF, of which Well 1 and 6 were sampled with different well measurement methodologies, causing a dissimilarity in sample depth between 2020 and 2021. In 2020, Well 1 and 6 were not purged before sampling, and measurements were taken close to water level. This was because the well was either under construction, or the pump not active. In 2021 the pump of the owner could be used to “flush” out the well before sampling, moving the sample depth to that of the bottom of the well. The EC in 2021 than 2020 shows to be higher for the MCF wells sampled at the bottom of the well. Well 2 was also measured in MCF, on the same terrain as Well 1, but the well could be purged in both years by using the pump of the well itself. For this well the salinity is similar for both years.

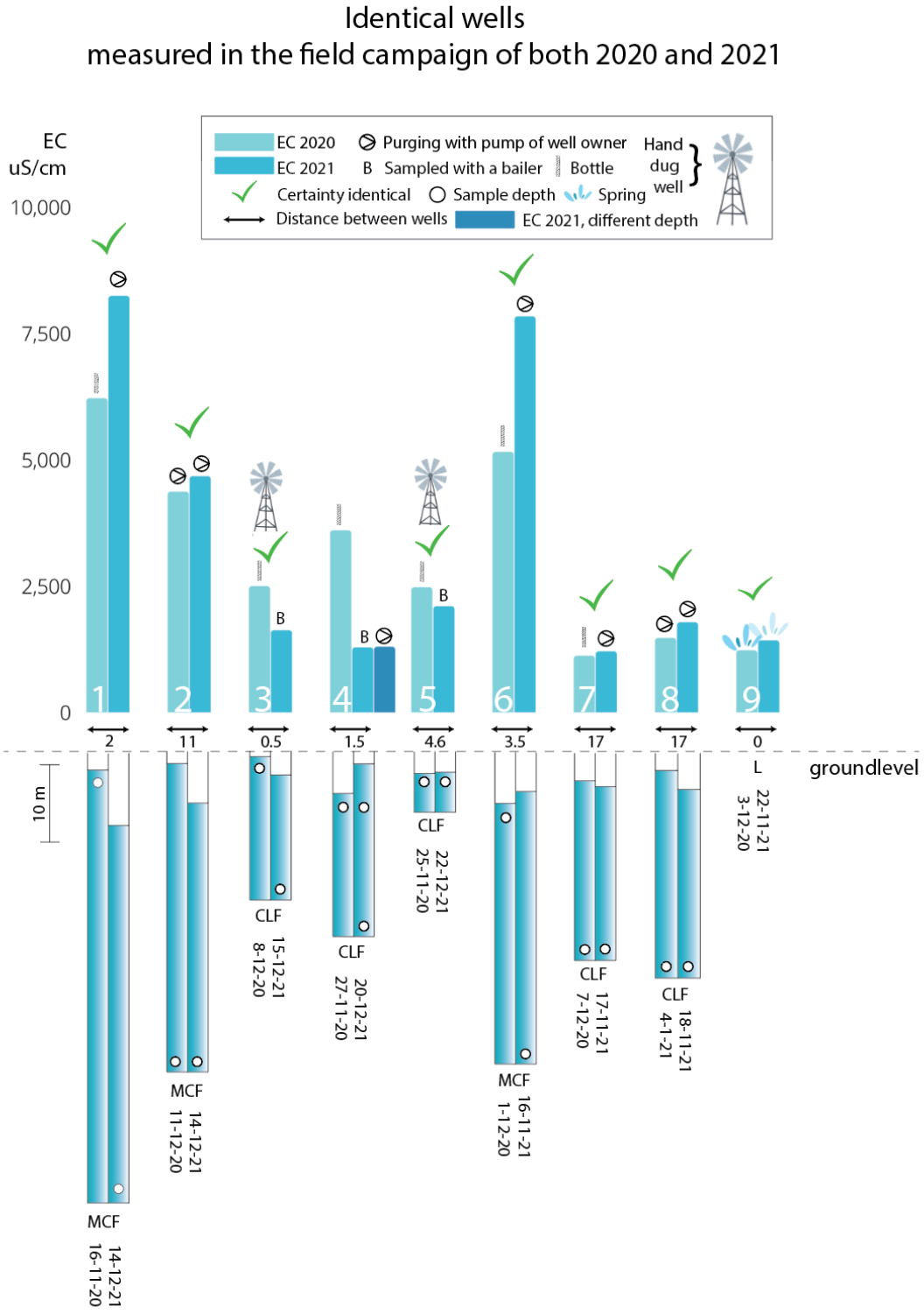

Figure 28. Identical wells measured in both 2020 and 2021 .. The 7-9 wells that were measured in both 2020 and 2021. Top part illustrates the EC value in µS/cm, the bottom part illustrates the actual wells with their depth and water levels to scale (scale = 10 m).There is symbology for sample depth, well depth and water level in relation to ground level, distance between wells 2020 and 2021 as based on QGIS, purging method per year (bailer, pump of owner or bottle), geology (CLF for Curaçao Lava formation, MCF for Mid Curaçao formation, L for Limestones), a mill symbol for hand dug wells, the date of sampling for both years and the certainty of if these are indeed identical wells. The numbering of the wells coincides with the information provided in ***Table 32****.*

Two of the wells (well 4 and well 6) match in terms of GPS (<5 meters distance from each other in QGIS), but have different descriptions of well type and location; it is therefore uncertain if these two wells were truly measured in both years. These wells are therefore not further considered. Well 3, 5, 7 and 8 are located in the CLF, of which 3 and 5 were noted to be hand dug in 2020. There are only slight differences in salinity of 17, 8 and 18%, respectively, regardless of sampling method. Well 9 is a spring close to Hato airport with a slight increase in salinity of 14%.

Table 32. Overview of "identical" wells, measured in both 2020 and 2021.

	Sample code	2020 – EC (mS/cm)	2021 – EC (mS/cm)	Geology	Distance* (m)	Water level (2021)	Depth** (2021)	Water level (2020)	Sample depth (2020) in m below water level	Comment
1	11.6 (2020) GW_44 (2021)	6.21 26-11-2020	8.33 14-12-2021	MCF	2	11.1	57	2.68	1-3	Pump owner used in 2021. Could not be pumped in 2020 because well wasn't finished. Certain that same well.
2	26.5A (2020) GW_45 (2021)	4.36 11-12-2020	4.67 14-12-2021	MCF	11	5.9	41	Closed well	Pumped with pump owner	Similar EC. Certain that same well. Pumped in both years.
3	GW_52 (2021) 22.12	2.49 8-12-2020	1.62 15-12-2021	CLF	0.5	11.1	19.6	9	1-3	Roadside well. Uncertain if same well in 2020-2021. Bailer was used in 2021.
4	12.12 (2020) GW_60 AB (2021)	3600 27-11-2020	1285 / 1297 20-12-2021	CLF	1.5	4.6	7.7 23.7	16.6	1-3	Uncertain if this is the same well for 2020 and 2021. Different description, even though <5 m distance in QGIS. Pump and bailer was used in 2021.
5	10.10 (2020) GW_65 (2021)	2.47 25-11-2020	2.10 22-12-2021	CLF	4.6	7.39 m	11.3	11.0	1-3	Owners shared that this well collects a lot of rainwater, even when the neighbors do not have any water, they do. Bailer was used in 2021.
6	16.3 (2020) GW_009 (2021)	5.15 – 7.50 1-12-2020	7.83 16-11-2021	MCF	3	11.88	40.0	14.1	1-3	In 2020 it was stated that the well depth was 65 m. Pumping was used in 2021.
7	24.1 (2020) GW_10 (2021)	1.11 7-12-2020	1.20 17-11-2021	CLF	17	11.38	25	10.0	Pumped with pump owner	Certain that this is same well, even with >5 meter distance in QGIS. Both years pumped.
8	41.2 (2020) GW_011 (2021)	1.47 4-1-2020	1.77 18-11-2021	CLF	17	7.71	>27	6.9	Pumped with pump owner	Certain that this is same well, even with >5 m distance in QGIS. Both years pumped.
9	Hato spring SP001	1.22 3-12-2021	1.42 22-11-2021	L	0	0	0	0	0	Certain that this is the same spring.

**This is the distance between the wells based on GPS locations of both years in QGIS3, measured with a straight line. ** Sample depth.*

4.1.8 Identical wells for 2020, 1992 and 1977

During the fieldwork period of 2020, 20 wells were accessed and measured that were also measured in the fieldwork period of 1992: 5 on the western side of Curaçao and 15 on the eastern side of Curaçao.

Of these 20 wells, 12 were also measured in 1977. For these wells, referred to as the “identical wells”, the field values for EC (Table 33 - Table 34; Figure 29 - Figure 33) and pH (Figure 34 - Figure 36; Table 35) were compared. The NO_3^- (Table 36; Figure 37;
Figure 39), SO_4^{2-} (Figure 38) and SAR (Figure 40 - Figure 41) are compared as well, but only for the identical wells on the eastern side of the island. In addition, during the fieldwork campaign of 2021, five wells were identical to the fieldwork of 1977; two of these five samples were also measured in 1992 (Figure 29). Overall, for EC, there is no significant difference over the decades for the identical wells of 1977, 1992, 2020 and 2021 (Table 34). For pH, there is a decrease over the years (Table 35).

Table 33. Overview EC (mS/cm) of identical wells measured in 1977, 1992 and 2020 (N=12). The comparison between 1992 and 2020 has a sample size of 20.

	1977	1992	2020	Average	STD
6z209	2.44	1.99	0.93	1.79	0.63
5z6	1.66	1.11	1.07	1.28	0.27
6z254	1.80	1.79	5.92	3.17	1.95
8n16	1.80	1.88	6.84	3.51	2.36
4z1	2.55	1.94	1.71	2.07	0.35
5n30	1.18	1.24	1.65	1.36	0.21
5z12	2.60	1.50	3.17	2.42	0.69
5n2	1.62	5.21	2.80	3.21	1.49
5n247	1.29	1.74	1.91	1.65	0.26
3n12*	1.88	1.42	1.55	1.62	0.19
2n30	1.64	1.30	1.43	1.46	0.14
1n1	1.42	1.63	1.20	1.42	0.18
Average	1.82	1.90	2.52		
STD	0.45	1.04	1.85		

*3n12 is a spring.

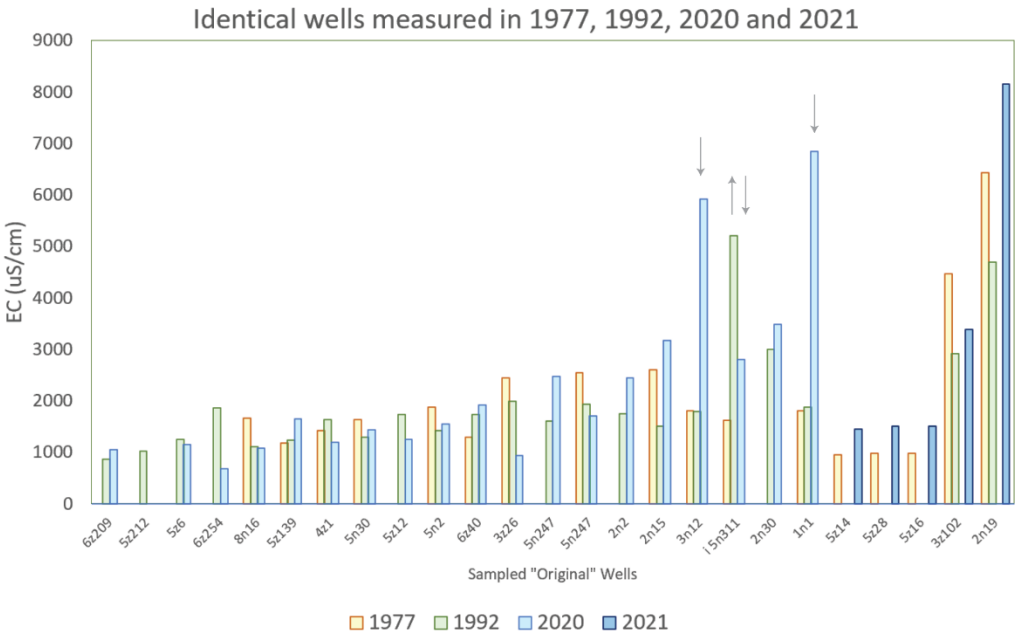

Figure 29. Comparison EC identical wells for 1977, 1992, 2020 and 2021.3n12 is a spring. The arrows point towards two wells that show a large increase (>300%) when

comparing 1977 and 2020. The up-and-down arrow point towards a well that increased (>300%) between 1977 and 1992, but then decreased in 2021.

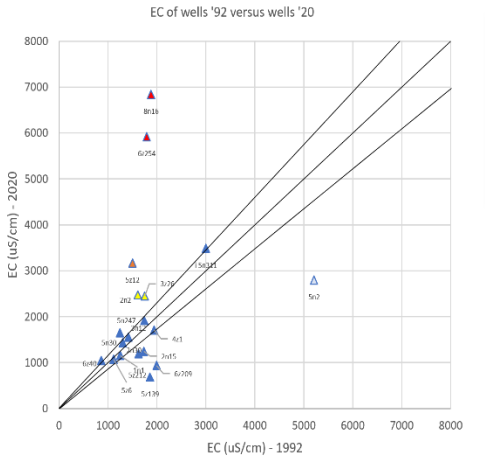

Figure 30. Scatterplot of EC in '92 and '20 of identical wells.. Red means that the increase >300%, yellow <15%, blue neutral, lightblue decrease.

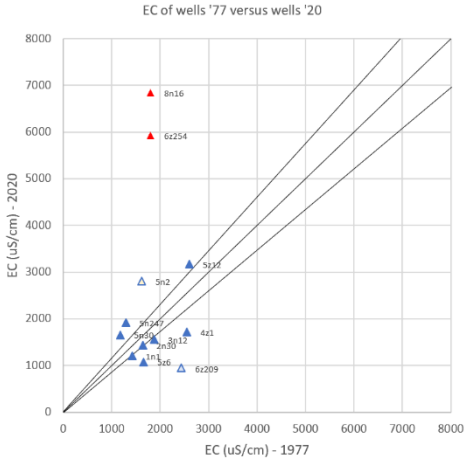

Figure 31. Scatterplot of EC in '77 and '20 of identical wells.. Red means that the increase >300%, yellow <15%, blue neutral, lightblue decrease.

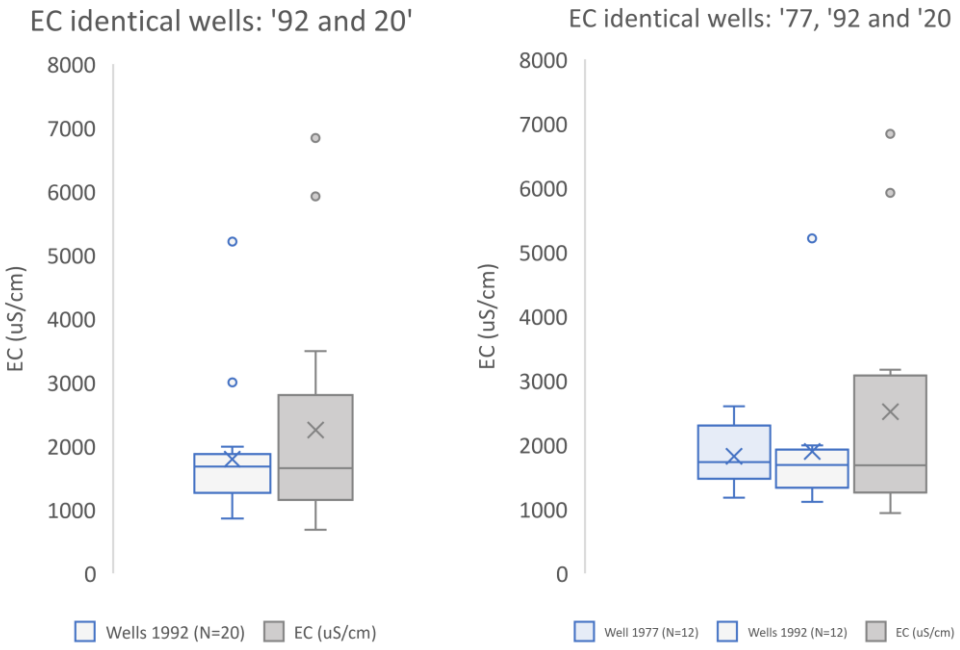

Figure 32. EC of identical wells measured in 1977, 1992 and 2020. (ns).

When comparing EC throughout the years for the identical wells, there is no significant difference (Anova, p = 0.317) between the years (Table 34). The average did increase for 2020, and more extreme salinity values were measured (Figure 29). On the western side of the island well 1n1 and 2n15 (Figure 33) have not gotten more saline over the years, despite being in close proximity to the coastline. For 1n1 the groundwater was shallow (<1.5 m) and it had recently rained. The highest increase happened on the eastern side of the island, for well 6z254 and 8n16 (Figure 31; Figure 33). The biggest decrease between 1992 and 2020 happened in well 5n2 (Figure 30); between 1992 – 1977 this same well increased in salinity (Figure 31). Compared to 1977, well 5n2 did not decrease in EC as much as it did

compared to 1992. The EC values for wells 8n16 and 6z254 are clearly higher in 2020 (5920 and 6840 µS/cm) than in 1992 (1790 and 1880 µS/cm) and 1977 (1800 and 1800 µS/cm)(Table 33; Figure 29). 5z12 increased as well, but to a lesser extent. For the 1992 – 2020 comparison 5n2 lowered in EC the most, yet decreased in EC compared to 1977. Other wells slightly decreased in salinity or were more or less in the same range (<15%) as previous years. Other wells that went down in salinity are well 5z139 and well 6z209. Overall there is no significant difference in EC between the 20 identical wells measured in both 1992 and 2020, and the 12 identical wells measured in 1977, 1992 and 2020 (Figure 32).

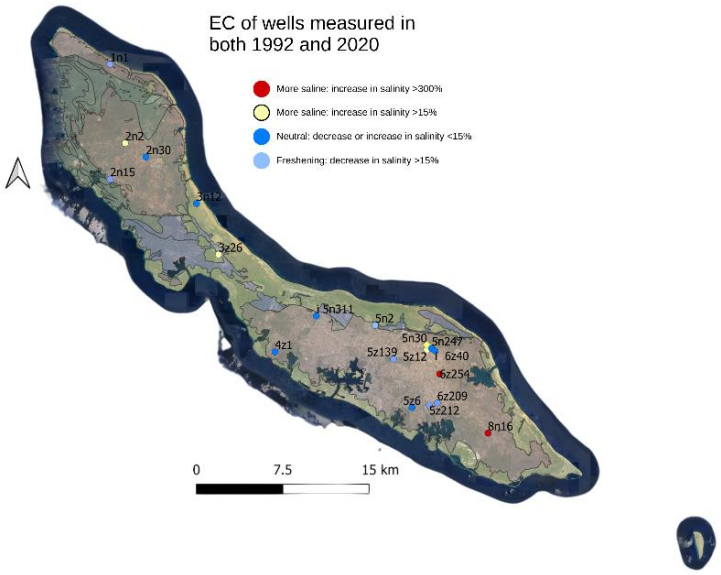

Figure 33. Increase or decrease in EC for identical wells of '92 and '20.

Table 34. Summary EC Identical wells

Groups	*Count*	*Sum*	*Average*	*Variance*
1977	12	21880	1823.33	225315.15
1992	12	22754	1896.17	1170947.24
2020	12	30202	2516.83	3723353.97

p-value Anova: 0.37

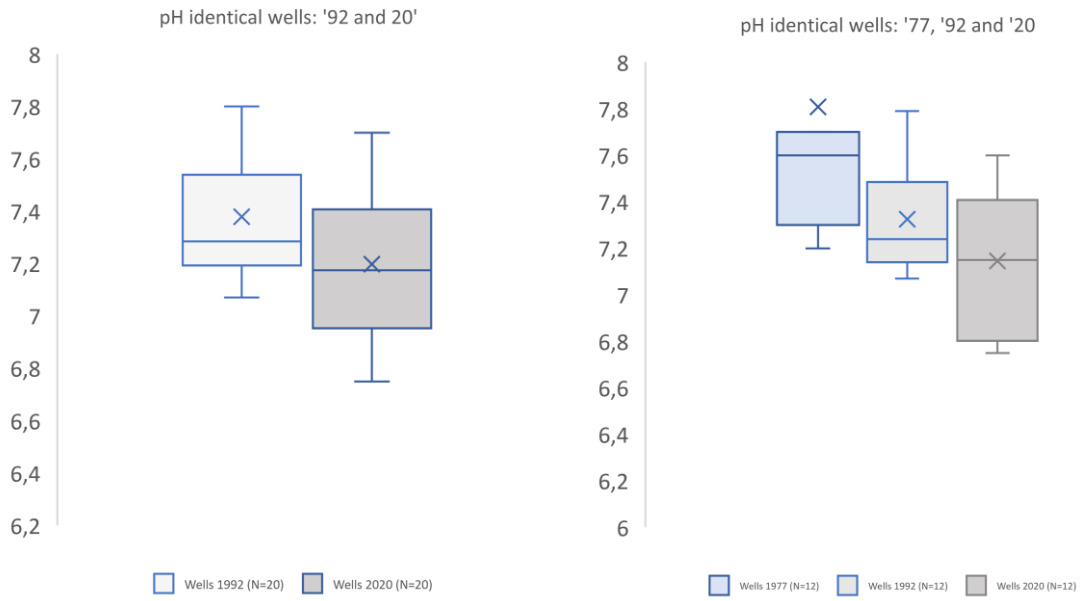

Figure 34. Boxplots of pH for identical wells.. a) 92 and ’20, b) ’77, ’92 and ‘20

Table 35. Summary pH identical wells

Groups	*Count*	*Sum*	*Average*	*Variance*
1977	12	93.7	7.8	0.673561
1992	12	87.9	7.3	0.057718
2020	12	85.75	7.1	0.089045

p-value Anova: 0.01

For the identical wells in ’77, ’92 and ’20 (*n*=12) there is a significant decrease in pH over the years (Anova, p-value = 0.01)(Table 35). When looking at Figure 35 and Figure 36, it can be witnessed that the pH with the highest drop are located in the west (3z26, 2n2), but some of the eastern wells also decreased (5z12, 6z209, 4z1). When comparing ’92 to ’20 (Figure 35), western wells 2n15, 2n2 and 3z26 decreased, and eastern wells 6z209, 8n16, 5z139, 5n247. For the SAR, sulphate and nitrate of the identical wells, only the fully analyzed samples of the eastern side are considered. For sulphate, there is only one well (5z139) where the change in concentrations exceeds 50% between ’92 and ’20 (Figure 38). Nitrate has increased for four wells (
Figure 39; Table 36), but also decreased for four to six wells. All other wells are close together in concentration. For the SAR of the eastern identical wells, the 2020 wells have decreased for almost all wells in comparison to 1992 (Figure 40), but in the boxplot comparing all years there is no significant decrease (Anova, p-value = 0.18) (Figure 41).

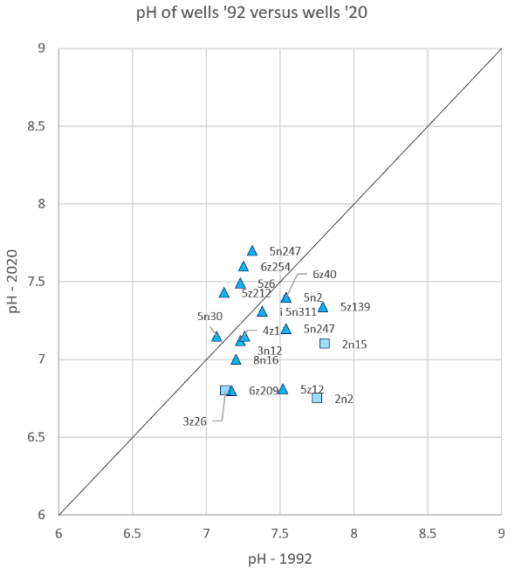

Figure 35. pH of wells in ’92 and ’20 plotted against each other. The squares are wells located in the west.

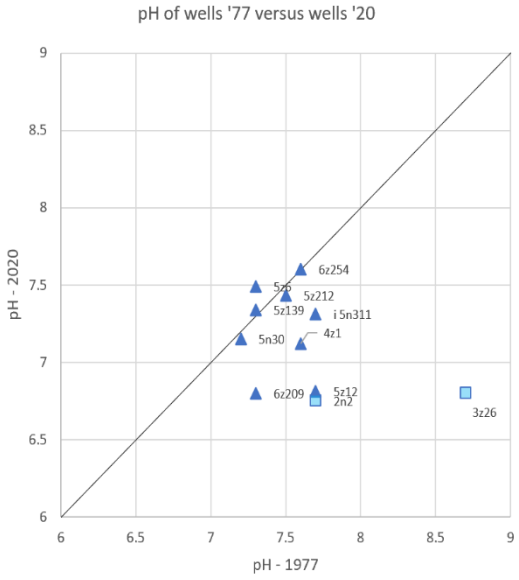

Figure 36. pH of wells in ’77 and ’20 plotted against each other. . The squares are wells located in the west.

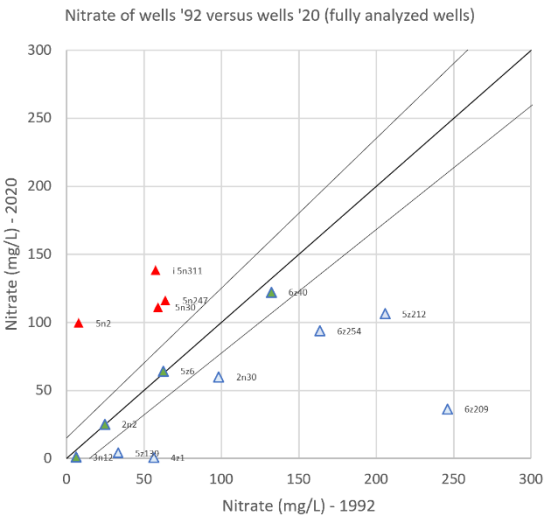

Figure 37. Nitrate concentration (IC) for wells '20 and '92.

This only includes the fully analysed wells. Wells with more than >15% increase between years are coloured red, >15% increase light blue, and between both darker blue.

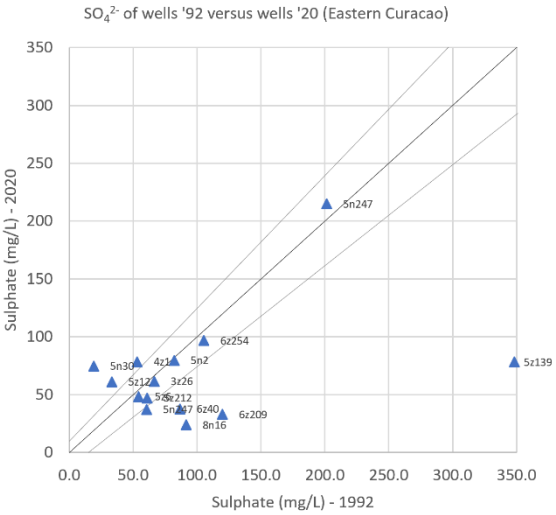

Figure 38. Sulphate concentration for wells '20 and '92.

This only includes the fully analysed wells.

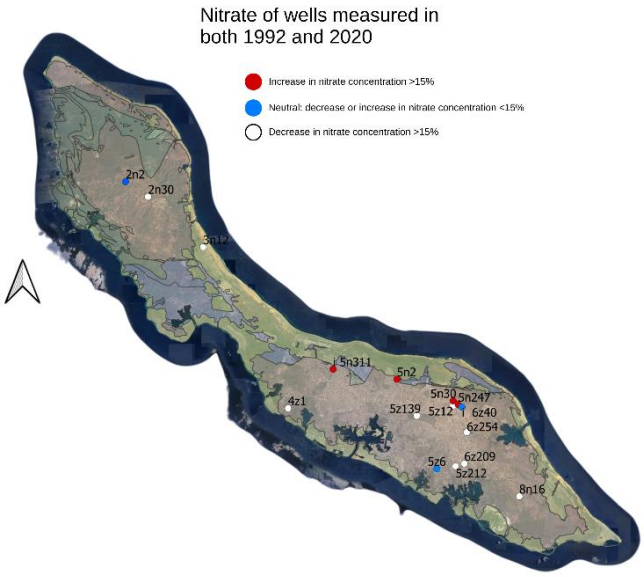

Figure 39. Increase or decrease in NO_3 for identical wells '92 and '20 .

Table 36. Nitrate concentrations in mg NO_3^- / L for 1992 and 2020 identical wells

	1992	2020
6z209	246	36
5z212	206	106
5z6	63	64
6z254	164	93
5z139	33	4
4z1	56	0.5
5n30	59	111
5n2	8	99
6z40	132	122
5n247	64	116
2n2	25	25
3n12	6	1
i 5n311	58	138
2n30	99	60

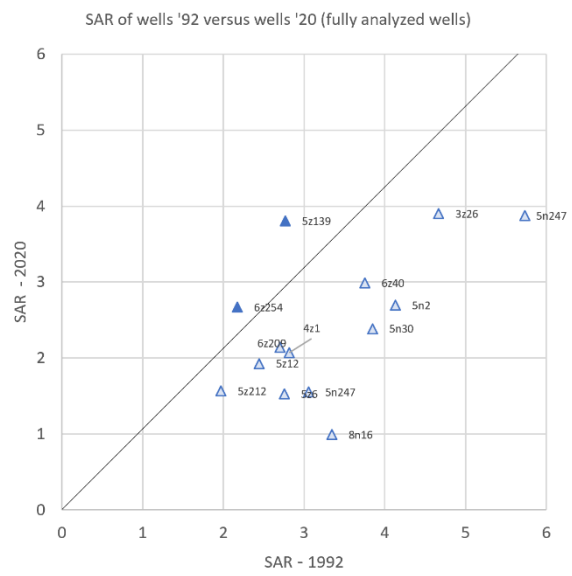

Figure 40. SAR of wells '92 versus '20.Only for eastern fully analyzed wells.

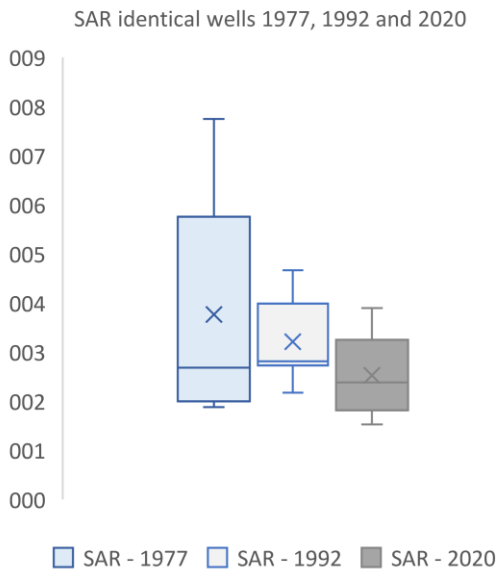

Figure 41. Boxplots of SAR eastern Curaçao for '77, '92 and '20.. Anova p-value of 0.18.

4.2 Multivariate Statistics

The skewness of the samples was checked with a normality test (Shapiro-Wilk), which showed that all parameters for 2021 and 1992 had p-values under 0.05, meaning that for both years all parameters deviate from a normal distribution. Parameters that also have a skewness coefficient that exceeds 2 or -2, were log transformed so that they can be used for further analyses. For the '21 dataset, this meant that the following parameters were transformed: B, Ca, Cl, Fe, HCO_3, K, Mg, Na, SO_4, PO_4 and NH_4 (pH, NO_3, Si had skewness coefficients <2 and were not transformed), and for the '92 dataset: B, Ca, Cl, F, Fe, HCO_3, K, Mg, Na, NH_4, NO_3, Si and PO_4 were transformed (Table 37). For the '21 analysis (14 parameters) the NH_4 is still skewed after transformation, and for the '92 analysis (19 parameters) Co, Cr and Cu are still skewed after transformation. Subsequently, all parameters were scaled before doing the Principle Component and Cluster Analyses.

Table 37. Skewness of parameters 1992, 2021

	1992	2021
Ca	6.01	5.15
Cl	4.62	5.82
Fe	4.97	7.67
HCO_3	2.94	4.46
K	8.65	4.08
Mg	6.06	6.53
Mn	3.60	6.65
Na	3.39	5.79
NH_4	9.24	8.61
NO_3	**1.73**	**0.87**
pH	**0.63**	**0.71**
PO_4	9.70	4.49
Si	**-0.64**	**-0.67**
SO_4	4.67	4.73

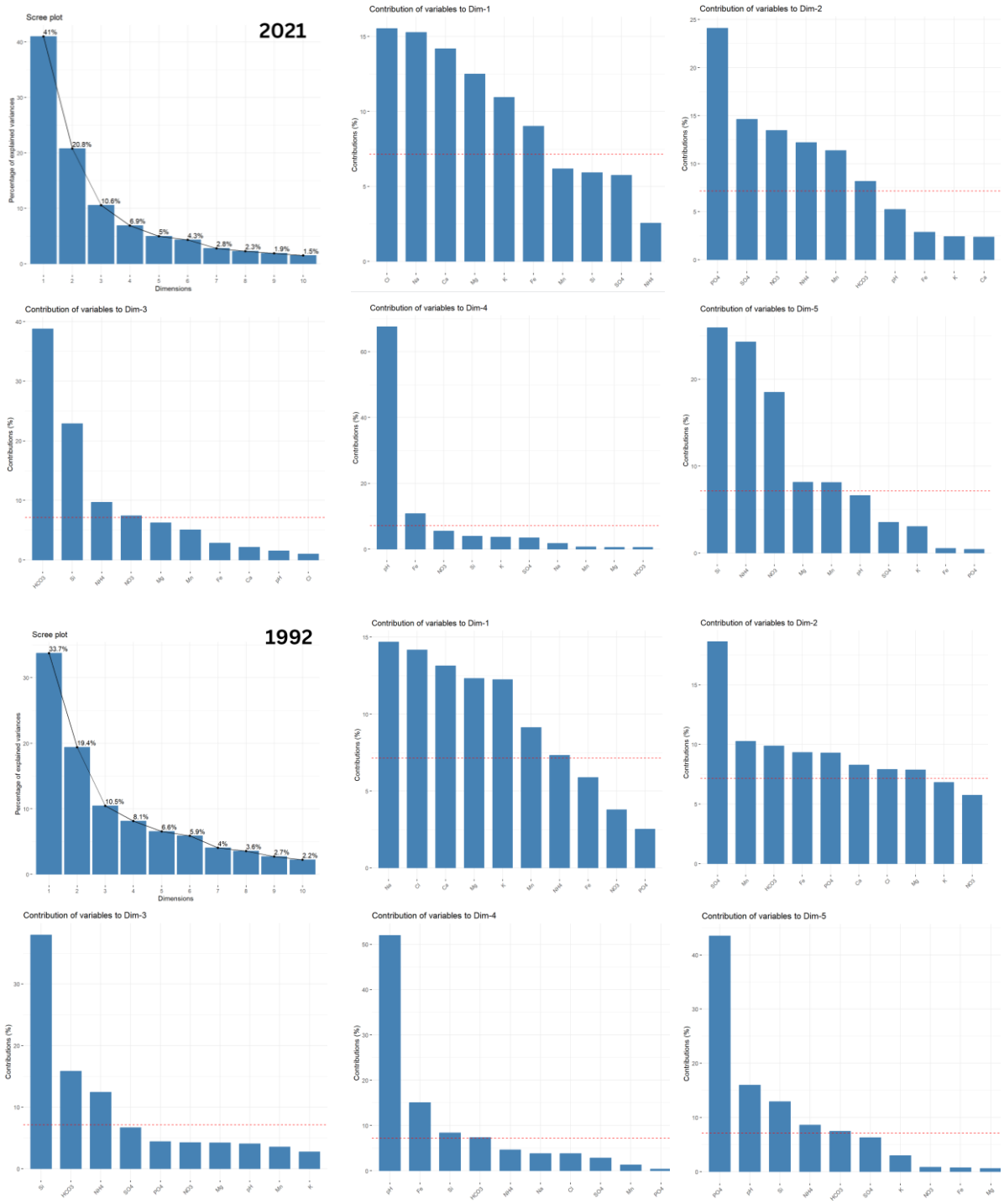

Figure 42. PCA for 2021 (top) and 1992 (bottom)

.

Principle Component Analyses

The principle component analyses for 2021 (Figure 42, top; Figure 43) shows that the first and second dimension of chemical variables account for 41% and 21% of the total variance, respectively. For 1992 (Figure 42, bottom; Figure 44) the first dimension explains 33% of the variability and the second dimension 19%. For both years Na, Mg, Cl and Ca contribute heavily to the first dimension, with a negative contribution of Si. In 1992 33% of the variability was explained with the first dimension

parameters, while in 2021 it's 41%. PO_4 (0.837), Mn (0.574), NH_4 (0.595), HCO_3 (0.487), SO_4 (-0.652) and NO_3 (-0.625) are key contributors for the second dimension in 2021. In 1992, SO_4 (0.711) dominates this component most, with a negative contribution from Mn (-0.528), PO_4 (-0.502), HCO_3 (-0.518), PO_4 (-0.502), K (-0.462) and Fe (-0.503) (Table 38; Table 39; Figure 43; Figure 44). For both 1992 and 2021, in the second dimension, NO_3 and SO_4 are of a different charge than the other parameters. Although the extent of contribution changes, the second dimension has similarities for PO_4, SO_4 and HCO_3 between the years; for 2021 the contribution of NO_3 has increased.

For both years the third dimension mostly consists of contributions by Si and HCO_3. For the fourth dimension, pH dominates in both 1992 and 2021. Where the fifth dimension is contributed to mostly by PO_4 in 1992, it can be witnessed that for 2021 there are no parameters exceeding a contribution of 0.5. The PCA of 1992 needs five dimensions to explain a cumulative 78.3% of the variability; the PCA of 2021 explains 79.2% with four dimensions and 84.2% with five.

K-means Clustering

Several (rigid and fuzzy) k-means clustering analyses were tested (Appendix VI), of which the rigid k-means clustering is presented for the '21 and '92 dataset with the following 14 parameters: pH, NH_4, Na, K, Ca, Mg, PO_4, Cl, SO_4, HCO_3, Mn, NO_3, Si and Fe. These are the same parameters as were used for the PCA within this thesis. These results are compared to each other, and also to the (fuzzy) k-means analyses that was done in the doctoral report on Curaçao's groundwaters based on the '92 dataset (de Bruijne & Louws, 1994). Two of the main differences between the k-means analyses in this thesis and the '94 report are:

1. The set of parameters

In '94 the following 19 parameters were (likely) used to cluster the '92 dataset with: pH, EC, Na, K, Ca, Mg, Cl, SO_4, HCO_3, and minor elements Al, Mn, Zn, Ti, Cd, Co, Cr, Cu, Ni and V. In this thesis Fe, NO_3, PO_4, NH_4, and Si were also included, and of the minor elements only Mn was used. EC was excluded for this thesis. This resulted in the following 14 parameters for this thesis: pH, NH_4, Na, K, Ca, Mg, PO_4, Cl, SO_4, HCO_3, Mn, NO_3, Si and Fe. Still in order to compare a test run was done with the 19 parameters that were likely used in 1992.

2. The number of wells

For the analyses of de Bruijne & Louws (1994), 88 groundwater wells were included for the analyses, whereas in this thesis all 97 wells measured in '92 were included, as it is not known which 9 wells were excluded from the fuzzy k-means of the '94 report; there are currently no available maps of the k-means analyses that was presented in the '94 report.

For this reason, a fuzzy and rigid k-means with 19 parameters that were used in the '94 report was also done, to see what type of clusters were formed and if they - to an extent - coincide with the results from the methods used within this thesis.

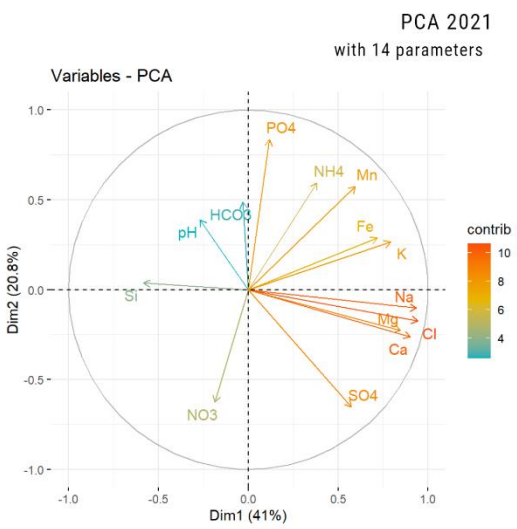

Figure 43. PCA for 2021 with 14 parameters.

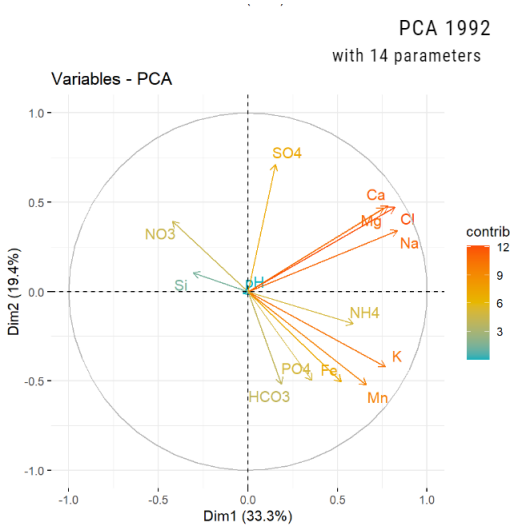

Figure 44. PCA for 1992 with 14 parameters..

Table 38. Correlations between parameters and dimensions for PCA Curaçao, 1992.

	Dimension 1 33%	Dimension 2 19%	Dimension 3 10%	Dimension 4 8%	Dimension 5 7%
Ca	**0.788**	0.474	0.134	-0.036	0.030
Cl	**0.818**	0.463	0.045	0.208	-0.022
Fe	*0.527*	*-0.503*	-0.184	-0.414	0.081
HCO_3	0.185	*-0.518*	*0.481*	0.289	-0.26
K	**0.760**	-0.430	-0.201	-0.027	0.164
Mg	**0.763**	0.462	0.248	-0.025	0.072
Mn	*0.657*	*-0.528*	-0.228	-0.121	0.001
Na	**0.833**	0.333	-0.073	0.208	-0.031
NH_4	*0.588*	-0.183	*0.426*	0.228	-0.280
NO_3	-0.423	0.395	0.249	0.062	0.085
pH	-0.290	-0.074	-0.243	**0.770**	0.383
PO_4	0.346	*-0.502*	0.253	0.066	**0.632**
Si	-0.288	0.117	**0.746**	-0.308	0.344
SO_4	0.159	**0.711**	-0.312	-0.179	0.240

Table 39. Correlations between parameters and dimensions for PCA Curaçao, 2021.

	Dimension 1 41%	Dimension 2 21%	Dimension 3 11%	Dimension 4 7%	Dimension 5 5%
Ca	**0.902**	-0.261	0.177	-0.068	0.031
Cl	**0.944**	-0.174	0.122	0.061	0.042
Fe	**0.719**	0.288	-0.204	-0.322	0.061
HCO_3	-0.029	0.487	**0.756**	0.074	0.040
K	**0.792**	0.264	-0.102	0.188	-0.146
Mg	**0.847**	-0.226	0.303	0.074	0.238
Mn	*0.595*	*0.574*	-0.273	-0.079	0.238
Na	**0.936**	-0.102	0.024	0.129	-0.029
NH_4	0.382	*0.595*	0.378	-0.037	-0.411
NO_3	-0.187	-0.625	0.331	0.231	-0.359
pH	-0.269	0.389	-0.151	**0.808**	0.215
PO_4	0.117	**0.837**	0.120	0.065	-0.054
Si	-0.583	0.036	*0.581*	-0.194	0.425
SO_4	*0.573*	-0.652	0.103	0.183	0.156

1992, check with 19 parameters

For the amount of clusters for 1992 a check was done with 19 parameters (Table 40; Figure 45). The choice was made to assess for five clusters (Table 43; Figure 48), as the configuration of wells is closest to what was tested for in the 1994 doctorate report, and the Bayesian Information Criterion (BIC) number is lowest for five clusters.

Table 40. Cluster size options for check of 1992 with 19 parameters

1992 dataset, with 19 parameters as in '94 doctorate (rigid k-means)				
Clusters	BIC number	Cluster size #2 – 19 parameters	Cluster grouping rigid k-means	
2	1654	1992_check_2c	25, 72	between_SS / total_SS = 18.9 %
3	1500	1992_check_3c	1, 74, 22	between_SS / total_SS = 32.1 %
4	1451	1992_check_4c (cluster size in '92)	56, 15, 25, 1	between_SS / total_SS = 39.5 %
5	**1444**	**1992_5c_check (cluster size in '23)**	**55, 19, 6, 16, 1**	**between_SS / total_SS = 44.6 %**
6	1449	1992_6c_check	6, 52, 16, 7, 15, 1	between_SS / total_SS = 49.1 %
7	1462	1992_7c_check	1, 13, 6, 54, 1, 16, 6	between_SS / total_SS = 53.2 %

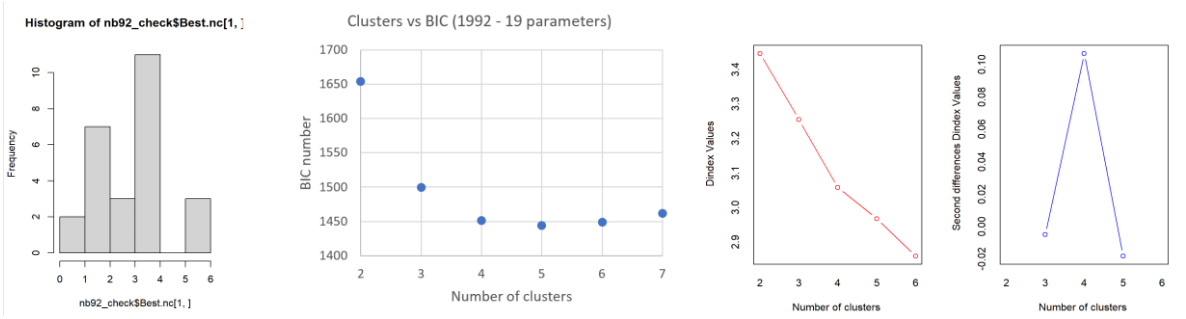

Figure 45. Choosing amount of clusters for 1992, check with 19 parameters. BIC number states that 5 clusters is optimum, whereas majority rule states that 4 clusters is the optimum. Cluster size in '94 was 4 clusters, but with different sizes (not 56, 15, 25, 1).

1992 with 14 parameters (pH, NH_4, Na, K, Ca, Mg, PO_4, Cl, SO_4, HCO_3, Mn, NO_3, Si and Fe)

A cluster analyses was then done for 1992 with 14 selected parameters (Table 41), where certain parameters were removed and others were added. The choice was made to assess for five clusters (Table 44; Figure 46) as this has the lowest BIC number and explains 46% of the variability, despite the majority rule suggesting 2, 3 or 6 clusters. In addition, it is easier to compare to the 1992 analyses where the choice was also made for 5 clusters.

When comparing the results of 1992 with 14 parameters, to the results of 1992 with 19 parameters, it is observed that the clusters are configured differently, yet the largest cluster is spatially very similar. The largest cluster (Cluster 2 for 14 parameters and Cluster 1 for 19 parameters) is of a similar size (47 wells with 14 parameters; 55 wells with 19 parameters).

Table 41. Cluster size options for 1992 with 14 parameters

1992 dataset, with 14 parameters (rigid k-means)					
Clusters	BIC number	Cluster size – 14 parameters	Cluster grouping rigid k-means		
2	1145	1992_2c	14, 83	between_SS total_SS = 24.3 %	/
3	1078	1992_3c	14, 39, 44	between_SS total_SS = 34.0 %	/
4	1051	1992_ 4c (cluster size in '92)	2, 12, 32, 51	between_SS total_SS = 40.8 %	/
5	**1049**	**1992_5c (cluster size in '23)**	**19, 47, 12, 2, 17**	**between_SS total_SS = 45.8 %**	**/**
6	1055	1992_6c	6, 2, 17, 8, 46, 18	between_SS total_SS = 50.0 %	/
7	1057	1992_7c	17, 45, 1, 17, 5, 10, 2	between_SS total_SS = 54.7 %	/

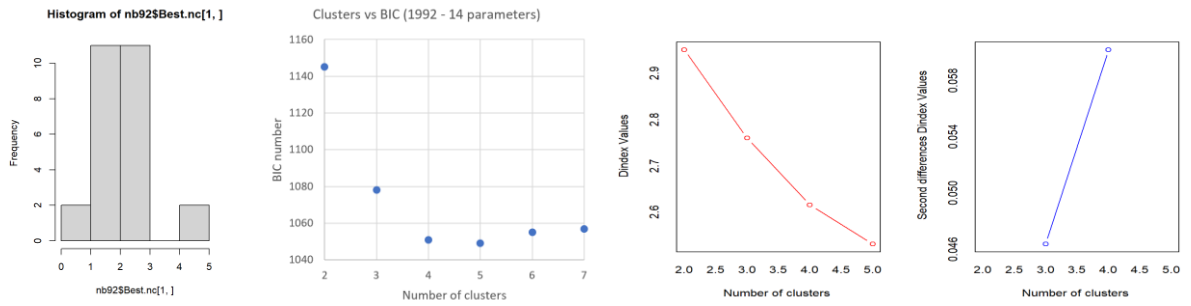

Figure 46. Choosing amount of clusters for 1992, with 14 parameters. BIC number states that 5 clusters is optimum, whereas majority rule states that 2 or 3 clusters is the optimum.

2021 with 14 parameters (pH, NH_4, Na, K, Ca, Mg, PO_4, Cl, SO_4, HCO_3, Mn, NO_3, Si and Fe)

A cluster analyses was then done for 2021 with the same 14 selected parameters as for the second analyses of 1992. The choice was made to assess for five clusters (Table 42; Table 44) as this also has the lowest BIC number and is consistent with how the previous cluster sizes were chosen for 1992.

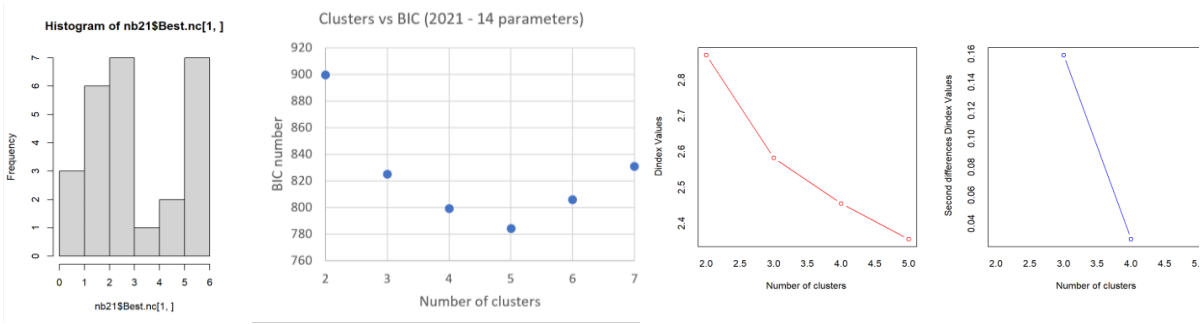

Figure 47. Choosing amount of clusters for 2021, with 14 parameters. BIC number states that 5 clusters is optimum, whereas majority rule states that 2, 3 or 6 clusters is the optimum.

Table 42. Cluster size options for 2021 with 14 parameters

2021 dataset, with 14 parameters (rigid k-means)				
Clusters	BIC number	Cluster size #2 – 19 parameters	Cluster grouping rigid k-means	
2	899,5	2021_2c	56, 22	between_SS / total_SS = 27.9 %
3	824,96	2021_3c	14, 44, 20	between_SS / total_SS = 40.4 %
4	799,11	2021_ 4c (cluster size in ’92)	15, 42, 14, 7	between_SS / total_SS = 48.5 %
5	**783,97**	**2021_5c**	**18, 4, 5, 35, 16**	**between_SS / total_SS = 55.6 %**
6	805,9	2021_6c	17, 4, 14, 5, 35, 3	between_SS / total_SS = 59.2 %
7	830,9	2021_7c	32, 2, 7, 6, 3, 13, 15	between_SS / total_SS = 62.5 %

Table 43. Cluster analyses for five clusters for 1992, with 19 parameters. As a check to compare to 1994 doctorate report.

Cluster size	Cluster 1: #55 wells		Cluster 2: #19 wells		Cluster 3: #6 wells		Cluster 4: #16 wells		Cluster 5: #1 well	
Parameters	C1_mean	C1_std	C2_mean	C2_std	C3_mean	C3_std	C4_mean	C4_std	C5_mean	C5_std
pH (-)	7,40	0,28	7,40	0,33	7,06	0,094	7,33	0,48	7,26	NA
EC (mS/cm)	1.7	0.50	1.6	0.85	15.8	8.3	5.3	2.5	22.3	NA
Na (mg/L)	182	103	217	113	2262	1191	789	606	3612	NA
K (mg/L)	1,2	1,5	7,8	6,2	48,4	58,3	9,3	14,5	618	NA
Ca (mg/L)	102	40	104	54	854	867	259	150	3430	NA
Mg (mg/L)	81	35	65	39	819	896	185	118	3155	NA
Cl (mg/L)	356	211	360	309	7128	5394	1648	942	14400	NA
SO_4 (mg/L)	111	82	70	55	827	1047	481	538	1074	NA
HCO_3 (mg/L)	443	100	502	174	846	899	411	162	195	NA
Al (mg/L)	0,052	0,0411	0,24	0,42	0,28	0,63	0,15	0,26	13,3	NA
Mn (mg/L)	0,030	0,1089	0,56	1,03	1,29	1,14	0,39	0,93	0,78	NA
Zn (mg/L)	0,104	0,1411	0,09	0,09	0,002	0	0,56	1,24	3,81	NA
Ti (mg/L)	0,002	0,0017	0,03	0,07	0,011	0,0260	0,0029	0,00477	3,3	NA
Cd (mg/L)	0,002	0,00073	0,00	0,0015	0,010	0,0237	0,0018	0,00243	0,0012	NA
Co (mg/L)	0,007	0,00540	0,02	0,0511	0,026	0,0575	0,0119	0,02229	3,03	NA
Cr (mg/L)	0,003	0,00087	0,02	0,0480	0,003	0	0,0031	0	1,86	NA
Cu (mg/L)	0,015	0,01063	0,04	0,0605	0,055	0,021	0,0031	0,01781	2,85	NA
Ni (mg/L)	0,006	0,00471	0,02	0,0201	0,004	0	0,0045	0	2,16	NA
V (mg/L)	0,085	0,04966	0,04	0,1033	0,002	0	0,0116	0,02925	3,39	NA

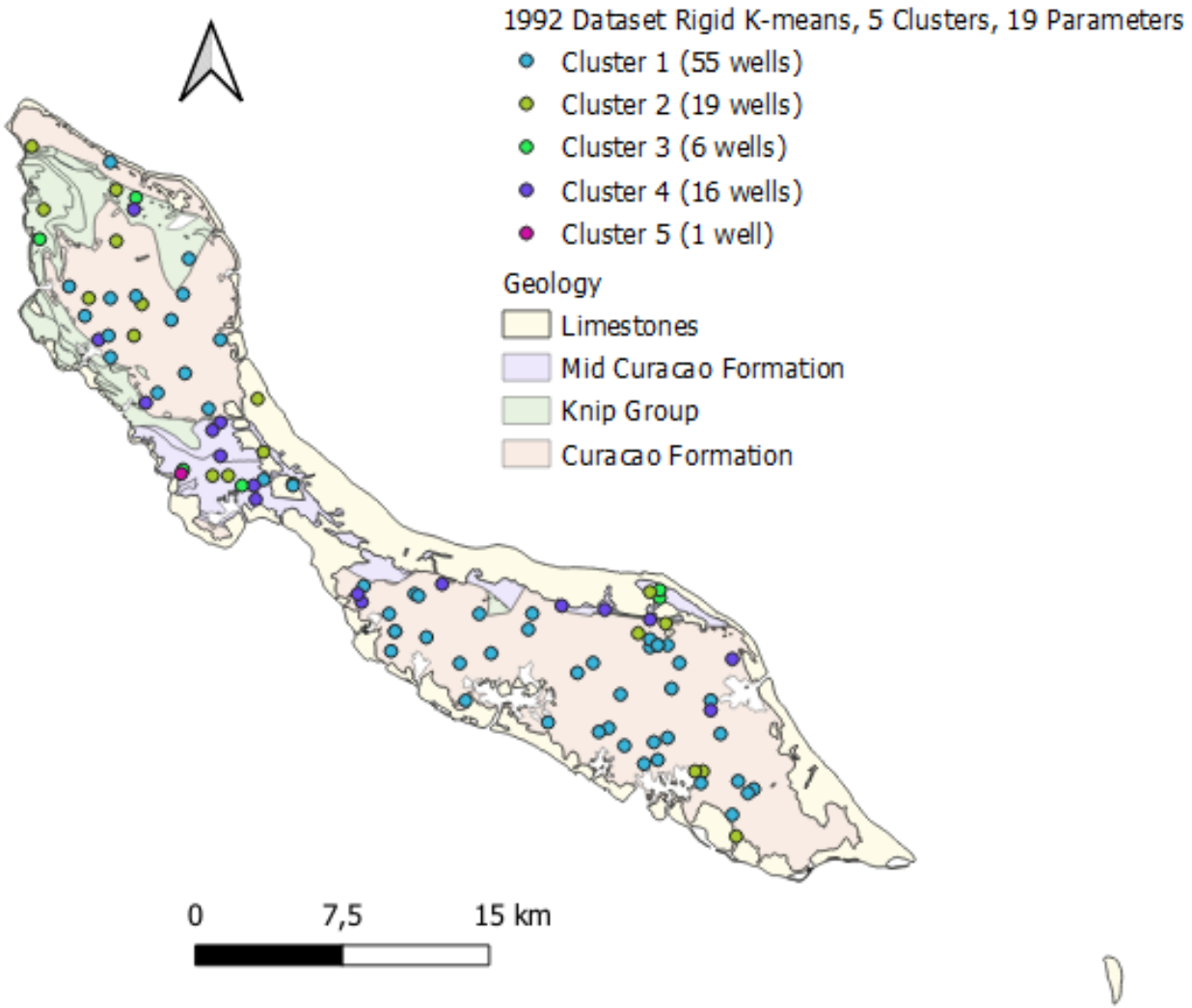

Figure 48. Rigid k-means Clusters Map Curaçao, 5 Clusters, 1992 (19 parameters)

Table 44. Cluster analyses for five clusters for 1992, with 14 parameters.

Cluster size	Cluster 1: #19 wells		Cluster 2: #47 wells		Cluster 3: #12 wells		Cluster 4: #2 wells		Cluster 5: #17 wells	
Parameters	C1_mean	C1_std	C2_mean	C2_std	C3_mean	C3_std	C4_mean	C4_std	C5_mean	C5_std
Ca (mg/L)	72,8	36,4	108,4	33,0	792,2	1013,3	457,4	NA	198,8	148,51
Cl (mg/L)	240,9	205,0	378,1	230,6	5041,8	5127,3	4219,3	NA	1097,4	927,53
Fe (mg/L)	0,5	0,6	0,1	0,1	2,1	3,2	2,9	NA	0,1	0,06
HCO_3 (mg/L)	443,8	136,9	490,2	82,1	436,7	135,9	1779,4	NA	235,2	331,26
K (mg/L)	6,7	6,0	1,6	2,6	72,2	165,3	89,6	NA	1,2	1,43
Mg (mg/L)	44,5	27,7	86,9	27,2	703,3	985,7	441,1	NA	146,8	115,29
Mn (mg/L)	0,3	0,7	0,1	0,1	1,0	1,1	3,2	NA	0,0	0,02
Na (mg/L)	201,9	158,0	193,4	91,3	1782,7	1225,7	934,6	NA	455,2	513,60
NH_4 (mg/L)	0,1	0,2	1,1	4,8	9,1	16,6	215,0	NA	0,2	0,71
NO_3 (mg/L)	21,7	33,7	62,0	61,4	5,4	3,7	4,8	NA	105,9	77,94
pH (-)	7,6	0,3	7,1	1,1	7,1	0,2	7,0	NA	7,5	0,37
PO_4 (mg/L)	1,2	1,3	0,5	0,5	171,9	566,8	5,5	NA	0,3	0,45
Si (mg/L)	20,6	7,6	32,2	3,7	20,9	10,7	15,2	NA	23,2	7,56
SO_4 (mg/L)	80,9	82,1	111,2	82,2	927,2	801,8	1,0	NA	192,2	102,58

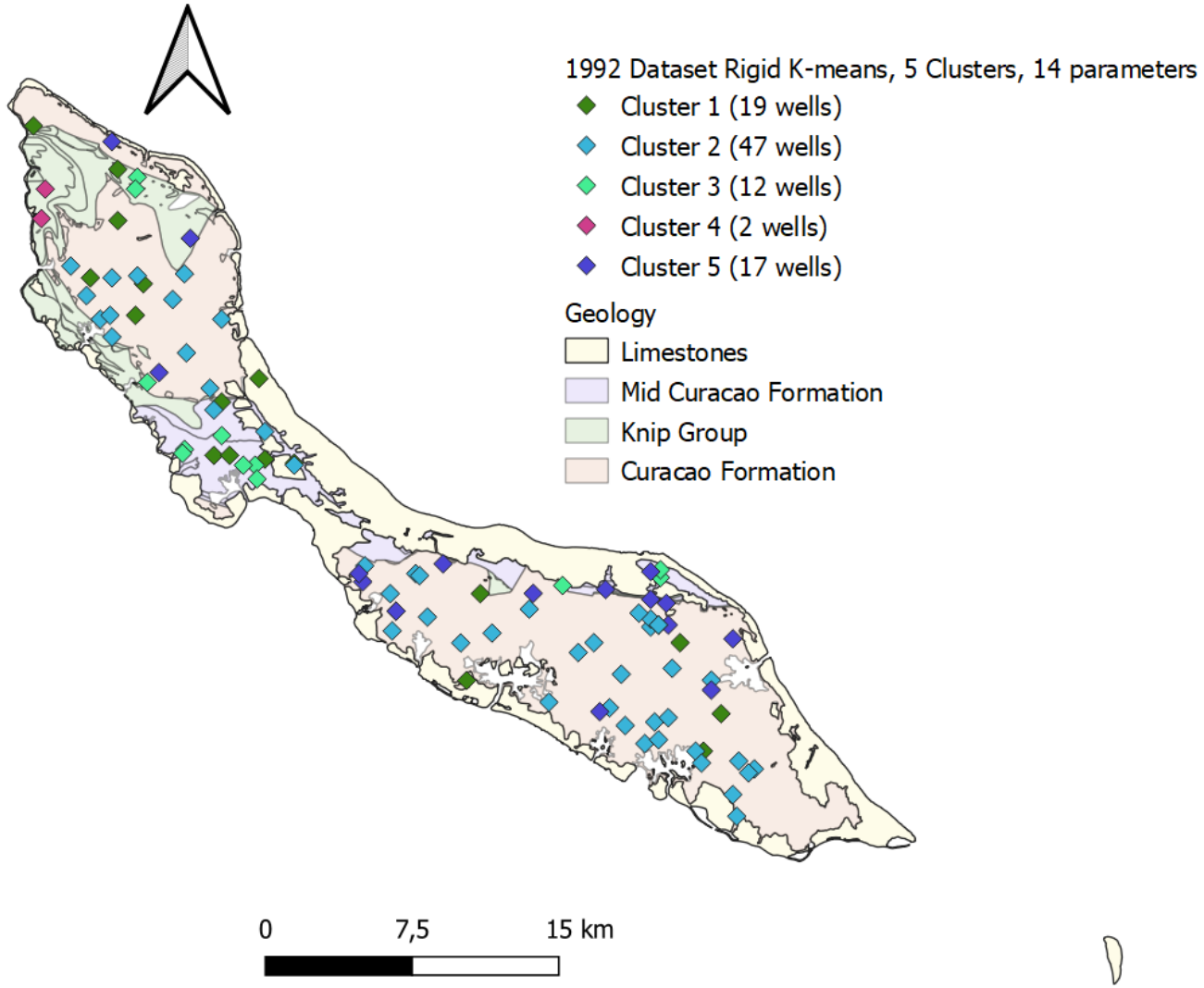

Figure 49. Rigid k-means Clusters Map Curaçao, 5 Clusters, 1992 (14 parameters

Table 45. Cluster analyses for five clusters for 2021, with 14 parameters.

Cluster size	Cluster 1: #18 wells		Cluster 2: #4 wells		Cluster 3: #5 wells		Cluster 4: #35 wells		Cluster 5: #16 wells	
Parameters	C1_mean	C1_std	C2_mean	C2_std	C3_mean	C3_std	C4_mean	C4_std	C5_mean	C5_std
Ca (mg/L)	97,7	49,8	246,3	99,6	1056,0	1239,1	138,5	101	337,0	219
Cl (mg/L)	356,7	429,8	990,6	824,5	5549,1	6762,1	368,9	477	1631,2	1621
Fe (mg/L)	0,2	0,5	0,0	0,0	5,8	7,8	0,0	0	0,0	0
HCO_3 (mg/L)	474,5	154,3	788,7	425,6	399,2	187,8	475,7	116	596,5	523
K (mg/L)	5,4	10,7	4,4	3,5	10,4	4,2	3,2	9	12,3	23
Mg (mg/L)	72,1	50,7	132,5	52,4	573,6	521,9	90,6	60	220,8	128
Mn (mg/L)	243,9	297,8	436,0	519,5	1348,6	1990,2	9,0	12	56,6	54
Na (mg/L)	216,5	218,9	452,5	406,3	2111,4	2269,8	204,8	176	698,0	755
NH_4 (mg/L)	0,4	0,3	1,8	1,8	0,3	0,1	0,2	0	5,0	19
NO_3 (mg/L)	17,4	33,0	71,8	78,1	23,7	47,3	74,6	54	63,3	71
pH (-)	7,4	0,4	6,9	0,2	7,0	0,2	7,1	0	7,1	0
PO_4 (mg/L)	1,5	1,5	4,6	5,2	0,2	0,2	0,8	3	1,9	5
Si (mg/L)	21,2	6,1	26,3	9,7	7,2	5,9	26,8	6	18,6	10
SO_4 (mg/L)	51,3	49,8	64,3	79,7	932,6	549,2	113,5	107	339,7	219

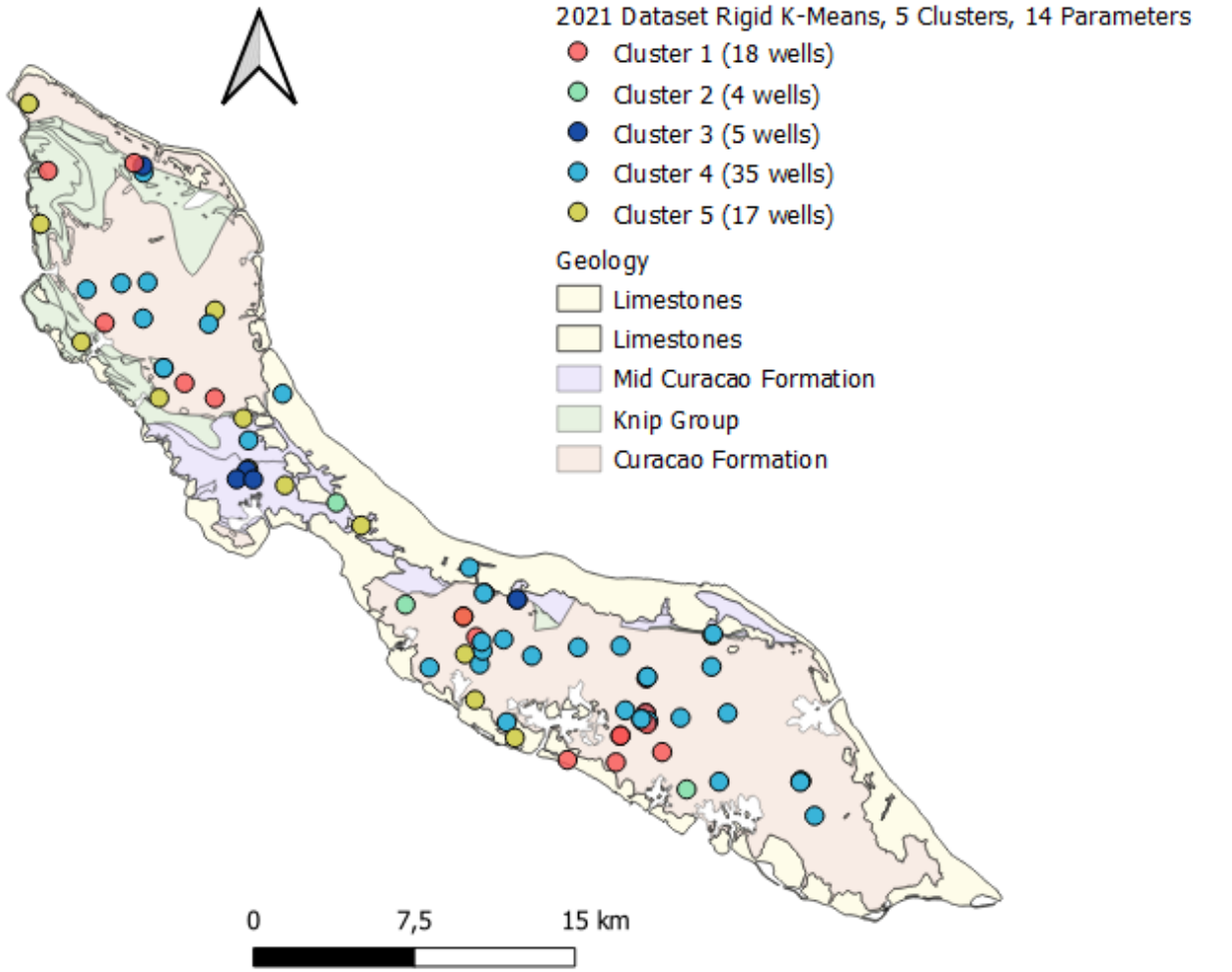

Figure 50. Rigid k-means Clusters Map Curaçao, 5 Clusters, 2021 (14 parameters)

4.3 Water use and well practices

This section describes what came forward in the 2020 fieldwork campaign on the purposes groundwater is used for in Curaçao as described by the well owners and the fate of the wells that were measured in 1992. As was mentioned in Chapter 3 Methodology (“Well selection”), the 97 wells that were measured in 1992 were tracked down in 2020, so that the exact same wells could be measured for better comparison. This was, however, more challenging than imagined and of the 97 wells, only 20 identical wells could be analyzed (20.6%). The reasons why the 77 wells could *not* be sampled can be categorized into: inaccessibility (23.7%), no (more) well (33%), access not granted (7.2%), no one home (13.4%) and unreliable sample (2.1%) (Figure 51 and Figure 52). Inaccessibility meant that there is still a well at the location, but that it is not accessible for measurement. This could be because the well itself is in accessible, e.g. overgrown by thorned bush that is too thick to get close to the well, or just the water was not accessible, e.g. the lid is closed off and specialized equipment is needed to access the well. At other times access was not granted, which meant that there was still a well, but it was either fenced off, it was hard to make an appointment, or people did not feel comfortable to allow us on their terrain to measure, which was mostly when there were visible agricultural practices. Additional reasons why wells could not be sampled the sample was that no one was home after several visits or that there was no well present at the GPS point (either because the well was filled in, a new neighborhood was built, or there was no trace of there ever being a well at all). For two wells a sample could be taken, but it was unreliable, due to dead animals in the well or urination.

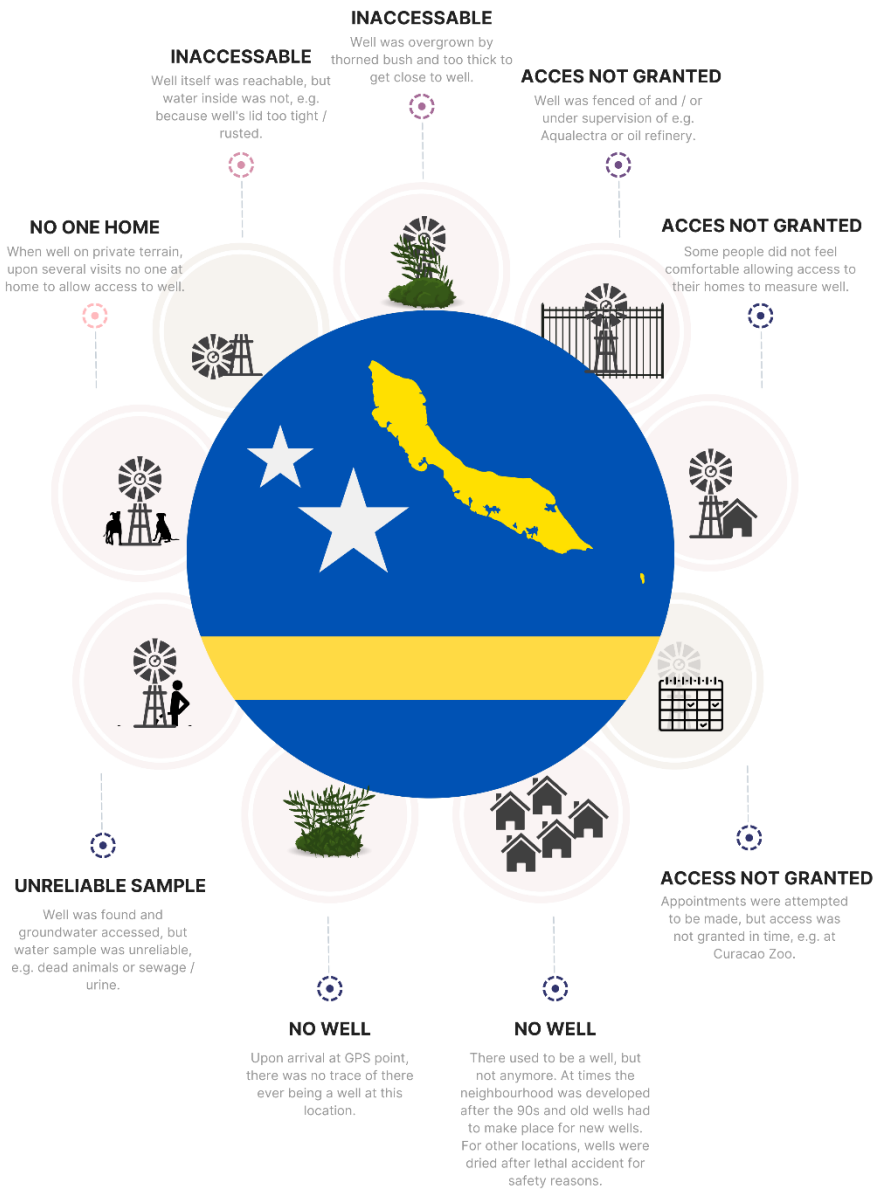

Figure 51. Reasons why 1992 wells could not be accessed or measured in 2020..

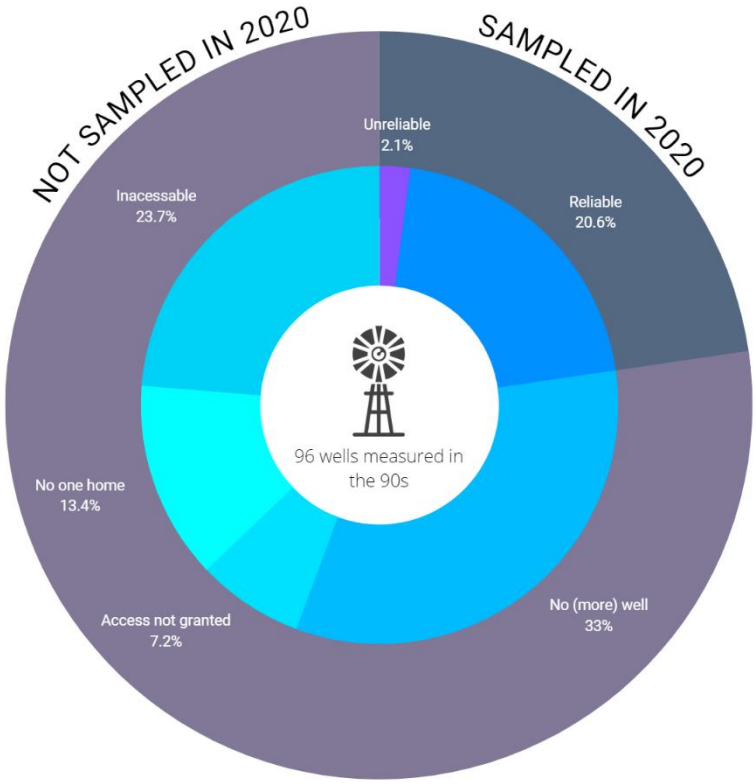

Figure 52. Fate of wells measured in 1992., as visited in 2020

After it became apparent that of the 96 wells in ’92, 80% could not be measured, another well sampling strategy was adopted (see: Methodology), where 71 more wells were measured. Of the visited wells (91 in total), 57 wells had bystanders or owners present that could be asked what the well’s water was used for (Figure 53 and Figure 54). For 44 wells the groundwater was only used for irrigation the agricultural fields (14), the garden (29) or to give to animals (1). For four households groundwater was used for both irrigation and household practices, and for three households groundwater was used for both irrigation

and filling the pool. All eight households that had a well ánd a pool, used groundwater to fill the pool with. Only one well owner used its groundwater to drink from.

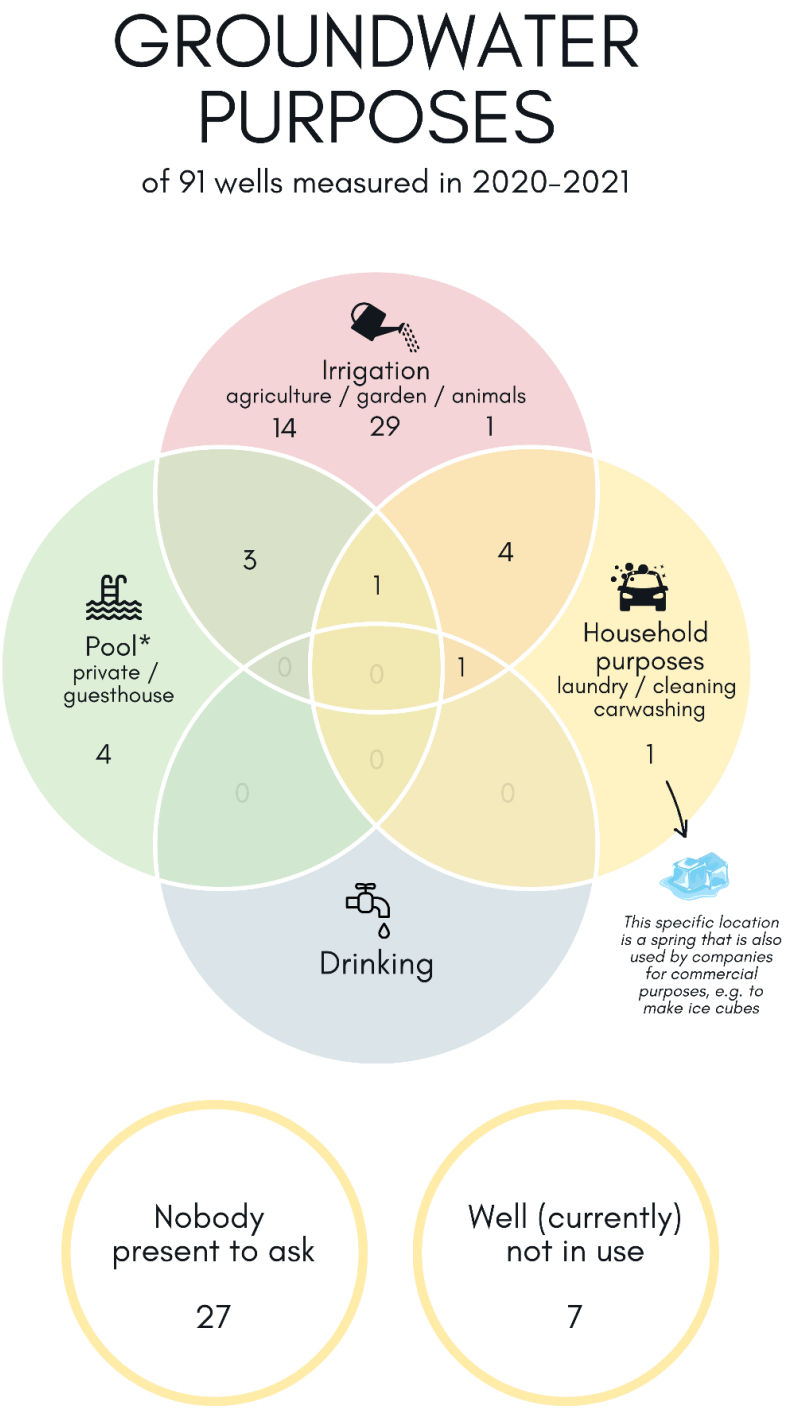

Figure 53. Results groundwater use .of 91 wells measured in 2020.

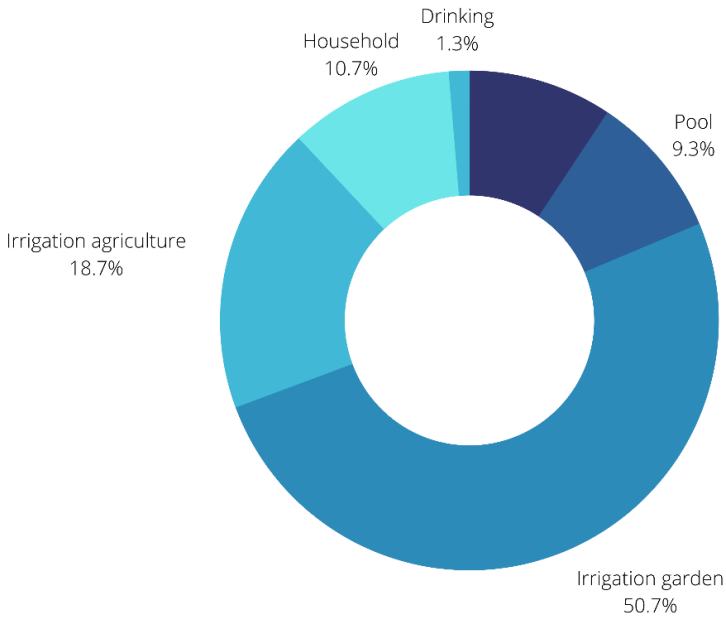

Figure 54. Groundwater use of wells 2020, percentage .of number of well locations per purpose, of which some could be overlapping.

4.4 Runoff and rainwater

In 2020 and 2021, explorative precipitation and surface runoff were taken over the island of Curaçao. The runoff streams were taken in both rural and urban locations. During the '20 fieldwork campaign, the biggest runoff stream was witnessed at Westpunt, Curaçao (Figure 55). For an impression of this runoff stream, please refer to the following video link. For an initial impression of chemical composition of precipitation and runoff the samples taken in 2020 and 2021 were joined together (Appendix IV and Table 46).

Figure 55. Runoff stream direction and flow as witnessed at Westpunt. Curaçao. Dashed arrows are added to illustrate where witnessed streams are expected to originate from as based on height map Curaçao. Estimation of length plume 1 after rainfall had stopped is roughly 80 meters (Google Maps Locations). Runoff streams entering the ocean at Westpunt, Right: Curaçao in November, 2020 during heavy rainfall. Picture taken from Restaurant Playa Forti. Plume 2 formed as rain continued.

Table 46. Significant differences between rain and runoff for samples joined of '20 and '21 (*p-value < 0.05).

Parameter	Rain AVG	Rain STD	Runoff AVG	Runoff STD
EC (µS/cm) ↑ *	63.97	53.08	322	346
HCO_3 (mg/L) ↑ *	10.80	4.43	85.12	28.43
pH ↑ *	6.81	0.52	7.66	0.63
Zn (µg/L) ↓ (*n*=2)	59.54	-	6.75	4.86
Si ↑ *	0.03	0.04	1.75	0.96
Turbidity (NTU) ↑ *	<0.01	-	49.50	9.34
E.coli (CFU/100 mL) ↑*	NM	NM	757767	1048177

EC, HCO_3, pH, Si, Ca and turbidity go up significantly when comparing runoff to precipitation Table 46. Zn goes down in concentration, but has only been measured in two rainwater samples. Notably, the three runoff samples that were measured in 2021 for E. Coli (*n*=3) also had a high coliform count. K, Mg, Na, NO_3, PO_4, SO_4 indicate different values: from low in rainwater, to (slightly) higher average in runoff water, but there is no significant difference between the measurements. For NO_3, K and SO_4 it is two of the 2021 runoff samples, of eight measurements taken in 2020 and 2021, that notably rise by doubling or tripling in concentration.

4.5 Key figures and tables of the results

For ease of reading the Discussion chapter, the key figures and tables of the results chapter are repeated so they can be easily referred to by the reader in order of appearance in the Discussion Chapter.

Differences between 2020 and 2021 dataset

Table 47. Key table. Significant difference of parameters between the '20 and '21 dataset, eastern Curaçao (t-test) and between east '77, '92 and '20.

Test Years. East	Anova, east 1977, 1992, 2020	Anova, east 1977, 1992, 2021	2020	2021	T-test, east 2020 – 2021
Alkalinity (as mg/L HCO_3)	ns	***	376±90	509±185	****
B	-	-			ns
Ca (mg/L)	ns	ns	104±59	147±114	*
Cl	ns	ns			ns
Fe (mg/L)	-	-	0.42±0.19	0.013±0.25	****
F	-	-			**
K (mg/L)	ns	ns	7±10	4±9	****
Mg (mg/L)	ns	*	73±45	104±76	*
Na	ns	ns			ns
NH_4	-	-			****
NO_3	-	-			ns
PO_4	-	-			****
Si	-	-			ns
SO_4	ns	ns			ns

Temperature	**	**	*

*Symbol meaning: ns p > 0.05, * p ≤ 0.05, ** p ≤ 0.01, *** p ≤ 0.001, **** p ≤ 0.0001. Alkalinity as mg/L $CaCO_3$, EC in µS/cm.*

Representativity: 2020, 2021 and comparison of all datasets

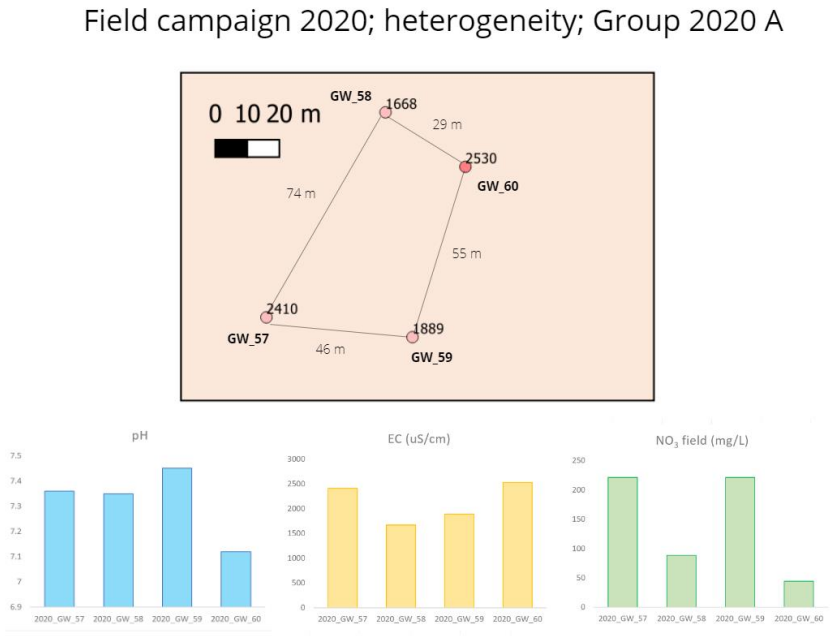

Figure 56. Key figure. Heterogeneity of four wells in the eastern section (group 2020 A). . The numbers in the map are the EC values for each of the wells in µS/cm*.*

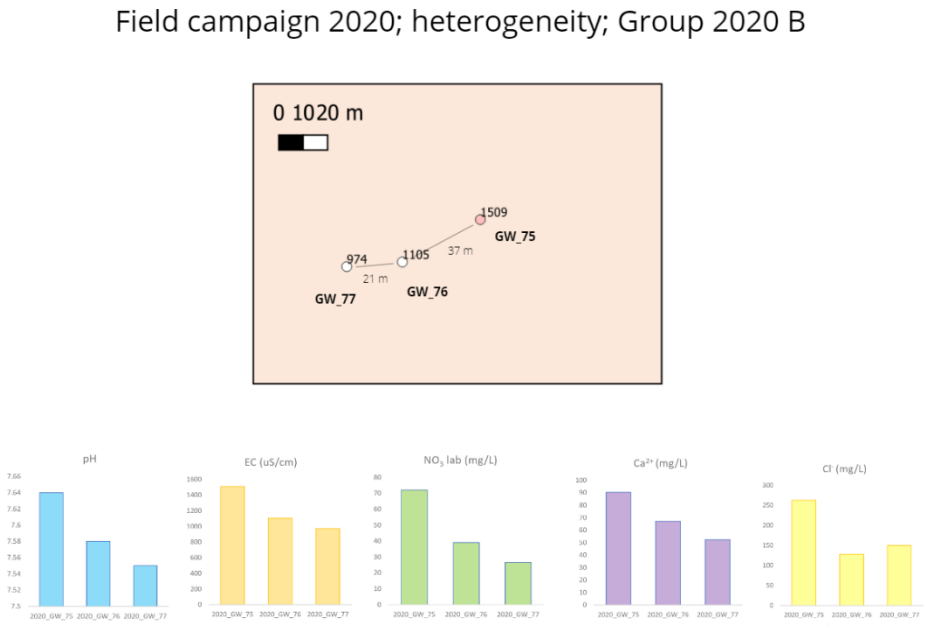

Figure 57. Key figure. Heterogeneity of three wells in the eastern section (group 2020 B). . The numbers in the map are the EC values for each of the wells in µS/cm*. All three wells had a geochemical analyses, and an E.B. < 10% , therefore NO3, Ca and Cl are showcased, besides EC and pH.*

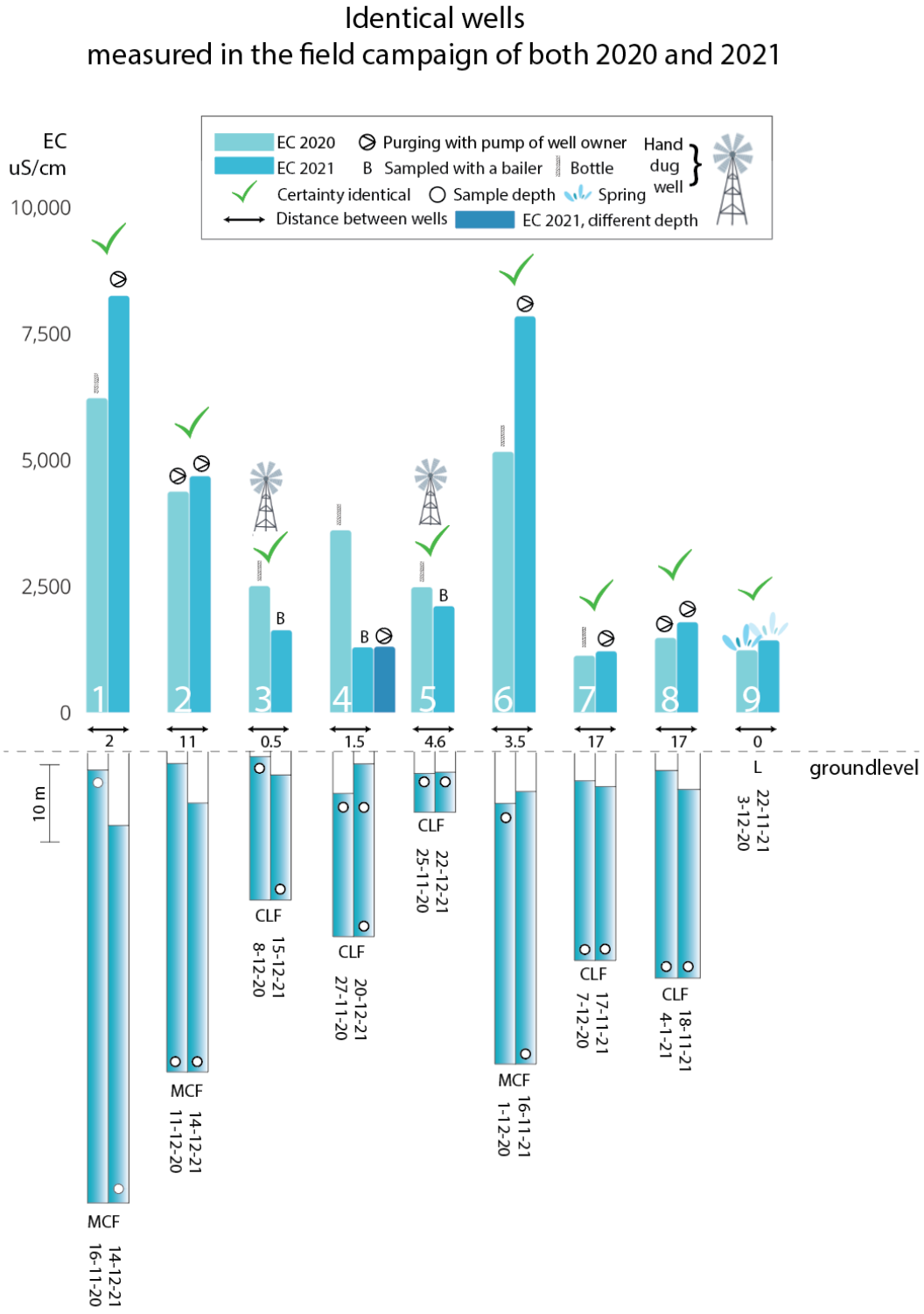

Figure 58. Key figure. Identical wells measured in both 2020 and 2021. The 7-9 wells that were measured in both 2020 and 2021. Top part illustrates the EC value in µS/cm, the bottom part illustrates the actual wells with their depth and water levels to scale (scale = 10 m).There is symbology for sample depth, well depth and water level in relation to ground level, distance between wells 2020 and 2021 as based on QGIS, purging method per year (bailer, pump of owner or bottle), geology (CLF for Curaçao Lava formation, MCF for Mid Curaçao formation, L for Limestones), a mill symbol for hand dug wells, the date of sampling for both years and the certainty of if these are indeed identical wells.

Chemical trend through the decades: groundwater freshening

Table 48. Key table. Significant difference of EC over the decades, between '77, '92, '20 and '21 dataset: for total island, eastern island, western island and per geology.

Parameter (anova)	1977-1992	1977-2020	1977-2021	1992-2020	1992-2021	2020-2021
[1]EC – total (*)	*↓	ns	ns	ns	ns	ns
[2]EC – east (***)	*↓	*** ↓	***↓	ns	ns	ns
[3]EC – west (ns)	ns	ns	ns	ns	ns	ns
[4]EC – Diabaas East (**)	*↓	**↓	**↓	ns	ns	ns
[5]EC – Diabaas West (ns)	ns	ns	ns	ns	ns	ns
[6]EC – Knip (ns)	ns	-	ns	-	ns	-
[7]EC – Limestones (ns)	ns	ns	-	ns	-	-
[8]EC – Mid Curaçao (ns)	ns	ns	ns	ns	ns	ns

*Symbol meaning: ns p > 0.05, * p ≤ 0.05, ** p ≤ 0.01, *** p ≤ 0.001, **** p ≤ 0.0001. Some geologies for certain years did not have any measurements, for those comparisons a "-" sign is present.*

Chemical trend through the decades: acidification and related processes

Table 49. Key table. Significant difference of pH and alkalinity (per year and geology), all of Curaçao.

Parameter (anova)	1977-1992	1977-2020	1977-2021	1992-2020	1992-2021	2020-2021
[1]pH – total (≥***)	****↓	****↓	****↓	ns	***↓	*↓
[2]pH – east (*)	**↓	ns	****↓	ns	ns	**↓
[3]pH – west (≥***)	***↓	****↓	****↓	*↓	**↓	ns
[4]pH – Diabaas East (≥***)	ns	ns	****↓	ns	ns	* ↓
[5]pH – Diabaas West (≥***)	***↓	****↓	****↓	*↓	**↓	ns / *↓
[6]pH – Knip (ns)	ns	-	ns	-	ns	-
[7]pH – Limestones (ns)	ns	ns	-	ns	-	-
[8]pH – Mid Curaçao (**)	*↓	**↓	**↓	ns	*↓	ns
[1]Alkalinity – total (**)	**↑	ns	****↑	**↑	ns	****↑
[2]Alkalinity– east (*)	**↑	ns	***↑	**↑	ns	****↑
[3]Alkalinity – west (ns)	ns	ns / -	ns	*↑ / -	ns	ns / -

*Symbol meaning: ns p > 0.05, * p ≤ 0.05, ** p ≤ 0.01, *** p ≤ 0.001, **** p ≤ 0.0001. HCO_3 measurements for '20 were taken with different methodology and most likely gave an underestimation of the alkalintiy. For alkalinity, the '20 results could in addition not be validated with the ion balance and therefore also have an "-" sign present.*

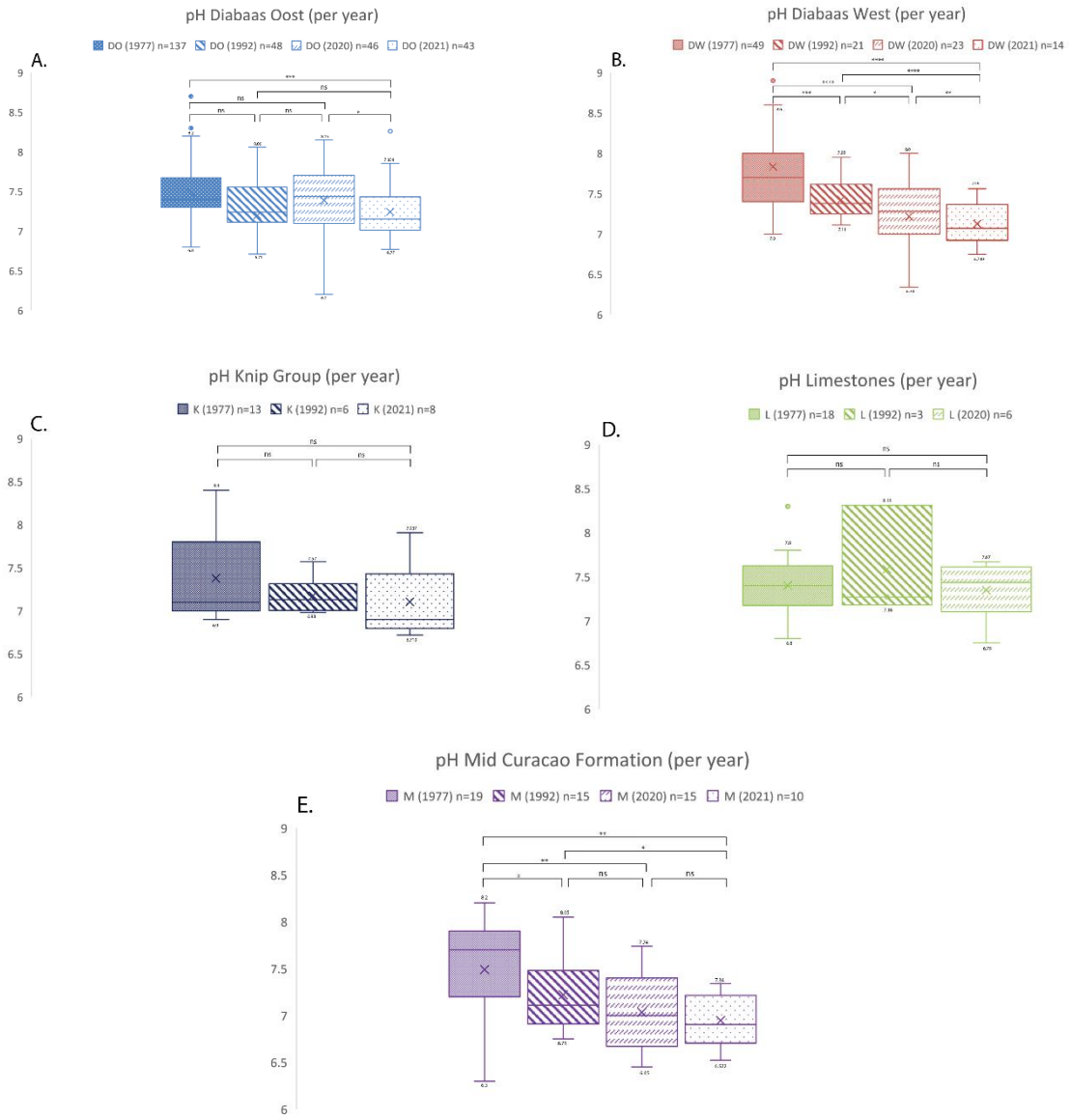

Figure 59. Key figure. Boxplot comparison of pH per geology over the decades.. A) pH of Diabaas East (Diabase East) for '77, '92, '20 and '21. B) pH of Diabaas West (Diabase West) for '77, '92, '20 and '21. C) pH of Knip Group for '77, '92, and '21. D) pH of Knip Group for '77, '92, and '20. E) pH of Mid Curaçao formation for '77, '92, '20 and '21.

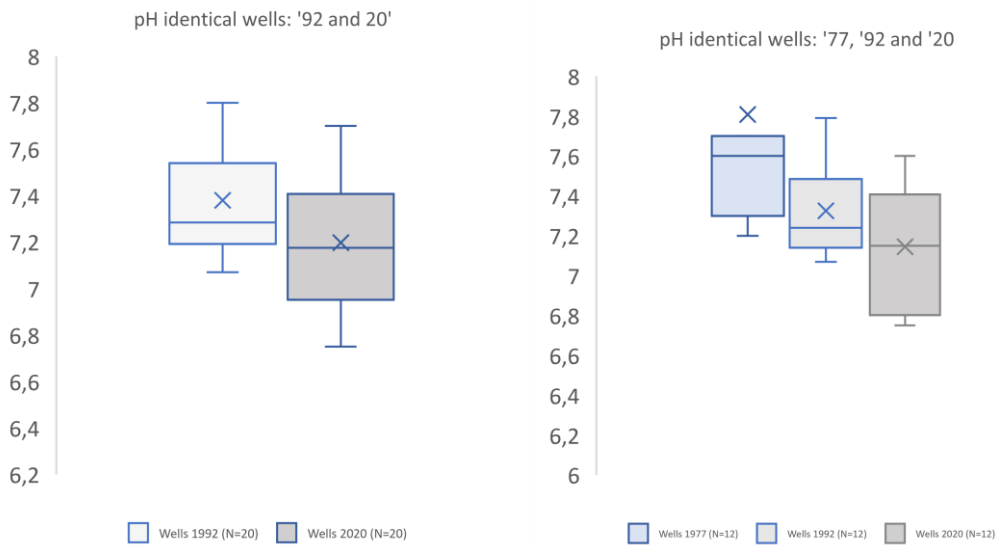

Figure 60. Key figure. Boxplots of pH for identical wells. a) 92 and '20, b) '77, '92 and '20

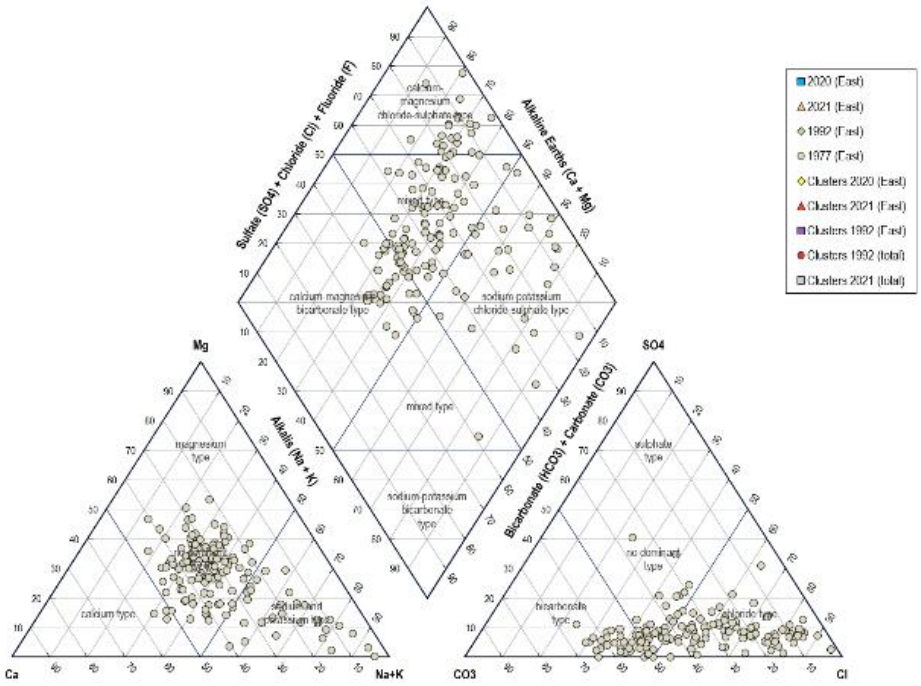

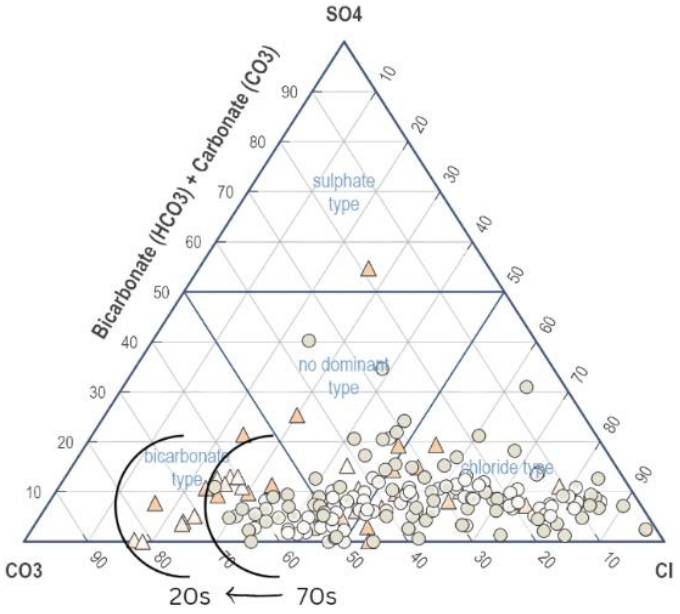

Figure 61. Key figure. Piper diagrams for different datasets, eastern side.Top) Piper diagram for 1977, east. Bottom) Zoom in anion side for '77 and '20-'21.

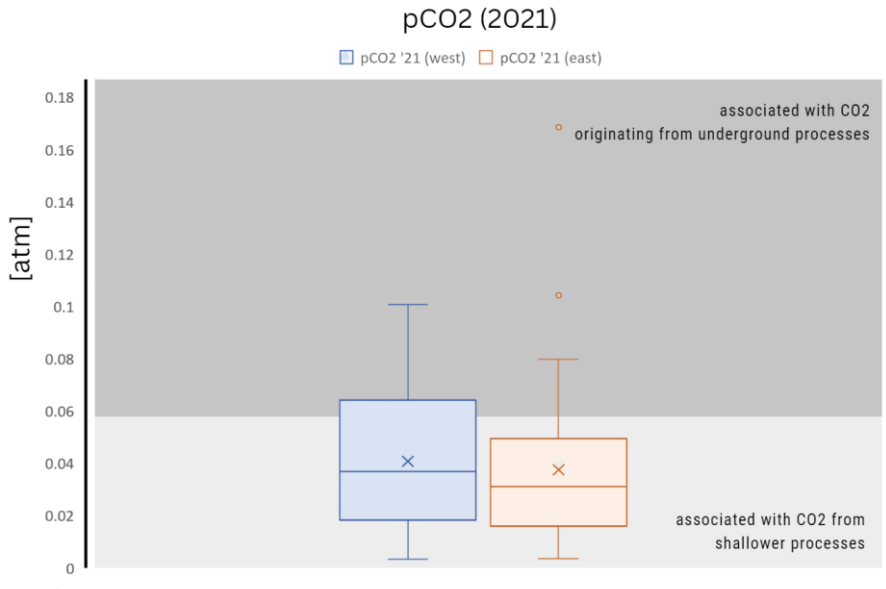

Figure 62. Key figure. pCO_2 for 2021. Unit in atm. pCO_2 east and pCO_2 west visualized in boxplots for 2021. Bottom is associated with shallower processes of CO_2, top is associated with processes of the deeper underground.

Table 50. Key table. SO_4 concentrations (mg/L) for different years (east-west), and their p-values.

	1977	1992	2020	2021
East	114 ± 123	134 ± 122	NA	116 ± 136
West	267 ± 423	334 ± 584	NA	433 ± 687
p-value	0.00016 (***)	0.22 (ns)	NA	0.011 (*)

*Symbol meaning: ns $p > 0.05$, * $p \leq 0.05$, ** $p \leq 0.01$, *** $p \leq 0.001$, **** $p \leq 0.0001$.*

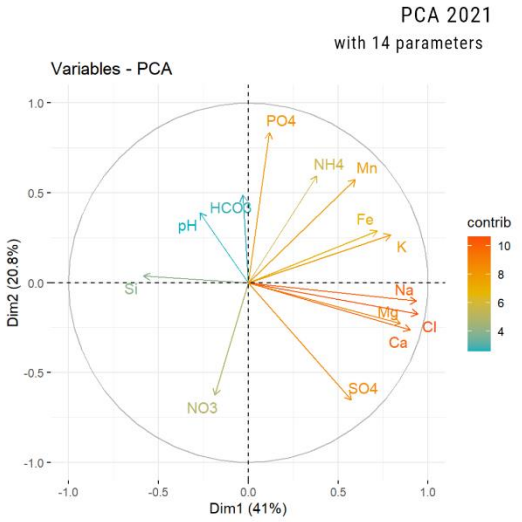

Figure 63. Key figure. PCA for 2021 with 14 parameters.

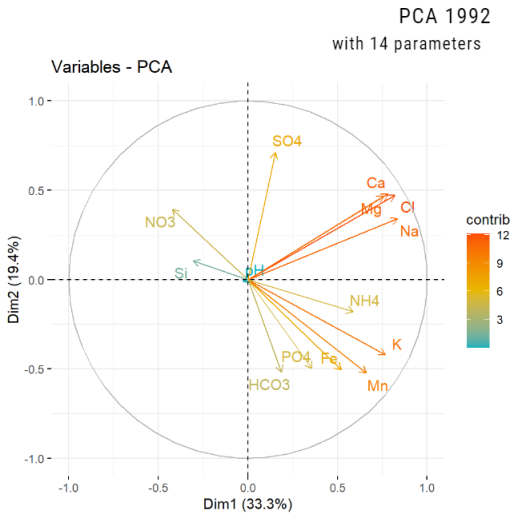

Figure 64. Key figure. PCA for 1992 with 14 parameters..

5 Discussion

In this chapter the results of this thesis' fieldwork campaign and its relation to older datasets will be discussed. For ease of reading the research questions as presented in Chapter 1 Introduction are followed to structure this Discussion chapter. At first the groundwater results for 2020 will be discussed (§5.1). Emphasis is put on the representativity of the dataset and its comparison with the field campaign of 2021. For the second section of the discussion (§5.2), the overall geochemical trend between all datasets over the decades is discussed ('77, '92, '20, '21) while addressing possible explanations of the underlying causes and reactions that could be related to the found changes over time. This section is subdivided in: §5.2.1 Salinization and freshening, §5.2.2. Groundwater Acidification and Related Processes, and §5.2.3. Nutrient pollution. In the third part of this chapter (§5.3) rain and runoff are discussed and in §5.4 the multivariate statistics over the '21 and '92 dataset are discussed: Principle Component Analyses and Cluster Analyses.

5.1 Representativity: 2020, 2021 and comparison of all datasets

One of the aims for this thesis was to determine the representativity of the '20 dataset and see how its findings differ or relate to the wells that were sampled in '21. The expectation was that there would be no significant differences between the groundwater chemistry of these adjacent years, as the field campaign in '20 and '21 had similar rain seasons, were sampled only one year apart in similar months, and had a similar distribution homogeneity over the island (Table 15; Methodology), even with only seven identical wells between the years. Having coinciding data could have allowed for the 2020 (n=91) and 2021 (n=71) dataset to be combined into one larger 2020/2021 (n=162–7=155) dataset. This was, however, not the case. As was witnessed in Table 47, the '20 and '21 differ significantly on a range of parameters, among which: alkalinity, Ca, Fe, F, K, Mg, NH_4, and PO_4. This means that, as of now, the '20 and '21 dataset cannot be combined.

Combining 2020-2021: Distortion in dataset

The most likely explanation for the differences between 2020-2021 would be that the incomplete dataset of '20 distorts the results for the 2020 field campaign, as not all samples could be fully analyzed (Methodology, Section 3.2.2; Results, Section 4.1.1) and 13 higher salinity samples were excluded from the eastern '20 dataset (*n*=52) (Appendix I). This means that the higher salinity wells are underrepresented, which is in line with nearly all parameters of '20 being significantly lower than '21. Having a complete 2020 dataset, and including the samples that are now missing when the ICP-MS of TU Delft's Waterlab is working again, will give more insight and confirm if this is indeed the case. However, even in a situation where all '20 samples are analyzed, caution must be taken before combining the results of '20 and '21, as there are various other factors that could also have played a role in the dissimilarities between the two datasets, which will be further discussed, namely:

- The difference in field methodology between the field campaigns
- Season and rainfall
- The well sampling strategy applied in both years

Combining 2020-2021: Differences in the field methodology

When comparing the field methodology for the '20 and '21 fieldwork period, there are clear differences in the approach for groundwater collection and purging (Methodology, Table 15). In 2020 groundwater

was retrieved with a weighted bottle from roughly one to three meters below water surface, but would un-avoidantly include water from surface level. Groundwater could only be pumped and purged if the owners had their own stationary pump. The extent of pumping depended on the activity of the well; if wells were used daily, less pumping was done than if they were mainly inactive. In 2021 the stationary well pumps of the well owners were also used when present, but when missing a bailer, hand pump or vacuum pump could be used to sample from greater depths than was possible for the field campaign in ’20.

This difference in sample collection could have had several effects on the groundwater quality. The field methodology that is applied for groundwater research can directly affect the quality of the collected data in any phase of the field campaign: from initial sampling, purging to timing of analyses and storage arrangements. It is even said that most systematic and random errors within groundwater research occur within the field, not the lab (Thornton, 2008). The chemical composition of groundwater can also have large variations, even at a small scale (several meters), due to stratification and mixing of layers and chemical reactions. Mixing can also happen during sampling, especially so for inactive wells with stagnant water or groundwater with a large surface in contact with air (Appelo & Postma, 2005). For this reason, purging properly is essential in order to introduce fresh groundwater into the well before collection. The extent of bias that can occur depends on several variables that influence the stagnant layer, such as the degree of isolation, direction of groundwater flow (vertical or horizontal), the activity of the well, exposure to the atmosphere and well design (Nielsen & Nielsen, 2005). Research has shown that the method used for purging can also directly influence groundwater quality, meaning that purging itself can significantly alter the water chemistry, again resulting in groundwater samples that are not representative (Thornton, 2008). It is therefore important to be consistent in purging methodology, whilst also finding the right balance between excessive and too little purging to be able to collect samples that actually reflect the in situ conditions of the aquifer. Appelo & Postma (2005) estimated that for general hydrological conditions, two to four replaced well volumes would be sufficient, although this can go up to ten replacements under certain conditions, depending on the local hydrological situation. If purging is not possible, it is recommended to take thorough fieldwork notes, so that information can still be collected, but the representativity of the well can later be determined in the data-analyses phase, and if needed excluded.

When looking at the results for ‘20 and ‘21, only seven identical wells could be compared one-on-one, a low sample size (Table 32). Nonetheless, it is already clear that there are differences between them, when looking at salinity (Figure 58). The wells that were actively used in both 2020 and 2021, or where a pump could be used for both years, have similar EC’s (Figure 58: well 2, 8, 9). The wells in MCF, where samples were taken from different depths due to different sampling methods, show a much larger difference in salinity between ’20 and ’21 (Figure 58: well 1 and 6). It is therefore likely that in ’20 more wells were sampled from a layer that was not representative of the actual aquifer, as there were more wells where purging could not occur due to lack of groundwater pumps. The difference is more apparent for the three MCF wells than the CLF wells. This could be because CLF generally has a different hydraulic conductivity than MCF (more permeable), lower salinity water, and also shallower wells, making a difference over depth not as distinctive as in MCF. Still, within CLF there are slight differences, but the differences in EC for the CLF (17%, 8% and 18%) and L are no more than what was considered normal or seasonal (< 20%) salinity fluctuations within the 1977 fieldwork campaign (Abtmaier, 1978).

When potentially combining the ’20 and ’21 dataset for future research purposes, it could be beneficial to look into establishing a correction factor based on depth for the wells of the 2020 dataset that are sampled at water level, especially for geologies where it seems to make a difference, such as MCF. Alternatively, it could also be an option to, as a general rule, only include the wells of ‘20 that were able to be sampled at greater depth, after purging, due to the presence of a working pump, and exclude those sampled at water level, depending on geology, well type and activity of the well. This seems to be a more favorable option than comparing, combining or correcting the EC of wells based on stratification found in proximate wells, as there is a large heterogeneity in water quality, even for wells in which the

same field methodology is used, and that are at very short distances of each other, such as 6 or 11 meters (Heterogeneity; Figure 56 and Figure 57).

In addition to sample depth, alkalinity was determined with different methods. Where in '21 titration was used, in '20 the Lovibond MD610 was used, a device that determines alkalinity through spectrophotometry. Although the method itself could have caused the lower alkalinity values that were found for '20 (Table 47), there is another reason that could explain the alkalinity of '20 being significantly (****) lower than '21, namely the degassing of CO_2 that occurs in water that is sampled closer to water level. The solubility of CO_2 is proportional to the length of the water column (10 meters depth is equal to 1 atm); this means that sampling at higher (stagnant) levels, can result in increased pH and decreased alkalinity, as shown in Eq. 5-1 and Eq. 5-2. Both equations shift to the right, reducing the H^+, HCO_3^- and some of the dissolved components, like Ca, Fe or Mn (Thornton, 2008).

$$H^+ + HCO_3^- \leftrightarrow H_2O + CO_2\ (g)\ (Eq.\ 5\text{-}1)$$

$$Ca^{2+} + 2\ HCO_3^- \leftrightarrow CaCO_3 + H_2O + CO_2\ \ (Eq.\ 5\text{-}2)$$

With stagnant layers, the top layer of water will also re-equilibrated with atmospheric pO_2, which can also result in lower concentrations for parameters that are redox-sensitive, such as Fe^{2+} (Eq. 5-3) a parameter that is also significantly lower for the '20 dataset (Table 47: ****).

$$O_2\ (g) + 4\ Fe^{2+} + 10\ H_2O\ \rightarrow 4\ Fe(OH)_3\ (ppt) + 8\ H^+\ (Eq.\ 5\text{-}3)$$

Combining 2020-2021: Season and rainfall

The expectation was that the influence of rainfall for comparison would be negligible, as wells in 2020 and 2021 were both measured in relatively wet rain seasons (Methodology; Table 15); also supported by the water balance of 1977, where it was stated that 4% of rainwater infiltrated as groundwater in the west, and 2% in the west (Abtmaier, 1977). The true influence is, however, unclear as the wells in '92, '20 and '21 groundwater were sampled as a single event, and the emphasis was on obtaining spatial distribution, not repetitive sampling in one location. Rain will also have a larger influence if the wells are sampled from the upper layers and / or not properly purged. In addition, the seasons in 1977 and 1992 were similar to each other, but dryer than 2020 – 2021, which could mean that the concentrations for recent years are potentially underestimated for the wells where rainwater did potentially influence due to lack of proper sampling technique. Overall, the consideration is still that the influence of rain is minimal, provided that that the sample is properly obtained - another reason to emphasize on adequate sampling methodologies.

Combining 2020-2021: Well sampling strategy and distribution

Although the definition for "representative" varies, it statistically entails a dataset that is of a smaller size, yet able to reflect the quality of whatever is being studied as closely as possible (Borovicka et al., 2012). For groundwater representativity this does not just relate to the quality of sampled water, but also to the amount of wells, referring back to the well sampling strategy and distribution over the island. If the datasets would not have significantly differed, the general assumption could have been that the amount of wells samples in 2020 and 2021 (70-90) is a large enough group to be able to say something about large-scale chemical processes and trends that have occurred over the decades, and will balance out any of the heterogeneity that was witnessed on a smaller scale (Figure 56; Figure 57).

An approach to reduce the influence of location and "well type" as a contributor to heterogeneity between datasets, the exact same wells as previous years could be measured. This could aid in a better overall comparison when gathering enough data points or increasing the sample size is challenging, and could potentially reduce the effects of local variability, such as distance from septic tank influencing e.g. nitrate concentration, or well type influencing e.g. pH (Verstappen, 2022). For this reason, the initial well

sampling strategy of the ’20 field campaign was to hunt down the exact same wells as were measured in ‘92 (Methodology; Well Sampling Strategy). This was, however, not realistic and not possible. All wells that were sampled in ‘92 wells were attempted to visit, but only 20 out of 96 wells could actually be sampled. Reasons for this varied widely (Figure 51). Due to the expenses that come with maintaining these older fashioned wells and mills (Personal communication, 2021), many are now abandoned and overgrown (Methodology; Figure 52).

Representativity: Datasets of 1977 and 1992

It is important to note that the field methodologies did not just differ between 2020 and 2021, but also between 2020 – 2021, 1992 and 1977 (Methodology, **Table 15**). It is unclear what purging technique was used in 1992, but it seemed to have been done with a weighted bottle similar to 2020. During the 2021, 2020 and 1992 field campaigns pH was measured directly after sampling. For 1977, however, it is unclear if pH was measured in the lab or field, as it is not mentioned in the report and the Annex containing the lab analysis is missing from the available documents. If pH was indeed measured in the lab, degassing, as shown in Eq. 5-1 and Eq. 5-2, might have occurred, precipitating the $CaCO_3$, and increasing the pH. This is also the reason why groundwater pH must be measured in rapidly, preferably within 15 minutes of sampling. This means that even with proper purging and sampling, the pH will not be representative of the water quality in the aquifer if not measured within the window. The potential effects of pH measuring and long-term trends are further discussed in section §5.2.2. Groundwater Acidification and Related Processes.

Besides sample collection methodology and timing, other variations could be caused by different measurement moments within the season, equipment type, calibration or handling. Although a uniform sampling methodology has now been set up by PhD-candidate M. Wit for the SEALINK project to avoid discrepancies in sampling for current and future groundwater research, the mentioned effects of field methodology differences must still be taken into consideration when comparing current and future data with the 90s and 70s for long-term trends.

Overall, gathering a representative dataset can be challenging, as groundwater research is a dynamic field, that requires improvisation and flexibility from the researcher – especially in regions such as Curaçao where social and logistic challenges can overshadow scientific and hydrogeochemical preferences for sample collection. With a scientific standard that is too high, one might risk not gathering enough samples to obtain a large enough dataset, but with a standard that is too low, one might obtain many samples, but that are not representative of the in situ aquifers. Without a network of well-maintained monitoring wells, it remains to be a balancing act.

Summary interpretation of representativity:

The 2020 and 2021 dataset cannot be combined, because they significantly differ on a range of parameters. There are different potential causes for the significant difference, namely: the distortion in dataset due to problems with the ICP-MS, the differences in field methodology between the field campaigns, and the well sampling strategy applied in both years
The most obvious explanation is the distortion in the ’20 dataset, which can be ruled out once the complete ’20 dataset has been re-analyzed. If after this full analyses there is:

- a significant difference between ’20 and ‘21, the datasets should still not be combined as differences in field methodology and/or sampling strategy are likely at play.
- no significant difference between’20 and ’21, the datasets could potentially be combined.

It is advised to exclude the non-representative ’20 wells upon completion of the dataset. This could be assessed by judging the sampling conditions on a well-to-well basis using the ’20 fieldwork notes on well type, sampling methodology, handling of sample, purging technique applied, sample depth, material, timing of sampling and other possible (logistic) causes that could have influenced the results.

One-on-one comparisons for the identical wells of 2020-2021 (*n*=8) showed that field methodology (purging technique and/or sampling depth) can influence the EC of the sample. Season and rainfall are expected to have a minimal influence on the sample results of ’20 and ’21, provided that sampling is done from a representative depth (shallower will have more effect from rain). Field methodology can have an influence on groundwater results. Differences in field methodology might not just have affected the results for ’20 and ’21, but also ’77 and ’92. With the information that is currently available it is hard to determine how the results could have been influenced, and to what extent. Overall, building a representative dataset that is scientifically up to par remains to be a balancing act between gathering enough data points, whilst also making sure the collected data is of scientific quality.

5.2 Chemical trend through the decades (’77, ’92, ’20, ’21)

As mentioned in section §5.1, for the rest of the interpretation the results of ’20 and ’21 are considered as separate datasets as they cannot (yet) be combined. Just as with the ’20 and ’21 dataset, caution still has to be taken with the comparison between the decades as ’77, ’92 and ’20-’21 as different methodologies have been used.

This section is focused on the main research aim, namely retrieving the overall chemical trend for both sides of Curaçao from 1977 to 2021. While Verstappen (2022) focused mainly on the comparisons between ’77-’92 and ’21 over the entire island, for this thesis the findings were split in an eastern and western side of Curaçao. The expectation was that for the eastern side more subtle differences would become visible, as the western side of Curaçao consists of wells that have the highest salinity on the island. In addition, the expectation was that the influence of geology is minimized for the east, yet anthropogenic influence is much more apparent due to a much higher population density. From the comparisons over the decades, the following key findings emerged:

- A freshening of groundwater is witnessed in the east, but not in the west
  Further discussed in 5.2.1 Groundwater salinization and freshening
- A decrease in pH is witnessed for both the west and east of Curaçao, but more distinctly for the west
  Further discussed in 5.2.2 Groundwater acidification and related processes.
- A significant rise in alkalinity is observed for the east, but not in the west
  Further discussed in 5.2.2 Groundwater acidification and related processes.
- No significant trend is witnessed in nutrient concentrations, yet nitrate levels are beyond acceptable levels for all years, especially in the east
  Further discussed in 5.2.2 Nutrient pollution.

5.2.1 Groundwater salinization and freshening

Verstappen (2022) has shown that salinization is an important process in Curaçao’s groundwaters, based on strong correlations that were found between several parameters (Cl, Na, Mg, Br, B, K, Ca and SO_4) and scatterplots for the 2021 dataset that indicated seawater intrusion. However, when looking at the EC throughout the years a significant decrease in salinity, not increase, is observed between the years 1977 – 1992 (van Sambeek et al., 2000; (Table 25) and 1977 - 2021 (Table 25) on the eastern side of the island; on the western side there is no significant difference in salinity between any of the datasets (Table 25). For the east, most increase in freshening is observed between 1977 – 1992, after which the extent of freshening declines, as a difference is not witnessed as a shorter-term effect between the ‘92-‘20/21 datasets, but *is* visible as a long-term effect between 1977 – 2020/2021 datasets. Same as for the larger ’92 and ’20 dataset, the identical wells (*n* = 20 for ’92 and ’20, east *n* =) have no significant difference in EC between ’92 and ’20 (Table 33 - Table 34; Figure 29 - Figure 32), although

it can be witnessed that in the east some wells have become more saline, some freshened and some remained the same (Figure 33).

The overall decline in groundwater EC that is witnessed between ’77 and ’92, and ’77 and ‘20/’21 could be attributed to leaking drinking wastewater pipelines or leaking wastewater effluent from sewer collection or septic tanks, as was also mentioned by Sambeek et al. (2000). This is in line with the salinity decrease only occurring on the eastern side, as this urbanized region of Curaçao has a higher population density, with more drinking water infrastructure and exposure to wastewater effluent. The extent of freshening declining between 1992 - 2020/2021 (Table 25), could be attributed to the fact that leakage of lower-salinity water had been solved from the 90s onwards, or by the fact that salinization processes (over-extraction and/or seawater intrusion) have increased within this period as well, balancing out the freshening of leaking wastewater and/or drinking water. This would result in no significant difference for EC between 1992 and 2020/2021, while in reality both freshening and salinization occurred. Although it is hard to pinpoint the exact causation within this context, simultaneous desalination and salinization processes are the most presumable, as the findings of Verstappen (2022) also imply that there has been an increase in seawater intrusion and salinization processes for Curaçao over the last decades.

It is more likely that the observed freshening is caused by wastewater as opposed to drinking water leakage, as the multivariate statistics also indicated that salinization and wastewater pollution were the dominant underlying processes explaining the hydrochemistry of the island. Nonetheless, the influence of drinking water leakage in the east could be further researched through stable isotope analyses, as drinking water in Curaçao consists of seawater that is desalinated through reverse osmosis (RO) (Bonnélye et al., 2007) and RO-derived waters can be traced through isotopes (Ganot et al., 2018). Furthermore, the eastern wells of ’21 could be selected to see if the same indicators for salinization that were found looking at the entire island as a whole by Verstappen (2022) are also found when focusing on the east and Diabaas East only.

5.2.2 Groundwater Acidification and Related Processes

There is a significant decrease in pH that is witnessed in the group of 17 identical wells measured in both 2020 and 1992 (Figure 34 - Figure 36; Table 35), and also in the complete datasets of ’77, ’92, ’20 and ’21 (Table 28; Table 29; Figure 20; Figure 21). For these datasets, and in the identical wells, the decrease in pH is more distinctly witnessed on the western side of Curaçao. On the long run there is a significant increase in alkalinity for the east (Table 28; Figure 23).

For ease of reading, this is best summarized in the following key tables and figures: Table 48, Table 49, Figure 59 and Figure 60.

Although the drop in pH is more distinct in the west, there is no significant difference in the west for alkalinity. In this section the potential causes will be discussed as follows:

- Acidification & geological buffering capacity
- Acidification & pyrite oxidation
- Acidification & organic degradation, pCO_2, vegetation
- Acidification & wastewater, fertilizer
- Acidification & well type
- Acidification & field methodology,
- Acidification & atmospheric pollution.

Acidification & geological buffering capacity

One of the ways that groundwater can acidify is through the introduction of CO_2. There are several ways through which CO_2 could enter (ground)water: from the atmosphere, from magma degassing, from oil degradation, from the degradation of organic material in wastewater or from plant respiration, and more (Delkhahi et al., 2020). Regardless of origin, as CO_2 dissolves in water (Eq. 5-4) it either exists as dissolved free CO_2 or in its hydrated form as carbonic acid H_2CO_3, both referred to as CO_2*. When aqueous CO_2* contacts lithology, different rock-water reactions will occur as a response to the influx of carbonic acid. In silicate-containing geology, different minerals, such as K-feldspar, will take up the proton(s) of H_2CO_3, leaving HCO_3^- and CO_3^{2-} in the water (Eq. 5-5).

$$CO_{2(aq)} + H_2O \rightarrow H_2CO_3 \ (Eq.\text{5-4})$$

$$H_2CO_3 \rightarrow H^+ + HCO_3^- \rightarrow 2\,H^+ + CO_3^{2-} \ (Eq.\text{5-5})$$

In carbonate containing rock, calcite will react with carbonic acid to bicarbonate (Eq. 5-6). Rocks that contain a majority of carbonate are not likely to have acidified groundwater, as the rapid carbonate dissolution buffers the addition of protons very well (Appelo & Postma, 2005). For 2021 it was shown that 90% of the groundwater samples (*n*=63) were supersaturated with calcite (based on groundwater data from Verstappen, 2022). For silicate-rock, the reactions are slower, and often insufficient to resist acidification that originates from anthropogenic or polluting sources. Yet, silicate weathering is often still the most important neutralizing mechanism against acidification if carbonate is not present. As the silicate-relating weathering reactions are irreversible they are officially not called “buffering” mechanisms, even though they do counteract a drop in pH by consuming the acid and producing bicarbonate. The effect of these silicate-reactions on the composition of groundwater is mainly an increase in cations (Na, K, Mg, Ca) and dissolved silica (SiO_2) (Appelo & Postma, 2005). Over the years, the Mg, K and Ca concentrations have significantly increased in western Curaçao, and Mg concentrations in the east (Appendix II).

$$CaCO_3 + H_2CO_3 \leftrightarrow Ca^{2+} + 2\,HCO_3^- \ (Eq.\text{5-6})$$

When aluminum hydroxide, $Al(OH)_3$, is present, and the pH is low enough for it to dissolve (Eq. 5-7), Al-containing rocks can do some of the buffering as well (Appelo & Postma, 2005). In this moment, the pH of Curaçao’s groundwater is not low enough for this reaction to occur, it is, however, possible to if this acidification trend continues.

$$Al(OH)_3 + 3\,H^+ \rightarrow Al^{3+} + 3\,H_2O \ (Eq.\text{5-7})$$

So boiled down, as infiltrating CO_2*-containing water moves through the subsurface, the H_2CO_3 concentration will decrease and the CO_3 and HCO_3^- content will increase, due to several (buffering) mechanisms involving mineral dissolution that are activated by acidification. When these buffering or neutralizing mechanisms are no longer sufficient, the groundwater pH will decrease. As the geology between the east in the west is the same for Diabaas West and Diabaas East, yet the different trends

for the east and west are still clearly visible when looking at the western and eastern Diabaas, the differences found in the decrease in pH and rise in alkalinity for east and west cannot be attributed to a difference in lithological rock-water interactions, or geological buffering capacity, and there must be additional processes at play.

Acidification & pyrite oxidation

A geology-related reaction that actually contributes to the acidification of groundwater is the oxidation of pyrite (Eq. 5-8). It is unclear how much pyrite is present in the formations of Curaçao, but it is often found in small quantities in a range of reduced sediments (Appello & Postma, 2005). The doctorate report of Molengraaff (1927) on Curaçao's geology and geohydrology does mention several occurrences of pyrite-containing rocks that were observed during his geological fieldwork. Pyrite oxidation is one of the strongest naturally occurring acidification reactions, and whenever groundwater tables lower, pyrite oxidation can occur (Appelo & Postma, 2005). As the geology is the same for both DE and DW, but the drop in pH is still distinctly observed for DW (Table 49), pyrite oxidation is not considered as a determining factor for acidification. In addition, the SO_4^{2-} concentrations only significantly differ between the total east and total west, not between DW and DE (Appendix II).

$$2\,FeS_2 + \frac{15}{2}O_2 + H_2O \leftrightarrow 2\,FeOOH + 4\,SO_4^{2-} + 8\,H^+ \quad (Eq.\,5\text{-}8)$$

Acidification & organic degradation, pCO_2 and vegetation

As mentioned in "Geological buffering capacity", one of the ways to acidify groundwater is through the introduction of CO_2. Figure 62 showed that all 2021 wells have values above atmospheric pCO_2, indicating that underground processes occur of which the influx is higher and/or faster than can be counteracted by (geological) processes that resist the CO_2-influx. The organic matter that could be responsible for the production of CO_2 (Eq. 5-9) can come from sources like wastewater or from the respiration of plant debris. This means that an increase in vegetation on the western side of Curaçao could have increased the amount of groundwater CO_2, potentially playing a role in the acidification of groundwater over time being stronger in the west, as this is the section of the island that is less urban, has less wastewater exposure, but more forestation than the east.

$$CH_2O + O_2 \rightarrow CO_2 + H_2O \rightarrow H^+ + HCO_3^- \quad (Eq.\,5\text{-}9)$$

In 2021, the pCO_2 was not significantly different for the east and the west (Figure 62); 2021 is also the year where no significant difference was witnessed in the pH of the eastern and western side in this year (Table 29). For future research, the pCO_2 concentrations of '92 and '20 can also be reviewed, provided that the alkalinity was accurately measured, to see how they have developed for the different sides of the island over the decades, as opposed to focusing on one year, to determine how the changes in CO_2 levels are for the different sides of Curaçao.

Acidification & wastewater: pH, nitrate and alkalinity

When wastewater is discharged different oxidation reactions can occur in the unsaturated zone, such as the nitrification of NH_4^+ to NO_3^-, directly generating acidity (Eq. 5-10). The oxidation of organic matter from wastewater can also increase the CO_2 (Eq. 5-9), acidifying the groundwater through formation of carbonic acid, as also mentioned in section "Acidification & geological buffering capacity" and "Acidification & organic degradation, pCO_2 and vegetation". One major difference between the effects of CO_2 introduction through root respiration and introduction through wastewater, is that with root respiration CO_2 formation is close to the source, whereas with wastewater the dissolution of organic pollution allows for continuous conversion into CO_2, even beyond the source point of contamination (e.g. septic tank). The witnessed rise in HCO_3 only seen in the east (Figure 61) and the eastern negative correlation between pH and alkalinity is likely related to organic conversions due to wastewater pollution. Although this still does not explain why the pCO_2 levels are not significantly different for eastern and western Curaçao in 2021.

In the results of both 2020 and 2021 it is witnessed that NH_4^+ is only present in a minority of wells, whereas NO_3^- is present in the majority of wells. As NH_4^+ and NO_3^- will only occur together at sites with less oxidation, this indicates that the wastewater is well-oxidized and NH_4^+ conversion to nitrate can take place, just like the oxidation of organic matter (Eq. 5-10).

$$NH_4^+ + 2\,O_2 \rightarrow NO_3^- + 2\,H^+ + H_2O \;(Eq.\,5\text{-}10)$$

A neutralizing effect related to wastewater (or fertilizer) pollution could be the removal of nitrate through denitrification (Appelo & Postma, 2005) (Eq. 5-11). In reducing circumstances, nitrate could be transformed to N_2 through heterotrophic reactions with organic carbon as the energy source:

$$4\,NO_3^- + 5\,CH_2O \rightarrow 2\,N_2 + 4\,HCO_3^- + CO_2 + 3\,H_2O \;(Eq.\,5\text{-}11)$$

This would usually occur in areas that are enriched in (labile) organic carbon, the portion of organic carbon that can be readily decomposed by microorganisms in the soil (Abascal et al., 2022). There is, however, no indication that there is a distinction for this between the east and the west. In addition, there is an ubiquitous presence of nitrate in the groundwater, suggesting that nitrification plays a more prevalent role than denitrification, resulting in an overall net acidification effect.

Although, nitrate pollution is adamant, there is no significant increase (or decrease) in nitrate concentrations over the decades (Appendix II). An argument could be made that wastewater pollution has therefore not increased; this is, however, unlikely. More likely could be that nitrogen is spreading spatially (steady-state), as opposed to increasing in concentration per well point.

Besides the leaking of drain fields or wastewater infrastructure, exploratory field interviews during the field campaign of 2020 also showed that people deliberately take wastewater out of their septic tanks to irrigate their private gardens with, especially in regions where groundwater is too saline to use for gardening or landscaping. Another reason often mentioned for reverting to wastewater irrigation is that tap water is too expensive to use for gardening applications. To illustrate: tap water in Curaçao for domestic use costs between €5.14 and €10.14 per m^3 (Aqualectra, 2022), whereas it costs €0.87 per m^3 in the Netherlands (Waternet, 2022). Purposefully irrigating with septic tank wastewater also means that wastewater likely that has not fully undergone anaerobic treatment yet, before it is actively distributed. Besides human waste, wastewater in Curaçao also consists of detergents, soaps, solvents and other chemicals (Erdogan, 2021) that could contribute to alkalinity directly.

Verstappen (2022) fully attributed the decrease in pH between ’77, ’92 and ’21 to the continuous leaking of septic tanks in combination with irrigation water leaching NH_4^+ and organic material. Verstappen also stated that the alkalinity increased (Table 49), because (geological) buffering mechanisms were activated with the increase in H^+, although ultimately not enough to prevent acidification. Although wastewater pollution seems to certainly play a major role in the acidification of groundwater, it does not explain why acidification occurs mostly in the western section, while the eastern side of Curaçao is more exposed to the effects wastewater effluent – unless there are additional non-wastewater related processes at play in the west.

Acidification & well type

Verstappen (2022) found that older hand-dug wells had a slightly higher pH (roughly 0.3 unit point higher) than newer boreholes. This could have partly influenced the difference in pH between the 2021 and 1992-1977 dataset, as the majority of wells measured for the 2021 dataset were boreholes (36% hand-dug wells), whereas in 1992 and 1977 mainly hand-dug wells were measured (73% and 54%, respectively). However, when looking at the identical wells measured in 2020 and 1992/1977, the pH difference also clearly decreases throughout the years, while well type is no longer a variable, as the exact same wells were measured in 2020 as in 1977 and 1992. In addition, the drop in pH exceeds the 0.3 unit point that is found for well types for the western side of the island.

Acidification & field methodology

As mentioned in 5.1 Representativity, the field methodology can have a direct effect on the pH. It is unknown how the pH was measured in 1977, as the methodology is not stated in the field work report. However, if pH was measured in the lab as opposed to in the field, it would have likely been a systematic error and refer to all groundwater samples taken over the 1977-1979 period, yet in the 70s there is a clear difference between the east and west in terms of pH (west significantly higher than east). In addition, acidification is also witnessed from 1992 onwards, where the pH was measured in the field with certainty. The acidification trend that is witnessed for the east and the west is therefore not assumed to have been distorted by the field methodology, except for the 2020 wells that were potentially measured in the stagnant upper layer of the well, overestimating the pH.

Acidification & Atmospheric pollution

Another aspect to consider for groundwater acidification within Curaçao is atmospheric pollution. Curaçao is home to one of the largest petroleum refineries in the Wider Caribbean Region: the "Isla Refineria" (Pulster, 2015). The refinery is located next to Schottegat, Willemstad, and was operative from 1918 to the end of 2019 (Reuters, 2022). It is widely known that the emissions from industrial activities such as refineries contain components like NOx, SO_2, SO_3, particulate matter (PM) and polycyclic aromatic hydrocarbons (PAHs), that are linked to a range of detrimental consequences, for both human health and the environment (Pulster, 2015). These effects can be divided into: atmospheric inhalation, dry deposition and wet deposition.

With inhalation, the emitted pollutants are directly inhaled by people and animals and potentially cause several health problems, such as respiratory and cardiovascular events, chronic bronchitis and lung cancer (Pulster, 2015). With dry deposition the polluting components deposit to terrestrial surfaces directly, which can in turn be transported with precipitation events (EPA, n.d.). With wet deposition, atmospheric water will react with the emitted ambient nitrogen oxides, sulfur dioxide and sulfur trioxide to become sulfurous acid (H_2SO_3), nitric acid (HNO_3), nitrous acid (HNO_2), sulfuric acid (H_2SO_4) and form acid rain (Figure 68)(Eq. 5-12 – Eq. 5-15).

$$2\,SO_2 + O_2 \rightarrow 2\,SO_3 \; (Eq.\,5\text{-}12)$$

$$SO_3 + H_2O \rightarrow H_2SO_4 \; (Eq.\,5\text{-}13)$$

$$2\,NO_2 + H_2O \rightarrow HNO_2 + HNO_3 \; (Eq.\,5\text{-}14)$$

$$N_2O_4 + H_2O \rightarrow HNO_2 + HNO_3 \; (Eq.\,5\text{-}15)$$

Acid rain in the ocean can be detrimental for aquatic life and coral (Carlowicz, 2008); acid rain on land can have negative effects on flora, soil and groundwater quality (Nielsen et al., 1985), especially for geologies with acidic (crystalline) rocks that have little buffering capacity, and have a higher sensitivity to acidification. Although atmospheric pollution does not introduce CO_2 into the subsurface system in the same way that organic pollution (from e.g. wastewater or root respiration) does, for carbonate-rock containing formations, the acidity of rain and runoff would dissolve the carbonates (Eq. 5-16), similar to the introduction of carbonic acid:

$$CaCO_3 + H_2SO_4 \rightarrow CaSO_4 + H_2O + CO_2 \; (Eq.\,5\text{-}16)$$

Acid rain can also cause corrosion in distribution networks (Nielsen et al., 1985). The acid rain that does not infiltrate, “acid runoff”, can also have a negative effect on the ocean through both acidification and eutrophication. This is because the nitric and nitrous acid rain can be an additional N-source for oceans (MPCA, 1999), in addition to the other N-vectors, such as nitrogen-rich subsurface groundwater flow and runoff carrying nitrogen from fertilizers and (treated) wastewater towards the sea.

The RIVM uses the following indicators to observe the effect of acid rain on groundwater for regions that has been exposed to atmospheric pollution: an increase in sulfate, an increase in nitrate, an increase in

alkaline cations (such as Na, Mg, K, Ca), a drop in “acid neutralizing capacity” and a drop in pH (RIVM, 2014). The drop in pH, the increase in western Mg, K, Ca concentrations, and the higher sulfate concentrations for the west (Table 68) that are found within this research could be a consequence of acidification through atmospheric pollution and dry / wet deposition on the western side of the island. It must be added, however, that sulfate can also originate from many other sources such as fertilizer, pyrite oxidation, wastewater, seawater, release of stored S in the soil or decomposition of organic matter (0.1% S) (MPCA, 1999; Appelo & Postma, 2005). Furthermore, even though the western sulphate concentrations are higher than the east, they did not increase throughout the years. In addition, a significant difference between DW and DO for sulphate concentration was only witnessed for 1977 and not for 1992 and 2021. The total west sulfate concentrations are higher in the west for both ‘77 and ’21 (Appendix II). A more in-depth analyses would be needed to narrow down and substantiate possible causes.

Although it is unclear exactly how the refinery could have affected Curaçao’s natural environment and aquifers over the 100 years it was operative, research in 2015 did show that Curaçao's ambient sulfur dioxide concentration was found to be the highest in the world in 2011, 2012, 2013 and 2014, far exceeding annual emissions of majorly polluted areas in the world (Figure 65: right) (Pulster et al., 2018). An investigation carried about by TNO in 2006 sampled seven wells on a section of the Isla terrain, and six wells at households in the surrounding areas (north, east and west) of the refinery. Here it was also found that all wells were contaminated with oil – partly dissolved into the water, and partly present as a floating layer on top of the groundwater, also known as Light Non-Aquous Phase Liquid (LNAPL). Although most of the (contaminated) groundwater flows towards Schottegat, the withdrawals by local residents adjacent to the refinery can pull the contaminants towards the households. It is mostly LNAPL that forms a spread risk as the oil is present in its purest form. For all household wells contamination was found, either with mineral oil, PAHs or the metals Vanadium and Cupper. The oil, PAH and Cu were attributed to the refinery, the high Vd concentrations were attributed to geology and/or (historical) oil contamination. Overall, the contamination in the wells surrounding the refinery was found to be serious and severe, and recommendations were made to map the risks to which the residents are exposed (ter Meer et al., 2007).

In terms of atmospheric spread, it is clear that wind plays a large role in the spread of the ambient pollutants (Zhang et al., n.d.), it has even been shown that atmospheric particles can travel from America to Europe in less than four days (Appelo & Postma, 2005). The wind direction in Curaçao is predominantly east (Figure 65: Left), but can also be northeastern or southeastern, but to a much lesser extent. This would mean that NO_x and SO_2 would have mostly moved towards the ocean, and less frequently (roughly 5% of the time, as based on wind directions in 2021) over land towards the western side of the island (World Meteorological Organisation, 2022).

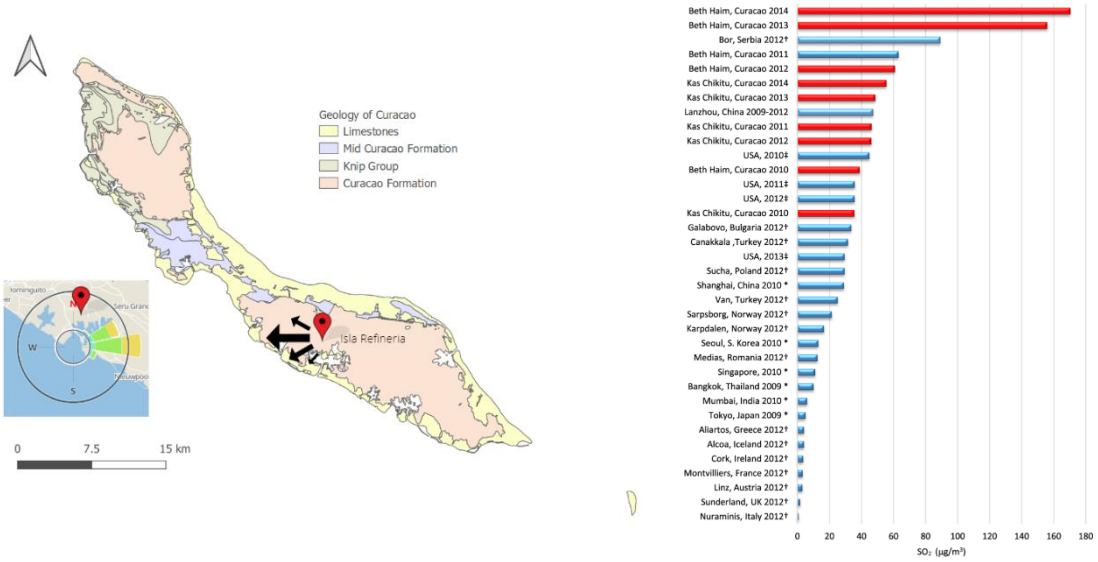

Figure 65. Atmospheric pollution potential in Curaçao. Left: Wind directions in Curaçao as based on 2021 in Windy.app application (World Meteorological Organisation, 2022). Right: Global SO_2 emission between 2010 and 2014. Curaçao takes in first and second place (2014 and 2013), and occupies seven positions in the global top 10 between 2010 and 2014.

If the refinery emissions moved with the southeastern wind 5% of the time, the *average* annual 24-hour SO_2 concentration would be below the European Commision's 24-hour maximum of 125 µg/m^3 (Pulster et al., 2018) for the western region of the island, but the southeastern wind event would still exceed daily guidelines and be enough to be seen as a considerable "singular episode". Nielsen et al. (1985) state that effects of acid rain may not only be a consequence of a cumulative build-up, but also from regional singular episodes. When considering 5% of Curaçao's total annual emission of 2014 as the effect of all the singular episodes transporting atmospheric pollution to the west, the yearly average of these singular episodes would still exceed the annual emission of Mumbai, India in 2010 (Figure 65: Right), a region that is also considered to have major air pollution. It is nonetheless unclear if this would have been sufficient to affect its surroundings over the years, with inconsistent and relatively infrequent dry or wet deposition due to refinery-related atmospheric pollution.

The exploratory quality measurements of rainwater during 2020 and 2021 show that rainwater is not acid (pH < 5.7), but the refinery has no longer been operative since late 2019. It is therefore, in this moment, not possible to do follow-up measurements downwind of the refinery. When exploring previous research, no papers were found where rainwater quality on Curaçao was researched during operation. However, a comparison could be made to the rainwater pH in Bor (Figure 65; row 3): a strongly polluted mining town in Serbia (Pacic, 2021) that had roughly half the SO_2 emissions in 2012 as Curaçao had in 2014 (Figure 65; row 1). Measurements done between 2010-2017 showed that rainwater in Serbia had an average pH of 4.39 (Keresztesi et al., 2019). Even though this might give an indication of what rainwater pH in Curaçao could have been like, it is not a substiantiated comparison, as there are other processes that can also influence the pH, such as mineral dust particles (e.g. calcareous soil dust) making their way from the African continent to different areas around the world, including Europe and the western Caribbean, buffering its rainwater (Carratala et al., 1996; Ramírez-Romero et al., 2021).

An assessment done by Rodhe (1989) does suggest that Venuzuela and the Southern Caribbean Sea are potential problem areas for acid deposition problems (Figure 66). In addition, the annual average pH of rainwater was assessed and modeled by Rodhe (2002) and shows that there is an acidified region right around the location of Curaçao, where a yellow-colored pH range of 4.5 – 4.8 is seen (Figure 67). Nonetheless, for wet deposition in Curaçao, wind direction during the precipitation event also plays a major role, as mentioned in above paragraphs. At the time of writing this thesis, there are negotiations to re-open the refinery (Reuters, 2022). For future research, if the refinery reopens, the potential effects and influence of the petrochemical emissions on rainwater and runoff pH should be measured and considered for hydrological and terrestrial assessments.

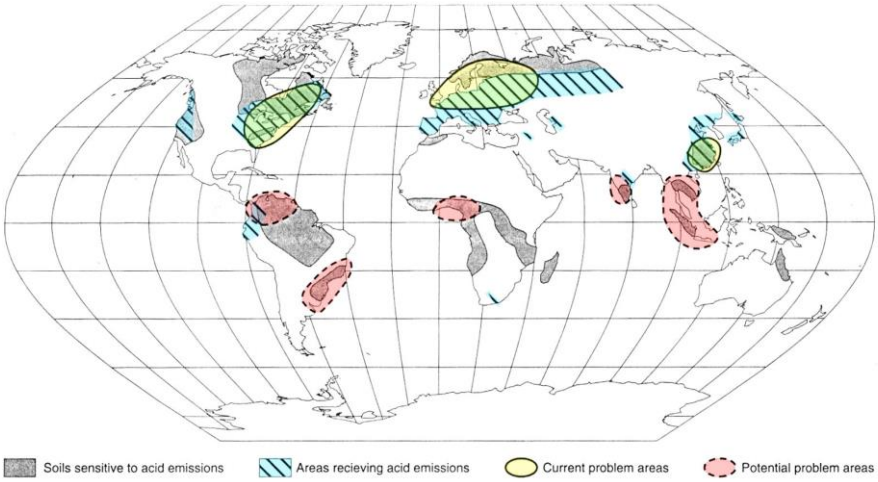

Figure 66. Areas in the world with current, future or potential problems with acid deposition (Rodhe, 1989).

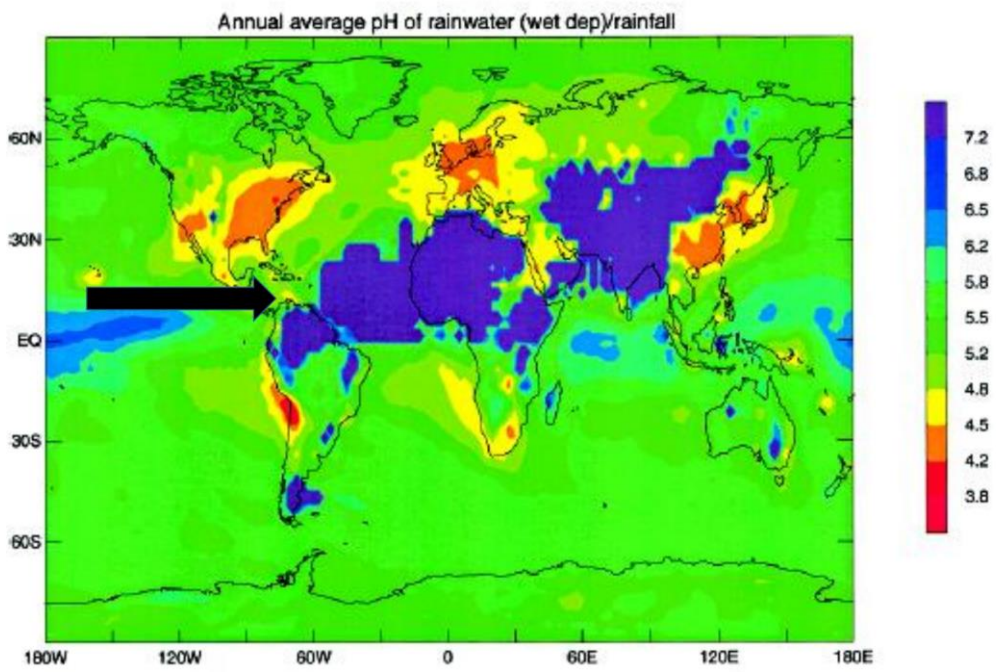

Figure 67. Global rainwater pH. The black arrow is pointing towards the region of Curaçao (Rodhe, 2002).

Summary interpretation of acidification trend in Curaçao

As the geology between the east in the west is the same for Diabaas West and Diabaas East, and the trends (a drop in pH that is more distinct for the west, and a rise in alkalinity only for the east) are still clearly visible when looking at eastern and western Diabaas only, the differences are likely unrelated to a difference in lithological rock-water interactions, such as **pyrite oxidation** or **geological buffering capacity**.

The long-term drop in pH is presumably also not due to differences in **field methodology** for ’77, ’92, ’20 and ’21. Nonetheless, there is still a lack of information to fully refute this. One of the main recommendations is therefore to obtain more information on historical fieldwork campaigns.

Verstappen (2022) found that hand dug wells were 0.3 unit point pH higher than bore holes in 2021. This could have meant that **well type** influenced the pH, as in 2020 and 2021 less hand dug wells were measured than in 1992 and 1977, lowering the pH. However, as the identical wells (where well type is

removed as variable) also showed a more distinct drop in pH for the west than the east, this is refuted as contributing factor to the acidification trend.
An initial assessment for pCO_2 of the wells of '21 showed no significant difference between the east and west. In this year, pH is also not significantly different for east and west.
Overall, these are complex processes and at this stage of understanding, it is hard to pinpoint the exact (simultaneous) processes that are behind the pH and alkalinity trend for the east and west. Nonetheless, it seems highly likely that eastern acidification is caused by wastewater pollution from acidifying nitrification and oxidation of dissolved organics, acidifying due to CO_2 dissolution and formation of carbonic acid. Acidification presumably started earlier in the east than in the west, explaining the higher western pH in 1977. Furthermore, acidification in the east due to eastern wastewater pollution is substantiated by: 1) higher nitrate concentration in the east than the west, 2) the fact that Willemstad is located in the east and most people and wastewater treatment facilities are located in this region, 3) the rise in alkalinity and correlation between HCO_3^- and H^+, which could be attributed to CO_2 and carbonic acid ($H_2CO_3 \rightarrow H^+ + HCO_3^-$) related acidification from dissolved organic carbon present in wastewater. Additionally, the results show that nitrification ($NH_4^+ + 2\ O_2 \rightarrow NO_3^- + 2\ H^+ + H_2O$) plays a more prevalent role than denitrification ($NO_3 + 5\ CH_2O \rightarrow 2\ N_2 + 4\ HCO_3^- + CO_2 + 3\ H_2O$), which is in line with an overall net acidification effect.
Wastewater could have also played a role for acidifying the west, but this is thought to play a much smaller role than the east as the west is less densely populated and has less exposure to wastewater pollution, also observed in the NO_3 concentrations being three times lower in the west than they are in the east. Still the west has a more distinct drop in pH than was witnessed in the west, and has no rise in alkalinity. This is plausibly caused by non-wastewater related acidifying processes, such as **atmospheric pollution** transported by southeastern winds while the Isla Refineria was still operating (1918-2019). **Increased vegetation**, increasing the subsurface degradation of organic matter, is also speculated to have an influence, but no detailed assessment was done. More in-depth analyses would be needed to substantiate or dismiss these causes, as major questions regarding these potential causes remain unanswered.

Table 51. Groundwater acidification in Curaçao: a summary of possible explanations, linked to Figure 68.

Topic	East	West
pH trend	Drop in pH ↓ (ΔpH = 0.25) Lower onset pH (pH = 7.49 (DE))	Drop in pH more distinctly ↓↓ (ΔpH = 0.7) Higher onset pH (pH = 7.83 (DW))
Alkalinity trend	Rise in alkalinity over the years ↑ Negative correlation between alkalinity and pH.	No significant difference in alkalinity over the years. No correlation between alkalinity and pH.
Wastewater presence	The east is more urban, with a higher population density, more septic tanks and the largest wastewater treatment facilities. These wastewater treatment facilities are not well maintained, and dispose of untreated or poorly treated wastewater (Erdogan, 2021).	More rural area with less exposure to wastewater effluent and wastewater pollution.
	For all wells in the east and west sampling often occurred close to people's houses, potentially causing a bias in increased witnessing of wastewater effects. There is no significant difference in E. Coli and NH_4 concentrations found in 2021 between the east and the west.	
Agriculture	In the eastern section of the east, agriculture occurs, but overall the eastern area is the most urban and industrial part of the island, accommodation near to 90% of the population.	The west in Curaçao is known for its agricultural practices. In Curaçao manure is mainly used for fertilization processes (Well interviews, 2020).
Nitrate	More nitrate pollution than in the west. Data from '21 shows that the average in the east is 74±63 mg/L, almost three times higher than in the west. No significant difference in nitrate between the years.	Less nitrogen pollution. Data from '21 shows that the average in the east is 27±44 mg/L. No significant difference in nitrate between the years.
	Nitrate presence is ubiquitous, suggesting that nitrification is most prevalent.	
Geology and water-rock interactions	The eastern and western Diabaas formations are of the same geology (Curaçao Lava Formation). When looking at Diabaas East (DE) and Diabaas West (DW) specifically, the drop in pH is also more distinct for the DW than the DE. In DE the rise in alkalinity is witnessed, whereas for DW it is not. The differences in pH and alkalinity are therefore not attributed to a difference in geological buffering capacity as the same rock-water interactions would occur in DE and DW. Other processes must be at play that cause the different trends in eastern and western Curaçao.	
Acid rain	Not subjected to events of acid rain.	Might have been subjected to singular events of wet or dry deposition due to atmospheric pollution from refinery Isla Refineria in Willemstad during operation between 1918 and 2019, when the wind would have come from a southeastern direction (5% of the time in 2021).
Vegetation	Less vegetation than in the west.	More and increasing vegetation when compared to the east. It is speculated that vegetation might have increased over the years, which would increase the subsurface degradation of organic matter possibly acidifying the groundwater, but there is no data and no analyses was done.

Cations	Mg rises between ’77 – ‘21 Ca rises only between ’91-‘21 K rises between ’77-’92, ’77-‘21 No difference for Na	Mg rises between ’77-‘21 No difference for Ca, K, Na
SO_4	Significantly higher concentration of SO_4 in the west than in the east (1977_{west} = 267±423; 2021_{west} = 433±687 mg/L), but no significant difference between the years for the west (1977-1992-2021)	Significantly lower concentration of SO_4 in the east than in the west (1977_{east} = 114±123; 2021_{east} = 116±136 mg/L), but no significant difference between the years for the east (1977-1992-2021).
pCO_2	In 2021, all wells have values above atmospheric pCO_2, indicating that underground processes occur to increase the level of pCO_2 in groundwater, but the groundwater wells in the east and west show no significant difference in pCO_2.	
EC	For DE and DW, there is no significant difference in salinity, excluding salinity as a cause for these differences. For the total east and west, however, a freshening is observed that is likely caused by wastewater and drinking water leakage on the eastern side. The extent of freshening declined between 92-21, likely due to simultaneous salinization processes.	

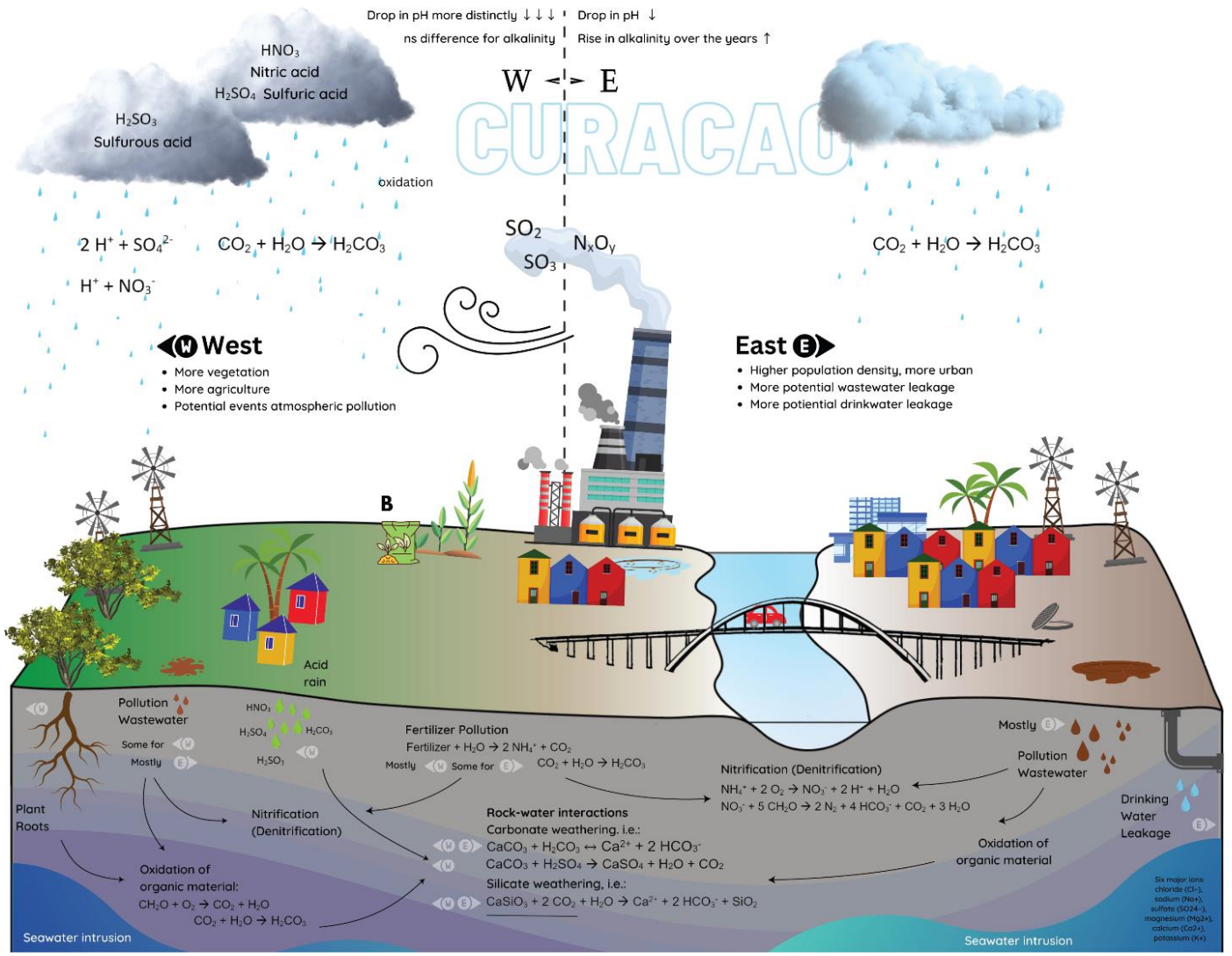

Figure 68. Illustration of western and eastern side of Curaçao., with reactions and possible causations of the geochemical differences between the east and the western side. Drawing done in Adobe Illustrator.

5.2.3 Nutrient Pollution

Although some of the processes related to nitrogen and wastewater discharge have already been mentioned under 5.2.2 Groundwater Acidification and Related Processes, the reactions and interrelations are discussed in more detail in this paragraph.

Nitrate
Nitrate can occur in groundwater naturally, but concentrations that exceed 1-3 mg/L are usually associated with human activity and contamination (Vadison & Brunett, 1985; Dubrovsky, 2010). Nitrate pollution can be caused by (partially) treated and untreated wastewater, atmospheric pollution, badly designed or old landfills, organic waste generated by animals, and agricultural practices with synthetic and organic fertilizer use (Lenntech, 2022). Although no significant difference is witnessed throughout the decades, the majority of samples are beyond acceptable levels and indicate nitrate pollution. A clear difference is observed for the east and the west, where the east has more nitrate pollution. Without studying the isotopic composition, it can be challenging to determine what the exact source of nitrate is (Robertson, 2021), but wastewater would likely play a large role, based on the level of exposure to discharge on the eastern side. It must be noted that for the 2021 dataset there is no significant difference for the E. Coli levels that were found on the eastern and western side, but E. Coli in the west could have possibly originated from manure as well. In addition, samples were often taken close to septic tanks, also in the west.

Phosphorus
Phosphorus can originate from wastewater, or from sources such as fertilizer and urban runoff (EPA, 2022). The concentration depends on the pH of the water and the reactions around minerals; in wastewater, the phosphorus concentration usually ranges between 5-15 mg/L total P, of which 70-85% is dissolved phosphate (PO_4^{3-}) (Roberson, 2021). The concentration of PO_4^{3-} for the '92, '20 and '21 dataset is lower than what would be expected for wastewater effluent concentration, but phosphorus can be adsorbed into the soil's unsaturated zone as there are minerals present with a positive charge. Although sorption does not completely stop phosphorus transport, it does strongly slow it down. In addition, with a lower pH, buffering reactions cause the phosphorus to precipitate and therefore remove the phosphate from the water (Robertson, 2021). These processes could be a possible explanation as to why the phosphorus concentration in groundwater is low for all datasets, and also why there is a significant decrease in phosphate over the years (1977-1992-2021; phosphate measurements for 2020 not taken into consideration).

5.3 Rain and Runoff

The expectation was that surface runoff would be a mix between ground- and rainwater, as heavy rainfall will activate the hydrological system, pushing out the groundwater. In addition, terrestrial contaminants, such as suspended solids and/or contaminants from fertilizers were expected. When comparing the runoff samples to rainwater it was already witnessed that EC, HCO_3, pH, Si, Ca and turbidity increased significantly. However, the sample size is small (*n*=8 for 2020 and 2021 combined) and the locations of sampling is diverse (urban to rural). More samples are needed to compare runoff to both groundwater and rainwater, and be more conclusory on the chemical composition of runoff and its subsequent potential influence on marine life / coral reefs.

5.4 Multivariate Statistics: PCA and cluster analyses

5.4.1 Interpretation PCA

The principle component analyses for 2021 showed that the first and second dimension of chemical variables account for 41% and 21% of the total variance, respectively (Figure 63; Figure 64). For 1992 the first dimension explains 33% of the variability and the second dimension 19% (Table 52). For both years Cl, Na, Ca, Mg, K, Fe and Mn contribute to the first dimension, with a negative loading for Si. This suggests that for this dimension these criteria vary together. The high loading of Cl, Na, Ca, Mg, K, Fe suggest that the first dimension of both 1992 and 2021 are primarily influenced by underlying salinization processes, as was also mentioned in Verstappen (2021). The positive contribution of Na, Mg and

Ca could also indicate that cation exchange is an additional underlying process in this dimension, but that would not be in line with the negative contribution of Si. If freshening would have played a more significant role, one would expect that HCO_3 would have had higher loadings, as the contribution is now low for the first dimensions of both years, namely -0.029 in 2021 and 0.185 in 1992.

For the second dimension, in 2021 SO_4, NO_3, PO_4, Mn, Fe and NH_4 are key contributors, followed by HCO_3. In 1992 it is SO_4, Mn, Fe and PO_4 that dominate this component most, followed by contributions from HCO_3 and NO_3.
NO_3, PO_4, HCO_3, and NH_4 indicate that the dominant process of this dimension is likely wastewater pollution. For both years when NO_3 increases, NH_4 decreases; this is expected as NH_4 is converted into NO_3 through nitrification. This is also seen in the two arrows representing NO_3 and NH_4 pointing in opposite directions (Figure 63; Figure 64). Looking at all parameters of the second dimension, when SO_4 and NO_3 increase, Mn, PO_4, HCO_3, K, NH_4 decrease. The negative correlation between NO_3-SO_4 and Mn-Fe also indicate that this dimension is influenced by reducing conditions, which could be linked to an increase in organic matter due to wastewater pollution.

When comparing the first and second dimension of 1992 to 2021, it is witnessed the dimensions entail the same underlying processes, namely salinization (dimension 1) and wastewater pollution (dimension 2), but the extent of variability that is explained by the first two dimension is larger in 2021 (62%) than in 2021 (52%). In addition, the contribution of both NO_3 and NH_4 to dimension 2 is larger in 2021 than it was in 1992. Both observations (more variability that is explained in 2021 and higher values for NO_3, PO_3 and NH_4), could be due to the fact that different wells were sampled in both years and conditions such as well type, geographic location and distance to septic tanks, have influenced the results. Alternatively, it could be due to a stronger correlation in 2021 between the parameters of the first two dimensions, meaning they could have become more dominant over time, explaining a larger percentage of the variance. When comparing the two plots of 1992 and 2021 (Figure 63; Figure 64), the similarities between the years for these dimensions are clearly observed, minding that the arrows are presented in mirror of each other.

For both years the third dimension mostly consists of contributions by Si and HCO_3, indicating geological mineral dissolution. While in 1992 Si has a higher contribution, in 2021 HCO_3 does. The percentage in contribution to variance has dropped to 10% and 11% for 1992 and 2021, respectively. For the fourth dimension, pH dominates for both 1992 (7%) and 2021 (5%). Where the fifth dimension is contributed to mostly by PO_4 in 1992, it is witnessed that for 2021 there are no distinct parameters in this dimension and contains more noise than all previous dimensions. This is expected as the PCA of 1992 needs five dimensions to explain a cumulative 78.3% of the variability, whereas the PCA of 2021 explains 79.2% with four dimensions and 84.2% with five, resulting in a fifth dimension for 2021 with less distinct parameters.

Table 52. Interpretation of Principle Component Analyses 1992 and 2021. Only contributions exceeding 0.7 (bold) and 0.5 (normal) are included, or contributions of below 0.5 that are important for the comparison between years (italic).

Dimension	**PCA – 1992**	**PCA – 2021**	**Interpretation**
1	Explains 33% **Na (0.833), Cl (0.818), Ca (0.788), Mg (0.763)**, **K (0.760),** Mn (0.657), NH_4 (0.588), Fe (0.527) *Si (-0.288)*	Explains 41% **Cl (0.944), Na (0.936), Ca (0.902), Mg (0.847), K (0.792), Fe (0.719),** Mn (0.595), SO_4 (0.573) Si (-0.583)	The first dimension shows underlying salinization processes, possibly seawater intrusion.
2	Explains 19% **SO_4 (0.711)**, *NO_3 (0.395)* Mn (-0.528), Fe (-0.503), PO_4 (-0.502), HCO_3 (-0.518), *K (-0.462), NH_4 (-0.183)*	Explains 21% SO_4 (-0.625), NO_3 (-0.625) **PO_4 (0.837)**, Mn (0.574), NH_4 (0.595), *HCO_3 (0.487), Fe (0.288), K (0.264)*	For both years, the second dimension shows contributions of SO_4 and NO_3 in one direction, and Mn, Fe, NH_4, HCO_3, PO_4 in the other direction. This indicates that 19 and 21% of the variability can be explained by different processes related to wastewater pollution. Notably, the contribution of PO_4,

			NO_3 and NH_4 to this dimension is higher in 2021 than in 1992.
3	Explains 10% **Si (0.711)**, *HCO_3 (0.481)*	Explains 11% **HCO_3 (0.756)**, Si (0.581)	Influence of geology is witnessed for both years in the third dimension, as dissolution of minerals is observed. For 2021 the contribution of HCO_3 is higher than Si, whereas in 1992 this is reversed.
4	Explains 8% **pH (0.770)**	Explains 7% **pH (0.808)**	In the fourth dimension it is observed that 8% and 7% of the variability is explained by pH, for 1992 and 2021, respectively.
5	Explains 7% *PO_4 (0.632)*, nothing else over 0.5	Explains 5%	The fifth dimension does not have parameters that distinctly jump out, , with the exception of PO_4 exceeding 0.5 in 1992. There is more noise than in the other dimensions.

Overall, the PCA indicates that salinization and wastewater pollution are the dominant underlying processes for the first two dimensions of both 1992 and 2021, and explain the majority of the variability in hydrochemistry of Curaçao's groundwater, followed by mineral dissolution and pH.

5.4.2 Interpretation Cluster Analyses

1992, check with 19 parameters

For the amount of clusters for 1992 a check was done with 19 parameters. The choice was made to assess for five clusters (Table 43), as the configuration of wells is closest to what was tested for in the 1994 doctorate report (Table 53), and the Bayesian Information Criterion (BIC) number is lowest for five clusters.

Table 53. Clusters of 1992 and mean seawater composition as presented in Louws & De Bruijne, 1994.

Parameter	Cluster 1 (n = 18) Precipitation		Cluster 2 (n = 35) Sub-oxidized		Cluster 3 (n = 25) Arid-zone		Cluster 4 (n = 10) Seawater		Mean Seawater Compo-sition
	CC	CM	CC	CM	CC	CM	CC	CM	
pH	7.54	7.58	7.23	7.00	7.457.54		7.117.09		8.2
EC	1.14	1.03	1.68	1.63	2.853.28		11.214.4		32.8
Na	131	134	175	178	313	405	1643	2146	10760
K	2.02	4.49	0.74	1.84	2.074.70		17.395.3		399
Ca	64.2	62.5	101	103	156	177	527	977	411
Mg	41.8	39.9	76.1	79.6	116 138		442892		1290
Cl	157	148	310	317	760	1010	4057	6394	19350
SO_4	36.6	45.7	82.2	95.9	152 198		562986		2710
HCO_3	419	432	467	483	400	419	412	637	142
Eh	*	-221	*	-129	*	-193	*	-157	?
SAR	*	3.25	*	3.20	*	5.54	*	11.94	?
NO_3	*	33.7	*	67.1	*	74.6	*	11.7	0.1
Si	*	23.7	*	32.1	*	24.2	*	21.1	2
Fe	*	0.37	*	0.11	*	0.27	*	2.26	0.002

* Non-clustered parameters.
Note that the CC's are less than the CM's which is in accordance with the fact that when q nears infinty all clustercentres are identical (Vriend, 1988).

Although caution must be taken when comparing the cluster analyses of this thesis to the one done in 1994, similarities are witnessed between the precipitation cluster and seawater cluster between the 1994 analyses and the check performed in this thesis (Table 53; Table 54). However, the arid-zone and sub-oxidized cluster that were found in the

1994 doctorate report of Louws & de Bruijne are not distinctly recognized in the analyses done in this thesis with rigid k-means method.

Table 54. Comparison 1992 dataset with 19 parameters, fuzzy c and rigid k-means.

1992 (19 parameters), 88 wells 1994 doctorate report (Louws & De Bruijne, 1994). Method: Fuzzy C	1992 (19 parameters), 96 wells this thesis. Method: rigid k-means (check)		
Precipitation Cluster (Cluster 1, 18 wells)	Cluster 2 (19 wells)	Cluster 1 and Cluster 2 overlap coincide as fresh water clusters.	Overlap
Seawater Cluster (Cluster 4, 10 wells)	Cluster 3 (6 wells)	Cluster 4 and Cluster 3 coincide as seawater clusters.	Overlap
Sub-oxidized (Cluster 2, 35 wells)	Cluster 1 (55 wells)	The sub-oxidized and arid-zone clusters of the 1994 doctorate report are not recognized in the 1992 analyses in this thesis.	Differs
Arid-zone (Cluster 3, 25 wells)	Cluster 4 (16 wells)		Differs

This could be due to the fact that different analyses were done (rigid k-means versus fuzzy-c means), or because there are differences in the amount of wells that were used from the 1992 dataset for both analyses. Louws & de Bruijne only used 88 wells of the 96 wells in the 1992 dataset for cluster analyses. For the analyses in this thesis 96 wells were used, as it was unknown which wells were left out by Loues & de Bruijne. Furthermore, the wells of each cluster were not included in the sections of the report that are currently available, which meant the geographical locations were not available, further complicating the comparison. The 1994 analyses of the 1992 dataset is therefore not used for further analyses or comparison.

1992 with 14 parameters (pH, NH_4, Na, K, Ca, Mg, PO_4, Cl, SO_4, HCO_3, Mn, NO_3, Si and Fe)

A cluster analyses was then done for 1992 with 14 selected parameters, where certain parameters were removed and others were added. The choice was made to assess for five clusters, as this has the lowest BIC number and explains 46% of the variability, despite the majority rule suggesting 2, 3 or 6 clusters. In addition, it is easier to compare to the 1992 analyses where the choice also fell on five clusters.

Due to the removal of EC as attributing parameter in the analyses, it is seen that EC is less of a contributing factor in the configuration of clusters for 1992 with 14 parameter than with 19 parameters (Figure 69). This could also indicate how seemingly small altercations could potentially influence cluster size. Nonetheless, the overall spatial spread of clustered wells is similar to the 1992 analyses done with 19 parameters (and also with the rigid-k method), especially for the larger clusters. For smaller clusters, more changes are seen. This underlines the value of doing a fuzzy-c clustering as opposed to a rigid clustering, as with the fuzzy c-means method, one well gets a weight as to which cluster it is attributed, and can therefore “belong” to several clusters. The high PO_4 concentrations that are seen for cluster 3 (1992, 14 parameters, this thesis; Table 44) are due to one well having a high concentration (>2000 mg/L PO_4) in the 1992 dataset. This well is likely one of the wells that was left out for the fuzzy c-means that was done in 1994, as this is not seen for the 1994 analyses.

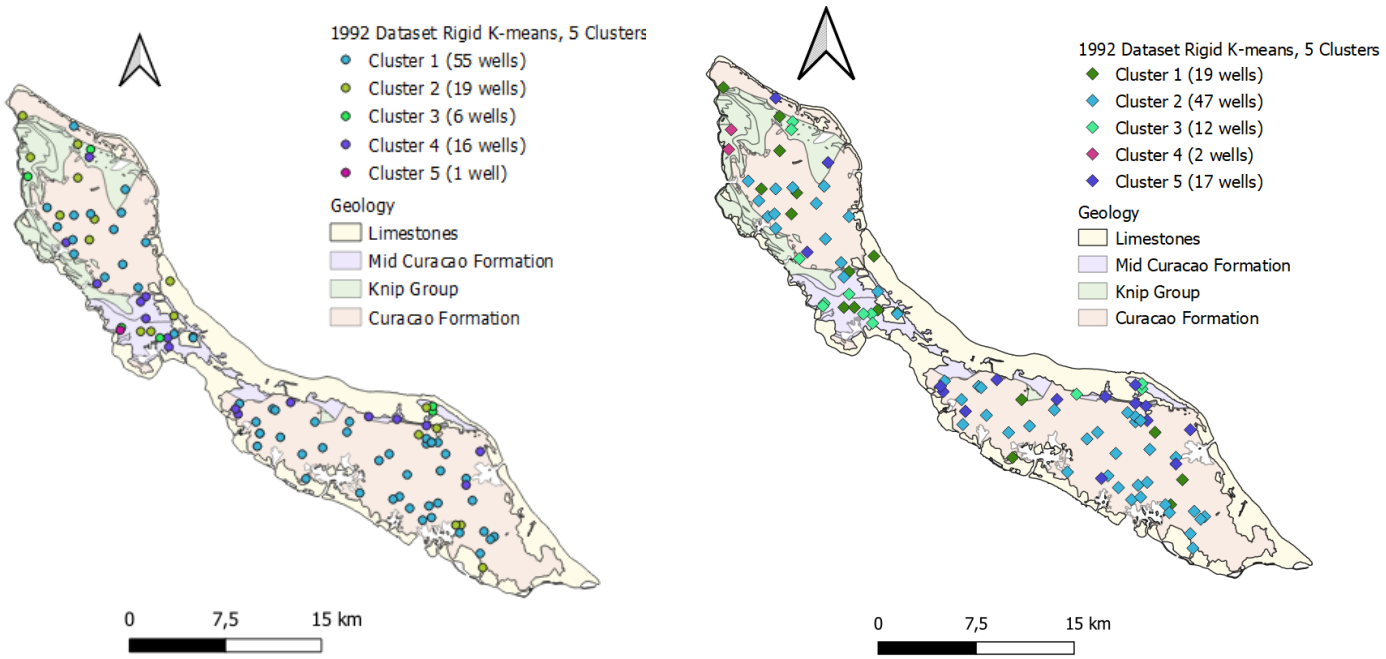

Figure 69. Rigid k-means for 1992 dataset with 19 parameters (left) and with 14 parameters (right).

Cluster analyses 2021 with 14 parameters (pH, NH_4, Na, K, Ca, Mg, PO_4, Cl, SO_4, HCO_3, Mn, NO_3, Si and Fe)

A cluster analyses was then done for 2021 with the same 14 selected parameters as for the second analyses of 1992 (Table 57). Again, the choice was made to assess for five clusters. as this also has the lowest BIC number and is consistent with how the previous cluster sizes were chosen for 1992. The hydrochemistry of the five clusters of 2021 (Table 57) is compared against standard values (Table 56), interpreted below and subsequently summarized (Table 55).

Cluster 1 – freshest cluster

The first cluster (*n*=19) has the lowest Ca, Cl, Mg, and NO_3 concentrations of all clusters. Spatially the wells are located around the edges of Cluster 4 (low brackish anthropogenic cluster), both in east and west (Figure 70, left). Although all clusters are mixed water types, Cluster 1 is closest to a Ca-Mg-HCO_3 water type (Figure 72). The EC of cluster 1 and 4 are similar at 1.7±1.3 and 1.9±1.4 mS/cm, respectively. The EC of other clusters is higher, ranging from 3.8±2.2 mS/cm (Cluster 2) to 12.8±11.0 mS/cm (Cluster 5), making Cluster 1 the freshest cluster, followed by Cluster 4. While Cluster 1 and 4 are similar in EC, Cluster 4 is likely influenced by wastewater pollution, and Cluster 1 is not, or to a much lesser extent. This is seen in the different NO_3 concentrations ($NO_{3\ Cluster\ 1}$=17±33 mg/L;$NO_{3\ Cluster\ 4}$=74±54 mg/L); in addition to the relatively higher contribution of Ca+Mg that is observed in Cluster 4 (Figure 72), which can be driven by wastewater pollution and is not observed in any of the other clusters, including Cluster 1.

Cluster 2 and Cluster 5 - two brackish clusters

Cluster 2 (*n*=4) is the smallest cluster and has an EC of 3.8±2.2 mS/m. Cluster 2 and Cluster 5 (*n*=16) are similar to each other as that they both fall in the brackish range, but Cluster 2 has lower salinity than Cluster 5 (EC=5.5±4.1mS/cm) and relatively less SO_4 (Figure 72). The Si (26±10 mg/L) and HCO_3 (789±426 mg/L) concentrations are higher in Cluster 2, which could mean that Cluster 2 is more exposed to mineral dissolution. Both clusters have relatively high NO_3 concentrations. In terms of location, no distinct geographical clustering of Cluster 2 is witnessed. For Cluster 5, some wells are located close to the coastline, but there are also wells situated more inland (Figure 70, left); what these wells do have in common is that they are somewhat located along the edges that surround Cluster 1 and 4.

Cluster 3 – reduced fossil seawater (Mid Curaçao) cluster

Cluster 3 (*n*=5) is characterized by the highest concentrations of Ca, Cl, Na, SO_4, and lowest Si (7.2 ± 5.9 mg/L). This cluster also has the highest EC (12.8±11 mS/cm), and the Cl concentration is 29% of that of seawater (Table 56). Of all clusters, Cluster 3 is closest to a Ca-Mg-Cl-SO_4 water type. Most Cluster 3 wells are located in the Mid Curaçao Formation (Figure 70, left) and could therefore be influenced by fossil seawater trapped in the lower permeable layers of the Mid Curaçao formation ((van Leeuwen, 2022). possibly explaining the higher salinity levels. The Mn and Fe concentrations are also highest for this cluster, indicating reducing circumstances.

Cluster 4 – low brackish anthropogenic (Curaçao Lava) cluster

Cluster 4 (*n*=35) is the largest cluster and distinctly located in the Curaçao Lava Formation, on both the eastern and western side (Diabaas East and west). Cluster 4 is more inland than the other clusters (Figure 70, left) and its Ca, Cl and Na concentrations indicate low brackish water (Table 56). Together with Cluster 2, Cluster 4 has the highest Si concentration (27±6 mg/L). As mentioned in the paragraph on Cluster 1, the hydrochemistry of Cluster 4 shows anthropogenic influences related to wastewater. Despite having a similar EC as Cluster 1, Cluster 4 has higher NO_3 concentrations (74±54 mg/L). In addition, when reviewing the piper diagram plotting all five 2021 clusters (Figure 72), it is witnessed that Cluster 4 is the only cluster that has relatively more Ca+Mg (roughly 10%), whereas all other clusters have the same Ca, Mg, Na, K cation ratio. Cluster 4 also has the lowest Mn and Fe concentrations of all clusters. Notably, Cluster 4 (2021) is very similar to Cluster 2 (1992, *n*=47) of the 1992 analyses (Figure 71). They are both the biggest clusters, both located in the Curaçao Lava Formation, and when comparing the concentrations (Table 58), similarities are clearly observed for Ca, Cl, HCO_3, Mg, NO_3, PO_4, Si and SO_4. This could indicate that the processes behind Cluster 4, low brackish water located in the Curaçao Lava formation experiencing wastewater pollution, were also at play in 1992.

Table 55. Rigid k-means Cluster Analyses for 2021.

Cluster	Cluster name	Key characteristics
Cluster 1 (*n*=18)	Freshest	Freshest cluster with low brackish water located around the edges of Cluster 4 Lowest EC; closest to a Ca-Mg-HCO_3 water type; lowest Ca, Cl, Mg; lowest NO_3.
Cluster 2 (*n*=4)	Brackish I	Small brackish cluster with medium EC and influences from geology Medium EC; Cluster 5 also brackish, but Cluster 2 has lower EC, Cl, Na, Mg, and SO_4 and higher HCO_3; highest Si (together with Cluster 4)
Cluster 3 (*n*=5)	Reduced fossil seawater (MCF)	A reduced fossil seawater cluster located in the Mid Curaçao Formation Highest EC, Ca, Na, SO_4 and Cl (29% of seawater); highest Mn and Fe; lowest Si; closest to a Ca-Mg-Cl-SO_4 water type.
Cluster 4 (*n*=35)	Curaca Lava (low brackish anthropogenic)	Low brackish cluster located in the Curaçao Lava Formation exposed to wastewater pollution Largest cluster; most inland; highest Si (together with Cluster 2); only cluster with relatively more Ca+Mg (Figure 72); similar EC as Cluster 1, but higher NO_3 concentrations; lowest Mn and Fe; similar to the second cluster of the 1992 dataset.
Cluster 5 (*n*=16)	Brackish II	Brackish cluster with medium-high EC on outside of Cluster 1 and 4 Medium-high EC; Cluster 2 also brackish, but Cluster 5 higher EC, Cl, Mg, Na and SO_4.

Recommendations

Clustering is a valuable tool to help determine the underlying processes that influence the hydrochemistry, yet there are several aspects and limitations to be taken into consideration. With the rigid k-means clustering used in this thesis, the results are sensitive to the initial choice of the amount of clusters especially when there is no previous knowledge on the amount of accurate clusters. When different methods (Elbow, BIC number, rule of majority) were applied to determine the amount of clusters, conflicting suggestions were given as to what amount of clusters should be chosen. For a more in-depth analyses, different cluster sizes for the rigid k-means clustering method could be assessed in more detail, or alternative clustering methods can be used, such as the fuzzy-c means analyses. The latter would be especially beneficial for a deeper understanding of the wells that are now categorized into more scattered or smaller clusters, such as the non-CLF clusters. In addition, it is recommended to obtain the exact analyses that was done in 1992, so it can be better mimicked and compared. Lastly, seawater and rainwater samples can also be included in the cluster analyses, which could benefit the results as the algorithm is trained to detect certain ratios and differences on the outskirts of the spectrum.

Multivariate statistics of 1992 and 2021

The multivariate statistics of the 1992 and 2021 dataset show that underlying salinization and wastewater pollution processes drive and explain most of the variance found in Curaçao's groundwater hydrochemistry. Salinization is observed in the first dimensions of the PCA, for both 1992 and 2021. In addition, the rigid k-means clustering of 2021 indicates that salinity plays a significant role in how clusters are distinguished. Cluster 1-4 (1.7-1.9 mS/cm), Cluster 2 (3.8 mS/cm), Cluster 5 (5.5 mS/cm) and Cluster 3 (12.8 mS/cm) have increasing salinity levels, although the possible influence of more subtle processes are also observed, such as mineral dissolution and redox processes.

Wastewater pollution is witnessed in the second dimension of the PCA, for both 1992 and 2021, where 19-21% of the variability is explained by the relations between parameters such as NO_3, PO_4, HCO_3 and NH_4. In the cluster analyses, Cluster 1 and 4, that have similar EC, are distinguished by anthropogenic influences, where the wells of Cluster 4 are under influence of wastewater pollution, mostly seen in higher NO_3 concentrations.

For further research the eastern and western side of certain clusters could be zoomed in on, different cluster sizes could be tested and alternative methods for cluster analyses, such as fuzzy c-means clustering, could be applied to obtain a deeper understanding of the 1992 and 2021 dataset.

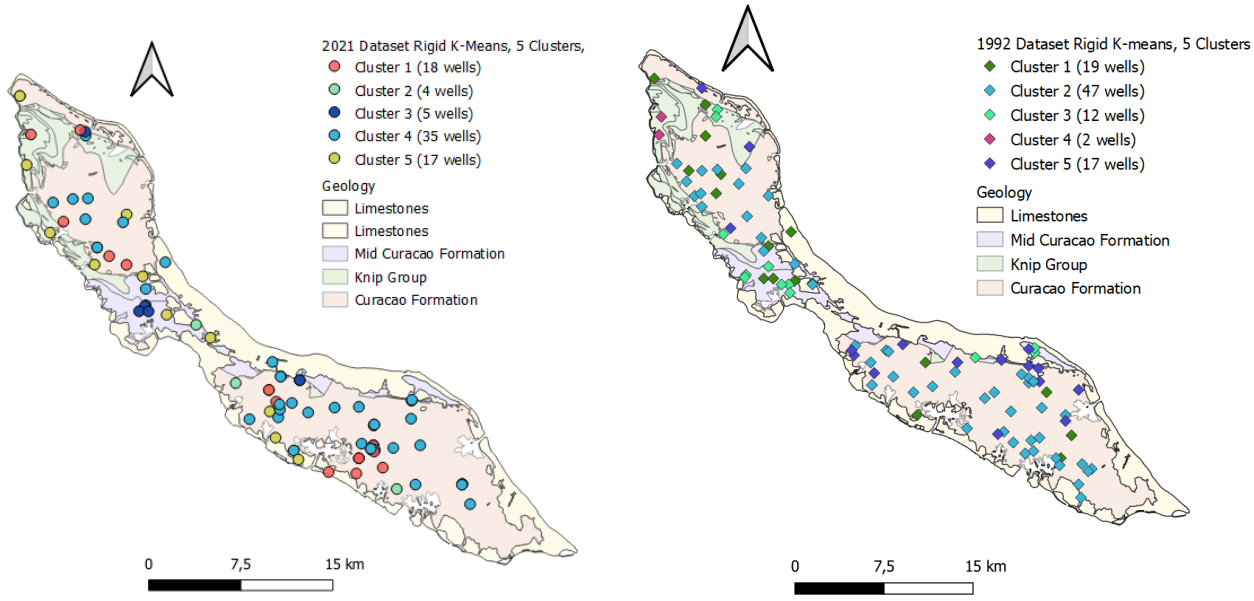

Figure 70. 2021 and 1992 cluster analyses maps next to each other for comparison.

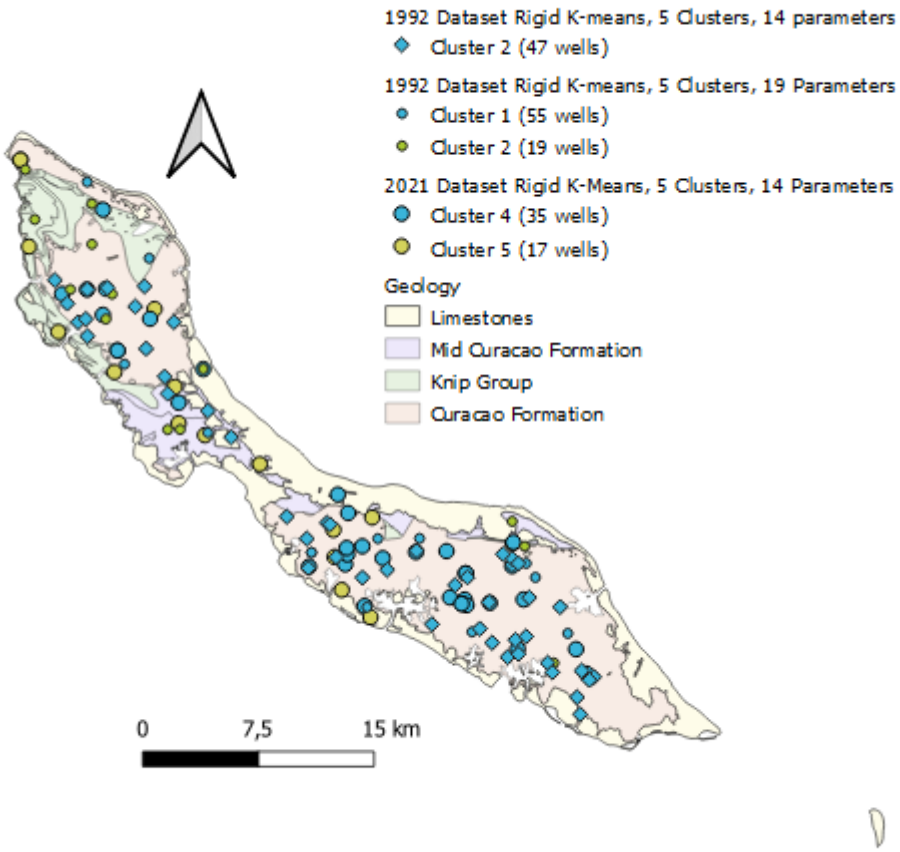

Figure 71. Rigid k-means Cluster Map with different clusters from 1992 and 2021 combined.

Table 56. Concentration standards of selected 14 parameters for different water types.

Parameter	Seawater	High Brackish	Low Brackish	Rainwater	Raw Wastewater	Drinking water
Ca (mg/L)	400	105	96	2.27 ± 0.87	-	-
Cl (mg/L)	18980	2970	191	14.32 ± 13.33	32 - 67	<150
Fe (mg/L)	-	-	-	0.01 ± 0.01	0.12 – 0.45	<0.2
HCO_3 (mg/L)	140	250	73	10.80 ± 4.43	60 – 370	>60
K (mg/L)	380	85	6.5	0.92 ± 0.23	22 - 26	-
Mg (mg/L)	1262	130	12	1.24 ± 0.90	-	-
Mn (mg/L)	-	-	-	4.10 ± 2.03	-	<0.05
Na (mg/L)	10566	1837	90	11.03 ± 8.28	49 - 54	<150
NH_4 (mg/L)	-	-	-	0.22 ± 0.08	4 - 108	-
NO_3 (mg/L)	-	-	-	0.20 ± 0.23	0.03 – 4.2	<50
pH (-)	-	-	-	6.81 ± 0.52	7.1 – 7.4	7.0<pH<9.5
PO_4 (mg/L)	-	-	-	0.05 ± 0.04	4 - 12	-
Si (mg/L)	1 (mg/L SiO_2)	17 (mg/L SiO_2)	24 (mg/L SiO_2)	0.03 ± 0.04	-	-
SO_4 (mg/L)	2649	479	159	3.16 ± 1.50	20 – 50	<150
EC (mS/cm)*				0.063 ± 0.053	1 – 2.5	<0.125
Source	Standard Seawater Composition (Lienhard et al., 2012)	High Brackish Composition (Lienhard et al., 2012)	Low Brackish Composition (Lienhard et al., 2012)	Rainwater results of fieldwork campaign ’20 and ’21 (Appendix IV)	Sampling from different papers mentioned in (Robertson, 2021)	Waterleiding Besluit, 2001 (Lenntech, 2022)

Table 57. Cluster analyses for five clusters for 2021, with 14 parameters

Cluster size	Cluster 1: #18 wells Freshest		Cluster 2: #4 wells Brackish I		Cluster 3: #5 wells Reduced Fossil Seawater (MCF)		Cluster 4: #35 wells Anthropogenic Low Brackish (CLF)		Cluster 5: #16 wells Brackish II	
Parameters	C1_mean	C1_std	C2_mean	C2_std	C3_mean	C3_std	C4_mean	C4_std	C5_mean	C5_std
Ca (mg/L)	97,7	49,8	246,3	99,6	1056,0	1239,1	138,5	101	337,0	219
Cl (mg/L)	356,7	429,8	990,6	824,5	5549,1	6762,1	368,9	477	1631,2	1621
Fe (mg/L)	0,2	0,5	0,0	0,0	5,8	7,8	0,0	0	0,0	0
HCO_3 (mg/L)	474,5	154,3	788,7	425,6	399,2	187,8	475,7	116	596,5	523
K (mg/L)	5,4	10,7	4,4	3,5	10,4	4,2	3,2	9	12,3	23
Mg (mg/L)	72,1	50,7	132,5	52,4	573,6	521,9	90,6	60	220,8	128
Mn (µg/L)	243,9	297,8	436,0	519,5	1348,6	1990,2	9,0	12	56,6	54
Na (mg/L)	216,5	218,9	452,5	406,3	2111,4	2269,8	204,8	176	698,0	755
NH_4 (mg/L)	0,4	0,3	1,8	1,8	0,3	0,1	0,2	0	5,0	19
NO_3 (mg/L)	17,4	33,0	71,8	78,1	23,7	47,3	74,6	54	63,3	71
pH (-)	7,4	0,4	6,9	0,2	7,0	0,2	7,1	0	7,1	0
PO_4 (mg/L)	1,5	1,5	4,6	5,2	0,2	0,2	0,8	3	1,9	5
Si (mg/L)	21,2	6,1	26,3	9,7	7,2	5,9	26,8	6	18,6	10
SO_4 (mg/L)	51,3	49,8	64,3	79,7	932,6	549,2	113,5	107	339,7	219
EC (mS/cm)	1,7	1,3	3,8	2,2	12,8	11,0	1,9	1,4	5,5	4,1
HCO_3 / EC	0,28		0,21		0,03		0,25		0,11	
Watertype	Mixed		Mixed		Mixed		Mixed		Mixed	

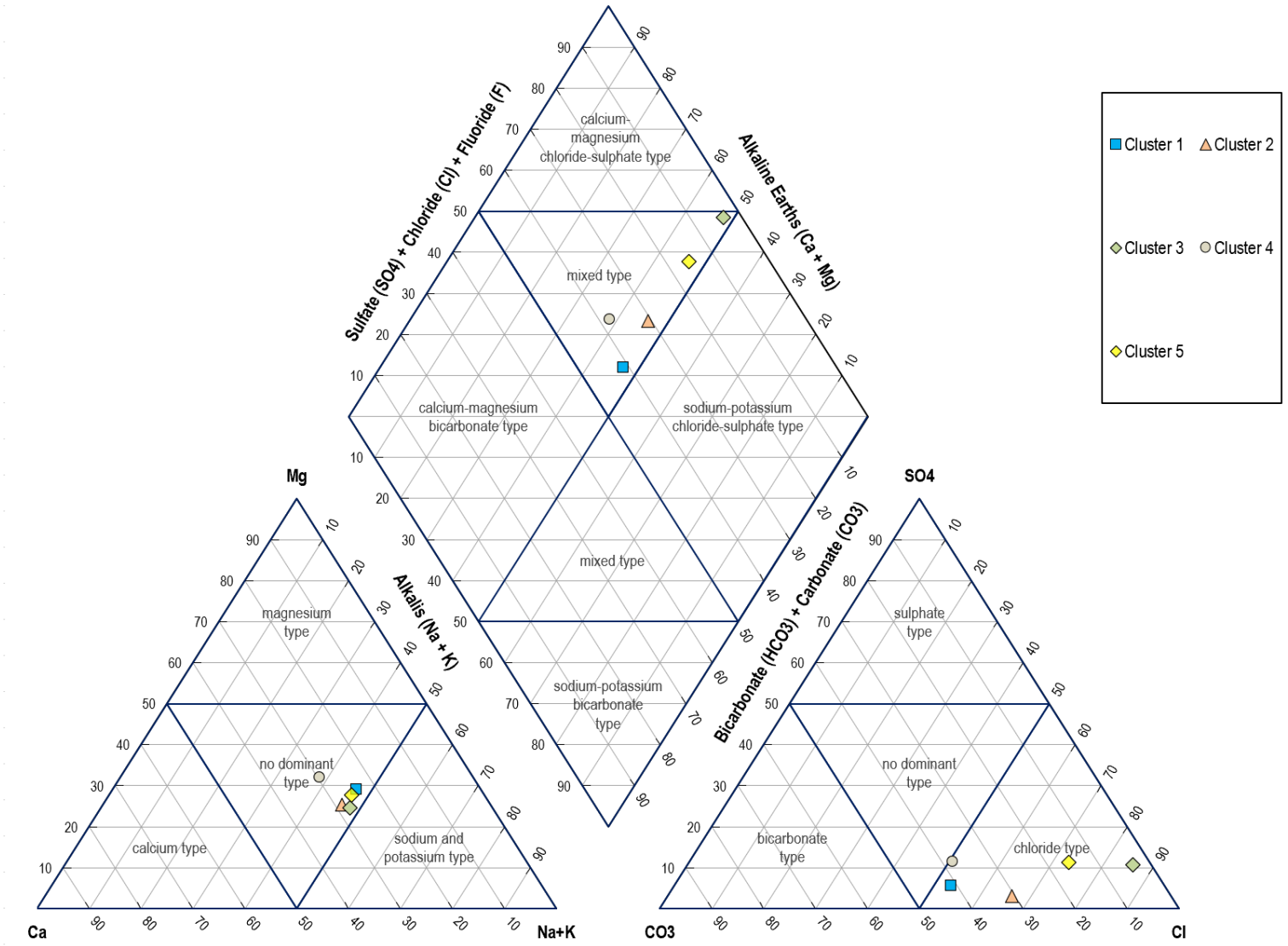

Figure 72. Piper diagram of different clusters of 2021 dataset.

Table 58. Comparison cluster analyses of biggest cluster (CLF) for 1992 and 2021.

Cluster size	Cluster 1992: #55 wells 19 parameters		Cluster 1992: #47 wells 14 parameters		Cluster 2021: #35 wells 14 parameters	
Parameters	C1_mean	C1_std	C2_mean	C2_std	C4_mean	C4_std
Ca (mg/L)	102	40	108	33	138	101
Cl (mg/L)	356	211	378	230	368	477
Fe (mg/L)	-	-	0,1	0,1	0,0	0
HCO_3 (mg/L)	443	100	490	82	475	116
K (mg/L)	1,2	1,5	1,6	2,6	3,2	9
Mg (mg/L)	81	35	86	27	90	60
Mn (mg/L)	0,03	0,1	0,1	0,1	9,0	12
Na (mg/L)	182	103	193	91	204	176
NH_4 (mg/L)	-	-	1,1	4,8	0,2	0
NO_3 (mg/L)	-	-	62	61	74	54
pH (-)	7,40	0,28	7,1	1,1	7,1	0
PO_4 (mg/L)	-	-	0,5	0,5	0,8	3
Si (mg/L)	-	-	32,2	3,7	26,8	6
SO_4 (mg/L)	111	82	111	82	113	107

6 Conclusion

A hydrochemical groundwater survey was carried out in 2020 on the Caribbean island Curaçao as part of the SEALINK project. The main objective of this thesis was to determine the current (2020) chemical state of Curaçao's groundwater, whilst also analyzing for long-term pollution trends with databases from the previous fieldwork campaigns, conducted in 1977 (Abtmaier, 1978), 1992 (Louws et al., 1997) and 2021 (Verstappen, 2022). In total, 27 quality parameters of the 2020 dataset have been analyzed and their relationships with other years were investigated to gain insight into the different processes influencing groundwater quality over the decades. Acquiring such knowledge can ultimately support in the protection of (ground)water resources against anthropogenic and natural hazards. In addition to geochemical trends, attention has been paid to the development of wells throughout the decades, and the representativity of the data.

Curaçao is a semi-arid climate and contains four geologies: Knip Group, Limestones, Mid Curaçao Formation (MCF), and Curaçao Lava/Diabaas Formation (DF), which is present as both Diabaas East (DE) and Diabaas West (DW). The Diabaas mainly constitutes of olivine, chlorite-like minerals, clinopyroxene, and plagioclase (Louws et al., 1997; Vries., 2000). Within this thesis, Curaçao was divided into a western and eastern section. Willemstad is located in the east, accommodating 170 000 people (United Nations, 2022) and has most of Curaçao's drinking/wastewater treatment plants and pipelines (Erdogan, 2021). The west is much less populated, mostly rural/agricultural and holds nature park Cristoffelpark (Restrepo et al., 2021). Due to problems with equipment in the Waterlab, TU Delft, only a sub-selection of 2020's eastern wells was fully analysed for its cation-content and suitable; the remaining samples were not used for the comparative assessments of non-field parameters (field: EC, pH, turbidity, NO_3).

Of the wells sampled in 2020, the EC ranged from 0.1 to 18.8 mS/cm: 29% of the wells were fresh, 53% slightly brackish (1.5–5 mS/cm), 17% brackish (5–15 mS/cm) and 1% saline, with most brackish and saline wells located in the west. The lowest ECs are on the eastern side of Curaçao in DE, the highest on the western side in the MCF. Groundwater pH ranged from 6.2 to 8.15, with the lowest in the west, and the highest in the Limestones formation. The majority of wells were used for private irrigation (51%), commercial agriculture (19%) or household practices (11%); all owners that had pool (n=8; 9%) used groundwater for filling; one well owner drank from his well. For irrigation, the eastern wells are at a low-medium sodium hazard, determined by the Sodium Adsorption Ratio and a medium-high salinity hazard. Some (n=8) deliberately irrigated with cesspit water, especially if groundwater was too high in salinity, and as tap water is expensive: €5.14 to €10.14 per m^3 (Aqualectra, 2022). 44% of wells are unsuitable for drinking, due to high NO_2, EC, turbidity, pH, NO_3 and NH_4 (WHO, 2022), but this is likely more, as 97% of wells were deemed unsuitable for drinking in 2021 (Verstappen, 2022), mainly because of bacterial contamination which was not assessed in 2020.

Of the 96 wells measured in 1992, 62 were identical to the 1977 fieldwork campaign. Sampling identical wells could result in more accurate comparative assessments. For this reason, the initial well sampling strategy was to measure the exact wells as was done in 1992. Although all 96 wells were visited, only 20 could actually be measured (21%), as several were now abandoned, overgrown, inaccessible (24%), no longer existed (33%) or access was not granted/nobody was home (21%). To acquire more data, an additional 71 wells were sampled, bringing the total to 91 (n_{east}=52; n_{west}=49). These wells were as homogeneously distributed across the island as fieldwork conditions allowed for, considering geology land use and the west-east division, but this was not always possible, as accessing wells remained to be a challenging practice. To gain insight into the effects of local heterogeneity, wells situated closely together (n=7, 21-74 m) were measured shortly after one other (<30min) to compare for EC, pH, NO_3, Ca, Cl, disclosing several quality differences, even at a smaller scale (ΔEC=0.5mS/cm, Δ35%, 52m; ΔCa=40mg/L, Δ54%, 52m). This underlined the value of measuring identical wells, and by lack thereof obtaining a dataset that has enough data points to overcome these local variabilities. It also showed the possible effects in wastewater-related components by sampling closer or further away from septic tanks/cesspits, e.g. nitrate (ΔNO_3=175 mg/L, Δ450% 21m).

As the fieldwork campaigns of 2020 and 2021 had similar wet seasons (2021: 623 mm; 2020: 646 mm (WMO, 2022)), and are only one year apart (10 Nov '20– 3 Jan -21; 23 Oct '21– 23 Dec '22), the expectation was that results would not significantly differ from each other, even with only eight identical wells between them. Yet, they differed on a range of parameters (i.e. alkalinity, pH, Ca, Fe, F, K, Mg, NH_4). Similar results would have allowed for the datasets to be combined as one moment in time, and would have also indicated that the current sample size (n=71-91) was sufficient to balance out local effects. The dissimilarities found between them are likely caused by a distortion of the 2020 dataset, related to the abovementioned lab problems, resulting in a 2020 sub-selection excluding higher salinity samples. The recommendation is to complete the 2020 analyses, and re-compare so that this factor could be ruled out.
The differences between 2020-2021 could have also been caused by the field methodology. In 2021 groundwater was collected with a bailer, hand pump or vacuum pump, whereas in 2020, only a weighted bottle was used. This meant that,

when stationary well pumps were not available, sampling in 2020 could only be done from shallower depths. This can have non-representative samples as a consequences of several processes, among which the degassing of CO_2 which results in higher pH, and lower alkalinity, Ca and Fe (Appelo & Postma, 2005), which, except for Fe, is witnessed in the 20-21 comparison. In addition, alkalinity was determined differently (spectrophotometry versus titration). When comparing wells that were measured in both 2020 and 2021 (*n*=8) for EC and sampling depth, it was also observed that wells without a pump, and therefore sampled from different depths, could differ in salinity (ΔEC=2.7mS/cm, <52%, MCF). Although there are indications that the methodology has affected the results, with the information that is currently available it is still hard to determine in what manner and to what extent. Nonetheless, it is advised to exclude certain (i.e. non-purged) wells upon completion of the 2020 dataset, which could be assessed by judging the sampling conditions on a well-to-well basis using fieldwork notes on well type, sampling methodology, handling, purging technique and sample depth.
A uniform sampling method has now been set up by PhD-candidate M. Wit to avoid discrepancies in sampling for current and future groundwater research, but the effects of field methodology differences must still be taken into consideration when comparing current and future data with 1992 and 1977 for long-term trends, as methods did not just differ between 2020-2021, but between all datasets. Before this can be accounted for, more information on historical fieldwork campaigns should be obtained as sections are missing in the only partially available reports of 1977 and 1992.

From the comparisons over the decades, the following key findings emerged (Table 59; Figure 73): freshening in the east, acidification that is more distinct in the west, a significant rise in alkalinity for the east, but not the west and no significant trend in nitrate, but nonetheless high nitrate concentrations, especially in the east.
The differences between east-west for pH and HCO_3 cannot be attributed to a more effective geological buffering capacity in the east, as the differences are also between in DE and DW, in which the same levels of neutralizing rock-water interactions would occur. The increase in Mg (east-west: ’77-’21), K (west) and Ca (west: ’92-’21) could also be an effect of this (Appelo & Postma, 2005). When comparing pCO_2/pH between east-west (2021), no difference is observed, but all wells, east and west, have values higher than atmospheric pCO_2, indicating underground processes with a higher influx than can be counteracted by neutralizing processes. Although pCO_2 gives insight into the amount of dissolved CO_2, it does not show the *origin* (e.g. wastewater and/or root respiration), where other indicators come in.
It is highly likely that eastern acidification is caused by leaking wastewater that resulted in the oxidation of dissolved organic matter ($CH_2O+O_2 \rightarrow CO_2+H_2O \rightarrow H_2CO_3 \rightarrow HCO_3^- + H^+$), and nitrification ($NH_4+2O_2 \rightarrow NO_3^- + 2H^+ + H_2O$). This is substantiated by higher eastern NO_3 concentrations, eastern exposure to Willemstad’s wastewater, the correlation between H^+/HCO_3 , and the observation that NH_4 is only present in a minority of wells (2020/2021), whereas NO_3 is present in the majority, indicating well-oxidized wastewater that resulted in an overall net acidification effect.
For the rural west, acidification is presumably also related to wastewater, but to a much smaller extent than in the east and presumably with an additional cause(s) for the pH drop. Exploratory assessments point towards potential acidification from atmospheric pollution (acid rain, dry deposition) spreading westward from the petrochemical facility “Isla Refinería” with a southeastern wind. An increase in western vegetation, which would have increased the subsurface degradation of organic matter, is also speculated to have an influence, but no detailed analyses was done.
For nitrate no trend was observed, yet nitrate pollution is present for all years, with several wells exceeding the indication for human activity of 1-3 mg/L (Vadison & Brunett, 1985; Dubrovsky, 2010) (NO_3>3 mg/L: 1992: 81%, 2020: 87%, 2021: 65%) and the WHO drinking water standard (2022) (NO_3>50 mg/L: 1992: 38%, 2020: 39%,2021: 47%), likely linked to wastewater and fertilizer inputs.
Eastern freshening is likely due to wastewater discharge and leaking drinking water infrastructure in the east. Simultaneous salinization processes (over-extraction and/or seawater intrusion) presumably caused the extent of eastern freshening to decline between ’92 and ‘20/’21, The identical wells of 1992-2020 (*n*=20) showed no significant difference between them, which is in line with the findings of the larger non-identical datasets.
With the cluster analyses done on the ‘21 dataset five clusters were identified: freshest cluster, low brackish anthropogenic (Curaçao Lava) cluster, reduced fossil seawater (Mid Curaçao) cluster, and two brackish clusters.
In addition to the geochemical trend and representativity, exploratory assessments of runoff (video link) and rainwater were made to gain more insight into the surface processes that might link to the disruption of marine aquatic life. The results showed that EC, HCO_3, pH, Si, Ca and turbidity significantly increased when comparing runoff to precipitation. However, there were many practical challenges, limiting the ability for sufficient sampling and conclusive results.

As was observed during this investigation, multi-annual datasets are valuable tools to elicit large-scale and long-term groundwater quality trends, such as contamination, freshening, salinization and acidification. With increasing uncertainties surrounding anthropogenic and natural hazards (e.g. climate change, over-extraction, seawater intrusion, coral loss) such knowledge can greatly support governing parties in making well-informed decisions on the management of contamination sources, safeguarding (ground)water resources and protecting interlinked systems, such as marine aquatic life. However, gathering a representative dataset in Curaçao is challenging, as social and logistic challenges overshadow the scientific and hydrogeochemical preferences for sample collection. This stresses the importance of not just research in itself, but also establishing a network of maintained (monitoring) wells that allow for more accessible, efficient, and representative groundwater sampling than is currently possible.

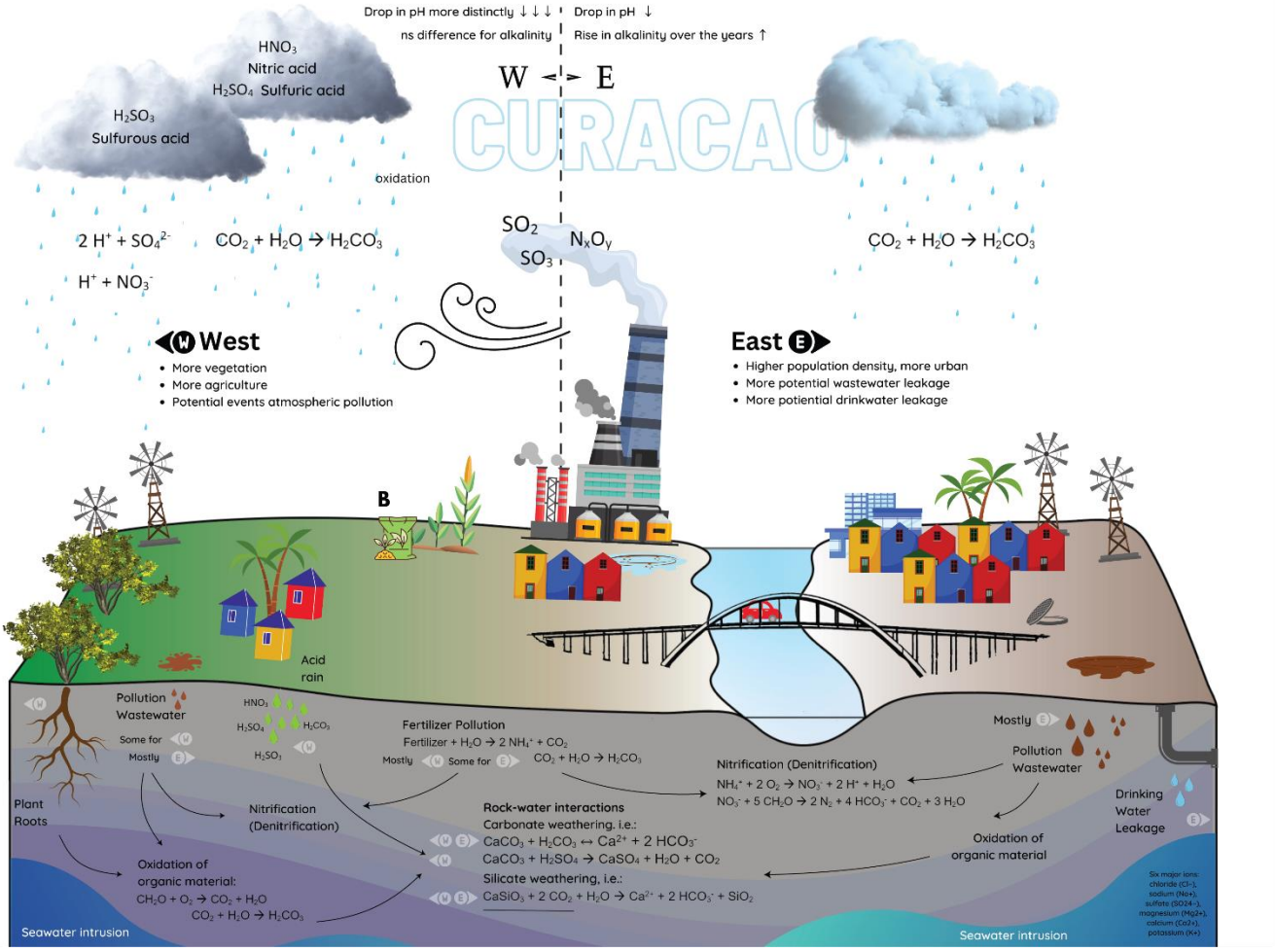

Figure 73. Conclusion: different processes and trends for western and eastern Curaçao.

Table 59. Conclusion: key findings for eastern and western Curaçao

	Total West & Diabaas West (DW)	Total East & Diabaas East (DE)
Land Use	Rural	Urbanized
Onset pH	pH = 7.83 (DW)	pH = 7.49 (DE)
pH drop	Large (∆pH = 0.7) (DW)	Considerable (∆pH = 0.25) (DE)
Alkalinity	Does not rise; no correlation between pH and alkalinity	Rises; negative correlation between pH and alkalinity
Nitrate	27±44 mg/L (’21)	74±63 mg/L (’21) (p-value < 0.0005)
Exposure to atmospheric pollution	Sometimes downwind from the refinery (5% of the time)	Upwind from refinery
Geological buffering capacity	Same for DW and DE	Same for DW and DE
SO_4	Higher in west (’77 and ’21)	Lower in east (’77 and ’21)
Mg, K, Ca, Na concentrations	Mg rises between ’77-‘21 Ca rises only between ’92-‘21 K rises between ’77-’92, ’77-‘21 No difference for Na	Mg rises between ’77-‘21 No difference for Ca, K, Na
EC	No significant difference over years	Freshening ‘77-‘92; ‘77-‘20/’21

7 Recommendations

All practical and scientific recommendations for future research that were mentioned in this thesis are listed in bullet point format in order of occurrence:

- **Establishing a network of monitoring wells**
  Overall, gathering a representative dataset in Curaçao has shown itself to be tremendously challenging. Groundwater research is already a dynamic field that requires improvisation and flexibility from the researcher – but especially so in regions such as Curaçao where social and logistic challenges overshadow scientific and hydrogeochemical preferences for sample collection. Now, with a scientific standard that is too high, one might risk not gathering enough samples to obtain a large enough dataset; with a standard that is too low, one might obtain many samples, but that are not representative of the in situ aquifers. Without a network of well-maintained monitoring wells, it remains to be a balancing act. In addition to following the measurement protocol now set up by PhD candidate M. Wit., more research could be done into the effects of local heterogeneity. This would allow for more insight into the amount of wells that are needed to overcome the effects of local heterogeneity that are present when it is not possible to sample the exact same wells as previous years. Alternatively, and preferably, a network of monitoring wells could be reintroduced in Curaçao, as this excludes well type and local spatial differences as variable and lays the foundation for easy, accessible, efficient and representative sampling. Such a network could be set up with existing wells or with novel wells that are designed specifically for monitoring.

- **Field methodology and information historical field campaigns**
  As mentioned within this thesis, the field methodology can influence the results. For this reason, it is valuable to have knowledge on the methods that were applied in previous fieldwork campaigns, so that if there are differences, they can be taken into consideration and if needed, accounted for. Although the assumption is that the fieldwork campaigns were up to scientific standard, for 1977 it is unknown how the pH was measured (directly in the field versus later in the lab), which could have influenced the pH. For 1992, it is unclear if wells were purged and how the sample water was collected. As purging and collection can influence the depth that a sample is taken at, it can also influence the results, as was observed within this thesis when comparing the results of 2020 and 2021. One of the main recommendations is therefore to obtain more information on historical fieldwork campaigns through retrieval of the fieldwork reports from the library of the University of Curaçao (1994 doctorate present under number: “OCLC-number: 743247193”), and if needed and possible also interview associated researchers to gather more insight into the methodology applied.

- **Completing the 2020 dataset, representativity and note taking**
  The dissimilarities found in this thesis between the 2020-2021 dataset are likely caused by a distortion of the 2020 dataset, related to problems that were encountered with the ICP-MS during lab analyses, which resulted in a sub-selection of sampled that excluded 13 higher salinity wells. The recommendation is to complete the 2020 analyses, as the samples are already ready to be measured, and re-compare the then complete 2020 dataset to 2021 so that it can be re-assessed if the 2020-2021 dataset are significantly different and if they can be joined together. In addition, upon completion of the 2020 dataset, it is advised to exclude non-representative (i.e. non-purged) samples from the 2020 dataset. This can be assessed with by judging the sampling conditions on a well-to-well basis using the 2020 fieldwork notes on well type, sampling methodology, handling, purging technique and sample depth. This also ties into the value of taking detailed field notes on *how* samples have been gathered that at a later stage it can be determined if this well is excluded, based on its assessed representativity. This also means that a well that is not “representative” enough upon first glance, can still be sampled, as one must also guard for not gathering enough samples when being too strict in the initial selection and assessment if a well is representative enough. With the current fieldwork challenges, it could otherwise mean that too many wells would be rejected as they are scientifically not fully “up to par”. When taking good notes, information can still be collected and inclusion and representativity can later be determined.

- **Nitrate spread**
  Even though the nitrate concentration is not significantly increasing throughout the years, NO_3 could be spreading spatially, as opposed to increasing in concentration, and further research can be done into this topic. In addition, the isotopic composition can be studied to determine what the exact source of nitrate is (Robertson, 2021), which without such analyses finding the origin of nitrate remains to be partially speculative and based on circumstantial evidence. Another possible method to determine the origin of nitrate, is to consider the nitrate/chloride ratio, which can give insight into pollution from fertilizer, rainwater, manure or domestic sewage pollution (Abascal et al., 2022).

- **Simultaneous salinization and freshening and drinking water leakage in the east of Curaçao**
  The causation behind the freshening that was observed in the east could be further researched through stable isotope analyses, as drinking water in Curaçao consists of seawater that is desalinated through reverse osmosis (RO) (Bonnélye et al., 2007) and RO-derived waters can be traced through isotopes (Ganot et al., 2018). This might also help distinguish between freshening that has occurred through drinking water leakage and freshening from wastewater discharge. Besides stable isotope analyses, there are a range of other methods (direct and indirect) to determine if groundwater has been affected by drinking water leakage, such as: using monitoring wells surrounding pipelines (to detect leaks with water level changes), pressure measurements, Groundwater Penetrating Radar, tracer chemicals or ratios within the results of the chemical analyses of groundwater (Amran et al., 2017). Monitoring wells only work if water levels are not already high or fluctuating. With chemical analyses comparisons (e.g. with chloride and bromide), it would be hard to determine if there is drinking water leakage, when simultaneous salination is also taking place, as is suggested within this thesis. The recommendation to determine drinking water leakage is therefore for stable isotope analyses.
  To determine eastern (simultaneous) salinization, the eastern wells of ’21 could be selected to see if the same indicators for salinization that were already found when observing the entire island as a whole by Verstappen (2022) are also found when focusing on the east and Diabaas East only. This could give more insight into the assumption that there is simultaneous salinization and freshening in the east, and that this is the reason that the extent of freshening has declined over the decades.

- **Western acidification and vegetation**
  For future research, it could be interesting to review pCO_2 concentrations of ’92 and ’20, as well as ’21, and see how it has developed for the different sides of the island over the decades, as opposed to focusing on one year only (’21) as was done within this thesis. Assessing pCO_2 over the years could provide more insight into (changes in) CO_2 originating from deep versus shallow sources (Delkhahi et al., 2020). It could also give information on if an increase in vegetation might have played a role in the acidification processes on the western side of Curaçao, provided that the alkalinity was accurately measured in these years. In addition, more information could be gathered on if and how vegetation might have increased on the western side of the island, for example with satellite imagery, with the Normalized Difference Vegetation Index (NDVI). NDVI is a common method to determine the vegetation density through remote sensing with a dimensionless inde (Pettorelli Nathalie, 2014). NDVI can also be used over a series of time with reconstruction techniques that would show changes in vegetation coverage over the decades (Li et al., 2021).

- **Atmospheric pollution & SO_4**
  Further analyses could be done related to sulfate concentrations, as (1) Verstappen (2022) found that there was an additional SO_4 -source, that could not be accounted for by seawater intrusion, and (2) there seemed to be plausibility for atmospheric pollution from the refinery located in the center of Curaçao playing a role in groundwater acidification for the west. At first, the sulfate and chloride can be plotted against each other for the east and the west, to determine if there are differences for both sides in terms of there being an additional source of sulfate, besides seawater. Sulfate can be used as an indicator for atmospheric pollution, but can also be attributed to a range of other sources (fertilizer, pyrite oxidation, wastewater, release of stored S in the soil or decomposition of organic matter (0.1% S)). Different methods could be used to identify the origins of SO_4, one of them is measuring the ratio of different isotopes of sulfur, which can provide information on the source of sulfur: δ34S from atmospheric pollution (3–12‰), fertilizers (7–21‰), detergent (−3.2–25.8‰), evaporites (−14–35‰), and pyrite (−15‰ to 4‰) (Wang & Zhang, 2019). Alternatively, a multi-isotopic approach could be used,

also measuring stable N-isotopes. This would not only give more insight into possible atmospheric pollution related N contamination, but also into wastewater and fertilizer as source of the nitrogen pollution (Torres-Martínez et al., 2021). In addition, the expected acidity of the rainwater during the refinery's operating years could be estimated by linking the expected pH of rainwater to the emission that were measured in 2014, 2015 by Pulster (2015). Relevance is there to determine causes of western acidification of the past datasets, but also for the future - especially with the current talks in Curaçao of re-opening the refinery.

- **Wastewater bias**
  Extra attention can be paid to the potential wastewater and fertilizer bias that exists with the current sampling and well strategy method, where sampled wells are often closely located to people's homes. Wastewater related pollution, e.g. nitrate, can be higher, as was also shown in this thesis where a distance of 21 and 38 meters between three different wells showed NO_3^- concentrations of roughly 72 mg/L, 39 mg/L and 27 mg/L NO_3, respectively – with the highest concentrations close to the house. Furthermore, there was no significant difference between E. Coli for the east and west within the '21 dataset, while the east has much more exposure to wastewater. Although E. Coli could have also originate from sources such as manure, it could have also been partially due to a bias towards in household wells that are measured close to septic tanks. For future research, it could be interesting to analyze the bias that occurs with sampling close to homes and septic tanks/cesspits so that it can be taken into consideration for the interpretation.

- **Rain and runoff samples**
  Just like groundwater, sampling rain and surface runoff was challenging, albeit there were different obstacles, as also mentioned in 3.1.7 Runoff and rain collection. For measuring runoff the recommendation is to be situated close to a known runoff stream (e.g. Westpunt, close to restaurant Playa Forti), as rainfall is very short-lived and localized, and hard to predict. Furthermore, a 4WD is great to make way through the unpaved and muddy nature of certain roads closer to the ocean. Equipment that is suited for the intense rainfall is also recommended. When more rainwater samples are collected, as opposed to the sparse amount of samples for 2020-2021, the comparison can also be made between groundwater and runoff, and not just between rainwater and runoff, as was done in this thesis. This is relevant because runoff does not just consist of rainwater; in heavy rainfall, rainwater will activate the hydrological system, pushing out groundwater as well. The expectation is that runoff is a mix between ground- and rainwater, with terrestrial components that are added as the stream makes it way over land, e.g. suspended solids, fertilizers. Furthermore, if the refinery reopens, assessments can be done for rainwater and runoff pH, especially within specific wind directions.

- **Valuing a social approach**
  Locals really are the experts of any region. If it wasn't for the warm and kind-hearted people of Curaçao I would still be making way through the thicket and thorns trying to access old wells. With a deeper understanding of the culture and a bigger social network, my thesis went from individual research to a community-matter, making it much easier to navigate through the island's challenges. On top of the support, local anecdotes also provided much-appreciated clues, for example on where runoff streams were located and in what areas salinization is taking place. The final recommendation is therefore to not underestimate the blessing that comes with local friendships, no matter how technical the research may be.

Bibliography

Abascal, E., Gómez-Coma, L., Ortiz, I., & Ortiz, A. (2022). Global diagnosis of nitrate pollution in groundwater and review of removal technologies. *Science of The Total Environment*, *810*, 152233. https://doi.org/10.1016/j.scitotenv.2021.152233

Abtmaier. (1978). *Groundwater investigation Curacao*.

Ahmad Cahyadi, Hendy Fatchurohman, & Indra Agus Riyanto. (n.d.). *Groundwater quality analysis in dry seasons in Panggang Cay, Kepulauan Seribu, Jakarta, Indonesia*.

Alcalá, F. J., & Custodio, E. (2008). Using the Cl/Br ratio as a tracer to identify the origin of salinity in aquifers in Spain and Portugal. *Journal of Hydrology*, *359*(1–2), 189–207. https://doi.org/10.1016/j.jhydrol.2008.06.028

Amran, T. S. T., Ismail, M. P., Ahmad, M. R., Amin, M. S. M., Sani, S., Masenwat, N. A., Ismail, M. A., & Hamid, S. H. A. (2017). Detection of underground water distribution piping system and leakages using Ground Penetrating Radar (GPR). *AIP Conference Proceedings*, *1799*. https://doi.org/10.1063/1.4972914

Appelo, C. A. J., & Postma, Dieke. (2005). *Geochemistry, groundwater and pollution*. Balkema.

Aqualectra. (2022, August 1). *Tariffs valid as of : 01 August 2022*.

Beets, D. J. (1972). Lithology and stratigraphy of the Cretaceous and Danian succession of Curaçao (Proefschrift). *P.18-104*.

Bijay-Singh, & Craswell, E. (2021). Fertilizers and nitrate pollution of surface and ground water: an increasingly pervasive global problem. In *SN Applied Sciences* (Vol. 3, Issue 4). Springer Nature. https://doi.org/10.1007/s42452-021-04521-8

Bonnélye, V., Sanz, M. A., Francisci, L., Beltran, F., Cremer, G., Colcuera, R., & Laraudogoitia, J. (2007). Curacao, Netherlands Antilles: A successful example of boron removal on a seawater desalination plant. *Desalination*, *205*(1–3), 200–205. https://doi.org/10.1016/j.desal.2006.04.045

Borovicka, T., Jirina, M., Kordik, P., & Jiri, M. (2012). Selecting Representative Data Sets. In *Advances in Data Mining Knowledge Discovery and Applications*. InTech. https://doi.org/10.5772/50787

Carratala, A., Bellot, J., Gomez, A., & Millan, M. (1996). *African Dust Influence on Rainwater on the Eastern Coast of Spain* (pp. 323–332). https://doi.org/10.1007/978-94-017-3354-0_32

Cashman, A. (2014). Water security and services in the Caribbean. *Water (Switzerland)*, *6*(5), 1187–1203. https://doi.org/10.3390/w6051187

Cashman, A., Nurse, L., & John, C. (2010). Climate change in the caribbean: The water management implications. *Journal of Environment and Development*, *19*(1), 42–67. https://doi.org/10.1177/1070496509347088

Central Bureau of Statistics Curaçao. (2022). *Central Bureau of Statistics Curaçao*. Https://Www.Cbs.Cw/Climate.

De Bruijne, R., & Louws, R. (1994). *GROUND WATERS OF CURAÇAO A Geochemical Survey* [Doctoraalverslag].

Debrot, A., & Wells, J. (2009). CURAÇAO. *Important Bird Areas in the Caribbean – Curaçao*. https://www.dcbd.nl/sites/default/files/documents/IBA_curacao.pdf

Delkhahi, B., Nassery, H. R., Vilarrasa, V., Alijani, F., & Ayora, C. (2020). Impacts of natural CO2 leakage on groundwater chemistry of aquifers from the Hamadan Province, Iran. *International Journal of Greenhouse Gas Control*, *96*. https://doi.org/10.1016/j.ijggc.2020.103001

Erdogan, E. (2021). *The terrestrial consequences of poor wastewater management in Curaçao: How exploring public health risks and ground water quality levels can provide insights into establishing its sustainable management for small island development states*. https://studenttheses.uu.nl/bitstream/handle/20.500.12932/1274/Erdogan_MSThesis_SD.pdf?sequence=1&isAllowed=y

Estep, Sandin, & Vermeij. (2017). *The State of Curaçao's Coral Reefs*.

Fabricius, K. E. (2005). Effects of terrestrial runoff on the ecology of corals and coral reefs: Review and synthesis. *Marine Pollution Bulletin*, *50*(2), 125–146. https://doi.org/10.1016/j.marpolbul.2004.11.028

FAO. (1985). *Water quality for agriculture*.

Farrell, D., Nurse, L., & Moseley, L. (2010). *MANAGING WATER RESOURCES IN THE FACE OF CLIMATE CHANGE: A CARIBBEAN PERSPECTIVE*.

Ganot, Y., Holtzman, R., Weisbrod, N., Bernstein, A., Siebner, H., Katz, Y., & Kurtzman, D. (2018). Managed aquifer recharge with reverse-osmosis desalinated seawater: Modeling the spreading in groundwater using stable water isotopes. *Hydrology and Earth System Sciences*, *22*(12), 6323–6333. https://doi.org/10.5194/hess-22-6323-2018

Geology. (2022). Geology.Com. *Https://Geology.Com/Minerals/Pyroxene.Shtml*.

Ging, P. B., Long, D. T., & Lee, R. W. (1996). *Selected Geochemical Characteristics of Ground Water from the Marshall Aquifer in the Central Lower Peninsula of Michigan*.

Grontmij, & Sogreah. (1968). *Water and land resources development plan for the islands of Aruba, Bonaire and Curacao. Report Gro ntmij (De Bilt): 133 pp*.

Jager. (2017). *Curacao Environmental Statistics Compendium (2017)*.

ter Meer, J., Henk Verhagen, & Diana Slijkerman. (2007). *Samenwerkingsverband tussen Milieudienst Curaçao en TNO ter vergroting van expertise milieuonderzoek*.
Jones, J. A. A. (2011). *Sustaining Groundwater Resources A Critical Element in the Global Water Crisis*. http://www.springer.com/series/8096
Keresztesi, Á., Birsan, M.-V., Nita, I.-A., Bodor, Z., & Szép, R. (2019). Assessing the neutralisation, wet deposition and source contributions of the precipitation chemistry over Europe during 2000–2017. *Environmental Sciences Europe*, *31*(1), 50. https://doi.org/10.1186/s12302-019-0234-9
Khan, M. N., Mobin, M., Abbas, Z. K., & Alamri, S. A. (2017). Fertilizers and their contaminants in soils, surface and groundwater. In *Encyclopedia of the Anthropocene* (Vols 1–5, pp. 225–240). Elsevier. https://doi.org/10.1016/B978-0-12-809665-9.09888-8
Li, S., Xu, L., Jing, Y., Yin, H., Li, X., & Guan, X. (2021). High-quality vegetation index product generation: A review of NDVI time series reconstruction techniques. *International Journal of Applied Earth Observation and Geoinformation*, *105*, 102640. https://doi.org/10.1016/j.jag.2021.102640
Lienhard, J., Antar, M. A., Bilton, A., Blanco, J., & Zaragoza, G. (2012). SOLAR DESALINATION. *Annual Review of Heat Transfer*, *15*(15), 277–347. https://doi.org/10.1615/AnnualRevHeatTransfer.2012004659
Marine Caribbean. (n.d.). *Offshore Services*. Http://Marinecaribbean.Com/Contact-Us/.
Martis, A., Jan van Oldenborgh, G., & Burgers, G. (2001). *Predicting rainfall in the Dutch Caribbean-more than El Niño?*
Mindat. (2022). *Chlorite Group*. Https://Www.Mindat.Org/Min-1016.Html.
Mordt, M., González De Alba, I., Jaramillo, G., Auricchio, B., Abdullahi, U., Abdulkadri, O., Rei, D., King, E., Brielle, J., Taylor, N., Pizarro, G., & Ortiz-Juárez, E. (2018). *The UNSDG MAPS mission in Curaçao was composed of the following team members*.
Naily, W., & Sudaryanto. (2018). Cl/Br Ratio to Determine Groundwater Quality. *IOP Conference Series: Earth and Environmental Science*, *118*(1). https://doi.org/10.1088/1755-1315/118/1/012020
Nationaal Archief Curacao. (n.d.). *Fisher Collection*. Https://Canoncuracao.Cw/43-Omgaan-Natuur/.
Nielsen, D. M., & Nielsen, G. L. (2005). *Handbook of Groundwater Sampling - The Essential*.
Pacic, N. (2021). Bor: Serbia's Pollution Crisis in Pictures. *Https://Balkaninsight.Com/2021/10/21/Bor-Serbias-Pollution-Crisis-in-Pictures/*.
Paytan, A., Shellenbarger, G. G., Street, J. H., Gonneea, M. E., Davis, K., Young, M. B., & Moore, W. S. (2006). Submarine groundwater discharge: An important source of new inorganic nitrogen to coral reef ecosystems. *Limnology and Oceanography*, *51*(1 I), 343–348. https://doi.org/10.4319/lo.2006.51.1.0343
Pettorelli Nathalie. (2014). The Normalized Difference Vegetation Index. *ISBN: 9780199693160*, *Oxford*.
Pulster, E. L. (2015). *Scholar Commons Assessment of Public Health Risks Associated with Petrochemical Emissions Surrounding an Oil Refinery*. http://scholarcommons.usf.edu/etdhttp://scholarcommons.usf.edu/etd/5761
Ramírez-Romero, C., Jaramillo, A., Córdoba, M. F., Raga, G. B., Miranda, J., Alvarez-Ospina, H., Rosas, D., Amador, T., Kim, J. S., Yakobi-Hancock, J., Baumgardner, D., & Ladino, L. A. (2021). African dust particles over the western Caribbean – Part I: Impact on air quality over the Yucatán Peninsula. *Atmospheric Chemistry and Physics*, *21*(1), 239–253. https://doi.org/10.5194/acp-21-239-2021
Reuters. (2022, June). *Curacao sets talks with U.S.-Brazilian consortium to run island's oil refinery*. Reuters.
Robertson, W. (2021). *Septic System Impacts on Groundwater Quality*.
Sadoff, Claudia., & Muller, Mike. (2009). *Water management, water security and climate change adaptation early impacts and essential responses*. Global Water Partnership.
Santo Tomás Seccional Tunja, U., Smith Prieto, F., Lesmes Fabian, C., Wilson Ibañez, J., & Caro Camargo, C. (2018). *Groundwater Sustainability Assessment in Small Islands: The Case Study of San Andres in the Caribbean Sea*. https://doi.org/10.20944/preprints201807.0449.v1
Shahid, S., Wang, X., & Eslamian, S. (2017). *Climate Change Impacts on and Adaptation to Groundwater The Effect of Dust on the Suspended and Bed Load of Karkheh River View project Climate change View project*. https://www.researchgate.net/publication/319101949
Thornton, S. F. (2008). *Principles and Practice for the Collection of Representative Groundwater Samples*. https://doi.org/10.13140/RG.2.2.10865.07522
Torres-Martínez, J. A., Mora, A., Mahlknecht, J., Kaown, D., & Barceló, D. (2021). Determining nitrate and sulfate pollution sources and transformations in a coastal aquifer impacted by seawater intrusion—A multi-isotopic approach combined with self-organizing maps and a Bayesian mixing model. *Journal of Hazardous Materials*, *417*, 126103. https://doi.org/10.1016/j.jhazmat.2021.126103
United Nations. (2021). *UNITED NATIONS WORLD WATER DEVELOPMENT REPORT 2021 : valuing water.* UNITED NATIONS EDUCATIONA.
United Nations. (2022). *Demographic UN Stats*.
UNOPS. (2018). *EVIDENCE-BASED INFRASTRUCTURE: CURACAO NATIONAL INFRASTRUCTURE SYSTEMS MODELLING TO SUPPORT SUSTAINABLE AND RESILIENT INFRASTRUCTURE DEVELOPMENT*.
Van Buurt, G. (2018). *Water conservation in Curaçao; using traditional earthen dams*.
Van Houselt, G. J. (2021). *A Rainwater Harvesting System based Blueprint for Excess Runoff Management on Caribbean Small Island Developing States Investigating the Feasibility of the Rigofill System Combined with New Dam Structures in the Coral Estate Resort-Curacao*.

Van Leeuwen. (2017). *Terrestrial molluscs of Aruba, Bonaire and Curaçao in the Dutch Caribbean: an updated checklist and guide to identification Terrestial molluscs of Saba (Netherlands Antilles) View project Onderzoek Algemene Rekenkamer View project*. https://www.researchgate.net/publication/324165329

van Leeuwen. (2022). *The Hydrogeology of Curaçao: an electrical resistivity study*. Hydrology and Quantitative Water Management Group Wageningen University, April 2022.

Van Sambeek, M. H. G., Eggenkamp, H. G. M., & Vissers, M. J. M. (2000). The groundwater quality of Aruba, Bonaire and Curaçao: A hydrogeochemical study. *Geologie En Mijnbouw/Netherlands Journal of Geosciences*, *79*(4), 459–466. https://doi.org/10.1017/s0016774600021958

Verstappen, I. (2022). *Hydrogeochemical investigation of the groundwater of Curaçao*.

Waitt. (2016). *Economic Valuation of Curaçao's Marine Resources*.

Wang, H., & Zhang, Q. (2019). Research Advances in Identifying Sulfate Contamination Sources of Water Environment by Using Stable Isotopes. *International Journal of Environmental Research and Public Health*, *16*(11), 1914. https://doi.org/10.3390/ijerph16111914

WHO. (2022). *Fourth edition incorporating the first and second addenda Guidelines for drinking-water quality*.

8 Appendix I

8.1.1 Smaller (*n* = 52) versus larger (*n*=91) dataset of '20

This sections shows different options regarding the representativity of the incomplete dataset of fieldwork 2020. At first the representativity of the smaller (*n*=59) dataset in regards of the complete dataset of 2020 is checked, with locations over the entire island. In order to determine this, the following aspects are added below:

- N. mean, average and range of salinity for both the complete (*n*=59) and incomplete (total, *n*=91) dataset
- Occurrence in percentages and N within the different geologies for both the complete (*n*=59) and incomplete (total, *n*=91) dataset
- Map of locations of the different samples in order to determine if the locations of the completed sample are just as well spread out as the samples that were not all completed, of the total dataset

Total amount of groundwater samples is 91, of which 59 are completely measured, 34 are not completely measured, but will be once the ICPMS is working again, and 1 sample is not completely measured, and will also not be measured in the ICPMS (Table 60; Table 61). As is witnessed in Figure 74-Figure 75, the dataset with 59 complete samples, has much lower salinity values than the complete dataset (n=91) and is therefore not taken to be representative of the entire dataset.

Table 60. Overview of salinity of full dataset, including the samples that are not fully analysed yet in ICPMS. Unit: µS/cm

	N	Min	Max	Average	Median	STD
Salinity DS1	90	113	18770	2920	1799	2917
Salinity DS2	59	113	6580	2117	1668	1549

Table 61. Occurrence of datapoints in different geologies for DS1 and DS2.

	N	CLF	K	L	LM	MCF
DS1	90*	65	0	6	0	14
DS2 (incl)	59*	46	0	5	0	3
DS3 (excl)	31	19	0	1	0	11

**DS1 is the complete dataset, including samples that have not been fully measured by the ICP-MS. DS2 is the incomplete dataset, excluding the part of the groundwater samples that are awaiting the ICP-MS analysis. DS3 is the section of samples that is excluded on the basis that they cannot yet be analyzed in the ICP-MS.*

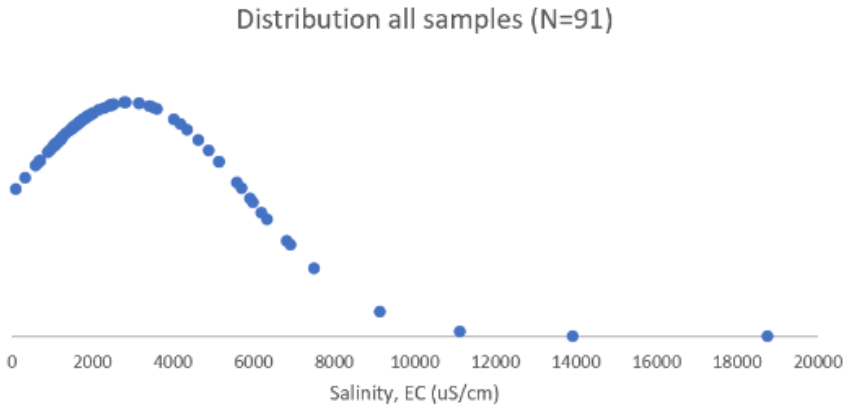

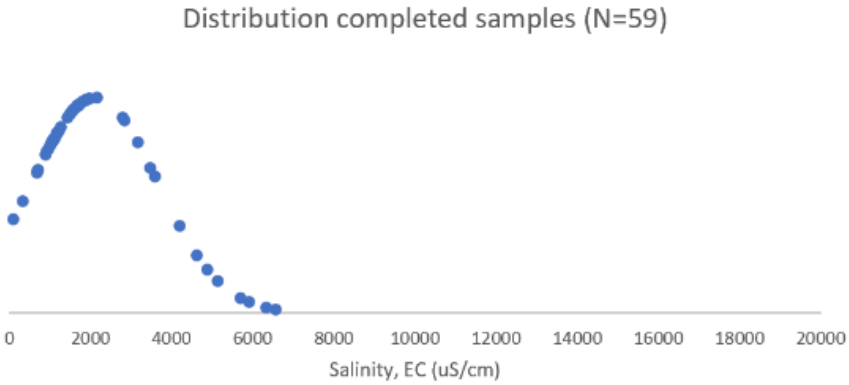

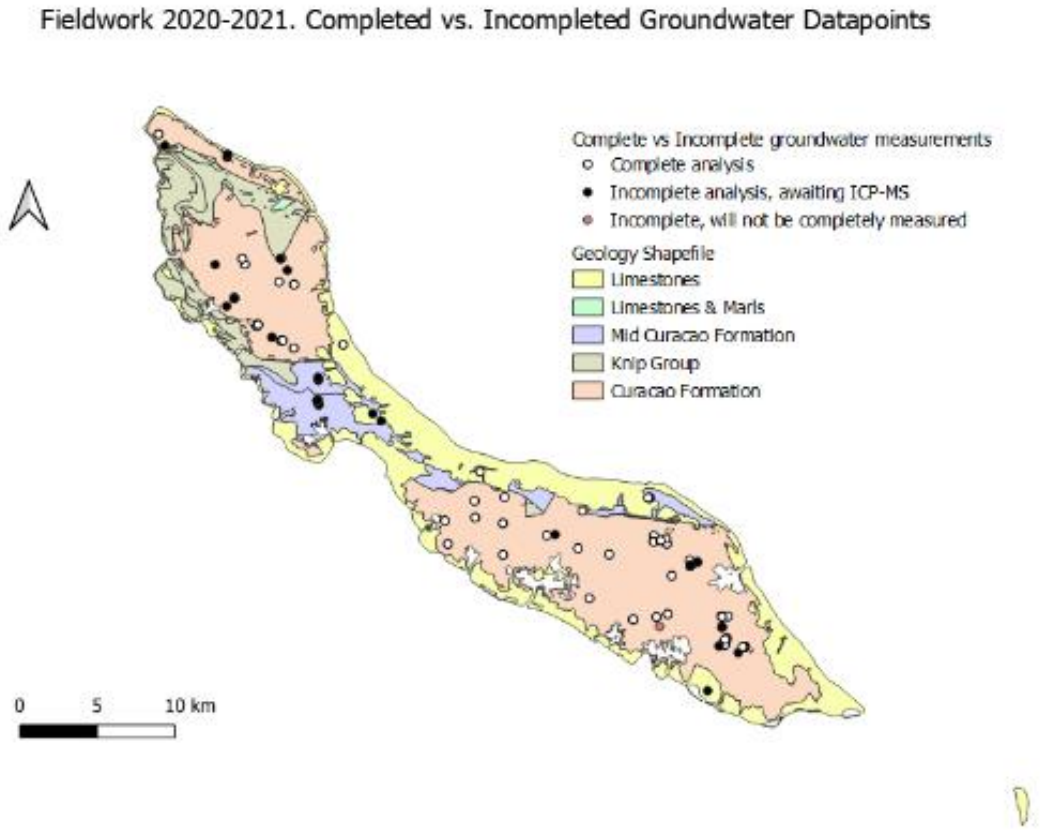

Figure 74. Measured fully analysed versus not fully analysed sample point 2020 .Top left: normal distribution all samples. Top right: normal distribution of samples that were fully measured. Bottom: Map of groundwater well locations where there is a complete analysis (white), incomplete analyses (black). Relatively speaking, the Mid Curaçao Formation has the most samples that are now awaiting ICP-MS analysis.

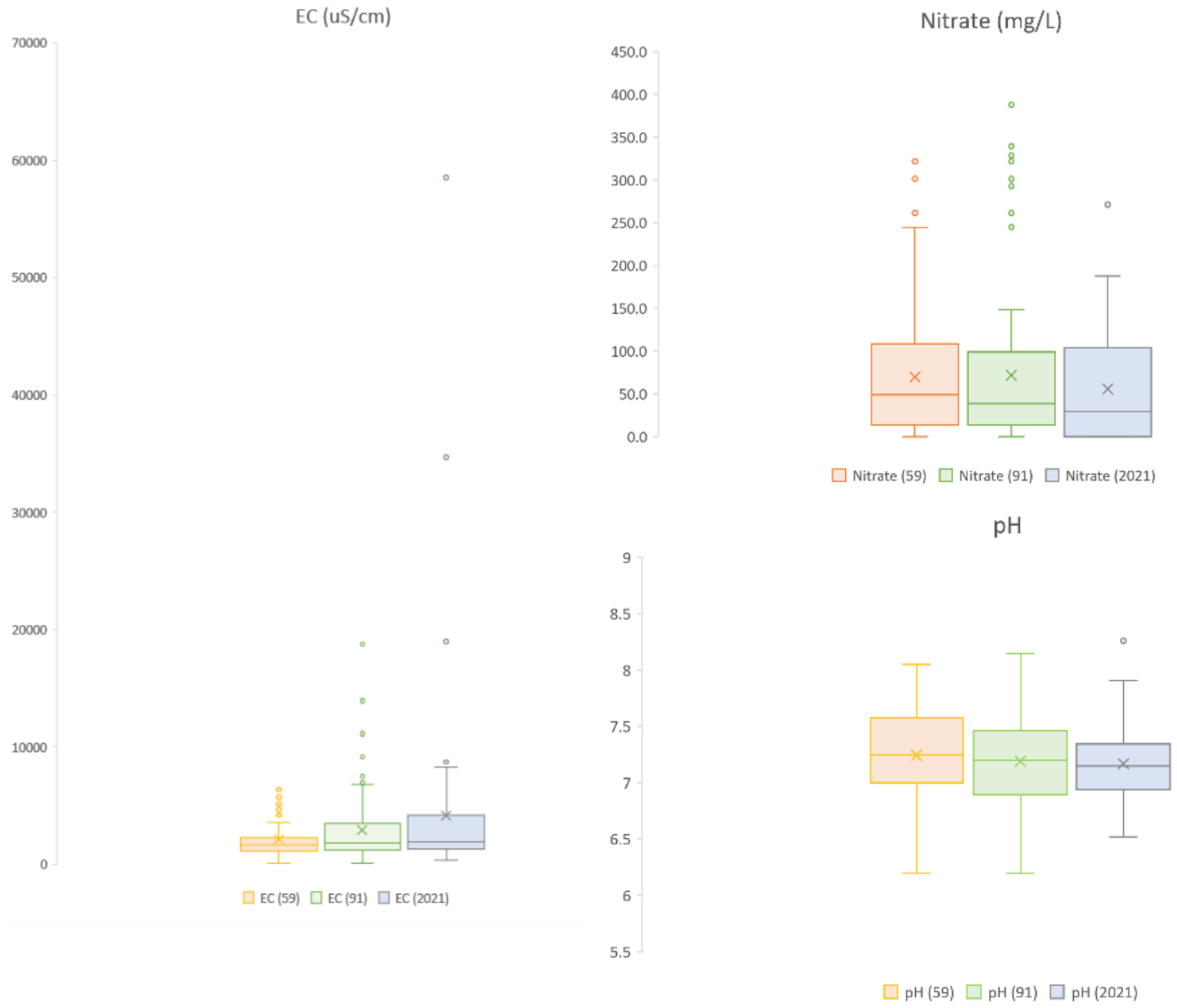

Figure 75. Boxplots fully analysed versus not fully analysed sample points 2020... Left: Boxplots EC of 2020 completed dataset (N=59), 2020 total dataset including non-completed samples (N=91) and total dataset of 2021. Top right: Boxplots nitrate of 2020 completed dataset (N=59), 2020 total dataset including non-completed samples (N=91) and total dataset of 2021. Bottom right: Boxplots pH of 2020 completed dataset (N=59), 2020 total dataset including non-completed samples (N=91) and total dataset of 2021.

8.1.2 Eastern dataset versus western dataset 2020

This sections concerns the representativity of the incomplete eastern dataset of fieldwork 2020. In the previous section the representativity of the smaller (N=59) dataset in regards of the complete dataset of 2020 was checked, which was determined not to be representative. It can be seen that the EC and pH are slightly higher for the total eastern dataset, than for the eastern dataset with completed samples (Figure 76-Figure 78; **Table 62**-**Table 63**), but the difference is not as significant as it was in the previous section. Nitrate is very similar, both for the total eastern dataset of '20 as the eastern dataset with only the complete samples. Although there will still be a distortion, due to the missing samples in the eastern dataset; for 2020 the eastern dataset will be used for data analyses and comparisons with other years.

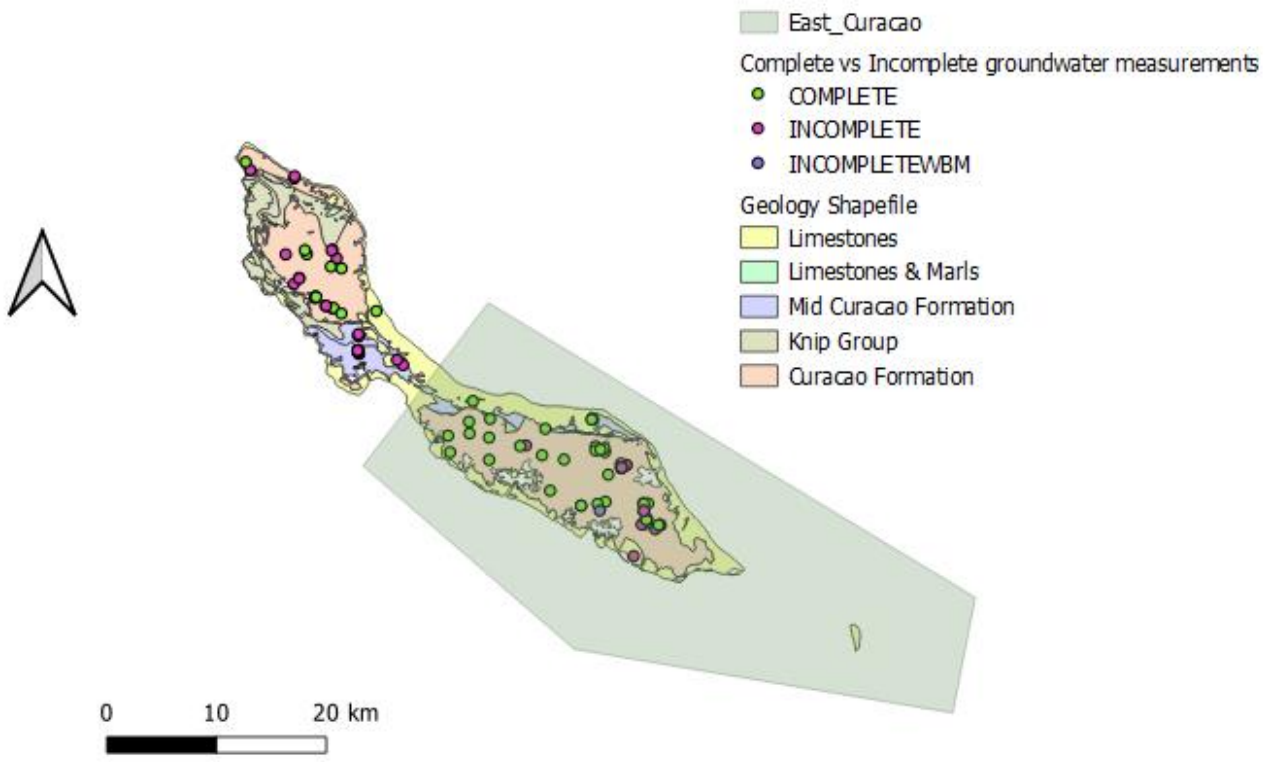

Figure 76. Eastern versus western dataset, fully analysed and not fully-analysed samples 2020 . "Complete" are the groundwater samples with complete analysis (N=59). "Incomplete" are the groundwater samples with incomplete analyses (awaiting ICP-MS to work again) (N=91).

Table 62. Total dataset, versus eastern dataset total and complete (uS/cm)

Salinity	N	Min	Max	Average	Median	STD
Total dataset (east + west)	91	113	18770	2920	1799	2917
Eastern dataset (total)*	53	113	6920	1897	1647	1351
Eastern dataset (complete)	42	113	5920	1615	1546	963

**Eastern dataset (total) are all groundwater samples present in the eastern section of the island (both with complete and incomplete analysis). Eastern dataset (complete) are only the groundwater samples that have a complete analysis in the eastern side.*

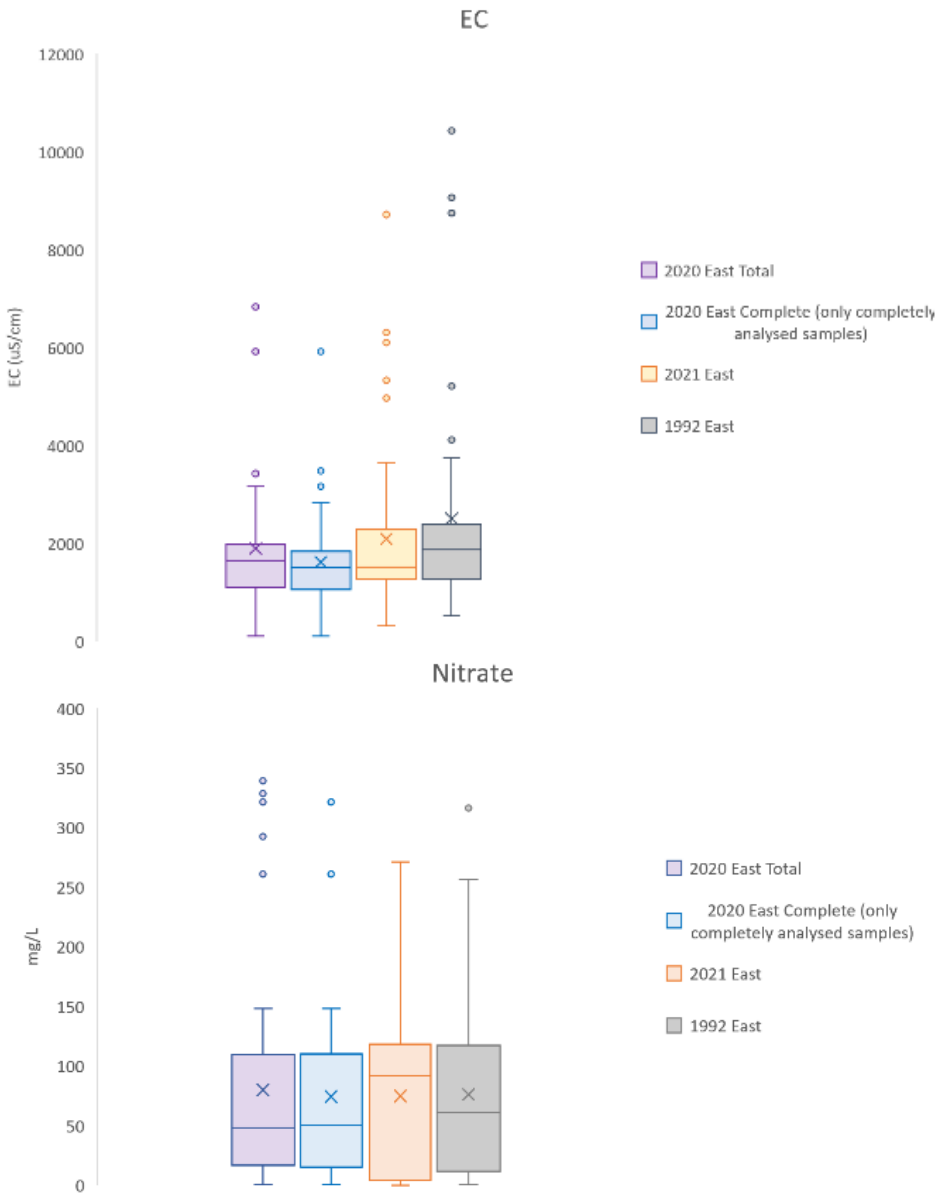

Figure 77. Boxplots EC completed and non-completed samples east . Left: Boxplots for EC (µS/cm) over eastern side (2020 total, 2020 complete, 2021 dataset, 1992 dataset). Right: Boxplots for nitrate over eastern side (2020 total, 2020 complete, 2021 dataset, 1992 dataset).

Table 63. Amount of datapoints per dataset on the eastern side of the island, per geology type.

Geology East	N	CLF	K	L	LM	MCF
Eastern dataset (all samples) '20	53	46	0	5	-	1
Eastern dataset (complete) '20	42	37	0	4z	-	1
Eastern dataset '21	44	40	0	3	-	1
Eastern dataset '92	56	52	0	0	-	4
Eastern dataset '77	>142	125	1	5	-	11

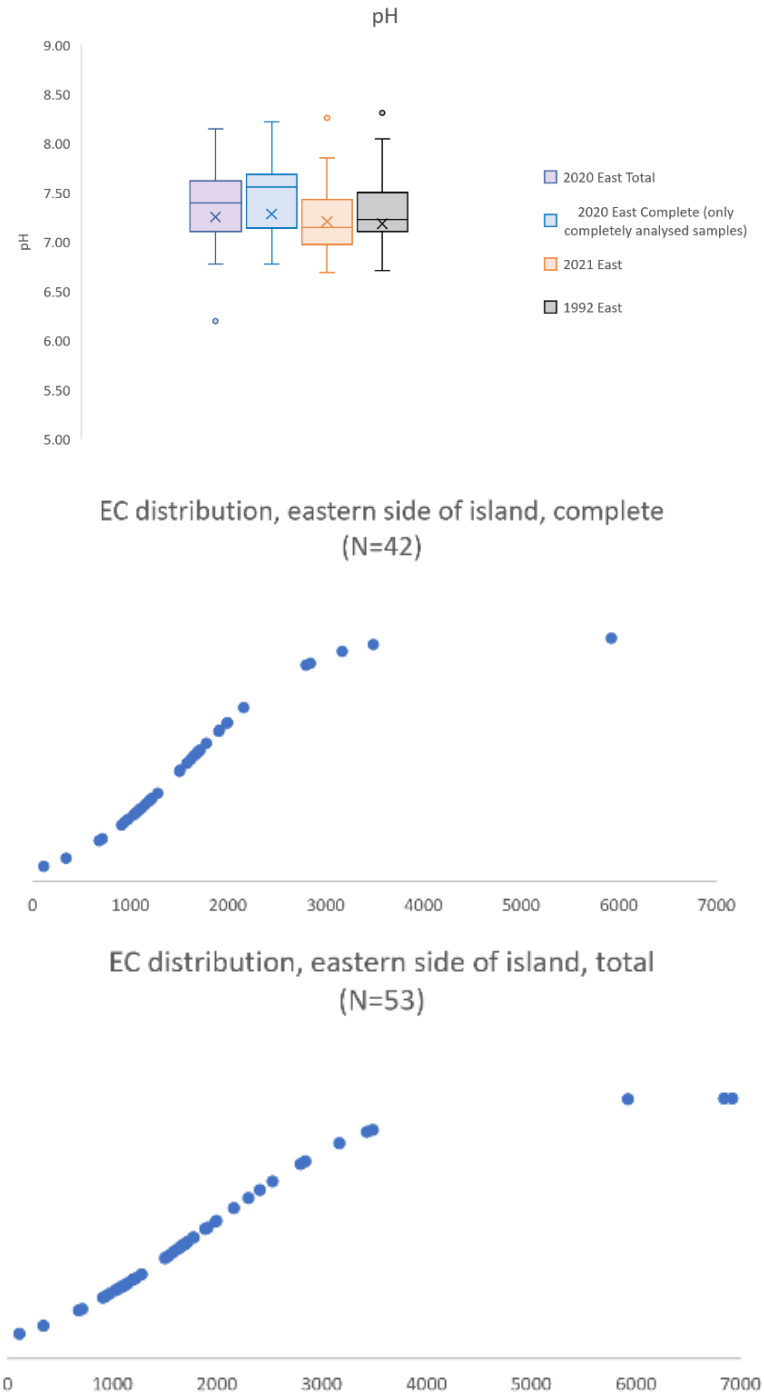

Figure 78. Boxplots pH completed and non-completed samples east. Left: Boxplots for pH over eastern side (2020 total, 2020 complete, 2021 dataset, 1992 dataset). Top right: Distribution EC total, eastern Curaçao (total: all groundwater samples, n=53). Bottom right: Distribution EC measured samples, eastern Curaçao (fully measured groundwater samples, n=42).

8.1.3 Overrange samples

M. Wit (PhD candidate SEALINK) has done a check to see if with his analyses of groundwater samples taken in ’21 of Curaçao, the initial results that were overrange differed greatly from the final results after re-analyses in the ICP-MS. What was shown (Figure 79) is that the concentrations indeed differed and cannot be considered as accurate prior to analyses.

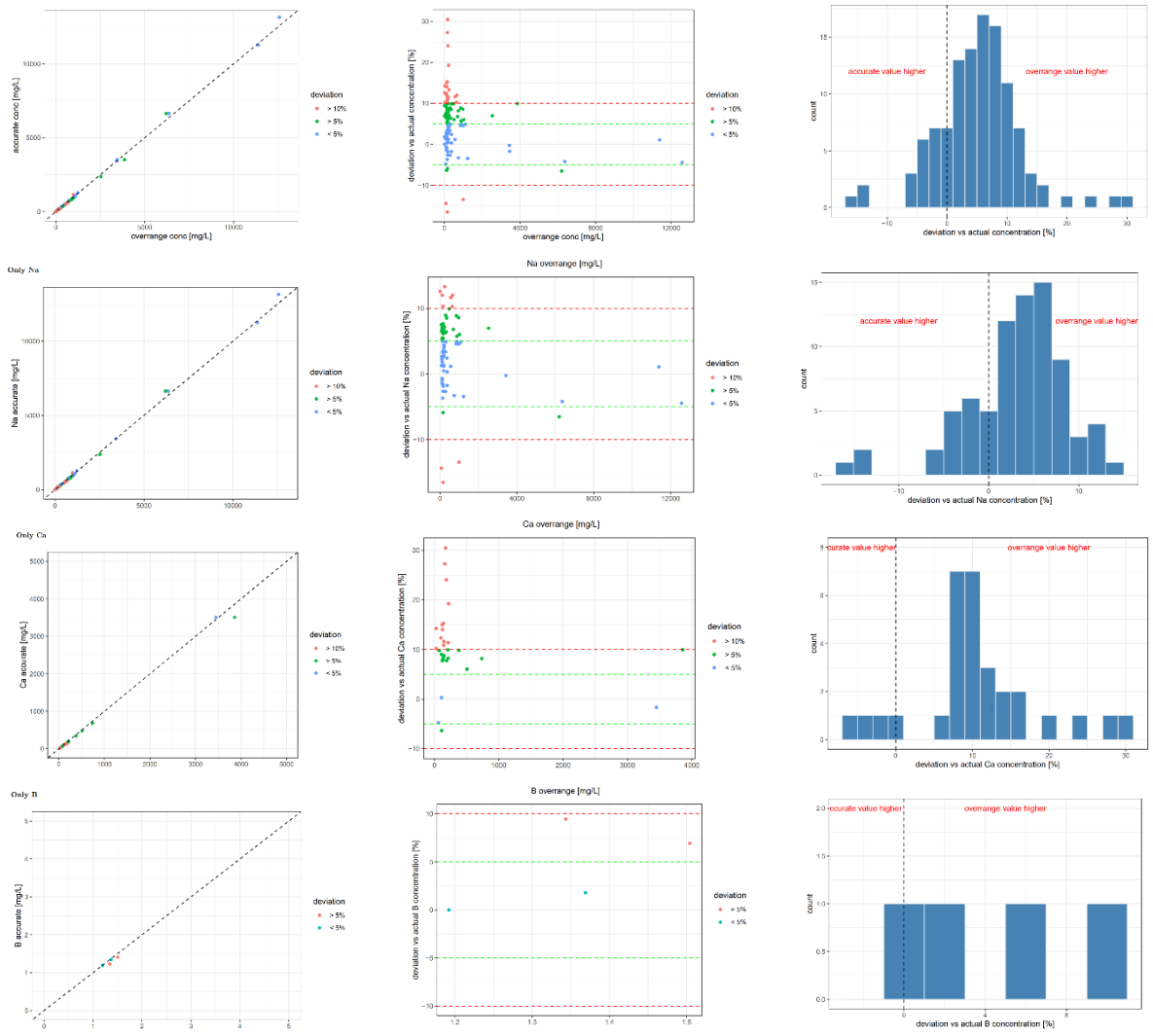

Figure 79. 2021 results that were overrange versus accurate result

8.1.4 Lab results versus field results

Lab results versus field results for NO_3 and alkalinity are shown in Figure 80.

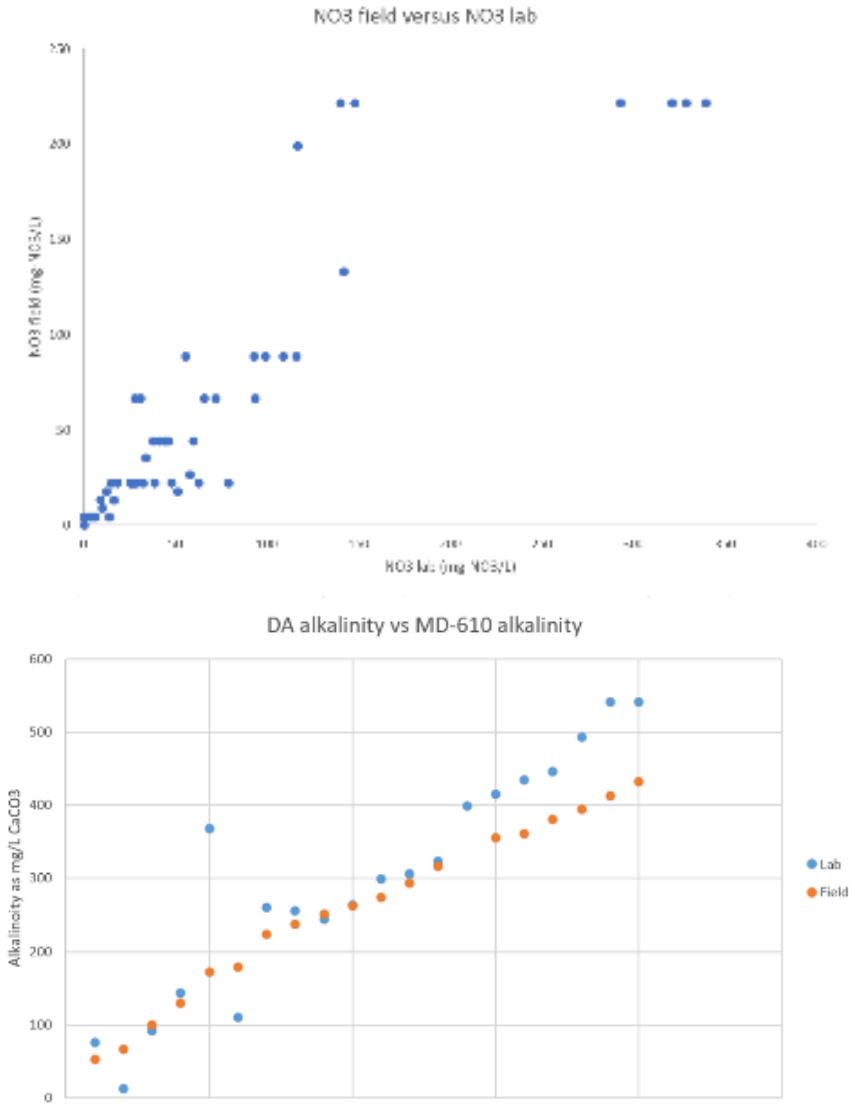

Figure 80. Lab versus field results 2020: nitrate and alkalinity. Left: Nitrate field versus nitrate in lab, both in mg-NO_3/L. Right: Alkalinity field versus alkalinity in lab, both in mg-$CaCO_3$

9 Appendix II

The comparisons over the years (1977 – 2021) are shown in tables of Ca (**Table 64**), Mg (**Table 65**), K (**Table 66**), Na (**Table 67**), SO_4 (**Table 68** -**Table 69**), and in boxplots for EC (Figure 81 -Figure 83), nitrate (Figure 84), sodium (Figure 85), chloride (Figure 86), magnesium (Figure 87), calcium (Figure 88), SAR (Figure 89) and alkalinity (Figure 90).

Table 64. Comparison between datasets for Ca concentrations, student t-test for significant difference.

	Total	East	West
1977 – 1992	ns	ns	ns
1992 – 2021	ns	ns	rises (*) from 300±647 to 461±763 mg/L
1977 - 2021	ns	ns	ns

*Symbol meaning: ns p > 0.05, * p ≤ 0.05, ** p ≤ 0.01, *** p ≤ 0.001, **** p ≤ 0.0001.*

Table 65. Comparison between datasets for Mg concentrations, student t-test for significant difference.

	Total	East	West
1977 – 1992	rises (*) from 115±171 to 173±413 mg/L	drops (*) from 101±136 to 100±67 mg/L	ns
1992 – 2021	ns	ns	ns
1977 - 2021	rises (*) from 115±171 to 189±430 mg/L	rises (*) from 101±136 to 104±76 mg/L	rises (**) from 141±219 to 334±673 mg/L

*Symbol meaning: ns p > 0.05, * p ≤ 0.05, ** p ≤ 0.01, *** p ≤ 0.001, **** p ≤ 0.0001.*

Table 66. Comparison between datasets for K concentrations, student t-test for significant difference.

	Total	East	West
1977 – 1992	ns	ns	rises (*) from 7.15±17.7 to 26.5±98.2 mg/L
1992 – 2021	ns	ns	ns
1977 - 2021	rises (**) from 3.73±11.36 to 6.6±14.1 mg/L	ns	rises (*) from 7.15±17.7 to 10.7±19.2 mg/L

*Symbol meaning: ns p > 0.05, * p ≤ 0.05, ** p ≤ 0.01, *** p ≤ 0.001, **** p ≤ 0.0001.*

Table 67. Comparison between datasets for Na concentrations, student t-test for significant difference.

	Total	East	West
1977 – 1992	ns	ns	ns

1992 – 2021	ns	ns	ns
1977 - 2021	ns	ns	ns

*Symbol meaning: ns p > 0.05, * p ≤ 0.05, ** p ≤ 0.01, *** p ≤ 0.001, **** p ≤ 0.0001.*

Table 68 . SO_4 concentrations for different years (mg/L), and significant differences in last row.

	1977	1992	2020	2021
East	114 ± 123	134 ± 122	NA	116 ± 136
West	267 ± 423	334 ± 584	NA	433 ± 687
p-value	0.00016 (***)	0.22 (ns)	NA	0.011 (*)

*Symbol meaning: ns p > 0.05, * p ≤ 0.05, ** p ≤ 0.01, *** p ≤ 0.001, **** p ≤ 0.0001.*

Table 69. Comparison between datasets for SO_4 concentration, Wilcoxon t-test for significant differences (mg/L).

	West	East
1977 – 1992	0.9811 (ns)	0.1024 (ns)
1977 – 2021	0.3797 (ns)	0.9108 (ns)
1992 – 2021	0.4076 (ns)	0.317 (ns)

*Symbol meaning: ns p > 0.05, * p ≤ 0.05, ** p ≤ 0.01, *** p ≤ 0.001, **** p ≤ 0.0001.*

Boxplots over the years ’77, ’92, ’20 and ’21

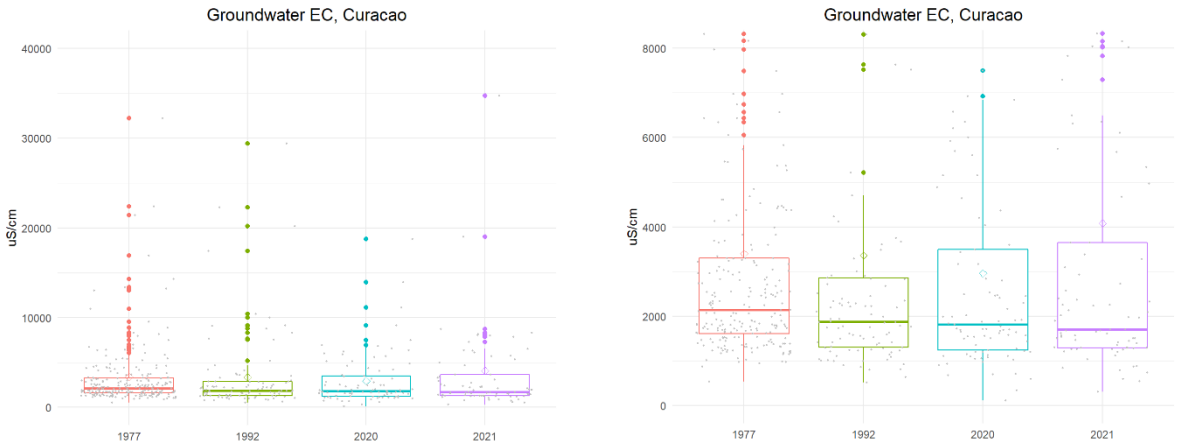

*Figure 81. Boxplot EC comparison of groundwater EC over the entire island of Curaçao between 1977, 1992, 2020 and 2021. **A)** Near to complete scale **B)** Zoomed in between 0 and 8000 µS/cm.*

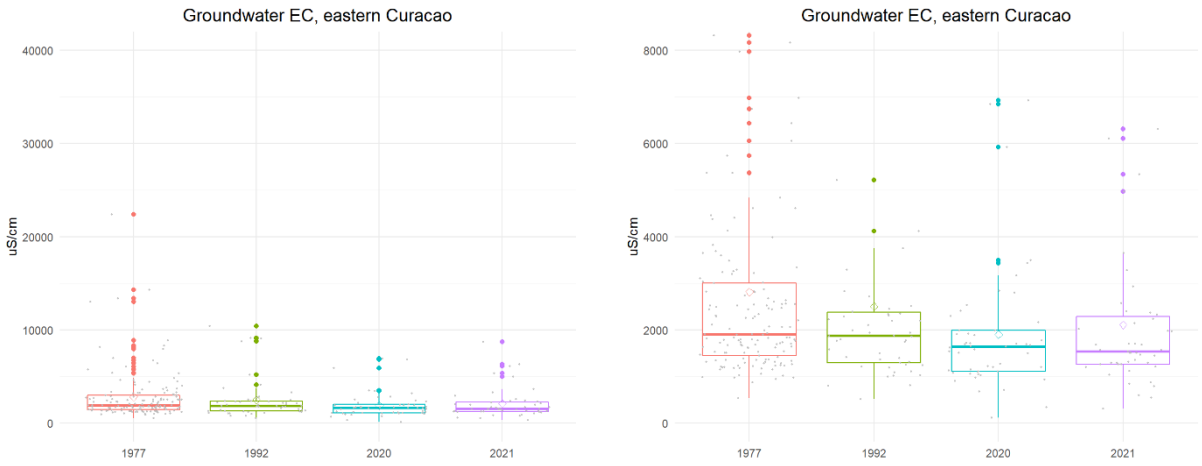

Figure 82. Boxplot EC groundwater comparison for eastern island between 1977, 1992, 2020 and 2021. ***A)*** *Complete scale.* ***B)*** *Zoomed in between 0 and 8000 µS/cm.*

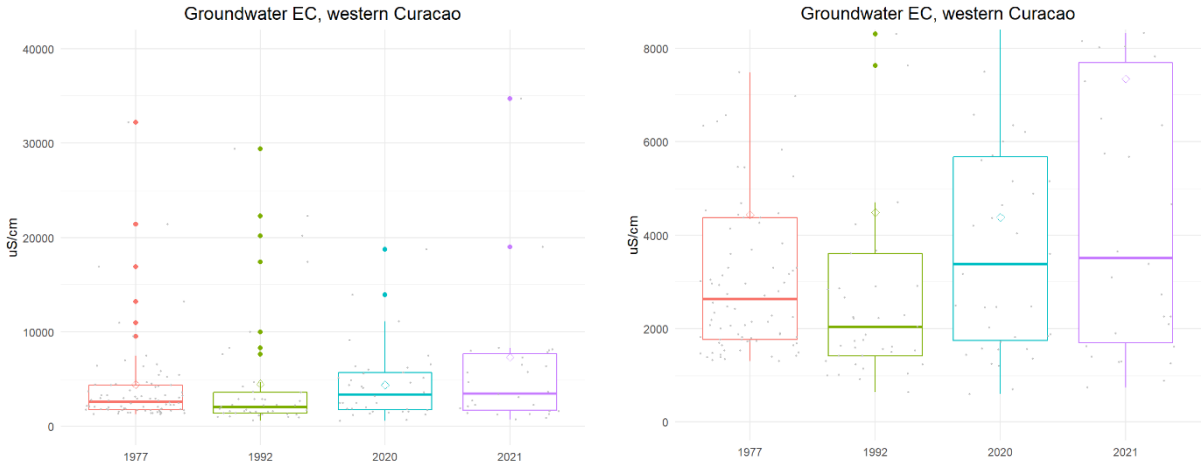

Figure 83. Boxplot EC groundwater comparison for western island between 1977, 1992, 2020 and 2021. ***A)*** *Near to complete scale.* ***B)*** *Zoomed in between 0 and 8000 µS/cm.*

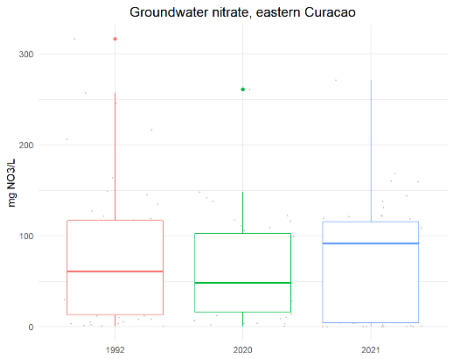

Figure 84. Boxplot nitrate groundwater comparison for eastern island between 1992, 2020 and 2021. No significant difference in NO_3 over the years.

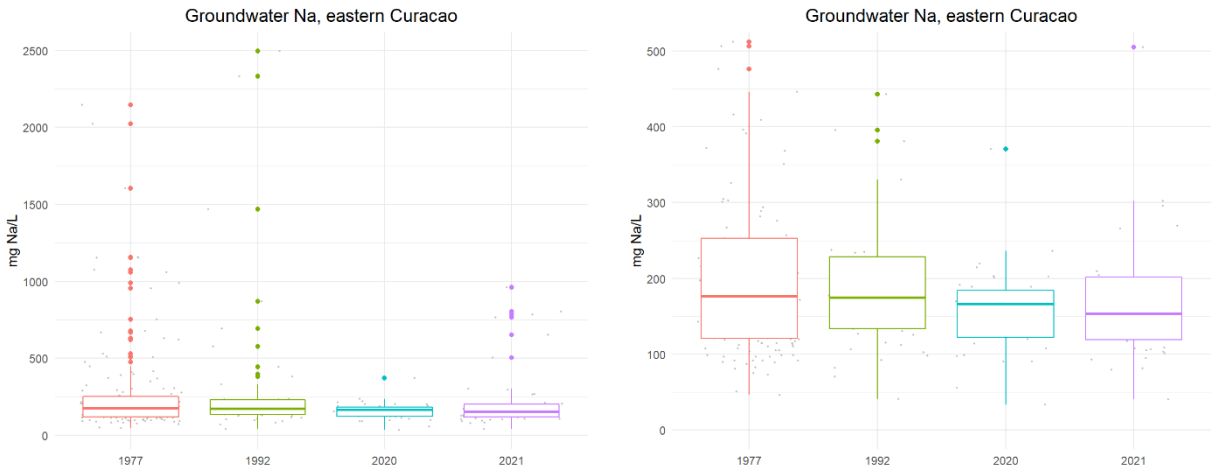

Figure 85. Boxplot sodium groundwater comparison for eastern island between 1977, 1992, 2020 and 2021.

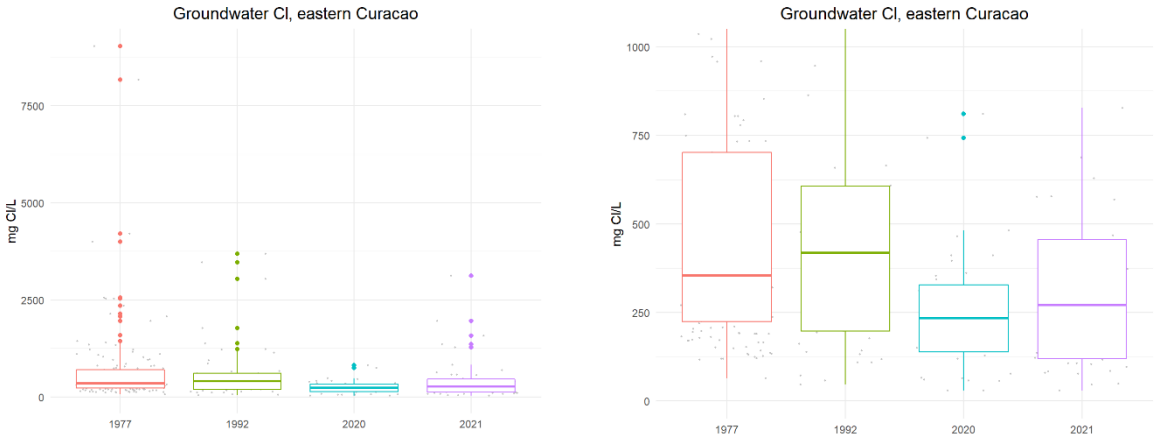

Figure 86. Boxplot chloride groundwater comparison for eastern island between 1977, 1992, 2020 and 2021.

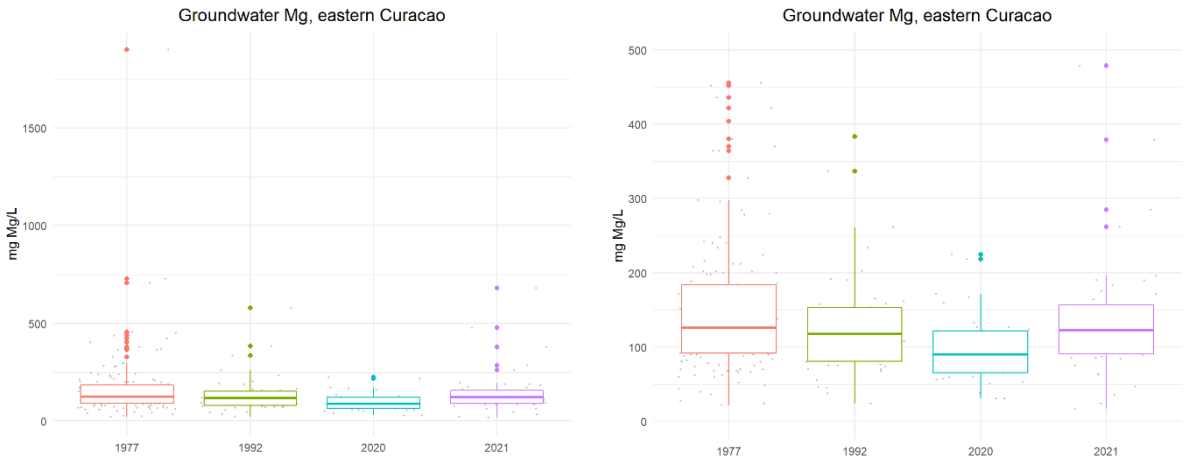

Figure 87. Boxplot magnesium groundwater comparison for eastern island between 1977, 1992, 2020 and 2021.

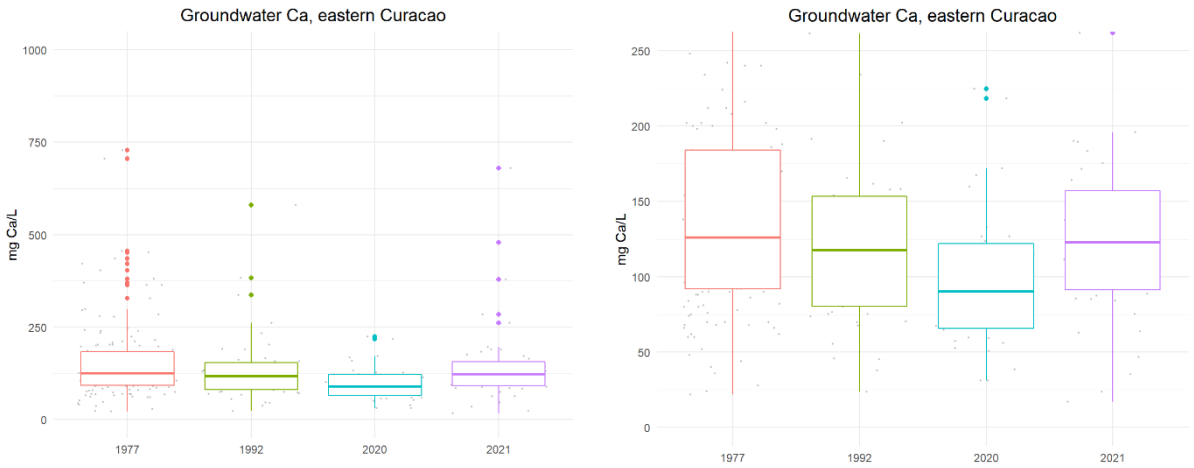

Figure 88. Boxplot calcium groundwater comparison for eastern island between 1977, 1992, 2020 and 2021.

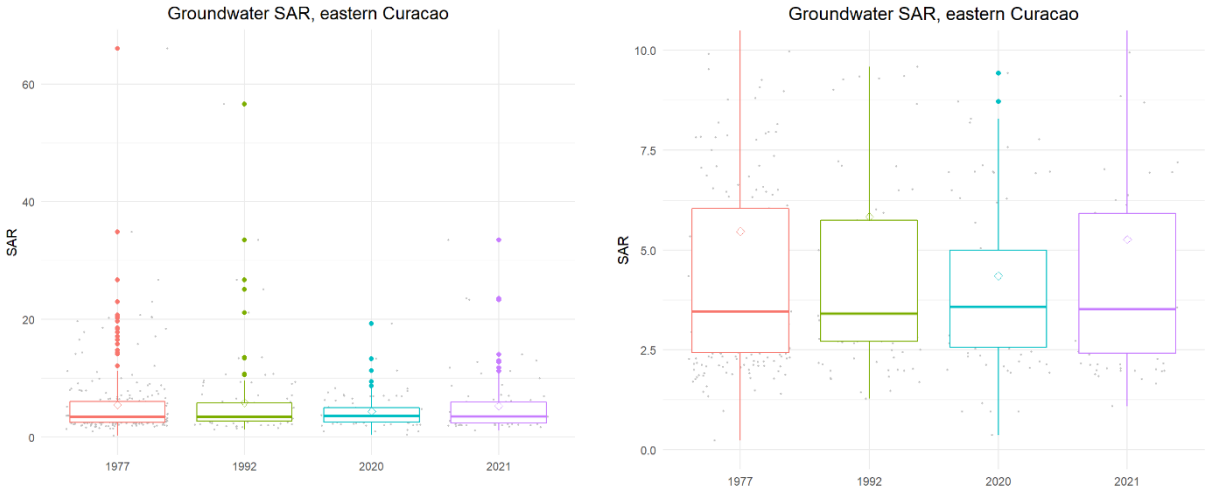

Figure 89. Boxplot SAR groundwater comparison for eastern island between 1977, 1992, 2020 and 2021 (ns).

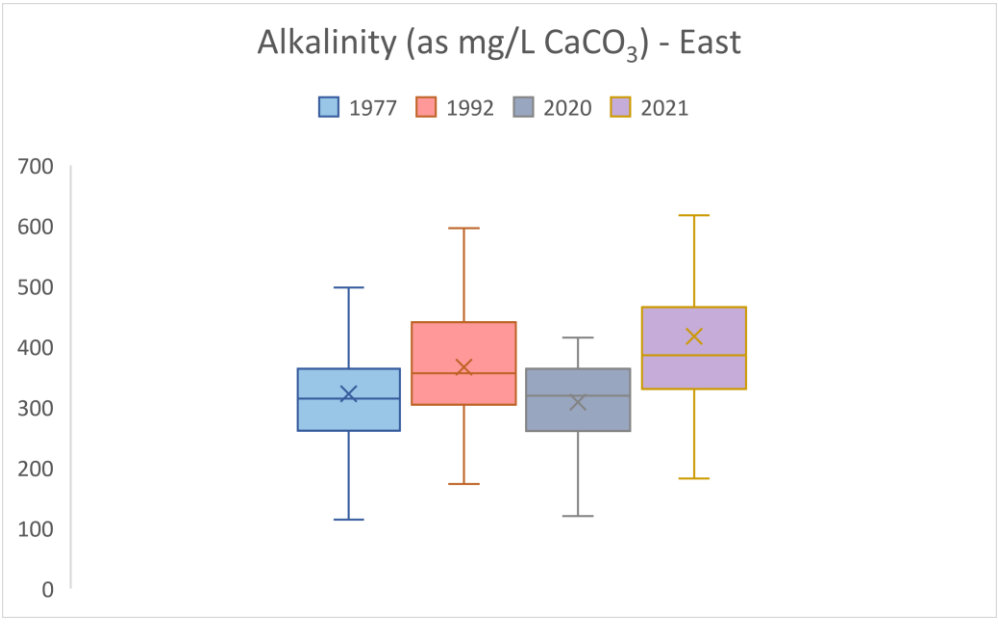

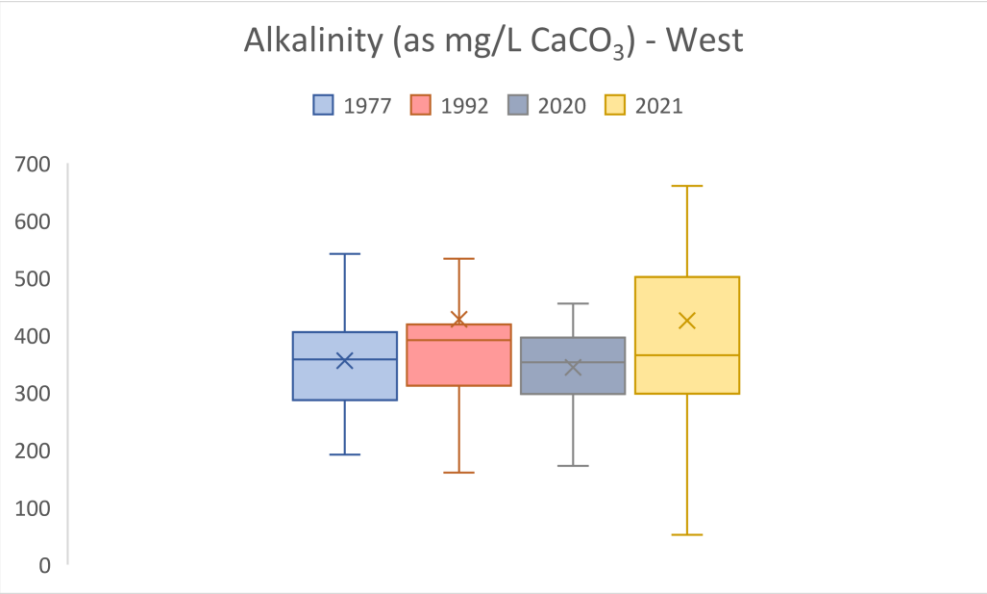

Figure 90. Western and eastern alkalinity over the years.

10 Appendix III

Cl/Br ratio and St. Joris Baai

The Cl/Br ratio versus Cl concentration is a measure to indicate mixing of seawater with fresh water, and can also be used to distinguish between different processes affecting the quality of groundwater (***Table 70***; Figure 91-Figure 96). For seawater, this is because the Cl/Br ratio remains largely unchanged when mixing occurs, while the actual concentration correlates inversely to distance from the ocean. This means that without other ratio-altering influences, the Cl/Br ratio (R = 655 + - 4) remains constant if salinization is caused by seawater mixing. It must be noted that the chemical analyses must be very precise, as the variability is not wide. (Naily & Sudaryanto, 2018)

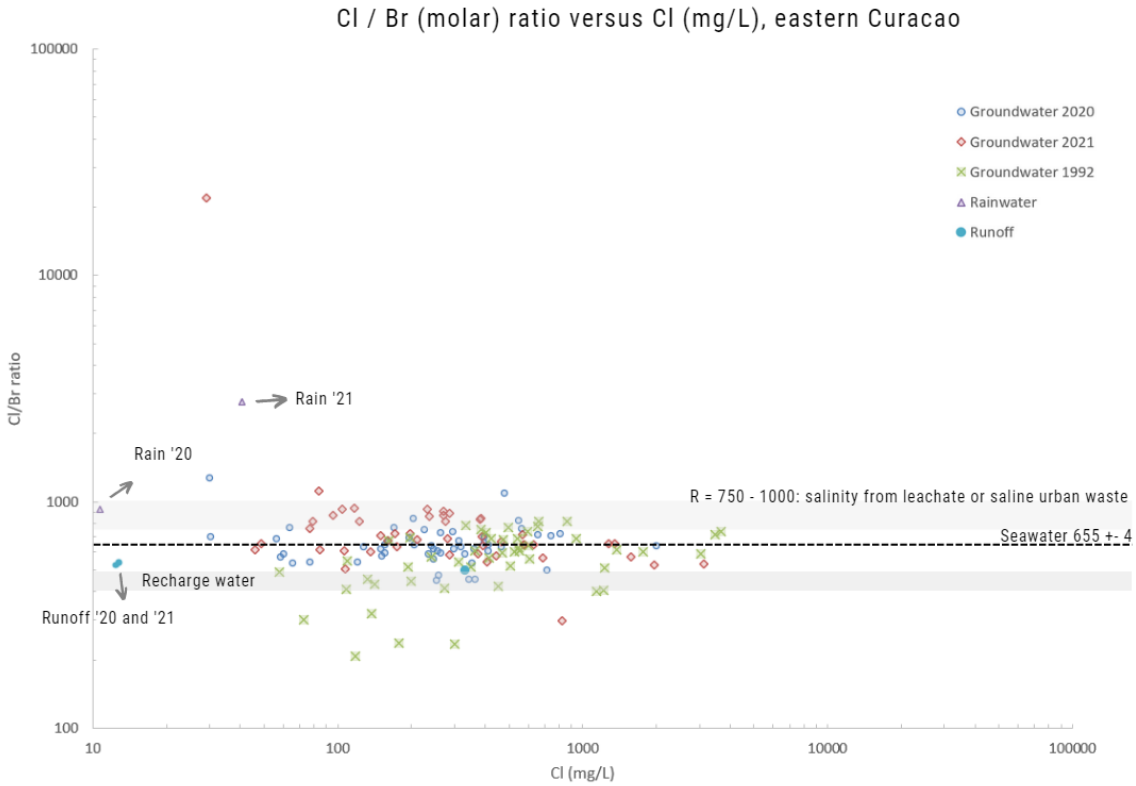

Figure 91. Plots of Cl/Br molar ratio versus chloride concentration for '92, '20 and '21, eastern Curaçao. Figure's background originating from results for aquifers in Spain and Portugal (Naily & Sudaryanto, 2018).

The Cl/Br ratio of rainwater close to the shore would be similar to that of seawater, but there might be some deviations due to processes that occur near the sea surface and coastal continent that could favor Br, reducing the Cl/Br ratio slightly. This is, however, different for regions that are windy and coastal, where ratios up to 1000 have been found in atmospheric contribution, and therefore rainwater. It is unclear to what this could exactly be attributed, but there is mention of the formation of small halite crystals (that are poor in Br); this formation would occur during the evaporation of seawater droplets on the edge of waves, to later be deposited and affect the Cl/Br ratio of the water sample. The Cl/Br ratio can be higher than that of seawater (>1500) due to the leaching of solid waste or because of wastewater loaded with sodium chloride. The Cl/Br ratio can be lower than that of seawater, because of the addition of pesticides than contain Br, or because of pollution from septic waste or manure and animal waste. Recharge can also be indicated with the Cl/Br ratio; this is, however, on the condition that there is no extreme evaporation, and there are no other sources of Cl. Lithology can also contribute and affect the Cl/Br ratio of rainfall and groundwater. Halite blown by the wind can raise the Cl/Br ratio to higher than 800 or 1000. Furthermore, anywhere where water moves only through only a short unsaturated zone, and the atmospheric composition directly affects the groundwater ratio. (Alcalá & Custodio, 2008)

When looking at the Cl/Br ratios for the entire eastern side of ’92, ’20 and ’21 (Figure 91), it can be seen that eastern wells for ’92 have more wells that have a Cl/Br ratio that is lower than that of seawater and that the Cl/Br has significantly risen from 1992 to 2020 and 2021. The rainwater samples taken in ’20 and ’21 have an R that exceeds that of seawater. Runoff samples taken in ’20 and ’21 have an R that is lower than that of seawater and is closer to the R that is associated with recharge water.

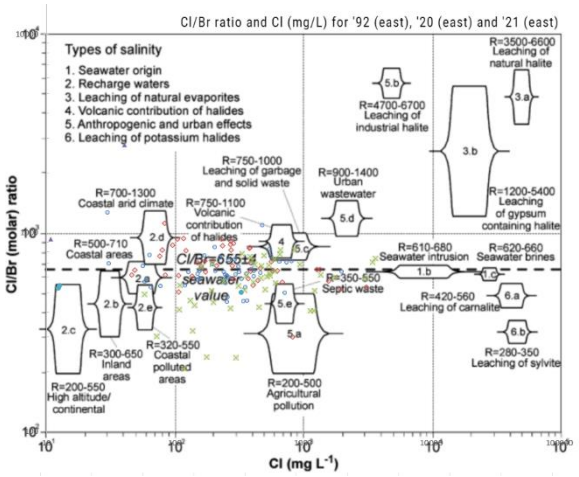

Figure 92. Plots of Cl/Br molar ratio versus chloride concentration for ’92, ’20 and ’21, eastern Curaçao. Figure’s background originating from results for aquifers in Spain and Portugal (Naily & Sudaryanto, 2018).

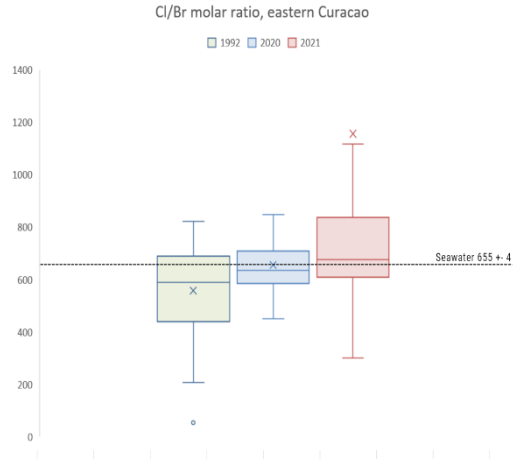

Figure 93. Boxplots of Cl/Br molar ratio ’92, ’20 and ’21, eastern Curaçao. There is significant difference between 1992-2020 (*) and 1992-2021 (**); there is no significant difference between 2020 and 2021.

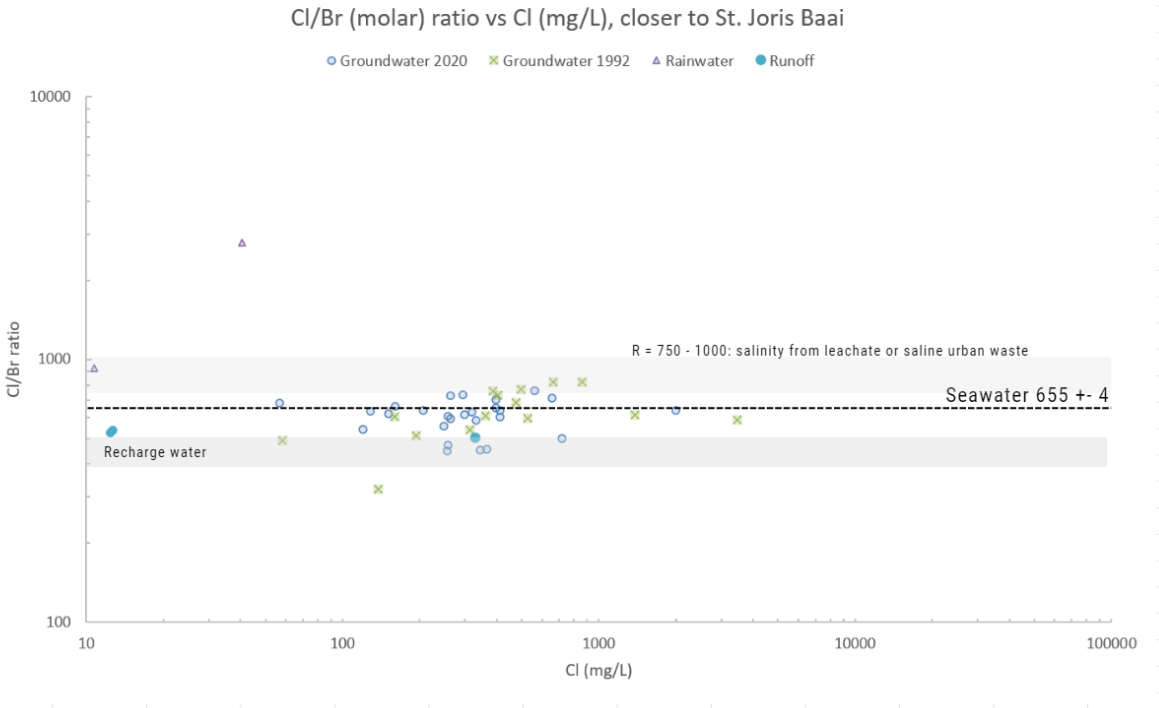

Figure 94. Cl / Br ratio for wells closer to St. Joris Baai: the eastern section of the eastern side of Curaçao.

When zooming in on the area around St. Joris Baai only, for ’92 and ’20 (Figure 94), 16 wells are considered from the ’92 dataset, namely: i 6z3, 6z118, 6z124, i 6z424, 8n58, 8n16, 8n12, 8n56, 8n52, 8n20, 8n22, 8n25, 6z209, 6z254, 6z53 and 6n7, and 26 wells are considered from the ’20 dataset: well 1 (6z209), 5 (6z254), 6 (8n16), 13, 14 (i 6z40), 37, 53, 54, 56, 57, 58, 59, 60, 68, 70, 71, 72, 73, 74, 75, 76, 77, 78, 81, 83 and 84. It can be seen that the wells in ’92 generally

have a higher Cl/Br ratio, closer to that of seawater intrusion compared to the Cl/Br of the entire eastern side of Curaçao in ’92, yet there the groundwater has a lower Cl concentration. Between ’92 and ’20 there is, however, no significant difference (Figure 96) and the Cl/Br ratio has not shifted as much around St. Joris Baai throughout the years

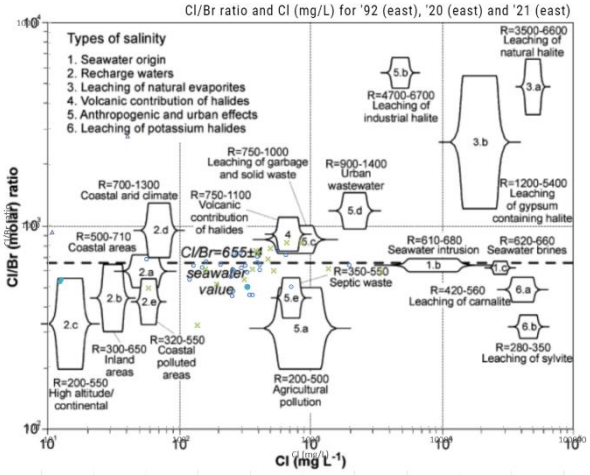

Figure 95. Plots of Cl/Br molar ratio versus chloride concentration for ’92 and ’20, wells close to St. Joris Baai. Figure’s background originating from results for aquifers in Spain and Portugal (Naily & Sudaryanto, 2018).

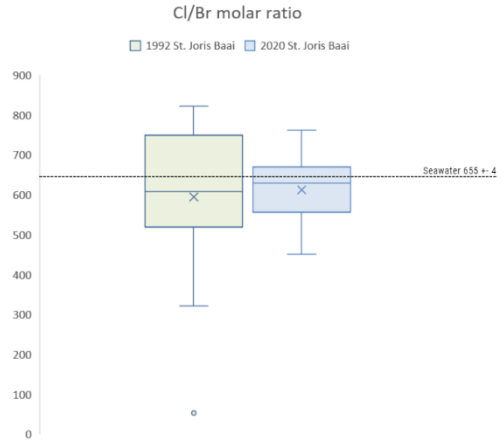

Figure 96. Boxplots of Cl/Br molar ratio ’92 and 20, wells closer to St. Joris Baai. There is no significant difference between 1992-2020.

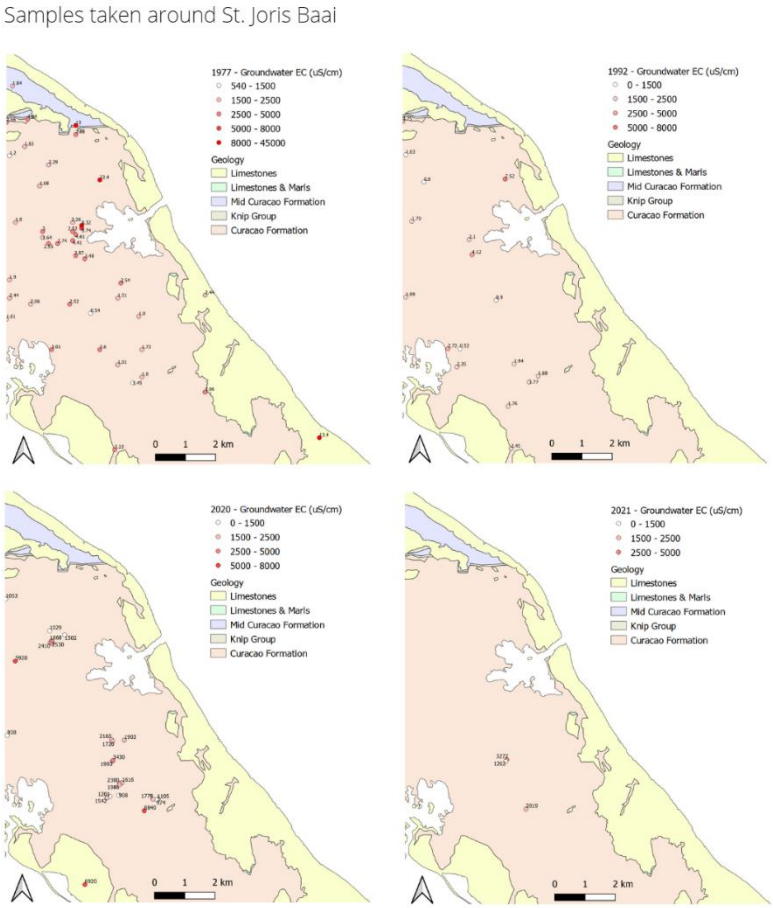

Figure 97. Wells sampled around St. Joris Baai in ’77, ’92, ’20 and ’21.

Table 70. Different molar ratio values R for Cl/Br

R	Water type
655 +- 4	Unpolluted marine water
400-500	Recharge water
50-650 (R<50 atmospheric pollution)	Continental rainwater
R close to marine value	Coastal rainwater
R > 800	Deposition from marine aerosol
750 -1000	Salinity from leachate or saline urban waste
450	Septic tank leachate
R < 650 (up to 900)	Volcanic gas contributing halides

Values retrieved from (Naily & Sudaryanto, 2018).

11 Appendix IV

Rain and runoff results for 2020 and 2021 are joined together in **Table 71** and **Table 72**.

Table 71. Explorative rainwater results for 2020 and 2021 joined together.

Parameter	Units	Average	STD	N*
Al	µg/l	117.90	161.16	3
As	µg/l	1.00	-	2
B	µg/l	17.56	4.56	3
Ba	µg/l	2.44	-	2
Br	mg/l	0.02	0.01	5
Ca	mg/l	2.27	0.87	3
Cl	mg/l	14.32	13.33	5
Cu	µg/l	2.61	-	2
DO	mg/l	7.52	-	2
DO	%	83.41	-	2
EC	µS/cm	63.97	53.08	4
Eh	mV	132.85	-	2
F	mg/l	0.04	0.06	5
Fe	mg/l	0.01	0.01	3
HCO_3	mg/l	10.80	4.43	5
K	mg/l	0.92	0.23	3
Li	µg/l	1.00	-	2
Mg	mg/l	1.24	0.90	3
Mn	µg/l	4.10	2.03	3
Na	mg/l	11.03	8.28	3
NH_4	mg/l	0.22	0.08	5
Ni	µg/l	1.81	-	2
NO_2	mg/l	0.01	0.00	5
NO_2 (field)	mg/l	0.00	-	2
NO_3	mg/l	0.20	0.23	5
NO_3 (field)	mg/l	0.00	-	2
P	mg/l	0.02	-	2
pH	-	6.81	0.52	4
PO_4	mg/l	0.05	0.04	5
Si	mg/l	0.03	0.04	3
SO_4	mg/l	3.16	1.50	5
Temp	C	26.60	-	1
Turbidity	NTU	<0.01	0	3
Zn	µg/l	59.54	-	2

**There are differences in the amount of samples taken as the 2020 rainwater samples are still waiting to go through the ICP-MS, but have been through the IC. For 2021 there is are certain parameters missing as well (e.g. EC and pH for one sample).*

Table 72. Explorative runoff results for combined runoff samples of 2020 and 2021 fieldwork campaign.

Parameter	Units	Average	STD	N
Al	µg/l	25.67	12.22	8
As	µg/l	1.03	0.40	8
B	µg/l	59.74	41.69	8
Ba	µg/l	7.38	8.23	8
Be	µg/l	1.00	0.00	4
Br	mg/l	0.21	0.48	8
Ca	mg/l	34.52	28.41	5
Cd	µg/l	1.00	0.00	4
Cl	mg/l	49.20	106.29	8
Co	µg/l	1.00	0.00	4
Cr	µg/l	1.61	0.30	4
Cu	µg/l	4.63	2.47	8
DO	mg/l	5.23	0.66	4
DO	%	61.38	9.17	4
EC	µS/cm	322	346	11
Eh	mV	104.43	16.54	4
F	mg/l	0.01	0.01	8
Fe	mg/l	0.04	0.03	8
HCO_3	mg/l	85.12	28.43	4
HCO_3	mg/l	82.61	30.29	4
K	mg/l	3.84	3.60	8
Li	µg/l	1.27	0.89	8
Mg	mg/l	5.32	6.43	8
Mn	µg/l	5.26	7.42	8
Mo	µg/l	1.73	0.70	4
Na	mg/l	32.70	61.60	7
NH4	mg/l	0.18	0.10	8
Ni	µg/l	1.53	0.77	8
NO_2	mg/l	0.03	0.06	8
NO_2 (field)	mg/l	0.00	0.00	4
NO_3	mg/l	3.04	4.95	8
NO_3 (field)	mg/l	6.64	9.13	4
P	mg/l	0.16	0.26	5
Pb	µg/l	0.67	0.39	8
pH		7.66	0.63	11
PO_4	mg/l	0.36	0.50	8
S	mg/l	3.95	3.35	5
Sb	µg/l	1.00	0.00	4
Se	µg/l	1.46	0.79	4
Si	mg/l	1.75	0.96	8
SO_4	mg/l	27.17	57.10	8
Temp	C	25.38	3.73	2
V	µg/l	14.18	7.27	8
Ti	µg/l	0.72	0.61	8
Zn	µg/l	6.75	4.86	8
Turbidity	NTU	49.50	9.34	4

E. Coli	CFU/100 ml	757767	1048177	3

12 Appendix V

Vegetation on the western side of Curaçao

Log pCO_2 versus SI calcite of wells in 2021 are shown in Figure 98. Figure 98. log pCO2 versus SI calcite of wells in 2021

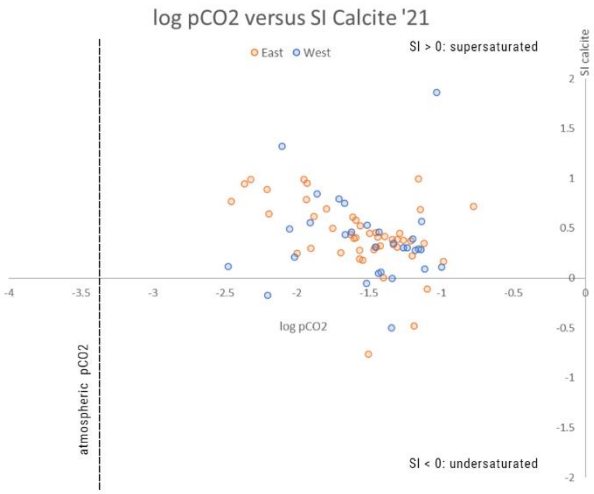

Figure 98. log pCO2 versus SI calcite of wells in 2021

13 Appendix VI

Multivariate statistics

The initial assessments on multivariate statistics are shown in Figure 99-Figure 106 and **Table 73**-**Table 81**.

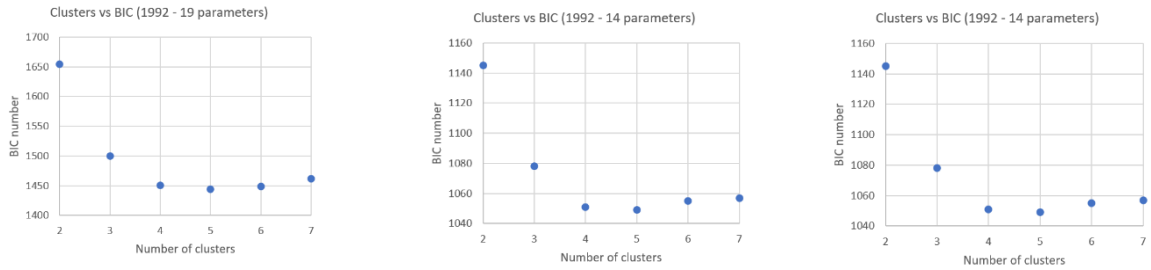

Figure 99. Different BIC numbers per number of cluster for the rigid k-means for 1992 (19 parameters), 1992 (14 parameters) and 2021 (14 parameters).

K-means clustering for 1992, 2020 and 2021 dataset

Table 73. K-means clustering with four clusters, eastern Curaçao (2020). Units mostly in mg/L or µg/L.

	Cluster 1	Cluster 2	Cluster 3	Cluster 4
Amount of wells	#15	#19	#1	#3
Well names (2020_GW_X)	10, 18, 31, 54, 58, 68, 69, 72, 74, 75, 78, 79, 8, 81, 82	1, 13, 14, 15, 2, 3, 38, 4, 40, 41, 42, 49, 53, 56, 64, 7, 76, 77, 80	5	12, 30, 9
B (µg/L)	348.3646	327.9709	387.2200	331.8183
Ca (mg/L)	108.6234	72.5823	122.0719	**189**.8918
Cl (mg/L)	298.7333	134.7895	206.0000	**585**.6667
EC (µS/cm)	**1737**	**960**	**5920**	**3043**
F (mg/L)	0.06084	0.07005263	0.05410000	0.04663333
Fe (mg/L)	0.405955	0.3257267	0.7692800	0.6356033
HCO_3 (mg/L)	371.368	368.5684	490.4400	341.6000
K (mg/L)	5.21426	7.056857	10.000000	6.664172
Mg (mg/L)	69.83783	44.84905	81.30789	**126**.25352
Na (mg/L)	179.2681	127.8660	191.4174	236.2388
NH4 (mg/L)	0.50629901	0.08471504	0.64394183	0.01285714
NO3 (mg/L)	60.28233	45.81579	93.60000	102.56667
pH (-)	7.453333	7.296842	7.490000	7.036667
Si (mg/L)	24.82961	26.31565	50.00000	29.20340
Temp (C)	29.90667	29.29474	29.20000	28.00000

Table 74. K-means clustering with three clusters, eastern Curaçao (2020). Units mostly in mg/L or µg/L.

	Cluster 1	Cluster 2	Cluster 3
Amount of wells	#18	#19	#1
Well names (2020_GW_X)	8, 9, 10, 12, 18, 30, 31, 54, 58, 68, 69, 72, 74, 75, 78, 79, 81, 82	1, 2, 3, 4, 7, 13, 14, 15, 38, 40, 41, 42, 49, 53, 56, 64, 7, 76, 77, 80	5
B (µg/L)	345.6069	327.9709	387.2200
Ca (mg/L)	122.1682	**72**.5823	122.0719
Cl (mg/L)	346.5556	**134**.7895	206.0000
EC (µS/cm)	**1955**	**960**	**5920**
F (mg/L)	0.05847222	0.07005263	0.05410000
Fe (mg/L)	0.4442297	0.3257267	0.7692800
HCO_3 (mg/L)	366.4067	368.5684	490.4400
K (mg/L)	5.455912	7.056857	10.000000
Mg (mg/L)	79.24044	44.84905	81.30789
Na (mg/L)	188.7632	127.8660	191.4174
NH4 (mg/L)	**0.42405870**	0.08471504	0.64394183
NO3 (mg/L)	67.32972	45.81579	93.60000
pH (-)	7.383889	7.296842	7.490000
Si (mg/L)	25.55858	26.31565	**50**.00000
Temp (C)	29.58889	29.29474	29.20000

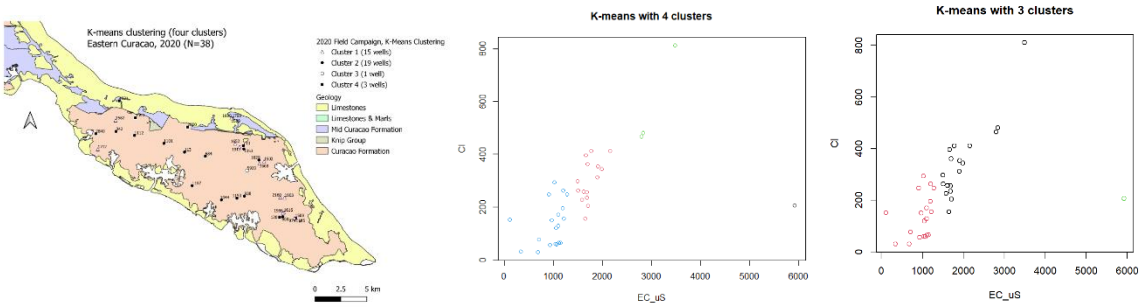

Figure 100. K-means clustering, 2020 (four clusters), eastern Curaçao.

2021 (east) (2)

Table 75. K-means clustering with four clusters, eastern Curaçao (2021). Units mostly in mg/L or µg/L

	Cluster 1	Cluster 2	Cluster 3	Cluster 4
Amount of wells	#29	#3	#8	#3
Well names (2021_GW_X)	1, 2, 3, 19, 11, 13, 15, 23, 24, 25, 26, 27, 28, 29, 34, 37, 38, 39, 40AB, 41, 42, 46, 47, 56, 57, 58, 63, 69, 70	6, 7, 20A	8, 14AB, 16, 22, 35, 36, 55, 64	20B, 43, 55B

Table 76. K-means clustering with three clusters, eastern Curaçao (2021). Units mostly in mg/L or µg/L. N=42.

Amount of wells	Cluster 1 #9	Cluster 2 #29	Cluster 3 #3
Well names (2021_GW_X)	8, 14AB, 16, 22, 35AB, 36, 43, 55AB, 64	1, 2, 3, 10, 11, 13, 15, 23, 24, 25, 26, 27, 28, 29, 34, 37, 38, 39, 40AB, 41, 42, 46, 47, 56, 57, 58, 63, 69, 70	6, 7, 20AB
B (µg/L)	397.3395	433.7917	1264.7714
Ca (mg/L)	184.2467	94.6292	373.5870
Cl (mg/L)	499.7671	185.2046	1929.8100
EC (µS/cm)	2489.333	1258.287	6525.250
F (mg/L)	0.1278333	0.2677667	0.6260000
Fe (mg/L)	0.01123473	0.01089361	0.03575560
HCO_3 (mg/L)	562.4967	485.2478	569.0100
K (mg/L)	2.288425	1.903064	24.382548
Mg (mg/L)	139.23937	65.86243	248.02212
Na (mg/L)	204.1459	151.4984	800.2262
NH4 (mg/L)	0.7606548	0.2689957	0.4140018
NO3 (mg/L)	87.64883	60.32160	87.59500
pH (-)	7.189750	7.260867	6.926250
Si (mg/L)	28.29977	25.08017	25.07301
Temp (C)	30.615	30.231	30.615

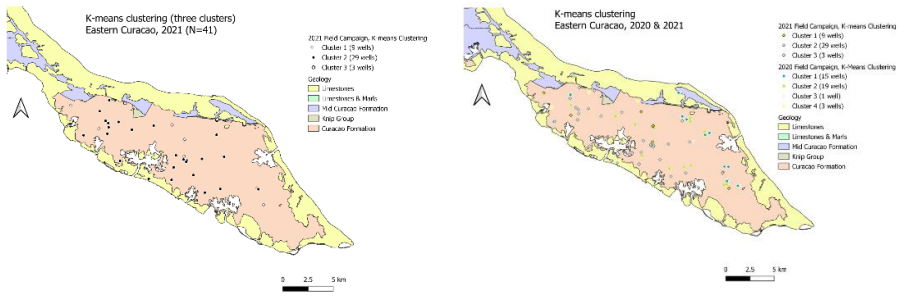

Figure 101. K-means clustering, 2021 (three clusters), eastern Curaçao.

Table 77. K-means clustering with three four clusters, eastern Curaçao (1992). Units mostly in mg/L or µg/L. N=50.

Amount of wells	Cluster 1 #6	Cluster 2 #40	Cluster 3 #4
Well names (1992_GW_X)	73, 14, 22, 70, 79, 83	All other wells	11, 12, 71, 84
EC (µS/cm)	3653.333	1650.600	9342.500
NO3 (mg/L)	53.16550	83.82423	35.48250
Ca	223.8369	107.7673	285.6257

Cl	1222.0592	340.9579	2851.2675
Fe	0.2028500	0.1490575	0.0677300
HCO_3 (mg/L)	374.5400	448.4122	534.9700
K (mg/L)	11.575483	1.573622	11.762100
Mg (mg/L)	148.92552	81.81285	217.60798
Na	390.2387	166.8161	1791.2940
pH (-)	7.183333	7.160500	7.452500
Si (mg/L)	28.51197	30.88612	24.24348

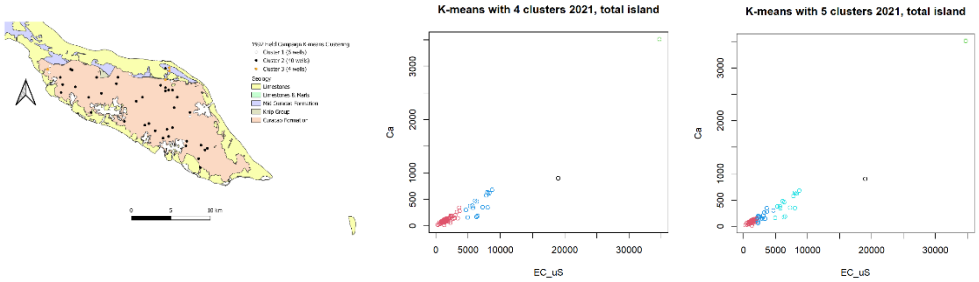

Figure 102. K-means clustering, 2021 (four clusters), eastern Curaçao.

Table 78. K-means clustering with four clusters, total Curaçao (2021). Units mostly in mg/L or µg/L. N=71

Amount of wells	Cluster 1 #1	Cluster 2 #56	Cluster 3 #1	Cluster 4 #13
Well names (1992_X)	4	All other wells	30	6, 7, 9, 20AB, 31, 44, 45, 49, 53AB, 54, 59, 67, 68
Ca (mg/L)	899.2867	119.3143	3509.0133	418.4356
Cl (mg/L)	7048.3200	302.9724	19027.8250	2055.1666
EC (µS/cm)	19000.000	1702.225	34710.000	6751.188
Fe (mg/L)	0.12437692	0.06621209	5.40739024	1.51122915
HCO_3 (mg/L)	2514.0200	490.5890	63.4600	491.9012
K (mg/L)	92.673039	2.302838	15.414424	14.292659
Mg (mg/L)	431.63058	82.47082	1598.57082	276.45550
Na (mg/L)	3438.4267	187.3762	6640.1917	829.9903
NO_3 (mg/L)	0.03000	54.33202	0.03000	67.58581
pH (-)	7.340000	7.218633	6.948000	6.950687
Si (mg/L)	7.645029	24.871331	0.001000	16.228086

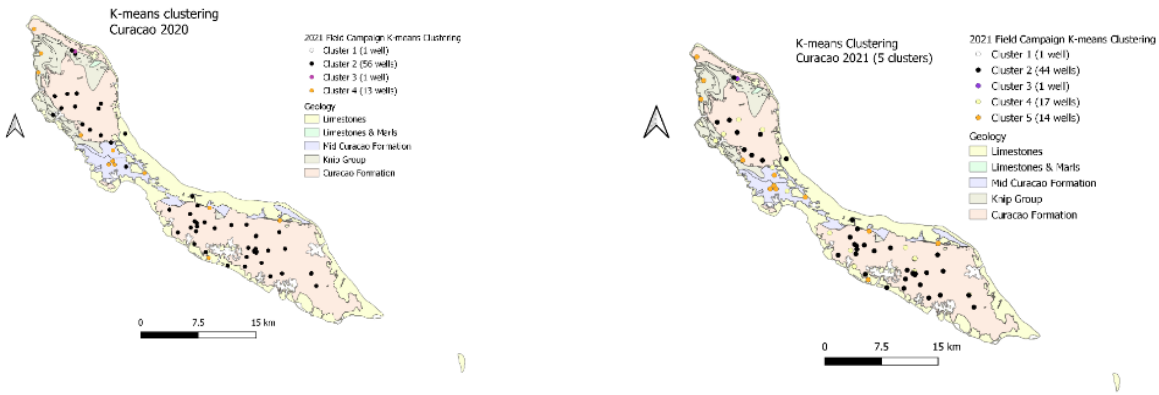

Figure 103. K-means clustering, 2021 (four clusters), eastern Curaçao.

Table 79. K-means clustering with five clusters, total Curaçao (2021). Units mostly in mg/L or µg/L. N=71

	Cluster 1	Cluster 2	Cluster 3	Cluster 4	Cluster 5

Amount of wells	#1	#40	#1	#16	#14
Well names (1992_X)	4, same as 4 clusters	All other wells	30, same as with 4 clusters	8, 14AB, 17, 18, 19, 22, 35AB, 36, 43, 44, 48, 50, 55B, 61, 65,	5, 6, 7, 9, 20AB, 31, 45, 49, 53AB, 54, 59, 67, 68
Ca (mg/L)	899.28669	96.59084	3509.01333	188.76821	426.31824
Cl (mg/L)	7048.3200	209.3965	19027.8250	597.8520	2112.2721
EC (µS/cm)	19000	1336	34710	2825.412	6890.200
Fe (mg/L)	0.12437692	0.08546049	5.40739024	0.01325408	1.61112074
HCO_3 (mg/L)	2514.0200	468.3209	63.4600	544.6629	496.0247
K (mg/L)	92.673039	1.980951	15.414424	3.381431	14.813778
Mg (mg/L)	431.6306	65.0406	1598.5708	133.0018	283.2480
Na (mg/L)	3438.4267	157.3301	6640.1917	286.5121	848.6123
NO_3 (mg/L)	0.03000	51.30561	0.03000	58.98141	72.07753
pH (-)	7.340000	7.222545	6.948000	7.177471	6.968000
Si (mg/L)	7.645029	24.958093	0.001000	23.585886	16.854206

1992 (total island) (5)

Table 80. K-means clustering with four clusters, total Curaçao (1992). Units mostly in mg/L or µg/L. *n*=97

Amount of wells	Cluster 1 #17	Cluster 2 #68	Cluster 3 #8	Cluster 4 #4
Well names (1992_X)	73, 14, 2, 22, 36, 41, 44, 47, 48, 62, 64, 67, 70, 79, 83, 85, 86	All other wells	11, 12, 3, 30, 31, 71, 84, 91	32, 37, 63, 96
EC (µS/cm)	3 458	1 576	8 856	22 335
NO_3 (mg/L)	37.81082	63.66127	23.98875	9.35500
Ca (mg/L)	189.22212	97.57796	357.08779	1892.01000
Cl (mg/L)	1053.605	311.088	2890.354	11938.890
Fe (mg/L)	0.5706765	0.2093309	1.0924787	3.4555000
F (mg/L)	All BLD (<0.1)	All BLD (<0.1)	All BLD (<0.1)	All BLD (<0.1)
HCO_3 (mg/L)	359.0853	454.4866	464.1337	886.6350
K (mg/L)	8.025941	2.652325	12.779288	212.753100
Mg (mg/L)	134.94080	73.79497	275.46943	1807.86375
Na (mg/L)	450.2689	174.2048	1537.8723	3030.2965
pH (-)	7.225294	7.284118	7.330000	7.147500
Si (mg/L)	23.55342	28.53208	18.38952	22.59743

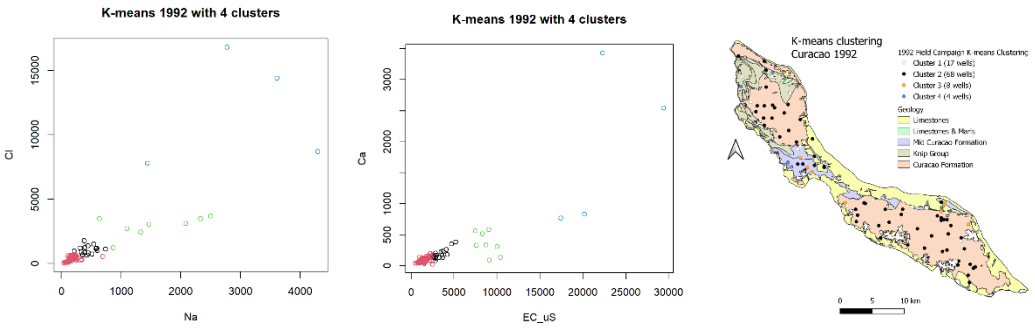

Figure 104. K-means clustering, 1992 (four clusters).

Comparison between 1992 and 2021

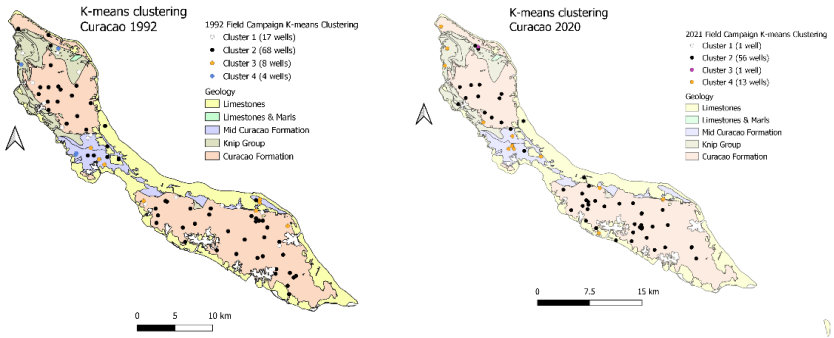

Figure 105. K-means clustering maps, 1992

Table 81. Comparison between cluster 2 2021 and 1992, most present in the CLF / DO formation.

Amount of wells	Cluster 2 - 2021 #17 Average	Cluster 2 - 1992 #56 Average
EC (µS/cm)	1702.225	1 576
NO_3 (mg/L)	54.33202	63.66127
Ca (mg/L)	119.3143	97.57796
Cl (mg/L)	302.9724	311.088
Fe (mg/L)	0.06621209	0.2093309
HCO_3 (mg/L)	490.5890	454.4866
K (mg/L)	2.302838	2.652325
Mg (mg/L)	82.47082	73.79497
Na (mg/L)	187.3762	174.2048
pH (-)	7.218633	7.284118
Si (mg/L)	24.871331	28.53208

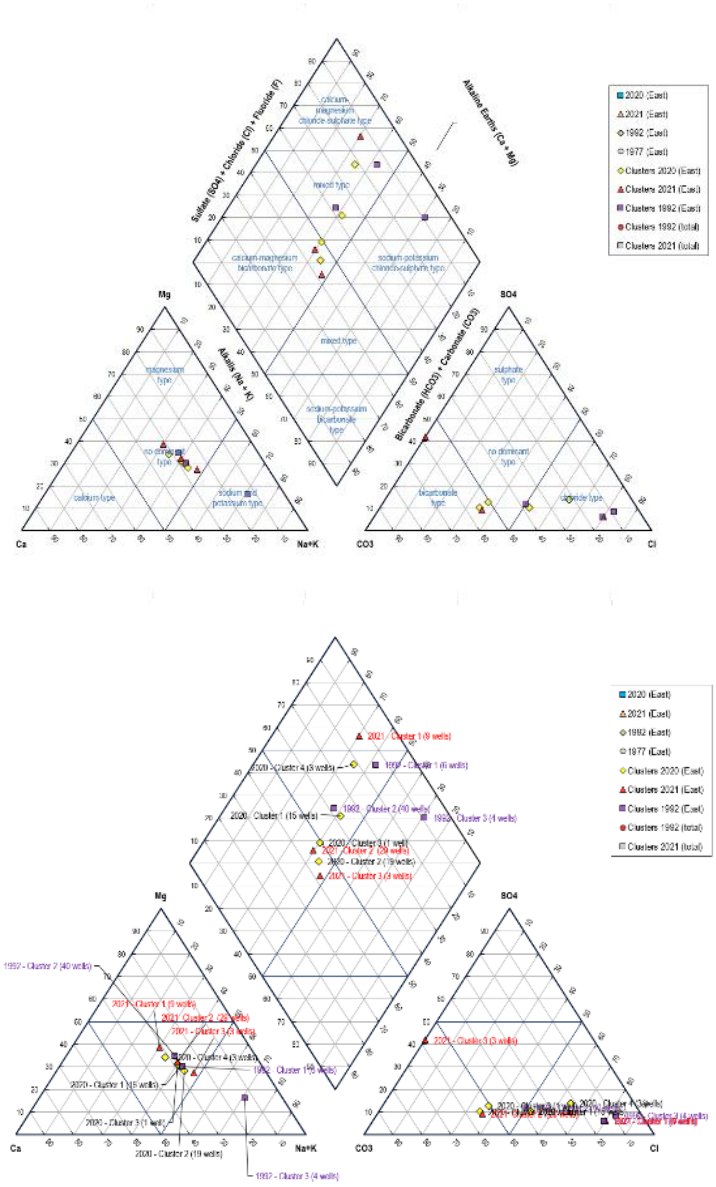

Figure 106. All clusters visualized in a piper diagram.